frontiers | Research Topics

Insights in zoological medicine 2023

Edited by
Irene Iglesias and Carlos Sacristán Yagüe

Published in
Frontiers in Veterinary Science

ISSN 1664-8714
ISBN 978-2-8325-6404-2
DOI 10.3389/978-2-8325-6404-2

About Frontiers

Frontiers is more than just an open access publisher of scholarly articles: it is a pioneering approach to the world of academia, radically improving the way scholarly research is managed. The grand vision of Frontiers is a world where all people have an equal opportunity to seek, share and generate knowledge. Frontiers provides immediate and permanent online open access to all its publications, but this alone is not enough to realize our grand goals.

Frontiers journal series

The Frontiers journal series is a multi-tier and interdisciplinary set of open-access, online journals, promising a paradigm shift from the current review, selection and dissemination processes in academic publishing. All Frontiers journals are driven by researchers for researchers; therefore, they constitute a service to the scholarly community. At the same time, the *Frontiers journal series* operates on a revolutionary invention, the tiered publishing system, initially addressing specific communities of scholars, and gradually climbing up to broader public understanding, thus serving the interests of the lay society, too.

Dedication to quality

Each Frontiers article is a landmark of the highest quality, thanks to genuinely collaborative interactions between authors and review editors, who include some of the world's best academicians. Research must be certified by peers before entering a stream of knowledge that may eventually reach the public - and shape society; therefore, Frontiers only applies the most rigorous and unbiased reviews. Frontiers revolutionizes research publishing by freely delivering the most outstanding research, evaluated with no bias from both the academic and social point of view. By applying the most advanced information technologies, Frontiers is catapulting scholarly publishing into a new generation.

What are Frontiers Research Topics?

Frontiers Research Topics are very popular trademarks of the *Frontiers journals series*: they are collections of at least ten articles, all centered on a particular subject. With their unique mix of varied contributions from Original Research to Review Articles, Frontiers Research Topics unify the most influential researchers, the latest key findings and historical advances in a hot research area.

Find out more on how to host your own Frontiers Research Topic or contribute to one as an author by contacting the Frontiers editorial office: frontiersin.org/about/contact

Insights in zoological medicine: 2023

Topic editors

Irene Iglesias — Animal Health Research Center, National Institute for Agricultural and Food Research and Technology, Spain

Carlos Sacristán Yagüe — Centro de Investigación en Sanidad Animal (CISA), Spain

Citation

Iglesias, I., Sacristán Yagüe, C., eds. (2025). *Insights in zoological medicine: 2023*. Lausanne: Frontiers Media SA. doi: 10.3389/978-2-8325-6404-2

Table of contents

frontiers | Frontiers in Veterinary Science

TYPE Editorial
PUBLISHED 07 May 2025
DOI 10.3389/fvets.2025.1603605

OPEN ACCESS

EDITED AND REVIEWED BY
Michael Kogut,
United States Department of Agriculture,
United States

*CORRESPONDENCE
Irene Iglesias
✉ iglesias@inia.csic.es
Carlos Sacristan
✉ carlos.sacristan@inia.csic.es

RECEIVED 31 March 2025
ACCEPTED 17 April 2025
PUBLISHED 07 May 2025

CITATION
Iglesias I and Sacristan C (2025) Editorial: Insights in zoological medicine: 2023.
Front. Vet. Sci. 12:1603605.
doi: 10.3389/fvets.2025.1603605

Editorial: Insights in zoological medicine: 2023

Irene Iglesias* and Carlos Sacristan*

Epidemiology and Environmental Health Group, Animal Health Research Center, National Institute for Agricultural and Food Research and Technology, Madrid, Spain

KEYWORDS

wildlife conservation, environmental and anthropogenic factors, infectious diseases, captive animal welfare, disease surveillance

Editorial on the Research Topic
Insights in zoological medicine: 2023

Over the past decade, remarkable progress has been made in zoological medicine through bold research initiatives and the application of innovative technologies. As we enter the third decade of the 21st century, it is crucial to understand not only the achievements but also the persistent and emerging challenges faced by wildlife in both natural ecosystems and human-altered environments. In the article series *"Insights in zoological medicine: 2023,"* we highlight the importance of wildlife studies in advancing knowledge on the Research Topic affecting these species and the interactions between wildlife, the environment, and human activities, emphasizing both achievements and outstanding challenges.

The studies by Tummeleht et al. and Haman et al. are notable examples of the interaction between wildlife and environmental risks, as well as the importance of early intervention and monitoring strategies. The first study examines the attraction of wild boar (*Sus scrofa*) carcasses to scavenging animals, which may serve as potential sources of African swine fever virus (ASFV) contamination in the environment. This research reveals the complexity of ASFV transmission routes, once interactions between wildlife —such as hooded crows (*Corvus cornix*) and red foxes (*Vulpes vulpes*)—and infected carcasses could facilitate the virus' spread. Additionally, the study underscores the need for proper carcass management to mitigate disease propagation among wildlife and in swine farming. Haman et al. investigated the significant mortality caused by the highly pathogenic avian influenza virus (HPAIV) H5N1 among seabirds (devastating bird colonies) and mammals along the Pacific coast of North America. Their findings highlight the necessity of coastal environment monitoring to better understand HPAIV epidemiology and mitigate its impact on vulnerable bird and mammal species.

The previous examples illustrate how human interventions can help wildlife conservation; however, human actions can also severely compromise the health and wellbeing of wild animals, particularly those kept in inadequate captive conditions. A pertinent example is the study by Stagni et al., which identified significant health problems in brown bears (*Ursus arctos*) rescued from suboptimal captivity. This retrospective research highlights common diseases and clinical abnormalities in these bears, including oral cavity and digestive system disorders, associated with the maintenance conditions before their rescue. Bears rescued from circuses and restaurants exhibited a higher prevalence of certain conditions, reinforcing the need for veterinary and captive management plans to improve their welfare. In another study conducted at a rescue

center in Vietnam, Ludi et al. analyzed foot-and-mouth disease outbreaks affecting bears, demonstrating how diseases can rapidly spread in confined spaces and emphasizing the need for surveillance and preventive management in these environments.

Another critical issue regarding captive wildlife is antimicrobial resistance. The study by Kim et al. explores the prevalence of bacterial resistance in animals housed in zoos. The detection of multidrug-resistant *E. coli* and *Enterococcus faecalis* suggests potential bacterial exchange between animals and humans, a significant concern for public health and captive wildlife management. Additionally, continuous animal welfare assessment in zoos is a fundamental concern, as explained by Liptovszky. Advanced data science techniques, such as syndromic surveillance (1) and comprehensive diagnostic examinations, as demonstrated by Vetere et al., can significantly enhance the quality of life of captive animals by ensuring efficient resource allocation and improvement of ongoing care and management.

Another study focusing on infectious agents in wildlife is the one by Carella et al., on the potential immunosuppressive effect of picornaviruses in the noble pen shell (*Pinna nobilis*)—a marine mollusk, illustrating the severe threat that viral pathogens pose to endangered species. This virus may cause mass mortality events in the Mediterranean Sea, highlighting the urgency of incorporating virological studies into marine conservation efforts to identify and mitigate similar risks.

Human activities also impact wildlife through climate change effects, as demonstrated in the study by Guan et al. on the gastrointestinal microbiome of three-toed box turtles (*Terrapene carolina triunguis*). This study suggests that the microbiome of this species may be resilient to rapid temperature changes, although the increased presence of pathogens such as *Erysipelothrix* sp. at higher temperatures could have adverse effects.

In summary, these studies demonstrate the value of a multidisciplinary approach to advancing zoological medicine and understanding the challenges faced by wildlife. Moreover, these investigations raise critical questions regarding the effects of human activities and environmental changes on wildlife health. The Research Topic and analysis of environmental data, alongside wildlife health monitoring, are essential to elaborate effective responses to these challenges. Such efforts also build a foundation for the development and implementation of more effective wildlife conservation and management policies. By addressing these Research Topic, we are better prepared to anticipate and mitigate risks posed by human activities and habitat alterations over wildlife health, ultimately ensuring long-term biodiversity preservation and ecosystem health.

Author contributions

II: Writing – original draft, Writing – review & editing. CS: Writing – original draft, Writing – review & editing.

Conflict of interest

The authors declare that the research was conducted in the absence of any commercial or financial relationships that could be construed as a potential conflict of interest.

The author(s) declared that they were an editorial board member of Frontiers, at the time of submission. This had no impact on the peer review process and the final decision.

Publisher's note

References

1. Ana A, Perez Andrés M, Julia P, Pedro P, Arno W, Kimberly VW, et al. Syndromic surveillance for West Nile virus using raptors in rehabilitation. *BMC Vet Res.* (2017) 13:1–10. doi: 10.1186/s12917-017-1292-0

frontiers | Frontiers in Veterinary Science

TYPE Original Research
PUBLISHED 13 December 2023
DOI 10.3389/fvets.2023.1299029

OPEN ACCESS

EDITED BY
Carlos Sacristán Yagüe,
Centro de Investigación en Sanidad Animal (CISA), Spain

REVIEWED BY
Azlan Che-Amat,
Putra Malaysia University, Malaysia
Michael James Murray,
Monterey Bay Aquarium, United States

*CORRESPONDENCE
Marta Brscic
✉ marta.brscic@unipd.it

RECEIVED 25 September 2023
ACCEPTED 20 November 2023
PUBLISHED 13 December 2023

CITATION
Stagni E, Sequeira S, Brscic M, Redtenba cher I and Hartmann S (2023) A retrospective study on the prevalence of main clinical findings in brown bears (*Ursus arctos*) rescued from substandard husbandry conditions. *Front. Vet. Sci.* 10:1299029. doi: 10.3389/fvets.2023.1299029

A retrospective study on the prevalence of main clinical findings in brown bears (*Ursus arctos*) rescued from substandard husbandry conditions

Elena Stagni[1], Sara Sequeira[1], Marta Brscic[2]*, Irene Redtenbacher[1] and Sabine Hartmann[1]

[1]VIER PFOTEN International, Linke Wienzeile, Vienna, Austria, [2]Department of Animal Medicine Production and Health (MAPS), University of Padova, Viale dell'Università, Legnaro PD, Italy

Brown bears (*Ursus arctos*) are kept under varied captive conditions, some of which may greatly compromise their welfare. FOUR PAWS is an NGO that rescues some of these bears kept in substandard conditions and houses them in species-appropriate sanctuaries, where preventive and reactive veterinary care is provided. This retrospective study aims to provide an overview of pathologies and clinical abnormalities reported in veterinary records and their prevalence according to body system affected and pre-rescue bear origin. Origin was categorised as subzoo (bears coming from substandard zoos), dancing (used to "dance" upon a music cue), restaurant (used to attract clients), private keeping (used for various purposes, such as photo props), circus (used for shows), and bear-baiting (exploited for hunting dog training in baiting stations). Clinical findings were extracted from reports of veterinary examinations done from 2006 to 2021, during rescue, routinely, in response to clinical signs, and/or *post-mortem*. Their prevalence was calculated according to the body system affected and neoplasia (specific group independent from the organ) over the findings' total number. Prevalence was also calculated according to pre-rescue origin (general and relative values in proportion to the number of reports per origin). Results refer to 302 veterinary reports of 114 bears examined, rescued from 1998 to 2021, with the age at rescue varying from a few months to 30 years (median 13 years). The total number of clinical findings was 1,003, and the systems with more findings were oral cavity (56.0%), abdominal cavity and digestive system (7.9%), integumentary (7.9%), ocular systems (7.7%), and musculoskeletal (7.6%). Findings involving other body systems and neoplasia were less prevalent (≤2.8%). Results showed a higher prevalence of some clinical findings for bears rescued from certain origins compared to others. Straightforward associations between pre-rescue origin and clinical findings were not feasible due to unknown anamnesis and details on pre-rescue conditions, and because some housing and management characteristics might be transversal to origins. Results suggest that bears rescued from certain origins were prone to specific clinical findings, supporting the need for the creation of *ad hoc* preventive veterinary and husbandry management plans after rescue, thus contributing to the improvement of captive bear welfare.

KEYWORDS

brown bear, health, keeping condition, animal welfare, pre-rescue bear origin, clinical finding

1 Introduction

Welfare is a multidisciplinary concept that includes, but is not limited to, physical health and emotional state, as described by Mellor et al. (1) in the Five Domains Model. In order to systematically and thoroughly assess animal welfare, this model identifies "health" as a domain that, together with "nutrition," "physical environment," and "behavioural interactions," form the foundations for inferences regarding the fifth domain, the mental state (1). Preserving the health of animals should therefore contribute to a good welfare state by enabling the performance of natural and positive behaviours, and minimising negative experiences such as pain and discomfort.

Welfare is a subjective state and similar experiences, rearing and housing conditions may lead to different perceptions by individual animals (2, 3). Not all animals, indeed, display the same response or clinical signs when exposed to pathogens, stressors, painful conditions, and other suboptimal conditions, with some being more resilient than others. It has been suggested that bears are extremely resilient, being able to physically resist severe environmental conditions, and this may potentially lead to their neglect in captivity (4). Moreover, bears can reach a considerable advanced age in captivity (5), and like most captive animals, they live longer than their conspecifics in the wild (6–8). This advancing age is connected to the development of age-related health issues, some of which may be very painful (9). The onset and progression of some of these health issues can be influenced by an appropriate environment and management. The environment bears are kept in should be carefully designed and managed to meet their physical, emotional, social, and behavioural needs and should vary according to the season and specific physiological states of the animals (10). For example, bear nutrition should not only meet the nutritional requirements targeted for the specific physiologic state but should also fulfil the feeding ecology, nutritional strategies, and nutritional wisdom of the animal (11, 12). Thus, feed type, quality, and way of provision in captivity play an important role in bear health and welfare status (10, 13).

Unfortunately, captive bears may be kept in conditions that do not meet their requirements (14), such as brown bears (*Ursus arctos*) in substandard zoos, circuses, private keeping, baiting stations, or even used as dancing bears. These keeping conditions share the low to very low welfare standards in which animals are kept, from inappropriate physical environments to inadequate nutrition to even forcing postures and movements that are unnatural to bears. Specifically, dancing bears were forced to perform dancing-like movements upon the cue of a violin, whilst being chained by a metal ring on their nose and upper lip. These animals were trained from a very young age, being placed on a hot metal plate whilst a violin was being played, and the pain caused by the heat of the plate triggered a stomping motion reaction, perceived as "dancing." The animal was thus conditioned, and the sound of the violin worked as the cue to "dance" (15). Bears in restaurants were used as props to attract clients and were usually kept in small, barren cages in front of the property. Both dancing and restaurant bears were often given alcohol (16, 17) in addition to an inadequate diet. Bears from private keeping were used for different purposes and kept in a variety of ways, from selfie bears that were chained by their nose ring and dragged around tourist locations so that people could take pictures with them (18) to bears kept as pets or in small enclosures as attractions in private properties or amusement parks. Bears kept in baiting stations were chained by their necks to a tree and used to train hunting dogs, whilst they spent the rest of their time in small and barren cages.

A gradual improvement of these bears' welfare is achieved after their rescue and housing in species-appropriate sanctuaries, where specialised veterinary care is provided, and husbandry and the natural environment aim at stimulating species-specific behaviours (19, 20). Since 1998, the animal welfare organisation FOUR PAWS International (FP) has rescued many bears and housed them in species-appropriate sanctuaries. The health status of these animals is assessed through veterinary examinations performed both on a regular basis and when provision of specific medical care is needed.

This retrospective study aims to provide an overview of pathologies and clinical abnormalities reported in veterinary records and the prevalence of these clinical findings clustered according to body system affected and pre-rescue bear origin.

2 Materials and methods

2.1 Animals and veterinary reports

The data for the study were extracted from veterinary reports of medical examinations performed between 2006 and 2021 on brown bears housed in FP Sanctuaries in Europe. The reports have been compiled during pre-rescue and rescue veterinary examinations, routine health check-ups, examinations conducted in response to specific clinical signs reported by caretakers, specialist visits, and *post-mortem* examinations. The diagnostic tools used in each examination varied and included blood and urine analysis, radiology, ultrasonography, computed tomography, endoscopy, histopathology, cytology, and bacterial and fungal culture. Consultations with veterinary specialists, such as dentists, ophthalmologists, and cardiologists, were carried out on a necessity basis.

All information written in the veterinary reports were exported onto Microsoft Excel (version 2201), and they were related to: identity of the bear examined; year of rescue; bear age at rescue; pre-rescue origin categorised as subzoo (bears coming from substandard zoos), dancing (used to perform dancing-like movements upon a music cue), restaurant (used to attract clients), private keeping (used for different purposes, such as photo props), circus (used for shows), and bear-baiting (exploited for hunting dog training in baiting stations); date of examination; name of the veterinarian performing the examination; type of visit/diagnostic performed; and clinical findings. The experimental unit for the extracted data was the veterinary report. The frequency distribution of reports of veterinary examinations performed *in vivo* and *post-mortem* and their distribution through the years were calculated. The reports *in vivo* were further grouped into pre-rescue, rescue, and post-rescue. The frequency distribution of reports for each bear was calculated as such and according to pre-rescue origin. Finally, the frequency of the different types of visits/diagnostics was calculated based on the total number of reports.

2.2 Clinical findings

Each finding reported during the veterinary examination was considered an independent occurrence, even if the pathogenesis was correlated (e.g., *periapical abscess and open root*; *mucopurulent ocular*

discharge and conjunctivitis). When the same finding on a bear was reported in more than one veterinary report over time, it was considered only once, unless the severity of the pathology changed (e.g., from *mild coxofemoral arthrosis* to *moderate coxofemoral arthrosis*) or the finding describing the pathology was at a different stage of progression (e.g., cavities and tooth destroyed). In case where a pathology concerned more than one anatomical part (e.g., two teeth), the finding (e.g., fracture) was considered once with the cumulative number of elements involved (e.g., fractures in two teeth).

In the second step, the prevalence of these clinical findings was calculated according to body system affected and neoplasia (allocated to a specific group, independently from the organs involved and counted only in the neoplasia group) as a percentage over the total number of findings. Laboratory results, such as bacteriological culture and histopathology, were included in the categories of body system affected and neoplasia. Parasitological examinations on faecal samples were not included in the dataset as feacal screenings are performed on a regular basis, independently from the veterinary examinations, and their results are managed in another data recording system. Each body system was subcategorised in order to group findings of a similar nature (e.g., *one or more missing teeth*; *lens luxation, uni- or bilateral cataract*). A further subgrouping was created within the subcategories for the oral and ophthalmic findings to reflect the variance found in the number of anatomical parts involved (e.g., *2 to 10 teeth missing*; *Bilateral cataract*). The groups of clinical findings and their descriptions are reported in Supplementary Table 1.

The prevalence of findings was also calculated according to pre-rescue origin (general and relative values in proportion to the number of reports for each origin).

3 Results

3.1 Animals and veterinary reports

The results of this study refer to 302 veterinary reports of 114 brown bears inspected. The bears were housed in six FP brown bear sanctuaries: Bear Sanctuary Müritz in Germany ($n = 24$) (18) ear Sanctuary Arbesbach in Austria ($n = 8$) (18) ear Sanctuary Belitsa in Bulgaria ($n = 33$) (18) ear Sanctuary Domazhyr in Ukraine ($n = 25$) (18) ear Sanctuary Prishtina in Kosovo ($n = 20$), and Arosa Bear Sanctuary in Switzerland ($n = 4$). They were rescued from 1998 to 2021 (Figure 1), and the highest number of bear rescues per year was 16 in 2013, followed by 10 rescues in 2019 and nine rescues in 2017 and 2020. Bear age at rescue varied from a few months to 30 years old, with a median value of 13 years. They were rescued from the following origins: 32 were from subzoos, 27 were dancing bears, 23 were kept next to restaurants, 16 were in private custody, 10 were used in circuses, and 6 were used for bear-baiting. The average age of the bears and length of stay in the FP sanctuaries until the end of 2021 or bear death according to pre-rescue origin are shown in Figure 2.

The number of reports of veterinary examinations performed *in vivo* and *post-mortem* was 278 and 24, respectively. Within the *in vivo* reports, 14 (5.0%) were compiled during pre-rescue, 23 (8.3%) during rescue, and 241 (86.7%) during post-rescue veterinary examinations. The distribution of the number of reports through the years is also shown in Figure 1. The number of reports of *in vivo* examinations increased progressively from 2015 to 2019, with a peak of 44 during 2019. The highest number of *post-mortem* reports was registered in 2020 ($n = 8$). The number of reports per bear varied: 30 bears had one report, 26 had two reports, 26 had three reports, 23 had four reports, 4 had five reports, and 5 had six reports. Of the 30 bears with only one report, six of them had only a *post-mortem* report.

The frequency distribution of the reports according to pre-rescue origin showed that the majority of reports were from dancing ($n = 90$), followed by subzoos ($n = 78$), restaurants ($n = 58$), private keeping ($n = 37$), circuses ($n = 25$), and bear-baiting bears ($n = 14$). The 37 reports of pre-rescue and rescue examinations were performed on 30 bears, divided according to their origin as follows: nine restaurants, six bear-baiting, five circuses, five private keepings, four subzoos, and one dancing.

Within the medical examinations of these reports, the most frequent type of visit or diagnostics applied was the general clinical examination (G, $n = 162$), followed by blood analysis (18), dentist examination (D, $n = 147$), ultrasound (U, $n = 109$) and radiology (X, $n = 84$), in 45 different combinations, as shown in Supplementary Table 2.

3.2 Clinical findings

The total number of clinical findings extracted was 1,003, and the systems with more findings recorded in the reports were: oral cavity (56.0%), abdominal cavity and digestive system (7.9%), integumentary (7.9%), ocular (7.7%), and musculoskeletal (7.6%) systems. The other body systems and neoplasia showed an overall prevalence of findings ≤2.8%: neoplasia (2.8%), urinary system (2.6%), cardiovascular system (2.5%), respiratory system (1.4%), reproductive system (1.1%), haematopoietic and lymphatic system (0.9%), poor nutritional status (0.8%), neurological system (0.5%), and endocrine system (0.4%).

The raw number of findings related to the most represented body systems and neoplasia and the respective percentages, calculated on the total number of findings relative to the same system/neoplasia, are reported in Table 1. The prevalence of clinical findings according to the pre-rescue origin of the bears is also reported in Table 1, which showed that some findings tend to be reported more often in bears rescued from certain origins compared to others. For example, within the ocular system, findings related to the lens, such as luxation or uni−/bilateral cataracts, seemed more present in dancing bears compared to bears from other origins. Within the oral cavity system, the findings of teeth fractured, destroyed, worn, or with attrition seemed more represented in bears used for bear-baiting, dancing, and restaurant bears. These findings were the most numerous group in the oral cavity, and the percentage of the different subcategories for each origin is represented in Figure 3. Regarding neoplasia, the majority were malignant, and circus, subzoo, and dancing bears showed the apparently highest prevalence.

4 Discussion

In this study, the prevalence of clinical findings reported in 302 veterinary records of examinations carried out on 114 brown bears was investigated across body systems. Results suggest that the most frequent findings in bears housed in FP sanctuaries rescued from

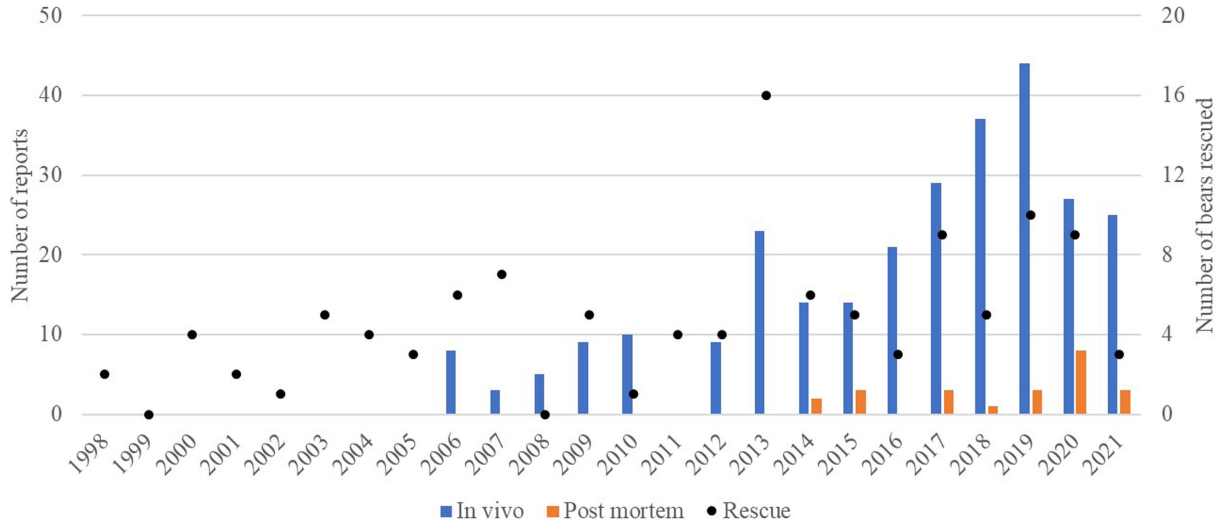

FIGURE 1
Distribution over years of the numbers of veterinary examination reports of brown bears (*Ursus arctos*) (no reports were collected before 2006): *in vivo* (blue) and *post-mortem* (orange) on the left axis scale. The points represent the number of bears rescued each year within the group of bears involved in this study (right axis scale).

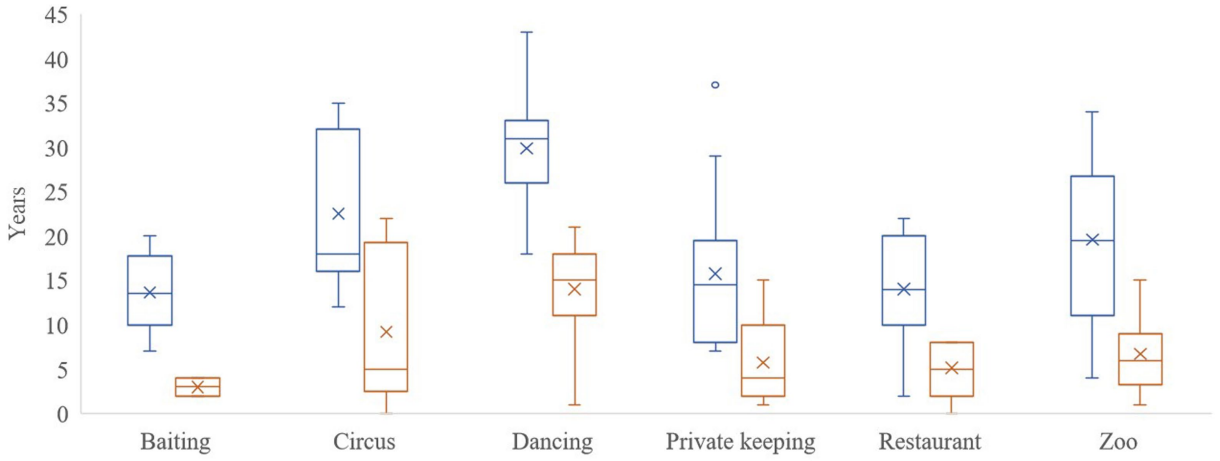

FIGURE 2
Box and whisker plot of the average age of the brown bears (*Ursus arctos*) (blue) and length of stay (orange) in FOUR PAWS sanctuaries until the end of 2021 or bear death, according to pre-rescue origin.

substandard conditions concern the oral cavity, abdominal cavity and digestive system, integumentary system, ocular system, and musculoskeletal apparatus, in decreasing order. According to the results of a survey conducted by Blake and Collins (21) in 50 North American zoos and aquaria, integumentary (54 cases), gastrointestinal (45 cases), and ocular diseases (17 cases) represented the majority of the clinical findings of 512 bears. The direct comparison of the distributions of findings across body systems between the current study and that by Blake and Collins (21) should be done with caution considering their different natures (direct data vs. survey data), study population, and statistical unit. In fact, the survey carried out by Blake and Collins (21) includes responses regarding bears in different rearing conditions and belonging to seven *Ursidae* species. The same direct comparison limitation applies to the results of most relevant diseases described in other retrospective studies, differing from the current one in that they were applied to subpopulations of captive bears of different species and ages, with a focus on specific anatomical systems, and/or assessed only *post-mortem* (22–25). For example, Clark et al. (26) focused on dental and temporomandibular joint pathologies, and Kitchener and MacDonald (27) focused on skeletal and dental pathologies. A few studies described the most common diseases developed in geriatric animals (4, 5, 27). Several others were based on data collected from autopsy results or skeleton examinations (23, 25, 26, 28, 29). To the best of the authors' knowledge, the current study represents the retrospective assessment of the largest collection of veterinary reports of captive brown bears across ages, including juvenile, adult, and geriatric animals that were examined *in vivo* and/or *post-mortem*.

TABLE 1 Raw number of clinical findings related to the most represented body systems and neoplasia in the veterinary examination reports ($n = 302$), their respective percentages (calculated on the total number of findings relative to the same body system/neoplasia, sum up to 100%), and percentages of clinical findings according to the pre-rescue origin [calculated on the total number of reports per origin (n of reports)] of the brown bears (*Ursus arctos*) rescued and housed in FOUR PAWS Sanctuaries ($n = 114$).

Clinical finding	Number of findings ($n = 1,003$)	% on total findings per system	Origin					
			Bear-baiting ($n = 14$)	Circus ($n = 25$)	Dancing ($n = 90$)	Private keeping ($n = 37$)	Restaurant ($n = 58$)	Subzoo ($n = 78$)
Oral cavity								
One or more teeth affected by cavities	30	5.3	14.3	8.0	18.9	8.1	3.4	5.1
One or more teeth fractured, destroyed, worn or with attrition	179	31.9	78.6	52.0	72.2	37.8	70.7	44.9
One or more missing teeth	65	11.6	21.4	12.0	44.4	21.6	15.5	2.6
One or more teeth discoloured, demineralised and/or with an enamel defect	32	5.7	7.1	4.0	1.1	29.7	20.7	7.7
One or more open root	138	24.6	35.7	28.0	58.9	37.8	51.7	37.2
Gum, buccal mucosa, tongue lesions, perio, and/or endodontitis	55	9.8	14.3	16.0	16.7	27.0	19.0	16.7
Apical/periapical lesions, osteomyelitis, osteolysis, purulent infection, abscess and/or fistula	60	10.7	14.3	20.0	27.8	16.2	12.1	19.2
Malocclusion	1	0.2	7.1	0.0	0.0	0.0	0.0	0.0
Persistent milk tooth	2	0.4	0.0	0.0	0.0	2.7	0.0	1.3
Abdominal cavity and digestive system								
Rectal prolapse and paralysis	2	2.5	14.3	0.0	0.0	0.0	0.0	0.0
Peritonitis	3	3.8	0.0	0.0	2.2	0.0	0.0	1.3
Abdominal fluid, ascites, and hemoabdomen	7	8.9	0.0	8.0	3.3	0.0	0.0	2.6
Alteration of the gallbladder and biliary duct	36	45.6	7.1	32.0	0.0	0.0	17.2	21.8
Hepatic modifications and degeneration	12	15.2	0.0	16.0	3.3	2.7	1.7	3.8
Liver perivasculitis and secondary hepatitis	2	2.5	0.0	0.0	0.0	0.0	0.0	2.6
Esophagitis, gastritis and gastroduodenitis, gastrointestinal gas accumulation, stomach rupture	10	12.7	0.0	0.0	5.6	2.7	0.0	5.1
Pathologies of the small intestine	7	8.9	0.0	4.0	0.0	0.0	0.0	7.7
Integumentary system								
Alopecia, adnexal atrophy, and fur quality	12	15.2	0.0	4.0	7.8	5.4	3.4	0.0
Alteration of one or more pads/soles and of one or more claws	28	35.4	7.1	16.0	4.4	13.5	13.8	7.7
Hyperkeratosis, acanthosis, and hyperpigmentation	3	3.8	0.0	0.0	3.3	0.0	0.0	0.0
Dermatitis, pyodermatitis, and erythema	6	7.6	0.0	0.0	2.2	0.0	5.2	1.3
Cutaneous or subcutaneous nodules or masses, suspect of papilloma.	5	6.3	0.0	0.0	1.1	2.7	1.7	2.6

(Continued)

10.3389/fvets.2023.1299029

TABLE 1 (Continued)

Clinical finding	Number of findings (*n* = 1,003)	% on total findings per system	Origin					
			Bear-baiting (*n* = 14)	Circus (*n* = 25)	Dancing (*n* = 90)	Private keeping (*n* = 37)	Restaurant (*n* = 58)	Subzoo (*n* = 78)
Abrasions and superficial ulcerations	2	2.5	0.0	0.0	1.1	0.0	0.0	1.3
Chronic or purulent abrasions, wounds, decubital lesions, and scars	23	29.1	7.1	4.0	3.3	21.6	5.2	9.0
Ocular system								
Signs of conjunctivitis and/or ocular discharge	8	10.4	0.0	0.0	1.1	5.4	8.6	0.0
Presence of *Thelazia* spp.	2	2.6	0.0	0.0	0.0	0.0	3.4	0.0
Foreign body in eye	1	1.3	0.0	0.0	0.0	0.0	1.7	0.0
Uni- or bilateral corneal hyperpigmentation, melanosis, and/or opacity	12	15.6	0.0	8.0	7.8	2.7	3.4	0.0
Uni- or bilateral corneal vascularization, edema, ulcer, and/or scar	4	5.2	0.0	0.0	1.1	8.1	0.0	0.0
Lens luxation, uni-, or bilateral cataract	25	32.5	0.0	4.0	21.1	5.4	1.7	2.6
Pathologies of uvea, sclera, and anterior chamber	8	10.4	0.0	0.0	6.7	2.7	0.0	1.3
Glaucoma	4	5.2	0.0	4.0	2.2	0.0	1.7	0.0
Unilateral retinal detachment or degeneration	7	9.1	0.0	4.0	6.7	0.0	0.0	0.0
Unilateral vitreous degeneration	1	1.3	0.0	0.0	1.1	0.0	0.0	0.0
Bilateral optical nerve degeneration	1	1.3	0.0	0.0	1.1	0.0	0.0	0.0
Unilateral phthisis bulbi	2	2.6	0.0	0.0	1.1	0.0	1.7	0.0
Unilateral microphakia	1	1.3	0.0	0.0	1.1	0.0	0.0	0.0
Unilateral microphthalmos	1	1.3	0.0	0.0	1.1	0.0	0.0	0.0
Musculoskeletal apparatus								
Alteration of the muscular tissue, muscle calcification, presence of radiodense material, and necrotic inflammation	6	7.9	7.1	4.0	1.1	2.7	0.0	2.6
Left or bilater femoropatellar/femorotibial arthrosis or tarsal arthrosis	11	14.5	0.0	4.0	5.6	0.0	1.7	5.1
Spine arthrosis and/or spondylosis, degenerative spine changes, vertebral dislocation, tissue formation on the side of the vertebral body, dens axis chip	16	21.1	0.0	0.0	4.4	0.0	1.7	14.1
One or more discs herniated or protruded, degenerative discopathies	4	5.3	0.0	0.0	0.0	0.0	0.0	5.1
Uni- or bilateral coxofemoral osteoarthritis	17	22.4	0.0	0.0	6.7	8.1	1.7	9.0

(Continued)

TABLE 1 (Continued)

Clinical finding	Number of findings (*n* = 1,003)	% on total findings per system	Origin					
			Bear-baiting (*n* = 14)	Circus (*n* = 25)	Dancing (*n* = 90)	Private keeping (*n* = 37)	Restaurant (*n* = 58)	Subzoo (*n* = 78)
Anatomical changes that caused modification of body structure and happened before the rescue	10	13.2	7.1	16.0	2.2	0.0	0.0	3.8
Uni- or bilateral elbow, carpal and metacarpal arthrosis, carpal sclerosis	9	11.8	0.0	4.0	1.1	0.0	1.7	7.7
Fracture, luxation or bone sclerotic changes	3	3.9	0.0	4.0	0.0	0.0	0.0	2.6
Neoplasia								
Benign neoplasia	7	25	7.1	0.0	1.1	2.7	0.0	5.1
Malignant neoplasia	21	75	0.0	12.0	10.0	2.7	0.0	10.3

The number of reports increased gradually throughout the years, with the exception of a spike of 23 reports in 2013, concomitant with a high number of rescues. This gradual increment of reports reflects the improvement of the record-keeping system in the organisation, the higher number of bears housed in the sanctuaries, and their ageing, which predisposes them to more frequent medical attention. The highest number of reports was recorded in 2019, when FP adopted the managerial choice of conducting as many routine veterinary examinations as possible, thus striving to preventively reduce the need for curative interventions.

As expected, bears were mainly examined post-rescue, and the limited number of pre- and during-rescue reports was due to restricted access to the bears during previous management. Moreover, poor examination conditions (e.g., no lighting) and limited time and resources (e.g., diagnostic tools) might have underestimated clinical findings, leading the authors to hypothesise that post-rescue findings reported by the veterinarians might have included health issues that were already present upon rescue. Other health issues might have developed after rescue and over time because of natural ageing processes or isolated events, such as accidents. The distinction between the period (pre- or post-rescue) of the onset of the health issue was, indeed, not the aim of the current study.

The system with the highest number of findings was the oral cavity, which is commonly affected in bears in captivity, as reported by Bourne et al. (9). Most of these findings were part of the category of teeth fractured, destroyed, worn, or with attrition, followed by open roots. Accordingly, Kitchener (4) described that the most common problem diagnosed on the skulls of captive bears was broken or open-tipped canines (>70%). This type of problem, together with wear and enamel erosion, can be attributed to compulsive chewing of the cage bars, a stereotypical behaviour developed in an inadequate environment (4, 9, 10). This bar-biting behaviour might also explain the high prevalence of teeth fractured, destroyed, worn, or with attrition reported for bears rescued from baiting stations, where they are usually kept in small barren cages when not used to train hunting dogs.

Dancing bears seem to be generally more at risk of developing health issues in the oral cavity than bears of other origins. The highest percentage of reported missing teeth might be associated with dietary and feeding aspects since an inappropriate diet has a role in developing medical issues of the oral cavity, although this managerial condition is reportedly common across origins. Moreover, missing teeth might be explained, on the one hand, by anecdotes reporting that previous owners of dancing bears extracted bears' teeth for their own personal safety, but no scientific evidence has been gathered of such a practice, making it a rather speculative statement. On the other hand, dancing bears have been under FP care for longer than other origins, and teeth might have been extracted due to their bad state during repeated veterinary interventions. In fact, dancing bears showed the highest percentage of cavities, open roots, and apical/periapical lesions, osteomyelitis, osteolysis, purulent infection, abscess, and/or fistula.

Regarding the abdominal cavity and digestive system, the highest prevalence of alterations of the gallbladder and biliary duct, hepatic modifications, and degeneration was reported for circus bears. According to Blake and Collins (21), hepatobiliary issues are not uncommon in bears in captivity. However, it is difficult to relate this finding to the circus origin, considering that alcohol and/or an inappropriate and unbalanced diet, which act as possible predisposing factors for liver degeneration (13), are traits that could be found across different pre-rescue origins. Gastroenteric and hepatobiliary systems are also commonly affected by neoplasia (10, 21), and in the current study, they represent the majority of malignant neoplasia found in bears housed by FP (11/21), although they have been considered altogether with neoplasia of other body systems following the example of Föllmi et al. (5).

Bears in captivity also frequently suffer from skin conditions, especially hair loss and rough hair coats, typically diagnosed in polar (*Ursus maritimus*) (30, 31) and Andean (*Tremarctos ornatus*) bears (32, 33). In fact, the brown bears included in this study were more frequently affected by alterations of pads/soles and claws, and chronic and purulent abrasions, wounds, decubital lesions, and scars than by alopecia and decreased fur quality. According to Collins (10), warm temperatures, a constantly moist environment, abrasive and hard substrates, and inappropriate surface cleanliness are to predispose factors for such findings. Moreover, the majority of the bears performed some type of stereotypical behaviour, typically pacing and circling or figure eight walking (34), which predisposes animals to sole issues when performed on abrasive substrates. Circus bears, along

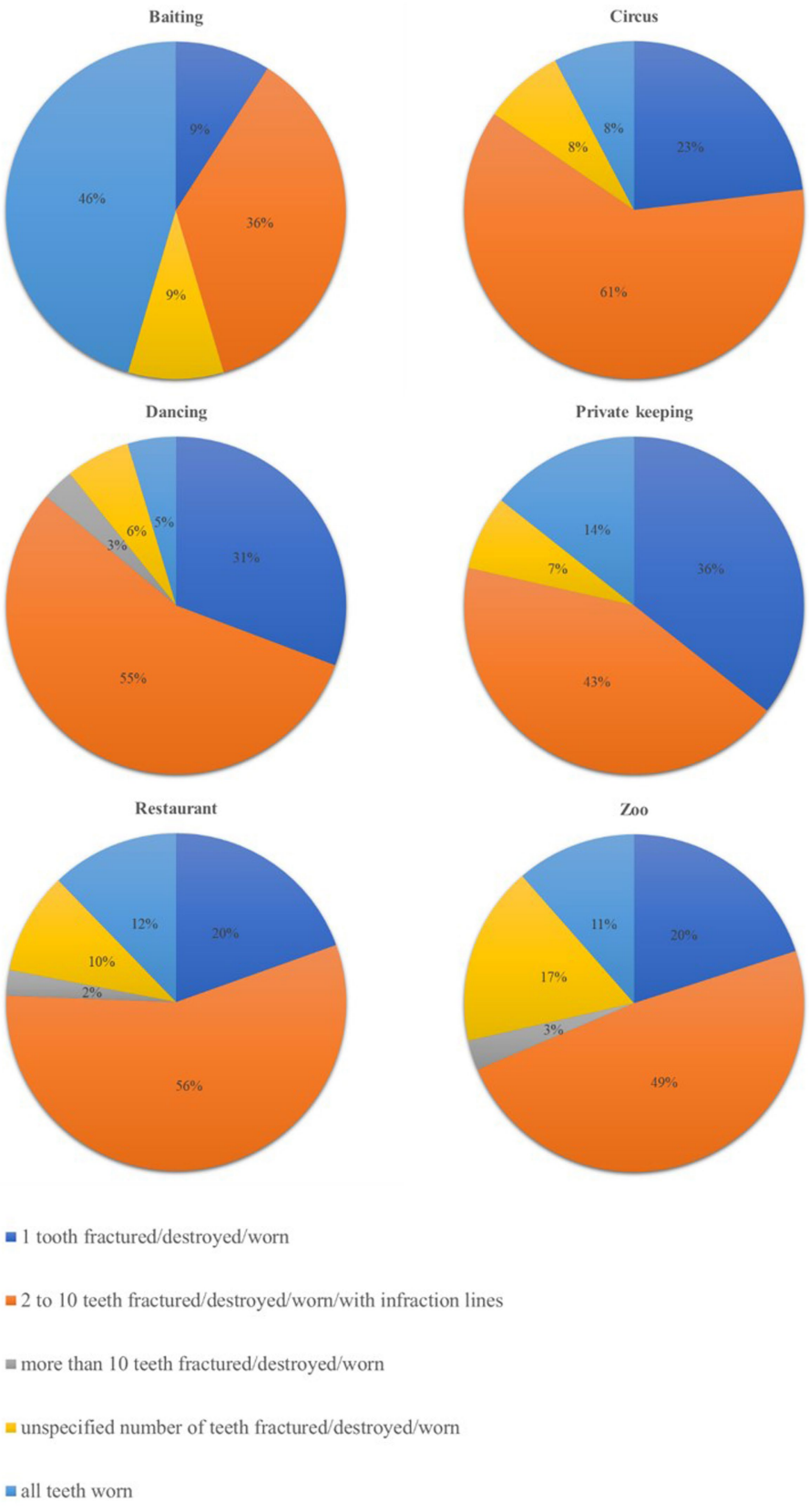

FIGURE 3
Distribution of the percentages of each subgroup of findings related to the subcategory of teeth fractured, destroyed, worn, or with attrition or infraction lines, according to the origin of the brown bears (*Ursus arctos*) in the dataset of the veterinary examination reports of the current study.

with those rescued from restaurants and private keeping, seem subject to the alteration of pads/soles and claws, likely sharing similar predisposing housing conditions. Private keeping, although varying in terms of housing and management, seems predisposing to a higher percentage of chronic and purulent abrasions, wounds, decubital lesions, and scars compared to other origins.

Ophthalmic pathologies are not commonly described in bears, except for some case studies (35–37), an epidemiological study on brown bears (38), and a survey on giant pandas (*Ailuropoda melanoleuca*) (39). In the current study, lens conditions, such as luxation and uni- or bilateral cataract, were the most commonly reported findings. The majority of ophthalmic alterations were found in reports of dancing bears, which could be expected to be the oldest group of bears in this study. It could also be related to the suggestion by Stades et al. (40) that the use of a stick on the face of dancing bears could be the cause of the lens luxation and retinal detachment.

Degenerative joint disease and consequent mobility problems represent a painful syndrome that develops over a number of years and might be caused by the ageing process, inflammation, or infection (9). Osteoarthritic changes have been found in all the bears radiographed by Föllmi (41); therefore, it is not surprising that the musculoskeletal system was one of the more represented systems in this study, with the greatest number of findings related to uni- or bilateral coxofemoral osteoarthritis. Kitchener (4) detected osteophytes in the sacral area and hip joint in more than 75% of the bear skeletons studied. In the current study, reports with findings related to this group were from bears rescued from subzoos, private keeping, and dancing, in decreasing order. Subzoo bears also showed the highest number of cases of spine arthrosis and/or spondylosis, degenerative spine changes, vertebral dislocation, tissue formation on the side of the vertebral body, and dens axis chip, which was the second most frequent group of findings. In fact, according to Nunn et al. (42), bears showed the highest prevalence of spondyloarthropathy among carnivores (27%), and it was detected in 96% of the skeletons examined by Kitchener (4). Obesity, a predisposing factor for osteoarthritis, has been described as a problem in several zoo animals, including bears (9). However, bears rescued from substandard zoos were rather underweight; therefore, obesity might not be the explanation for their observed higher prevalence in this study. In general, rescued bears were reported to show low body condition scores and signs of malnutrition, rather than being overweight. The importance of an adequate diet and physical exercise that guarantee a correct body mass according to the bear's physiological status has been reported to contribute to the prevention of joint problem development (9, 41). It is likely that these aspects were neglected in the previous keeping of these bears, regardless of their origin. Moreover, circus bears showed a higher prevalence of anatomical changes that caused body structure modifications, such as amputation or ankylosis, that were already present at rescue.

Inferential statistics from the results of this study on the brown bear population in captivity are limited due to the specificity of this study (convenience sample of bears rescued by FP and housed in FP sanctuaries). Moreover, the lack of precise information did not allow a straightforward association between pre-rescue bear origin and clinical findings. Particularly because of the unknown anamnesis and the difficulty to ascertain details on housing, environment, management, and handling of these bears prior to rescue. In addition, some characteristics, such as improper nutrition, a lack of enrichment, or species-appropriate stimuli, were likely transversal to all pre-rescue origins.

Data were presented as the prevalence of findings according to pre-rescue origin, although a limitation of this study is represented by the distribution of the number of veterinary reports among origins. Indeed, the majority of the reports belonged to dancing and subzoo bears, which could be explained by the fact that they were rescued in larger numbers and in earlier times. In the same way, it is not surprising that bears rescued from baiting stations were the least represented, as this practice became illegal only recently in Ukraine and is still practised in Russia. Thus, only a few of these bears have been somewhat recently rescued from illegal baiting or fighting stations in Ukraine. Furthermore, it could be argued that the number of veterinarians performing the examinations could cause a lack of standardisation, due to individual differences as well as different reporting methods (e.g., during dental examinations, different veterinarians may report cavity severity differently). In fact, human perception influences disease detection (43), and multiple people might assess the same conditions differently (44); therefore, the quality of the data should be considered before any quantitative analysis and interpretation (45). In favour of veterinarians performing examinations on bears housed by FP, it could be pointed out that they all had the same purpose of guaranteeing the maximum possible health and welfare state for each single animal, and this might have consequently reduced the possible bias due to individual perception. Moreover, the reports were collected by a centralised office, making sure the same kind of data was provided.

In conclusion, this retrospective study carried out on veterinary examination records provided an overview of the prevalence of disease and health issues in rescued brown bears in FP sanctuaries. The investigation of the conditions of captive wild animals, which are far less studied compared to those of farm and companion animals, is important to gather knowledge and provide evidence for decision-making at both practical and theoretical levels. The higher prevalence of some medical findings for bears rescued from certain pre-rescue origins may be used for the creation of *ad hoc* preventive veterinary and husbandry management plans, thus contributing to the improvement of captive brown bear welfare. Such plans should also consider the impact that each medical condition has on animal welfare, in terms of how pain, discomfort, or affected behaviours directly influence the mental state of the animal. The investigation of the role of specific husbandry and managerial aspects as possible preeminent predisposing factors, along with the strategies to overcome them, would be interesting topics for further studies.

Data availability statement

The datasets presented in this article are not readily available because the dataset can be requested to VIER PFOTEN International. Requests to access the datasets should be directed to Elena.Stagni@vier-pfoten.org.

Ethics statement

Ethical review and approval was not required for the study with animals in accordance with the local legislation and institutional requirements. Written informed consent from the owners of the

animals was not required to participate in this study in accordance with the national legislation and the institutional requirements.

Author contributions

ES: Conceptualization, Data curation, Investigation, Methodology, Project administration, Visualization, Writing – original draft, Writing – review & editing. SS: Data curation, Methodology, Writing – original draft, Writing – review & editing. MB: Conceptualization, Data curation, Methodology, Visualization, Writing – original draft, Writing – review & editing, Investigation. IR: Supervision, Writing – review & editing. SH: Funding acquisition, Supervision, Writing – review & editing.

Funding

The author(s) declare financial support was received for the research, authorship, and/or publication of this article. This study was supported by VIER PFOTEN International. The research has been planned and carried out by the authors independently of the organization, which did not participate in any aspect other than providing the funds and resources for the study. The publication fees were covered by the funds of the University of Padova.

Acknowledgments

The authors would like to thank Marlene Kirchner for her precious support at the beginning of this study, VIER PFOTEN International for the funding, and all the veterinarians who provided care to FOUR PAWS rescued animals, especially the Leibniz Institute for Zoo and Wildlife Research.

Conflict of interest

ES, SS, IR, and SH declare a conflict of interest being employed by the organisation that funded the research and that owns the sanctuaries were the bears examined are kept.

The remaining author declares that the research was conducted in the absence of any commercial or financial relationships that could be construed as a potential conflict of interest.

Publisher's note

Supplementary material

The Supplementary material for this article can be found online at: https://www.frontiersin.org/articles/10.3389/fvets.2023.1299029/full#supplementary-material

References

1. Mellor DJ, Beausoleil NJ, Littlewood KE, McLean AN, McGreevy PD, Jones B, et al. The 2020 five domains model: including human–animal interactions in assessments of animal welfare. *Animals*. (2020) 10:1870. doi: 10.3390/ani10101870

2. Hemsworth PH, Mellor DJ, Cronin GM, Tilbrook AJ. Scientific assessment of animal welfare. *N Z Vet J*. (2015) 63:24–30. doi: 10.1080/00480169.2014.966167

3. Mellor DJ. Animal emotions, behaviour and the promotion of positive welfare states. *N Z Vet J*. (2012) 60:1–8. doi: 10.1080/00480169.2011.619047

4. Kitchener AC. The problems of old bears in zoos. *Int Zoo News*. (2004) 51:282–93.

5. Föllmi J, Steiger A, Walzer C, Robert N, Geissbühler U, Doherr M, et al. A scoring system to evaluate physical condition and quality of life in geriatric zoo mammals. *Anim Welf*. (2007) 16:309–18. doi: 10.1017/S0962728600027123

6. Erwin J.M., Hof P.R., Ely J.J., Perl D.P. (2002). One gerontology: advancing understanding of aging through studies of great apes and other primates, In: Erwin JM, Hof PR, eds. *Aging in nonhuman primates*. Basel: Karger Publishers, pp. 1–21.

7. Longley L. A review of ageing studies in captive felids. *Int Zoo Yearbook*. (2011) 45:91–8. doi: 10.1111/j.1748-1090.2010.00125.x

8. Weigl R. *Longevity of mammals in captivity; from the living collections of the world*. Stuttgart, Germany: Schweizerbart Science Publishers (2005).

9. Bourne DC, Cracknell JM, Bacon HJ. Veterinary issues related to bears (*Ursidae*). *Int Zoo Yearbook*. (2010) 44:16–32. doi: 10.1111/j.1748-1090.2009.00097.x

10. Collins D. Ursidae In: E Miller and ME Fowler, editors. *Fowler's zoo and wild animal medicine*, vol. *8*. St. Louis, Missouri: Elsevier/Saunders (2015). 498–508.

11. LaDouceur EEB, Garner MM, Davis B, Tseng F. A retrospective study of end-stage renal disease in captive polar bears (*Ursus maritimus*). *J Zoo Wildl Med*. (2014) 45:69–77. doi: 10.1638/2013-0071R.1

12. Liu S, Lorenzen ED, Fumagalli M, Li B, Harris K, Xiong Z, et al. Population genomics reveal recent speciation and rapid evolutionary adaptation in polar bears. *Cells*. (2014) 157:785–94. doi: 10.1016/j.cell.2014.03.054

13. Robbins CT, Tollefson TN, Rode KD, Erlenbach JA, Ardente AJ. New insights into dietary management of polar bears (*Ursus maritimus*) and brown bears (*U. arctos*). *Zoo Biol*. (2021) 41:166–75. doi: 10.1002/zoo.21658

14. Maślak R, Sergiel A, Bowles D, Paśko Ł. The welfare of bears in zoos: a case study of Poland. *J Appl Anim Welf Sci*. (2016) 19:24–36. doi: 10.1080/10888705.2015.1071671

15. Tünaydin P. Pawing throught the history of bear dancing in Europa. *Freuzeit Info*. (2014) 24:51–60.

16. VIER PFOTEN International. Tomi, Gjina and Pashuk. SaddestBears – FOUR PAWS Campaign Help Bears. (2017). Available at:https://www.four-paws.org/our-stories/rescues-success-stories/rescue-bear-pashuk (accessed 22.9.23).

17. VIER PFOTEN International. The transformation of a rescued wild animal. FOUR PAWS Int. - Anim. Welf. Organ. (2022). Available at:https://www.four-paws.org/our-stories/publications-guides/the-transformation-of-a-rescued-wild-animal (accessed 22.9.23).

18. VIER PFOTEN International. FOUR PAWS brings Albanian bear Jeta to safety. FOUR PAWS Int. – Anim. Welf. Organ. (2017). Available at:https://www.four-paws.org/our-stories/rescues-success-stories/rescue-bear-riku (accessed 22.9.23).

19. Doyle C. Captive wildlife sanctuaries: definition, ethical considerations and public perception. *Anim. Stud. J.* (2017) 6:55–85.

20. Winders D. Captive wildlife at a crossroads–sanctuaries, accreditation, and humane-washing. *Anim Stud J*. (2017) 6:161–78.

21. Blake C., Collins D. (2002). Captive ursids: results and selected findings of a multi-institutional survey. In: Proceedings of the American Association of Zoo Veterinarians Annual Conference (C Baer. ed.), Milwaukee, Wisconsin.

22. Galateanu G., Göritz F., Saragusty J., Szentiks C.A., Wibbelt G., Hildebrandt T.B.. Bear watching for foot and spine osteopathology correlation in captive bears (*Ursidae*). Proceedings of the International Conference on Diseases of Zoo and Wild Animals, Warsaw. (2014). 122–125.

23. Kitchener AC, Asa CS. Editorial: bears and canids. *Int Zoo Yearbook*. (2010) 44:7–15. doi: 10.1111/j.1748-1090.2010.00112.x

24. Strömquist A, Fahlman Å, Arnemo JM, Pettersson A. Dental and periodontal health in free-ranging Swedish brown bears (*Ursus arctos*). *J Comp Pathol*. (2009) 141:170–6. doi: 10.1016/j.jcpa.2009.05.001

25. Wenker CJ, Stich H, Müller M, Lussi A. A retrospective study of dental conditions of captive brown bears (*Ursus arctos* spp.) compared with free-ranging Alaskan grizzlies (*Ursus arctos horribilis*). *J Zoo Wildl Med*. (1999) 30:208–21.

26. Clark EJ, Chesnutt SR, Winer JN, Kass PH, Verstraete FJM. Dental and temporomandibular joint pathology of the American black bear (*Ursus americanus*). *J Comp Pathol*. (2016) 156:240–50. doi: 10.1016/j.jcpa.2016.11.267

27. Kitchener A.C., Macdonald A.A.. The longevity legacy: the problem of old animals in zoos. Proceedings of the EAZA Conference, Kolmården. (2004). 132–137.

28. Balseiro A, Royo LJ, Gayo E, Balsera R, Alarcia O, García Marín JF. Mortality causes in free-ranging Eurasian brown bears (*Ursus arctos arctos*) in Spain 1998–2018. *Animals*. (2020) 10:1538. doi: 10.3390/ani10091538

29. Mörner T, Eriksson H, Bröjer C, Nilsson K, Uhlhorn H, Ågren E, et al. Diseases and mortality in free-range brown bears (*Ursus arctos*), gray wolf (*Canis lupus*), and wolverine (*Gulo gulo*) in Sweden. *J Wildl Dis*. (2005) 41:298–303. doi: 10.7589/0090-3558-41.2.298

30. AZA Bear TAG. *Polar bear (Ursus maritimus) care manual*. Silver Spring, MD: Association of Zoos and Aquariums (2009).

31. Bowen L, Keith Miles A, Stott J, Waters S, Atwood T. Enhanced biological processes associated with alopecia in polar bears (*Ursus maritimus*). *Sci Total Environ*. (2015) 529:114–20. doi: 10.1016/j.scitotenv.2015.05.039

32. Drake GJ, Nuttall T, López J, Magnone W, Leclerc A, Potier R, et al. Treatment success in three Andean bears (*Tremarctos ornatus*) with alopecia syndrome using oclacitinib maleate (Apoquel®). *J Zoo Wildl Med*. (2017) 48:818–28. doi: 10.1638/2016-0239.1

33. Nicolau A, Lemberger K, Mosca M, Leclerc A, Lécu A, Pin D. Clinical and histopathological aspects of an alopecia syndrome in captive Andean bears (*Tremarctos ornatus*). *Vet Dermatol*. (2018) 29:234–e85. doi: 10.1111/vde.12522

34. Montaudouin S, Le Pape G. Comparison between 28 zoological parks: stereotypic and social behaviours of captive brown bears (*Ursus arctos*). *Appl Anim Behav Sci*. (2005) 92:129–41. doi: 10.1016/j.applanim.2004.10.015

35. Boedeker NC, Walsh T, Murray S, Bromberg N. Case report: medical and surgical management of severe inflammation of the nictitating membrane in a Giant panda (*Ailuropoda melanoleuca*). *Vet Ophthalmol*. (2010) 13:109–15. doi: 10.1111/j.1463-5224.2010.00802.x

36. Dombrowski E, McGregor GF, Bauer BS, Parker D, Grahn BH. Blindness in a wild American black bear cub (*Ursus americanus*). *Vet Ophthalmol*. (2016) 19:340–6. doi: 10.1111/vop.12303

37. McLean IW, Bodman MG, Montali RJ. Retinal astrocytic hamartomas: unexpected findings in a giant panda. *Arch Ophthalmol*. (2003) 121:1786–90. doi: 10.1001/archopht.121.12.1786

38. Papadopoulos E, Komnenou A, Karamanlidis AA, Bezerra-Santos MA, Otranto D. Zoonotic *Thelazia callipaeda* eyeworm in brown bears (*Ursus arctos*): a new host record in Europe. *Transbound Emerg Dis*. (2021) 69:235–9. doi: 10.1111/tbed.14414

39. Miller S, Whelan N, Hope K, Marmolejo MGN, Knightly F, Sutherland-Smith M, et al. Survey of clinical ophtalmic disease in the giant panda (*Ailuropoda melanoleuca*) among North American zoological institutions. *J Zoo Wildl Med*. (2020) 50:837–44. doi: 10.1638/2018-0192

40. Stades FC, Dorrestein GM, Boeve MH, van de Sandt RRDM. Eye lesions in Turkish dancing bears. *Vet Q*. (1995) 17:45–6. doi: 10.1080/01652176.1995.9694591

41. Föllmi J.. Symptoms, radiographic examinations and pathologies: development of a scoring system to evaluate physical condition and quality of life in geriatric zoo mammals. (2005). Available at: https://www.tierschutz.vetsuisse.unibe.ch/research/publications/former_institute/index_eng.html (Accessed 6.11.23).

42. Nunn CL, Rothschild B, Gittleman JL. Why are some species more commonly afflicted by arthritis than others? A comparative study of spondyloarthropathy in primates and carnivores. *J Evol Biol*. (2007) 20:460–70. doi: 10.1111/j.1420-9101.2006.01276.x

43. Vaarst M, Paarup-Laursen B, Houe H, Fossing C, Andersen HJ. Farmers' choice of medical treatment of mastitis in Danish dairy herds based on qualitative research interviews. *J Dairy Sci*. (2002) 85:992–1001. doi: 10.3168/jds.S0022-0302(02)74159-3

44. Baadsgaard NP, Jørgensen E. A Bayesian approach to the accuracy of clinical observations. *Prev Vet Med*. (2003) 59:189–206. doi: 10.1016/S0167-5877(03)00100-4

45. Lastein DB, Vaarst M, Enevoldsen C. Veterinary decision making in relation to metritis - a qualitative approach to understand the background for variation and bias in veterinary medical records. *Acta Vet Scand*. (2009) 51:36. doi: 10.1186/1751-0147-51-36

frontiers | Frontiers in Veterinary Science

TYPE Original Research
PUBLISHED 13 December 2023
DOI 10.3389/fvets.2023.1273521

OPEN ACCESS

EDITED BY
Carlos Sacristán Yagüe,
Centro de Investigación en Sanidad Animal (CISA), Spain

REVIEWED BY
Ioannis A. Giantsis,
University of Western Macedonia, Greece
Carmelo Iaria,
University of Messina, Italy

*CORRESPONDENCE
Francesca Carella
✉ francesca.carella@unina.it

RECEIVED 06 August 2023
ACCEPTED 13 November 2023
PUBLISHED 13 December 2023

CITATION
Carella F, Prado P, De Vico G, Palić D, Villari G, García-March JR, Tena-Medialdea J, Cortés Melendreras E, Giménez-Casalduero F, Sigovini M and Aceto S (2023) A widespread picornavirus affects the hemocytes of the noble pen shell (*Pinna nobilis*), leading to its immunosuppression.
Front. Vet. Sci. 10:1273521.
doi: 10.3389/fvets.2023.1273521

A widespread picornavirus affects the hemocytes of the noble pen shell (*Pinna nobilis*), leading to its immunosuppression

Francesca Carella[1]*, Patricia Prado[2], Gionata De Vico[1], Dušan Palić[3], Grazia Villari[1], José Rafael García-March[4], José Tena-Medialdea[4], Emilio Cortés Melendreras[5], Francisca Giménez-Casalduero[6], Marco Sigovini[7] and Serena Aceto[1]

[1]Department of Biology, University of Naples Federico II, Naples, Italy, [2]Institute of Agrifood Research and Technology (IRTA)-Sant Carles de la Ràpita, Tarragona, Spain, [3]Chair for Fish Diseases and Fisheries Biology, Faculty of Veterinary Medicine, Ludwig-Maximilians-University Munich, Munich, Germany, [4]Instituto de Investigación en Medio Ambiente y Ciencia Marina, Universidad Católica de Valencia, Calpe, Spain, [5]Murcia University Aquarium, University of Murcia, Murcia, Spain, [6]Department of Marine Science and Applied Biology, Research Marine Centre in Santa Pola (CIMAR), University of Alicante, Alicante, Spain, [7]Consiglio Nazionale delle Ricerche, Istituto di Scienze Marine, Venice, Italy

Introduction: The widespread mass mortality of the noble pen shell (*Pinna nobilis*) has occurred in several Mediterranean countries in the past 7 years. Single-stranded RNA viruses affecting immune cells and leading to immune dysfunction have been widely reported in human and animal species. Here, we present data linking *P. nobilis* mass mortality events (MMEs) to hemocyte picornavirus (PV) infection. This study was performed on specimens from wild and captive populations.

Methods: We sampled *P. nobilis* from two regions of Spain [Catalonia (24 animals) and Murcia (four animals)] and one region in Italy [Venice (6 animals)]. Each of them were analyzed using transmission electron microscopy (TEM) to describe the morphology and self-assembly of virions. Illumina sequencing coupled to qPCR was performed to describe the identified virus and part of its genome.

Results and discussion: In 100% of our samples, ultrastructure revealed the presence of a virus (20 nm diameter) capable of replicating within granulocytes and hyalinocytes, leading to the accumulation of complex vesicles of different dimensions within the cytoplasm. As the PV infection progressed, dead hemocytes, infectious exosomes, and budding of extracellular vesicles were visible, along with endocytic vesicles entering other cells. The THC (total hemocyte count) values observed in both captive (eight animals) (3.5×10^4–1.60×10^5 ml^{-1} cells) and wild animals (14 samples) (1.90–2.42 × 105 ml^{-1} cells) were lower than those reported before MMEs. Sequencing of *P. nobilis* (six animals) hemocyte cDNA libraries revealed the presence of two main sequences of *Picornavirales*, family *Marnaviridae*. The highest number of reads belonged to animals that exhibited active replication phases and abundant viral particles from transmission electron microscopy (TEM) observations. These sequences correspond to the genus *Sogarnavirus*—a picornavirus identified in the marine diatom *Chaetoceros tenuissimus* (named *C. tenuissimus* RNA virus type II). Real-time PCR performed on the two most abundant RNA viruses previously identified by *in silico* analysis revealed positive results only for sequences similar to the *C. tenuissimus* RNA virus. These results may not conclusively identify picornavirus in noble pen shell hemocytes; therefore, further study is required. Our findings

suggest that picornavirus infection likely causes immunosuppression, making individuals prone to opportunistic infections, which is a potential cause for the MMEs observed in the Mediterranean.

KEYWORDS

immunosuppression, mass mortality, noble pen shell, RT-PCR, RNA virus

1 Introduction

Since June 2016, thousands of the noble pen shell *Pinna nobilis* individuals have died in the Mediterranean due to an extensive mass mortality event (MME) (1–7). The wide geographic range of the phenomenon makes the mass mortality of the species one of the largest known marine wildlife epizootic mortality events to date in the Mediterranean Sea (2, 8). The event was first observed along hundreds of kilometers of the southeastern coast of the Iberian Peninsula (9). Mass mortalities were subsequently observed in the northwestern Mediterranean (French and Italian coasts) and soon after in Greece, Cyprus, Turkey, Algeria, Tunisia, Morocco, Albania, and Croatia (1–5). The cause of this MME has been attributed to different pathogens, particularly *Haplosporidium pinnae* and *Mycobacterium* spp. (10–12). The presence of a great variety of pathogens associated with MMEs, including several potentially opportunistic pathogens, suggests that disease pathogenesis leading to animal mortality may have other unidentified causes (4, 13).

The order *Picornavirales* comprises positive-strand RNA viruses ranging between 7,000 and 12,500 nt in length (14). Within this order, the family *Picornaviridae* comprises 29 genera (https://ictv.global/report/chapter/picornaviridae/picornaviridae) of picornaviruses (PVs) (15). Picornaviruses are small, icosahedral viruses with single-stranded, highly diverse positive-sense RNA genomes associated with mild to severe diseases in vertebrates, invertebrates, and plants (16–18). The family *Picornaviridae* includes some of the most important groups in the development of virology, comprising poliovirus, rhinovirus, and hepatitis A virus (18, 19).

Virions consist of a capsid with no envelope surrounding a core of ssRNA measuring 22–33 nm in diameter (14, 20, 21). Next-generation sequencing (NGS) has significantly expanded the order *Picornavirales* in recent years through the identification of previously unknown viruses associated with various taxa, including aquatic vertebrates and invertebrates (22–27). The replication cycle takes place in the cytosol in close association with reorganized cytoplasmic membranous structures (28, 29). Infection with PV can induce numerous changes in infected cells, with the massive accumulation of cytosolic double-membraned vesicles (DMVs) and replication organelles possibly being the most important changes (30–32). Picornaviruses target intracellular membranes to generate complex membrane rearrangements of host organelles, such as the endoplasmic reticulum (ER), mitochondria, or endolysosomes (33, 34). Host intracellular membranes contain molecules, lipids, and proteins that serve as vehicles for intercellular communication in various (patho)physiological processes (35). The membrane may provide optimal platforms for viral RNA synthesis by concentrating viral replicative proteins and relevant host factors, as well as hiding replication intermediates, contributing to the evasion of host innate immune sensors (36).

Here, we report the discovery of a previously undescribed picornavirus infecting the immune cells of the noble pen shell *Pinna nobilis* sampled between 2021 and 2023 in different regions of Spain and Italy, where mortality events have been reported. Thirty specimens were analyzed using transmission electron microscopy (TEM) to describe the morphology and self-assembly of virions within the hemocyte cytoplasm and major structural transformations occurring in infected host cells. Illumina sequencing coupled to qPCR was performed to describe the identified virus and part of its genome.

2 Materials and methods

2.1 Hemolymph collection and investigation of viral agents in hemocytes

Due to its status as an endangered species, sampling of *P. nobilis* was carried out with the permission of regional and national authorities for animal welfare (for Spain, Generalitat de Catalunya—Identificació de l'expedient: SF/0003/23; Bank of species of the Mar Menor INF/2020/0017 promoted by the General Directorate of the Mar Menor and the University of Murcia; for Italy, Prot. MATTM 0016478 05/03/2020). A total of 30 animals were included in the study, collected from July 2021 to May 2023. Sampling was performed on natural populations along the Mediterranean coasts of Italy ($n = 4$) and Spain ($n = 18$) and on animals maintained in captivity in two facilities in Spain ($n = 8$). The natural sites in Spain and Italy were selected according to the presence of remaining populations of *P. nobilis*, despite the occurrence of mortality outbreaks (Figure 1).

In Catalonia (Spain), samples were collected from two estuarine populations in the Ebro Delta, where residual populations still exist: Fangar Bay (northern hemidelta) and Alfacs Bay (southern hemidelta), which are distributed in four different monitored areas (28). Mortality was first observed in 2018, leaving only a few individuals by 2021 (37). The mortality rate progressively increased from 33.5% in September 2021 to 75% in June 2023 (Prado pers. comm). Some of the remaining animals from this area are maintained in the aquarium facilities of the Instituto de Investigación en Medio Ambiente y Ciencia Marina (IMEDMAR) of the Universidad Católica de Valencia (UCV), in Valencia, Spain, and were included in the study. Another remaining population in

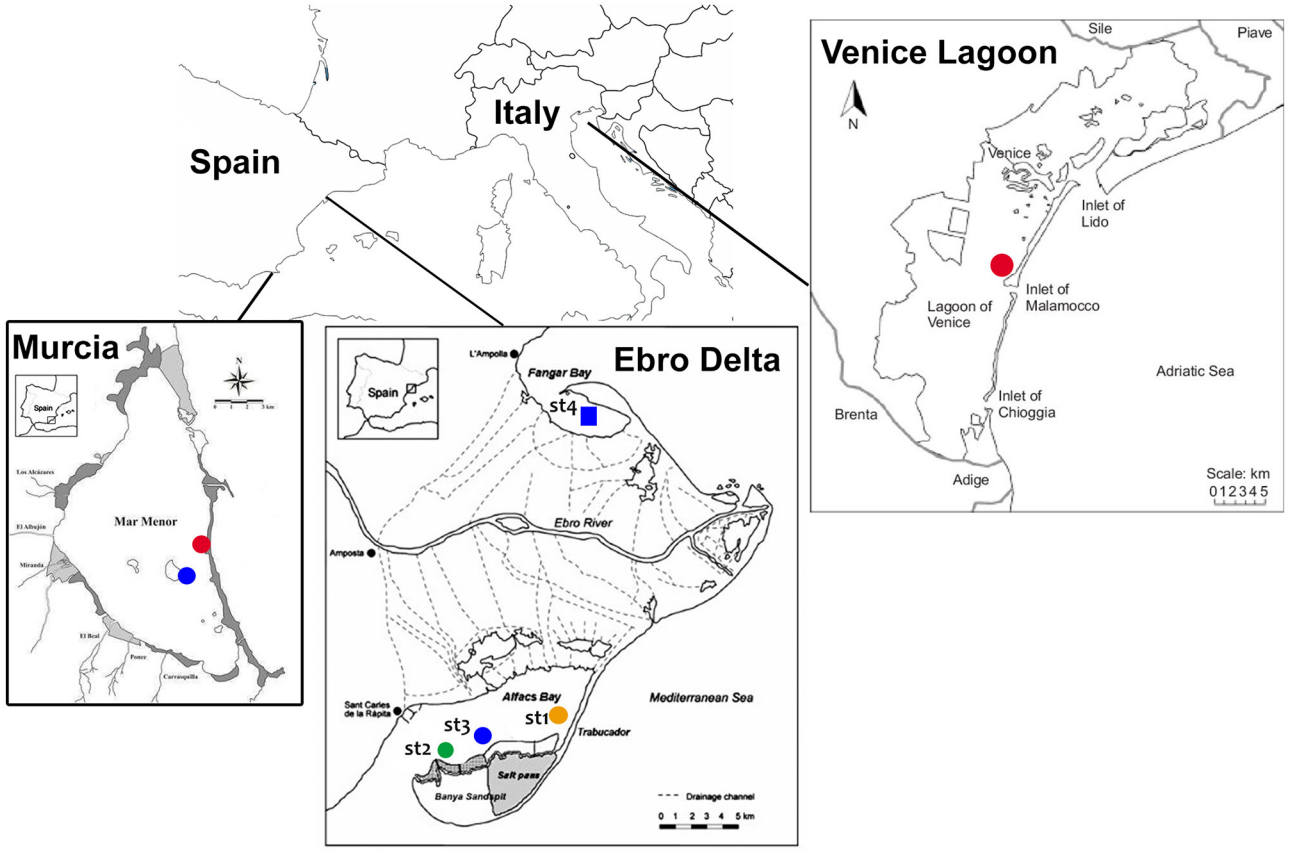

FIGURE 1
Map of the study areas where noble pen shell *Pinna nobilis* hemocytes were sampled in 2021–2023 in Murcia Baron (in blue), La Manga (in red), the Ebro Delta (sites 1–4), and the Venice Lagoon (Ottagono Alberoni).

Spain is the one located at the Mar Menor lagoon (Murcia), in the southwestern part of the Mediterranean. In this area, *P. nobilis* mortality was first observed in the summer of 2016. Initially, the *P. nobilis* mortality was correlated with an environmental collapse that became critical in 2016, 2019, and 2021 and reduced the population by >99% (38); for the present work, two surviving localities were sampled in the Baron and La Manga areas (39); some animals (n = 2) from this area were transferred to the seawater tanks of the University of Murcia Aquarium. Animals ($n = 6$) had been kept in captivity at IMEDMAR and Murcia Aquarium facilities for 6 months to 1 year. Until recently, *P. nobilis* was widely distributed in the Venice Lagoon (Italy), with the largest and densest colonies over marine tidal deltas and the outer part of central basins (40). Mortality onset was observed at the end of 2020, when the population decreased between 60 and 80% (unpublished data). The animals ($n = 4$) were sampled near Ottagono Aberoni Island, approximately 1 km away from the Malamocco inlet (Sigovini, personal communication).

For each animal included in the study (from the field and in captivity), 2 ml of hemolymph was collected via a 23-gauge needle from the posterior adductor muscle as a non-destructive sampling. The presence of clinical signs of disease was considered during sampling. Previous reports in the literature indicate that outward signs of disease start with behavioral changes, including shell gaping, slow valve closure speed when touched, and mantle retraction into the valves from the edge of the shell (11). These signs were difficult to recognize in animals in the field and those maintained in captivity since they mostly appear at very late stages of disease (11). In Catalonia, on July 21 and July/August 2022, most of the animals in the study (19) displayed apparent slow valve closure. In Venice Lagoon, in May 2023, animals displayed quick valve closure and visible mantle at the border of the valves instead. Nevertheless, 2 months later, remarkable mortality was observed in the sampling area. Animals maintained in the Murcia Aquarium and IMEDMAR-UCV did not show apparent signs of disease, but in both cases, up to 40–60% of the animals suffered sudden mortality in the following 6 months, primarily attributed to manipulation from artificial spawning attempts.

After the procedure, the animals were immediately relocated to the seabed/tanks, and their health was monitored over the following days. A volume of ~2 ml of hemolymph was collected for each animal. A 1 ml hemolymph aliquot was placed in a 1 ml RNA Later (Sigma-Aldrich, Italy)-labeled tube placed on ice for molecular analyses, and the other half was preserved for ultrastructural analyses. A small hemolymph aliquot (20 µl) was placed on a hemocytometer (Burker chamber) to determine the total cell number ($\times 10^5$/ml) and define the total hemocyte count (THC) (Table 1).

TABLE 1 List of collected samples of noble pen shell *P. nobilis* hemolymph in the Mediterranean Sea.

Site	Month and year	Number of collected animals evaluated by TEM	Sample type	Mean THC (ml^{-1}) of collected animals over the years
Alfacs site 1 Trabucador	July 2021 July 2022	6	Hemolymph	(4 in 2021): 2.35 ± 0.82 cells $\times 10^5$ (2 in 2022): 1.90 ± 0.33 cells $\times 10^5$
Alfacs site 2 Xiringuito	July 2021 July 2022	5	Hemolymph	(3 in 2021): 2.42 ± 0.42 cells $\times 10^5$ (2 in 2022): 2.15 ± 0.34 cells $\times 10^5$
Alfacs site 3 Barca	July 2021 August 2022	4	Hemolymph	(3 in 2021) 2.30 ± 1.0 cells $\times 10^5$ 2022 n.a.
Fangar site 4	May 2023	3	Hemolymph	n.a.
Murcia aquarium	September 22	4	Hemolymph	1.60 ± 0.22 cells $\times 10^5$
Tanks of IMEDMAR-UCV	July 21 May 2023	6	Hemolymph	(4 in 2021): 7.9 ± 0.3 cells $\times 10^4$ (2 in 2023) 3.5 ± 0.3 cells $\times 10^4$
Venice lagoon	May 2023	6	Hemolymph	n.a.

The number of samples analyzed per year is indicated in parentheses.
n.a., data not available; THC, total hemocyte count.

2.2 Transmission electron microscopy

For all the animals included in the study, part of the hemolymph was also fixed in 2.5% glutaraldehyde in PBS for 3 h. Cells were postfixed in 1% osmium tetroxide for 60 min and 0.25% uranyl acetate overnight. The cells were then dehydrated through a graded ethanol series and embedded in EPON resin overnight at 37°C, 1 day at 45°C, and 1 day at 60°C. Ultrathin sections (80 nm) were cut parallel to the substrate and placed onto a 200-mesh copper grid. Bright-field TEM images were obtained on the dried sample by using an FEI TECNAI G2 200 kV s-twin microscope operating at 120 kV (Thermo Fisher Scientific, Waltham, USA). Digital images were acquired with an Olympus VELETA camera.

2.3 RNA extraction, sequencing, and bioinformatic analysis

Total RNA was extracted from the hemocytes of six samples of *P. nobilis* collected from three sites of the wild population in Alfacs Bay, Catalonia (Table 2) using the PureLink RNA Mini Kit (Thermo Fisher Scientific, Waltham, Massachusetts, USA). Following DNase treatment, RNA concentration and quality were measured using a Nanodrop 2000 spectrophotometer (Thermo Fisher Scientific). Strand-specific cDNA libraries were prepared, and Illumina sequencing (NovaSeq 6000, 150 bp paired-end) was carried out by Eurofins Genomics (Ebersberg, Germany). Raw reads underwent trimming and adapter clipping using Trimmomatic 0.4 (41).

To identify RNA viruses eventually infecting the *P. nobilis* hemocytes, the trimmed, good-quality reads were aligned to the *P. nobilis* genome (ASM1616189v1) using Bowtie2 (42), and the unmapped reads were extracted using SAMtools (43).

A total of 33,097,808 paired unmapped reads were assembled using Trinity 2.12.0 (44), and the abundance estimation of contigs was performed with RSEM (45).

The Trinity-assembled contigs (140,922) were used as queries in a BLASTX search against the viral protein database (https://ftp.ncbi.nlm.nih.gov/refseq/release/viral/, downloaded on 6 June 2023). To focus the annotation on RNA viruses, the assembled contigs were analyzed using Virsorter2 (46) by selecting only the classification of RNA viruses. Additionally, VirBot, an RNA viral contig detector for metagenomic data (47), was utilized with the sensitive option. The contigs identified as positive by both VirSorter2 and VirBot were subjected to analysis using ORFfinder (https://www.ncbi.nlm.nih.gov/orffinder/). The resulting ORFs were then subjected to a BLASTP search against the UniProtKB/Swissprot, RefSeq protein, and non-redundant protein sequence databases on 4 July 2023.

The predicted sequences of the RNA-dependent RNA polymerase (RdRp) protein encoded by the identified RNA viruses were used for BLASTP searches against the viral protein database, and the highest scoring homologous sequences were downloaded. Multiple amino acid alignments of the selected RdRp sequences were performed using the Constraint-based Multiple Alignment Tool (COBALT, https://www.ncbi.nlm.nih.gov/tools/cobalt/re_cobalt.cgi). The best amino acid substitution model was searched, and the maximum likelihood tree was generated using the LG + G + I model and 500 bootstrap replicates using MEGAX (48), resulting in a final dataset of 317 characters.

2.4 Quantitative real-time PCR to detect the presence of the virus in *Pinna* hemocytes

Total RNA was extracted from the hemocytes of other 5 animals *P. nobilis* samples collected from different areas in Alfacs

TABLE 2 Samples of the noble pen shell *P. nobilis* used to extract RNA from hemocytes and raw data sequencing statistics.

Sample ID	Collection place	Collection date	Sequenced reads	Sequenced bases
Bar1	Alfacs Bay site 3	August 2022	25,189,100	7,556,730,000
Bar2	Alfacs Bay site 3	August 2022	28,331,700	8,499,510,000
Trab8a	Alfacs Bay site 1	July 2022	27,304,600	8,191,380,000
Trab8b	Alfacs Bay site 1	July 2022	29,977,200	8,993,160,000
Xir2a	Alfacs Bay site 2	July 2022	27,649,600	8,294,880,000
Xir5a	Alfacs Bay site 2	July 2022	23,687,100	7,106,130,000

TABLE 3 Samples of the noble pen shell *P. nobilis* used to extract RNA from hemocytes used for qPCR.

Sample ID	Collection place	Collection date
Bar6	Alfacs Bay site 3	August 2022
Bar7	Alfacs Bay site 3	August 2022
Trab3	Alfacs Bay site 1	July 2022
Trab5	Alfacs Bay site 1	July 2022
Xir6	Alfacs Bay site 2	July 2022

Bay, Catalonia (Table 3), as described before. RNA (500 ng) was reverse-transcribed using Maxima First Strand cDNA Synthesis (Thermo Scientific). Specific primer pairs were designed to amplify the two most abundant RNA viruses identified by the *in silico* analysis (Table 4), and quantitative real-time PCR experiments were conducted. Amplification reactions were performed in a total volume of 10 µl using 5 µl of PowerUp SYBR Green Master Mix (Applied Biosystems), 0.2 µM of each specific primer, and adjusted to 10 µl with distilled water. The reactions were conducted in technical duplicates using *P. nobilis* elongation factor-1 (*EF-1*) as a reporter gene (49, 50) (Table 4). The amplification conditions were as follows: 1 cycle for 2 min at 50°C; 1 cycle for 2 min at 95°C; 40 cycles of amplification at 95°C for 15 s; 60°C for 18 s; and 72°C for 1 min. The reactions were conducted in the QuantStudio 3 Real-Time PCR System (Thermo Scientific). The cDNA of the samples identified as Trab8a and XIR2a (the same used in the RNA-seq experiment) was subjected to real-time PCR amplification to confirm the results of the *in silico* analysis, and two negative controls were run without cDNA.

3 Results

3.1 Total hemocyte count, ultrastructure of infected hemocytes, and virus details

The THC values varied among individuals and areas over the years. The mean hemocyte count showed the lowest values from animals maintained in captivity in the IMEDMAR-UCV and Murcia Aquarium (between 3.5×10^4 and 1.60×10^5 ml^{-1} cells) compared with those from the natural population in Catalonia ($1.90–2.42 \times 10^5$ ml^{-1} cells) (Table 1). The most represented cells were granulocytes (~10 µm), displaying a small peripheral nucleus, and a small quantity of hyalinocytes (~7 µm), presenting a large central nucleus and small cytoplasm. All the hemocytes collected from animals in all areas of Italy and Spain from 2021 to 2023 (100%) displayed ultrastructural features of viral infection with associated cell death. These hemocytes all exhibited complex and unique membrane relocations, displaying numerous cytoplasmic vesicles associated with damaged mitochondria, a total lack of granules, the presence of protein aggregates, and, in some cases, cellular buddings. The formation of invaginations occurred at the membrane of various organelles, including the ER, endolysosomes, and mitochondria (Figures 2, 3). Features of viral infection at the hemocyte level are represented in Figure 2.

In all immune cells, aggregates of modified membranes occupied large areas of the perinuclear cytoplasm. Numerous membranous vesicles forming virions at various stages of self-assembly were visible. Vesicles in the cytoplasm were clearly associated with a dilated ER and nuclear membrane (Figures 3C, D). These vesicles had different dimensions and were constituted by double membranes, reported in the literature as DMVs or as autophagosome-like vesicles. The small vesicles measured 80–100 nm, whereas larger DMVs measured ~800–1,000 nm (Figures 3C–E). The presence of viral particles related to cytoplasmic vesicles, or mitochondrial membranes, was visible in all immune cells of *P. nobilis* (Figure 3F). Smaller vesicles were mostly used for virus genome replication at the cytoplasmic level, whereas larger DMVs supported a later step of virus production, specifically provirion maturation and the formation of complex factories. The DMVs displayed evident double or more complex membranes (Figure 4A). In earlier phases, the DMVs were filled by an unassembled viral amorphous and granular material; vesicles then showed one or two ring-like structures captured in the lumen vesicle, as also reported in other PVs (34) (Figure 4B). Viral replication factories are typically constituted by complex membrane remodeling emerging from DMVs formed by viral particles and proteins assembling mature virions, in some cases packed together. The virion is an icosahedral, non-enveloped, small (20 nm) particle with no discernible projections (Figures 4C, D).

Once the virus is assembled, viral release can occur through different mechanisms. Viruses can be released without lysis through so-called secretory autophagy, which occurs after the fusion of DMVs with the plasma membrane and are released as exosomes. Exosome typical dimensions ranged between 800 and 1,000 nm. Exosomes were secreted after their fusion with cell membrane vesicles and released as single-membraned virus-filled vesicles (Figures 4E, F). The four samples from Venice Lagoon, defined

TABLE 4 Primers used for the assessment of virus presence in noble pen shell *Pinna nobilis* hemocytes.

Primer	Sequence	Amplicon length (bp)	Reference seq accession number	Primer position on reference seq
PNChetoF	AGGGATGTTTGTGGGAGCAC	193	OR448788	5,561–5,580
PNChetoR	ACCGCCGAGGGTATTCTACT			5,753–5,734
PNPicornF	CGTCCGATGCCTCTCACTAC	167	OR448789	5,702–5,721
PNPicornR	AACCGGTCGAGCCAAGAAAT			5,868–5,849
EF1bivF	CTGGGTKTTGGACAAACTGAAG	211	XM_034472995.1	299–320
EF1bivR	GATACCAGCTTCAAATTCACCA			509–488

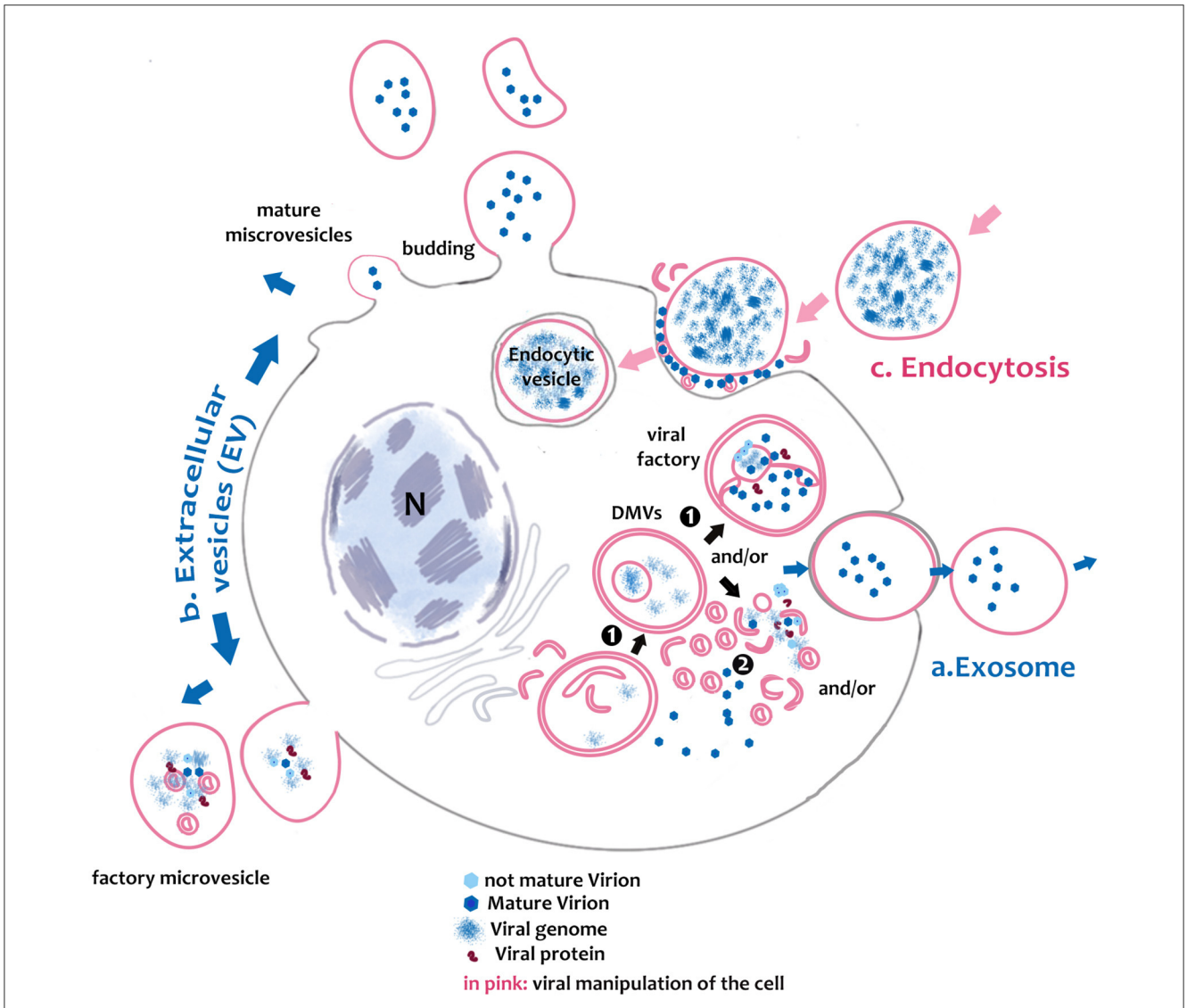

FIGURE 2
Schematic of picornavirus spread in noble pen shell *Pinna nobilis* hemocytes. Virus can form in large DMVs (1) or in small microvesicles (2), where the virus is freed in the cytoplasm. Then, viral replication and release may be performed using different pathways. a. Viruses may use the autophagic-like vesicles for viral spread, packaging virions, or viral factors that will be released to the extracellular medium as exosomes after fusion with the plasma membrane; b. Infectious microvesicle-like structures can either bud as evagination directly from the cytoplasm containing assembled virions and exit in extracellular vesicles (EVs) with mature virions or as factory microvesicles; then c. PV infective mechanism involves vesicles entering through the endocytic pathway.

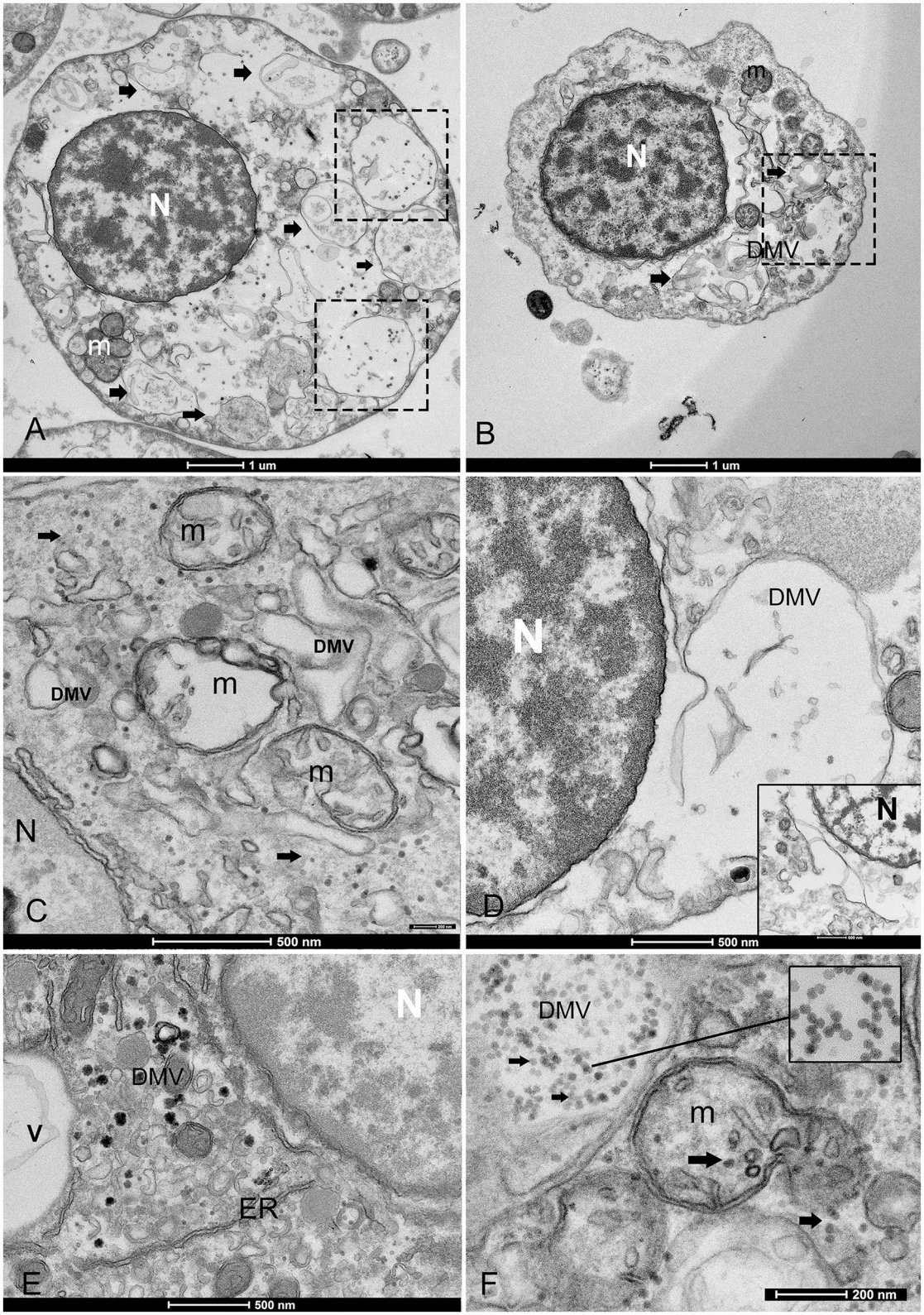

FIGURE 3
Overview of the morphological features of viral infection in the hemocytes of noble pen shell *Pinna nobilis*. **(A, B)** Granulocytes **(A)** and hyalinocytes **(B)** displaying double-membrane vesicles (DMVs) (arrows and squares). **(C)** Small vesicles (100–200 nm DMVs) and damaged mitochondria (m) with visible presence of viral particles in the cytoplasm (arrows); **(D)** Vesicle originates from the ER and nuclear membrane (inset); **(E)** Endoplasmic reticulum (ER) rearranged, forming DMV (v) and detail of zippered ER that consists of long stretches of ER-derived paired membranes. **(F)** Detail of vesicles containing viral particles (inset) and virus replication in a mitochondrion (m) but also present in the cell free in the cytoplasm (arrows). *N*, nucleus.

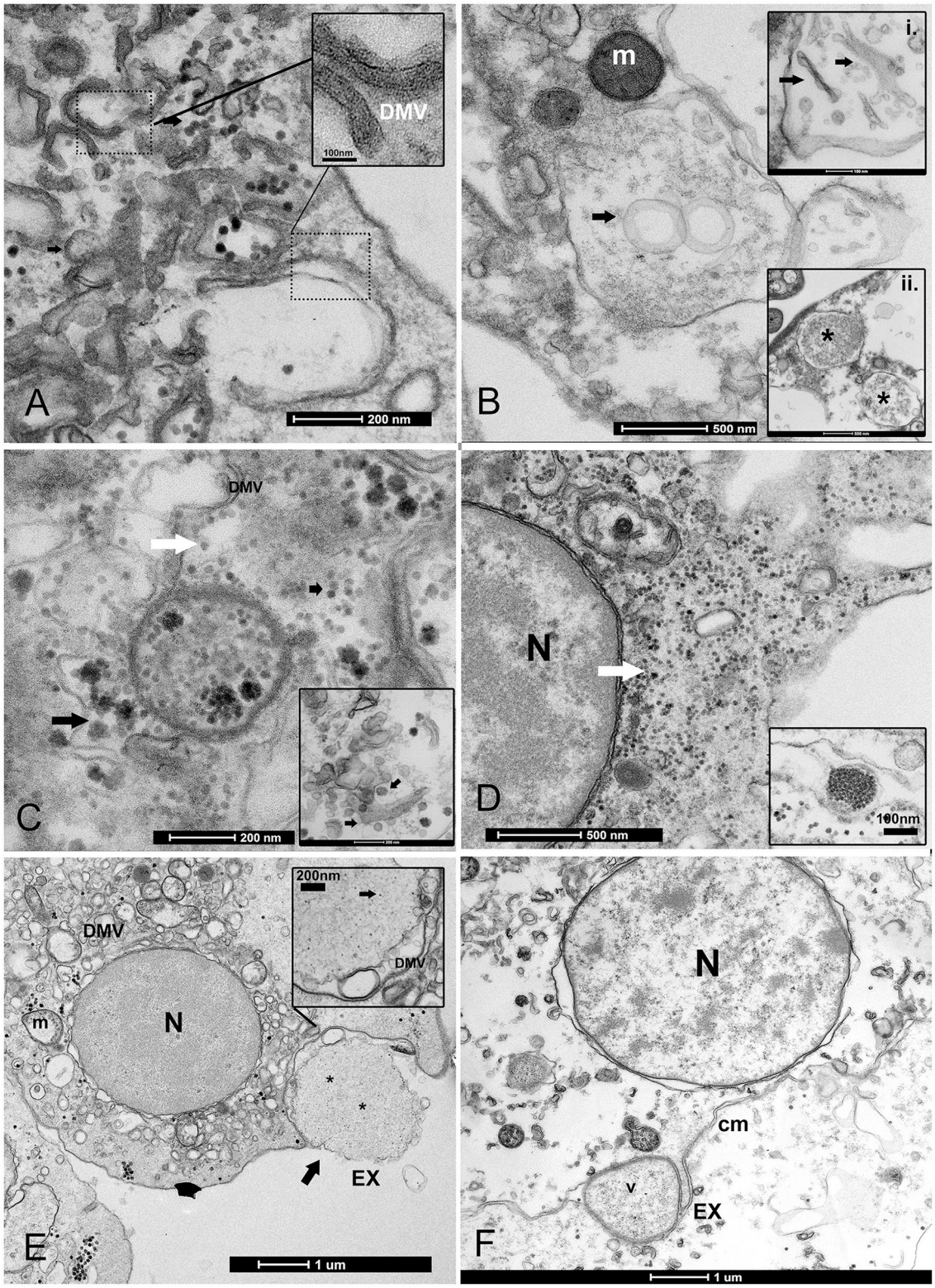

FIGURE 4
Biogenesis of double-membrane vesicles (DMVs) and exosome vesicles during PV replication. **(A)** Details of small and large DMVs with densely packed membranes that have an active role in viral RNA synthesis. **(B)** DMV biogenesis requires several membrane-remodeling steps: the biogenesis of DMVs can occur by the induction of positive membrane curvature through membrane pairing (inset i); these structures form cisternae that curve to finally seal and transform into a closed DMV and form ring-like vesicles, as reported in other picornaviruses where viral material can assemble (inset ii); **(C, D)** The virus replicates into factories through remodeled double membranes (inset), producing mature virions (white arrow) that accumulate in these large intracellular compartments from immature and forming ones (black arrow). **(D)** PV spreading into the granulocyte cytoplasm (white arrow); inset: grouped mature virions into vesicles. **(E, F)** Vesicles filled with viral particles (*) are released into the extracellular medium as exosomes (EX) after fusion with the cell membrane; viral egress involves the fusion of a double-membrane vesicle (V) with the cell membrane (CM); N, nucleus; m, mitochondria.

in the field as apparently healthy, displayed mature viral particles spreading into the cytoplasm (Figure 4D), small DMVs, and active factories.

The predominant infective strategy observed in the PV of *P. nobilis*, typical for non-enveloped viruses, was a non-lytic "unconventional secretion" using extracellular vesicles (EVs) (Figure 5). PV-infected cells secreted EVs carrying viral RNA particles. Vesicles ranged in diameter from 100 to 700 nm. Virions may be released from cells by a budding process from both granulocytes and hyalinocytes (Figures 5A–C). Infective vesicles were observed carrying either mature viral particles (Figure 5D) or vesicle factories containing still immature virions and DMVs (Figures 5E, F). EVs may be taken up by recipient cells by endocytosis or fusion with the plasma membrane. The vesicle is internalized, via endocytosis, in an endocytic vacuole surrounded by DMVs to form mature viral particles (Figures 6A, B). Infective vesicles transporting mature virions and injecting their contents were also visible (Figures 6C, D).

Dead hemocytes were observed during infections. The highest number of damaged cells was observed in animals maintained in captivity at IMEDMAR-UCV and Murcia Aquarium, surrounded by an elevated number of EVs or containing endocytic vesicles. Damaged cells appeared empty, shrunk, contained few vesicles, and presented membrane rupture and apoptotic bodies (Figure 7).

3.2 Identification of RNA viruses in *P. nobilis* hemocytes

Sequencing of six stranded cDNA libraries retrieved from hemocyte samples of six *P. nobilis* using Illumina technology generated a total of 162,139,300 paired-end raw reads (Table 2), subsequently deposited in the NCBI Sequence Read Archive (SRA) under the BioProject accession PRJNA999583. After trimming and mapping against the *P. nobilis* genome, the number of unmapped paired reads was 33,097,808 (20.4%). These unmapped reads were used to assemble the viral RNA genomes present in the *P. nobilis* hemocytes.

BLASTX analysis of the 140,922 contigs assembled using Trinity resulted in 61,634 positive matches (43.7%, e-value <10–20) against the viral protein database, encompassing DNA and RNA viruses as well as bacteriophages. Since this study was performed to identify RNA viruses in *P. nobilis* hemocytes, we focused specifically on this viral group using VirSorter2 and VirBot software tools. Both analyses identified the same set of five contigs, ranging from 5,210 to 8,876 nucleotides (nt) in length, all classified, with a score of 1 (the highest possible score with Virsorter2), into the realm *Riboviria*.

These five sequences exhibited the highest BLASTX matches with different *Riboviria* polyproteins 1 and 2 (Table 5), mainly of *Picornavirales*. Notably, two of these contigs (TRINITY_DN35348_c1_g1 and TRINITY_DN9545_c0_g1) displayed the highest number of mapped reads, particularly in the Trab samples (Site 1, Trabucador), indicating their abundance among the five identified viruses. Additionally, during the global BLASTX analysis, we discovered the contig TRINITY_DN58105_c0_g1_i1 (841 nt), which matched the predicted replication-associated protein of *Chaetoceros tenuissimus* RNA virus type II (BAP99820.1). Manual overlap with TRINITY_DN35348_c1_g1 (5,210 nt, matched with the predicted structural protein of *Chaetoceros tenuissimus* RNA virus type II, BAP99821.1) resulted in a 6,023 nt consensus sequence.

Figure 8 presents the genomic organization of the two most prevalent viruses identified herein. The sequence consensus_DN35348_c1_g1_DN58105_c0_g1 **(A)** is partial, lacking the complete 5′-end, while the DN9545_c0_g1 sequence **(B)** is complete. These two sequences were deposited in GenBank under accessions OR448788 and OR448789. The ORFfinder analysis identified two large ORFs encoding two viral polyproteins in both sequences. Within polyprotein 1, there were conserved domains of RdRp and RNA helicase (the latter was detected only in sequence DN9545). In contrast, structural polyproteins 2 have two rhv-like domains (picornavirus capsid protein domain-like), a CRPV capsid domain (a family of capsid proteins found in positive stranded ssRNA viruses), and a short VP4 domain (a family of minor capsid proteins located within the viral capsid at the interface between the external protein shell and packaged RNA genome). The presence of two large ORFs encoding these specific domains suggests that these viral sequences belong to the *Picornavirales* order.

The genomic organization of the remaining three viruses identified in *P. nobilis* hemocytes found herein (DN33054, DN37302, and DN33329) was deposited in GenBank under accession numbers OR448790, OR448791, and OR448792, respectively (Supplementary Figure 1). Similar to the two most abundant viruses, the genomic organization of DN33054 and DN37302 presented two large ORFs, with ORF1 encoding RdRp and RNA helicase and ORF2 encoding two rhv-like domains, a CRPV capsid domain and a short VP4 domain. In contrast, the genomic organization of DN33329 was quite different, with three partially overlapping main ORFs encoding a peptidase and RdRp, similar to the structure of the *Sobelivirales* order.

The maximum likelihood tree was generated based on the alignment of the conserved region of the RdRp proteins of the viruses identified in the *P. nobilis* hemocytes with homologous sequences downloaded from GenBank (Figure 9). Almost all of the RdRp sequences downloaded from GenBank belonged to *Picornavirales* from marine or freshwater environmental samples. A restricted number of sequences belonged to *Sobelivirales*, and two of them (*Penaeus vannamei* picornavirus and Wenzhou shrimp virus 8) to *Dicistoviridae*, which are associated with mollusk and crustacean diseases (27, 51). Among the viral sequences identified in *P. nobilis* hemocytes, DN33329 clustered with those in the order *Sobelivirales*, along with viruses from rivers, soil, and plants, agreeing with the genomic organization previously described (Supplementary Figure 1). Additionally, the remaining four sequences from *P. nobilis* belonged to the order *Picornavirales*, as expected from their genomic organization; among them, the two most abundant were clustered within the family *Marnaviridae*.

In terms of ultrastructure, both samples from the Trabucador area (Trab8a and Trab8b) that had the highest number of mapped viral reads displayed numerous cytoplasmic viral factories and

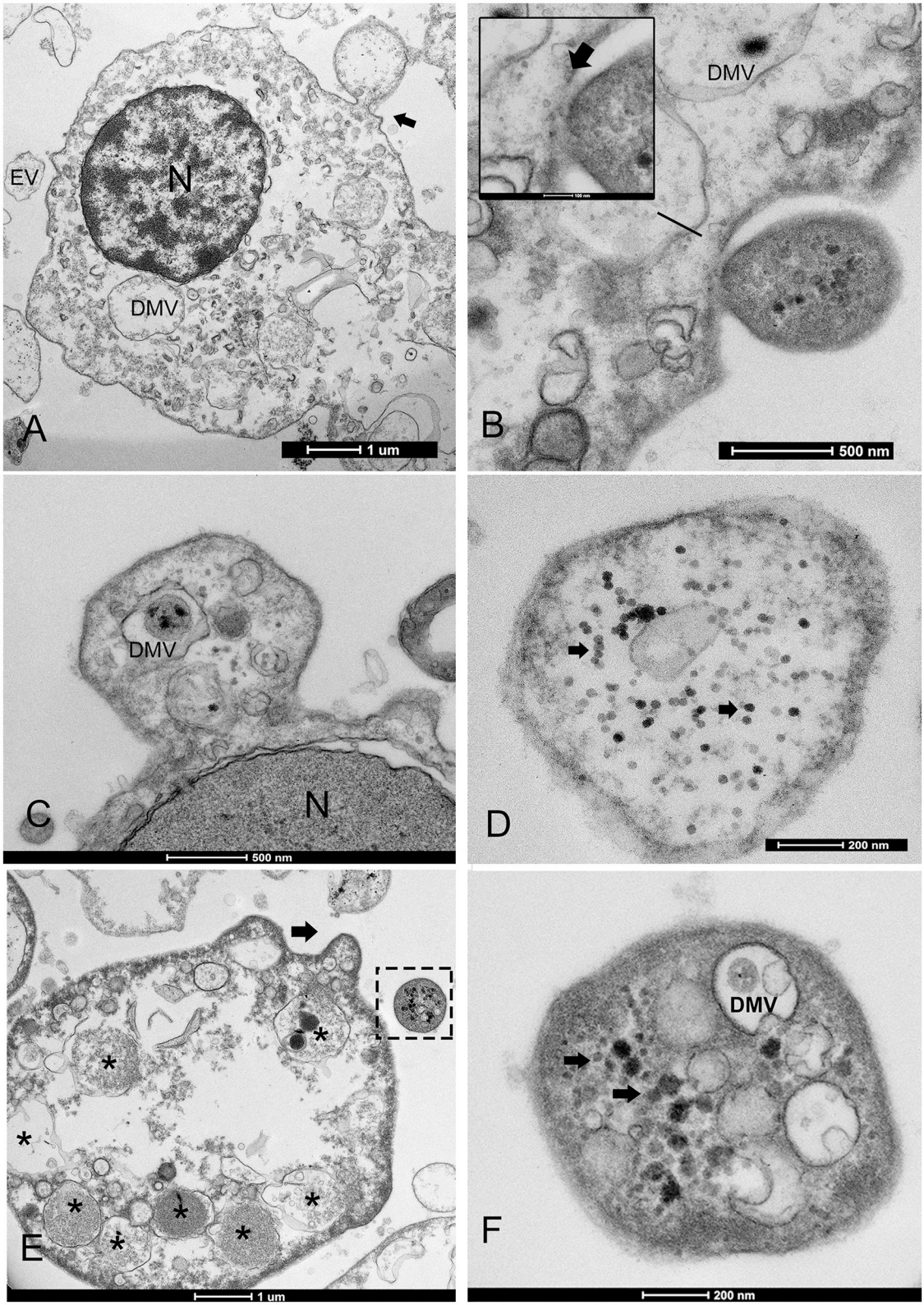

FIGURE 5
Extracellular vesicle (EV) formation during PV infection. **(A, B)** The EV lipid membrane mediates the release of virions through budding formation (arrow) with shedding microvesicles. **(B)** Details of budding from the cell membrane (arrow). **(C)** Hyaloncyte budding formation; **(D)** Vesicles might contain mature virions (arrows) or viral and/or host factor viral components (*) and induced/altered host factors **(E, F)**; N, nucleus; DMV, double-membrane vesicles within the EV.

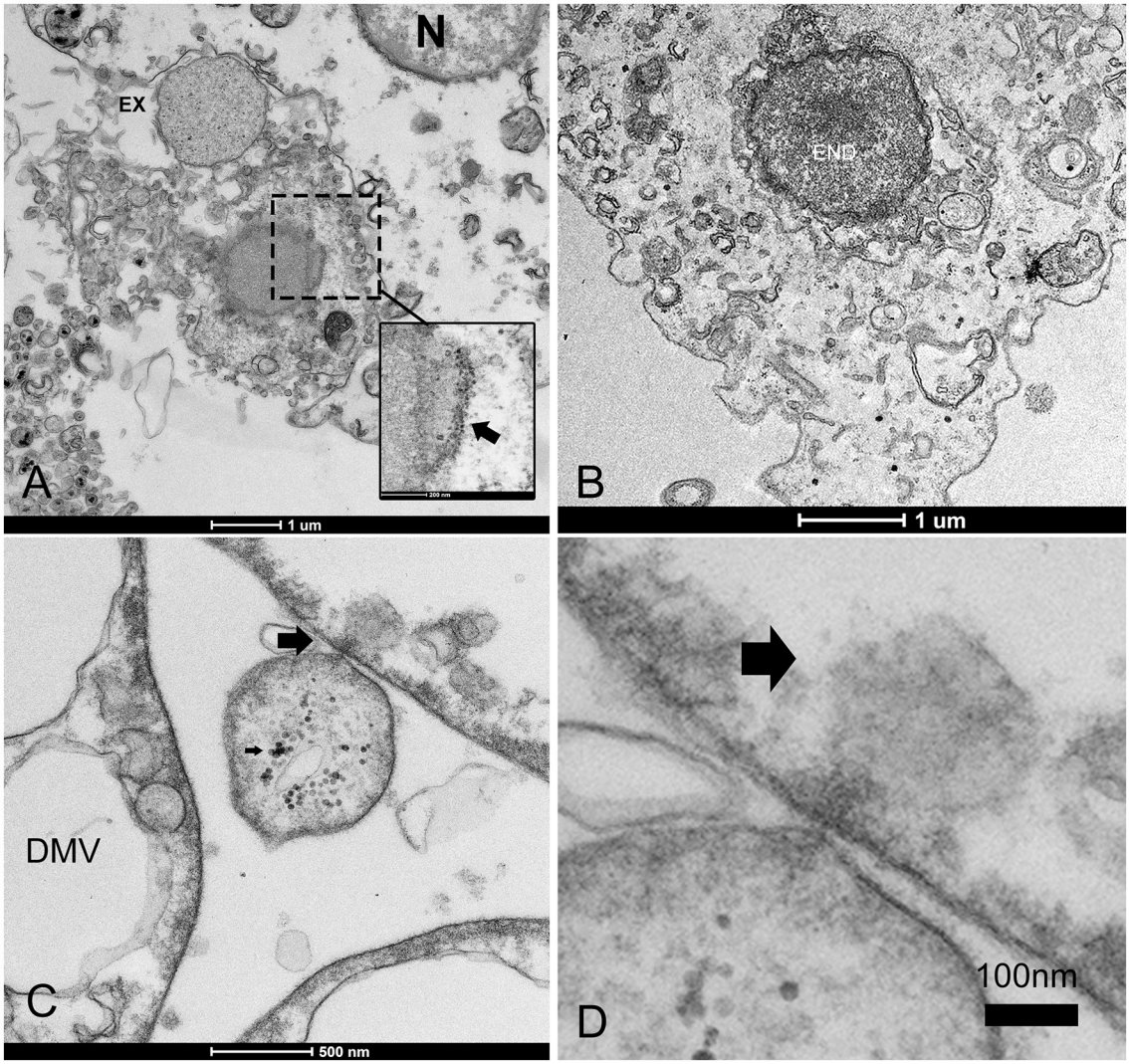

FIGURE 6
Infectious vesicles containing viral particles enter the cells. **(A, B)** Infective vesicles containing unassembled viral particles can enter through endocytosis, fusing with the cellular membrane and forming virions (inset, arrow) during the release of exosomes (EXs), which are then transported as late endosomes (ENDs) close to the nucleus **(B)**; **(C, D)** The vesicle can inject its content into other cells (arrows).

extracellular infective vesicles spreading into the hemolymph, suggesting an active infective phase.

3.3 Detection of RNA virus in *P. nobilis* hemocytes by quantitative real-time PCR

The quantitative real-time PCR experiments conducted on the cDNA of the *P. nobilis* hemocytes collected at different sampling points in Catalonia were positive for the primer pair PNChetoF/R designed on the reconstructed DN35348_DN58105 sequence, similar to a *Chaetoceros tenuissimus* RNA virus type II. These results confirm the *in silico* analysis of viral read abundance (Table 5), with Trab8a and XIR2a showing the highest infection level and XIR5 showing a low infection level (Figure 10). With the same primer pair, viral RNA was detected in all other examined samples, presenting variable infection levels. The primer pair PNPicorF/R designed for the sequence DN9545 did not provide a detectable amplification signal.

4 Discussion

This study reports the discovery of a picornavirus affecting *P. nobilis* hemocytes in Spain and Italy during MMEs (1, 4, 52). Previous studies investigating the etiological agent involved in MMEs showed a complex pattern: disease diagnosis repeatedly confirmed the simultaneous presence of several agents, such as *Haplosporidium pinnae* and *Mycobacterium* spp. (1, 4, 13), *Vibrio mediterranei* (53), and in some cases *Perkinsus* spp., suggesting that a common primary cause, not yet identified, could be linked to these phenomena (4). Based on our observations, this picornavirus could be the underlying cause of these events, as the virus was actively replicating and infecting *P. nobilis* shell immune cells in

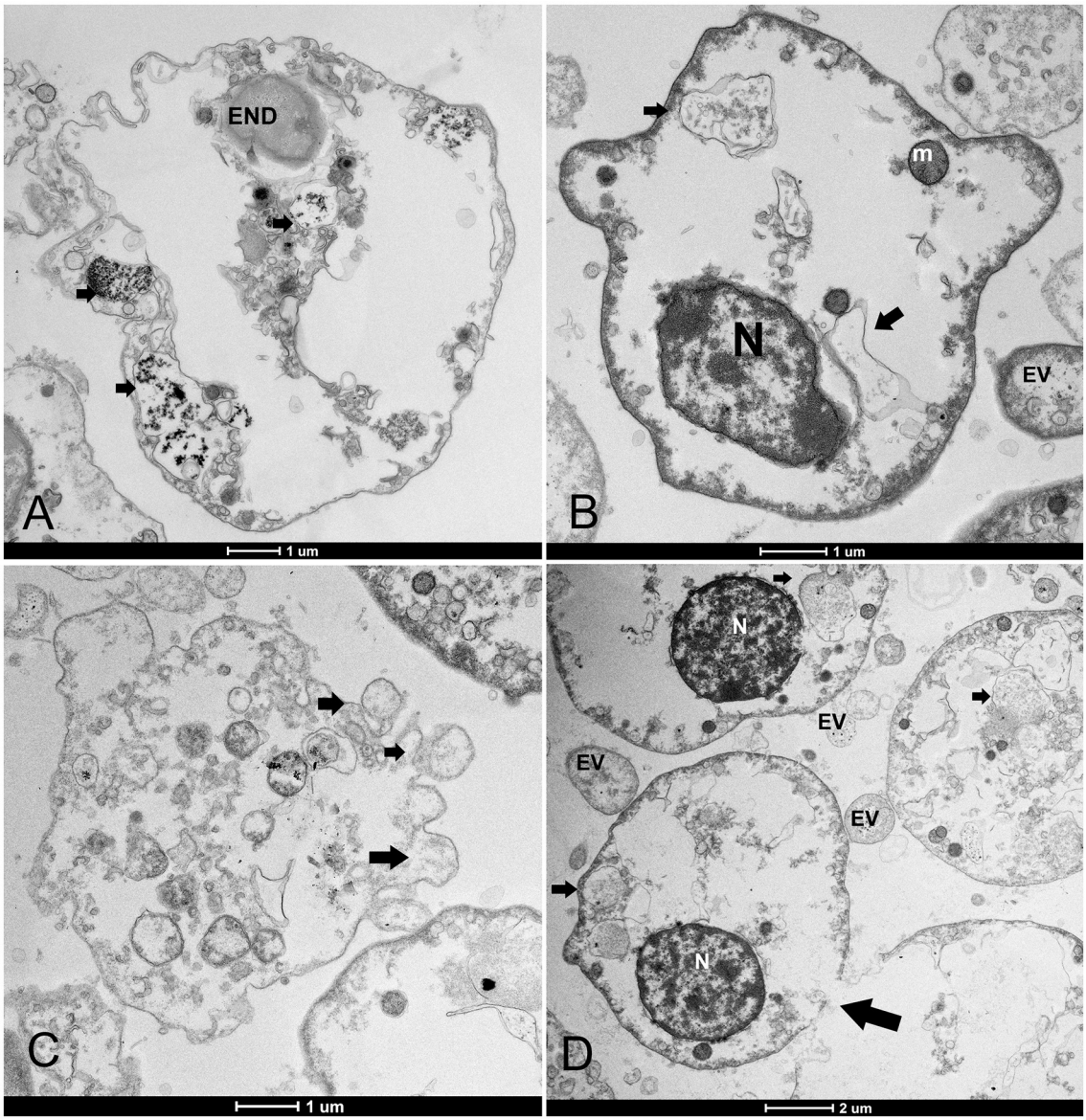

FIGURE 7
Hemocyte cell death. **(A, B)** Changes mainly include empty cytoplasm with residual vesicles (arrows) or endocytotic vesicles (ENDs) surrounded by extracellular vesicles (EVs); **(C)** blebbing of the plasma membrane and formation of apoptotic bodies (arrows) and loss of nuclei; **(D)** membrane rupture (arrows). N, nucleus; m, mitochondria.

100% of the examined residual populations in Italy and Spain from 2021 to 2023. In fact, the detection of this virus in the same populations over a 2-year period suggests that animals can maintain persistent infections until the disease becomes chronic, weakening them and making them susceptible to opportunistic infections, as also reported in other immunosuppressive viruses (54). This could explain the apparent resistance of the residual individuals who are slowly dying in all areas. The affected animals remain apparently healthy for months to years before the immune system begins to collapse, as reported by many scientists (3, 11, 52).

In this study, the observed picornavirus affecting *P. nobilis* in Italy and Spain used granulocytes and hyalinocytes as vessels for dissemination, replication, and long-term persistence, interfering with hemocyte immune abilities, as observed in other picornaviruses (55). Multiple known immunoregulatory mechanisms play a role in persistent viral infections, resulting in immunosuppression (56). Immunodeficiency viruses have been reported worldwide in felid, bovine (dairy cattle), and primate (chimpanzee) species and have been observed actively replicating in blood and lymphoid tissues (57). As a result of complete or unsuccessful viral replication, immunodeficiency viruses may functionally lyse or impair immune cells such as lymphocytes, as observed in parvovirus infections of B lymphocytes, in infectious mononucleosis due to Epstein–Barr virus, and in $CD4^+$ T lymphocytes and macrophages in AIDs caused by HIV lentivirus (58, 59). In other cases, viruses can infect, and damage cells involved in phagocytosis, such as macrophages, as seen in influenza virus and dengue virus infections (60, 61). Similarly, PV can block the

TABLE 5 Assembled contigs classified into the realm *Riboviria* by VirSorter2 and VirBot analysis, the results of their annotation through BLASTX vs. the viral protein database, and read abundance in the different noble pen shell *Pinna nobilis* samples expressed as raw counts.

Trinity contig name	Length (nt)	Best BLASTX hit	Bar1	Bar2	Trab8a	Trab8b	XIR2a	XIR5
TRINITY_DN35348_c1_g1	5,210	Predicted structural protein [*Chaetoceros tenuissimus* RNA virus type II] BAP99821.1	102	57	6,544	4,113	255	89
TRINITY_DN9545_c0_g1	8,505	Polyprotein [*Picornavirales* sp.] UNY42036.1	13	3,755	3,675	4,432	19	11
TRINITY_DN33054_c0_g1	8,876	Putative non-structural protein [*Picornavirales* N_OV_064] putative structural protein, partial [*Picornavirales* N_OV_064] ASG92536.1	3	364	406	509	2	1
TRINITY_DN33329_c0_g1	5,810	P1–P2 fusion protein [Pepo aphid-borne yellows virus] ANF99514.1	1.05	411.89	345.38	413.98	2.09	0
TRINITY_DN37302_c0_g1	8,567	Polyprotein [marine RNA virus BC-7] AYD68770.1	0	415	386	466	5	0

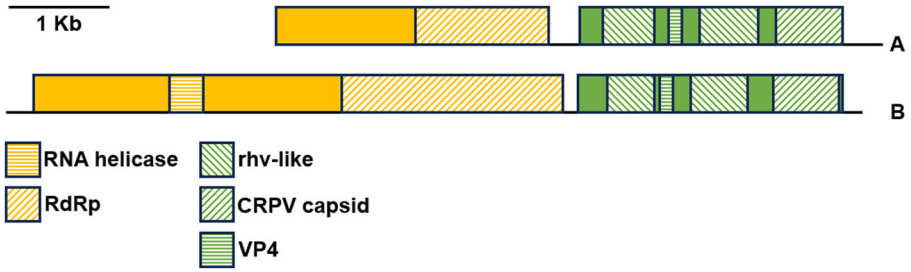

FIGURE 8
Genomic organization of the most abundant RNA viruses identified in the noble pen shell *Pinna nobilis* hemocytes. The colored boxes represent the ORFs of genes 1 (yellow) and 2 (green) encoding viral polyproteins 1 and 2, respectively. The different colored motifs represent the regions encoding specific viral proteins. **(A)** Trinity-assembled contigs DN35348_c1_g1 and DN58105_c0_g1, 5′-end partial (accession number OR448788); **(B)** Trinity-assembled contig DN9545_c0_g1 (accession number OR448789).

production of type I interferon (IFN), leading to T-cell depletion, or modulate immune cell apoptosis and autophagy mechanisms (62–64). In bivalves, the primary role of hemocytes is pathogen killing and elimination through phagocytosis, encapsulation, production of cytotoxic molecules and antimicrobial peptides, and secretion of inflammatory cytokines (65–68). A morpho-functional description of *P. nobilis* hemocytes was performed prior to the mortality events in 2015, showing that healthy hemocytes were able to conduct phagocytosis (69). In our study, *P. nobilis* hemocytes from individuals sampled in Spain and Italy displayed damage in mitochondria, ER, and other organelles, which may have affected their regular immune function (70). This is also true considering that a preliminary study performed in *P. nobilis* shell hemocytes from the same areas in 2021–2022 already revealed strong immunodepression, represented by a decreased immune cell response to pathogenic stimuli following an *in vivo* challenge (11).

Immunosuppression is necessary for PVs to use cell components to promote infection (55). PVs have evolved the ability to usurp infected cells' endogenous functions, inducing (endo)membrane rearrangements that are referred to as viral replication organelles (71). Recent work revealed that picornaviruses pack multiple viral particles into a cellular microvesicle to promote the spread of several heterogeneous virions at a time (72). In this context, the production of EVs and endocytic vesicles plays an important role in the pathogenesis and establishment of viral genome persistence and latency; moreover, viruses that establish chronic infections have been shown to modulate the production and content of more infectious EVs, increasing their infective potential (73). Animals maintained in captivity in this study displayed a high number of infective vesicles and dead cells, which was also related to hemocytopenia. Persistent PV infection can induce lymphopenia in humans and animals, such as cows, cats, and birds, as a direct result of viral infection or indirectly through cytokine induction (55, 74). Along with other diagnostic indices, decreased THC is a critical condition in the progression of an infection or a disease in invertebrates (75). Heamocytopenia has been observed during chronic viral infections, such as abalone ganglioneuritis (76), and during bacterial and parasitic diseases in other mollusk species (77, 78). Typically, persistent infections bring a relatively small pool of hemocytes into the hemolymph sinuses and perivisceral beds, and such sequestration into tissues may lead to a dramatic decrease in hemocyte numbers (79). Before the observation of mass mortality in the Mediterranean, Matozzo et al. (69) reported a higher number

FIGURE 9
Maximum likelihood tree constructed using the amino acid alignment of the conserved region of the RpRd of the RNA viruses identified in the noble pen shell *Pinna nobilis* hemocytes and other RpRd proteins downloaded from GenBank (total 38 amino acid sequences). The tree with the highest log likelihood (−16,083.36) is shown. The tree is drawn to scale, with branch lengths measured in the number of substitutions per site. The red and green boxes highlight the most and least abundant RNA viruses identified, respectively. The bootstrap percentages inferred from 500 replicates are shown next to the branches. When available, the geographic origin and host of the samples are indicated within parentheses.

of circulating hemocytes (5×10^5 cells) in comparison to that in the current Spanish wild and captive populations. Based on our results, this finding could indicate an over-time immune cell decrease due to infection and a worsened situation for animals maintained in tanks. Apart from hemocyte sequestration into infected tissues, such hemocytopenia is also possibly caused by apoptosis due to hemocyte infection (80). This host-initiated process of programmed cell death is essential for normal cell turnover and functions as an antiviral mechanism to limit the spread of a virus (81, 82).

In the present study, we were able to assemble different *Riboviria* sequences of the orders *Picornavirales* and *Sobelivirales*, with NGS Illumina sequencing obtaining nearly five different genomes accompanied by phylogenetic analysis. Our findings support previous observations that bivalve and other invertebrate viromes harbor a broad diversity of viruses of the order *Picornavirales* (25, 83), matching the ultrastructural features of hemocyte PV infection. Picornaviruses are components of the virome associated with filter-feeding organisms under normal physiological conditions, as reported in metatranscriptomic studies in the absence of detectable disease (84). Among the five assembled *Riboviria*, the two most abundant sequences are clustered with the *Picornavirales* group within the family *Marnaviridae*, which comprises small non-enveloped viruses that infect various photosynthetic marine protists (85) and have also been reported in diatom populations (86). The most abundant reads placed the hemocyte PV close to a virus isolated in the marine diatom *Chaetoceros tenuissimus*, named *C. tenuissimus* RNA virus type II (86), belonging to the genus *Sogarnavirus*, while the second most abundant PV was identified as *Picornavirus*, belonging to the genus *Marnavirus*.

Microalgal cells infected by *Marnaviridae*, genus *Sogarnavirus*, can display extensive cytopathic effects with ultrastructural changes, including swelling of the endoplasmic reticulum, vacuolation, and disintegration of the cytoplasm (86, 87), as reported in our study. To the best of our knowledge, this is the first report of a sogarnavirus affecting an animal species. To confirm the NGS analysis, qPCR was performed to amplify the most represented *Sogarnavirus*. The primer pairs designed on the sequence of the *P. nobilis* picornavirus similar to the *C. tenuissimus* RNA virus type II were positive in the analyzed samples, while no amplification was obtained with the other primer pairs. These results may not be conclusive and need to be confirmed with other analyses.

In this study, both apparently healthy and sick animals showed ultrastructural features of viral infection. In confined waters across Mediterranean regions, such as lagoons, MMEs started later (52). For instance, in Venice Lagoon, mortality episodes began in 2020, which is after the *P. nobilis* populations started dying off of the Ebro Delta, which started in 2018 (4). The viral infection could have originated first in Spanish waters, years before mortalities became evident, subsequently reaching other areas, until animals presented

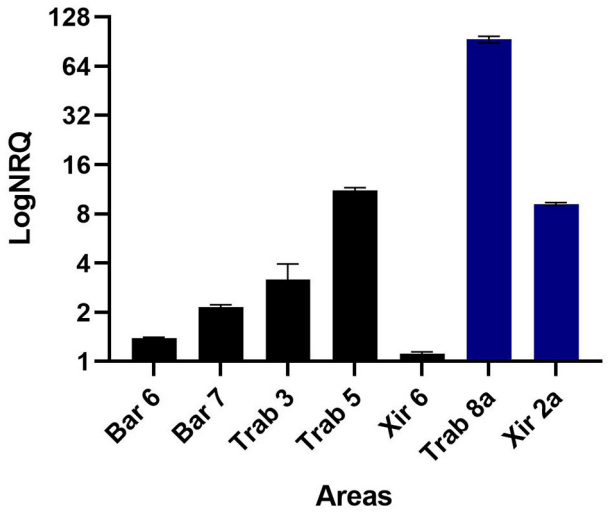

FIGURE 10
Results of the qPCR experiment conducted on the cDNA of the noble pen shell *Pinna nobilis* hemocytes collected in different areas using primer pairs specific for the *in silico* assembled Sogarnavirus (accession number OR448788). Bars represent the logarithm of the mean normalized relative quantification ± SEM using *P. nobilis* actin as an endogenous gene. The blue bars represent the samples used for the *in silico* RNA-seq experiment.

an acquired immunodeficiency (i.e., low count of hemocytes), as occurs with other immunodeficiency viruses. The disease, made up of periods of remission followed by disease progression over time, ends up gradually weakening the populations that start to display symptoms, leading to population decline. These individuals are exposed to a wide variety of bacterial and parasitic opportunistic infections, resulting in an unfavorable situation. In the Venice Lagoon, in the area where animals appeared apparently healthy in May 2023, remarkable mortality was observed 2 months later. In the four analyzed individuals, all immune cells presented actively replicating virus. This means that infection can be subclinical until very late in the process, which is when an opportunistic pathogen is more likely to take advantage of the situation.

As previously reported, recent findings suggest a more complex scenario than the one originally proposed in the first descriptions of *P. nobilis* MMEs (1, 4, 13). Diseases with complex etiology are influenced by various interacting drivers and frequently remain difficult to characterize. Indeed, this viral disease represents an epidemiological threat of unknown proportions for marine animal populations. Further studies are needed to determine the ecological importance of PV as an agent affecting the dynamics of *P. nobilis* MMEs in the analyzed areas and in other natural environments.

5 Conclusion

Few viruses, mainly those belonging to the families of *Alloherpesviridae* and *Iridoviridae*, have been associated with disease outbreaks and mortality in bivalves. Nevertheless, picornavirus-like particles have also been reported during disease outcomes (88–90). Here, we report the first description of an immunodeficiency virus in bivalves affecting *P. nobilis* hemocytes. Immune defense is a key determinant of fitness, underlying the capacity of animals to resist or tolerate potential infections. Immune function is not static and can be suppressed, depressed, or stimulated by exposure to environmental abiotic factors, food availability, and pathogens. Alteration of this response can directly affect population dynamics and survival. Recently, the emergence and spread of new and existing pathogens have posed a significant risk not only to human life and animal health but also to the conservation of wildlife. Future studies are needed to establish a clear and significant correlation between the genome of the picornaviruses assembled in *P. nobilis* hemocytes and the *P. nobilis* MMEs. First, the full length of the partial PV sequence assembled *in vitro* should be obtained using a 5′RACE approach. Second, viral isolation and cultivation attempts are needed to define virus characteristics. Finally, a fast and reliable diagnostic test (e.g., based on qPCR) should be developed to rapidly check the infection level of the surviving *P. nobilis* populations in other geographic areas. Virus presence should also be evaluated in the environment (water, plankton, sediments) and surrounding animals, which could be potential virus reservoirs.

Data availability statement

The original contributions presented in the study are publicly available. This data can be found here: https://www.ncbi.nlm.nih.gov/bioproject; PRJNA999583.

Ethics statement

The animal study was approved by MATTM Ministero dell'ambiente e della sicurezza energetica. The study was conducted in accordance with the local legislation and institutional requirements.

Author contributions

FC: Conceptualization, Data curation, Formal analysis, Funding acquisition, Investigation, Methodology, Supervision, Validation, Writing—original draft, Writing—review & editing. PP: Investigation, Resources, Writing—review & editing. GD: Writing—review & editing. DP: Writing—review & editing. GV: Methodology, Writing—review & editing. JG-M: Resources, Writing—review & editing. JT-M: Resources, Writing—review & editing. EC: Resources, Writing—review & editing. FG-C: Resources, Writing—review & editing. MS: Writing—review & editing. SA: Data curation, Formal analysis, Software, Supervision, Writing—original draft, Writing—review & editing.

Funding

The author(s) declare financial support was received for the research, authorship, and/or publication of this article. The research was partially supported by the EU LIFE Programme Project Protection and restoration of *Pinna nobilis* populations as

a response to the catastrophic pandemic started in 2016 (LIFE PINNARCA) (grant number LIFE20 NAT/ES/001265).

Acknowledgments

The authors thank Dr. Sergio Sorbo of the CeSMA, Section of Microscopy LaMMEC, University of Naples Federico II, and Dr. Antonella Giarra, Chemistry Department of the University of Naples Federico II, for technical support in electron microscopy. The authors also thank José Luis Costa and David Mateu Vilella (IRTA) and Roberto Vianello with Andrea Sabino (CNR-ISMAR) for technical assistance during fieldwork sampling in Catalonia and Venice, respectively.

Conflict of interest

The authors declare that the research was conducted in the absence of any commercial or financial relationships that could be construed as a potential conflict of interest.

The reviewer IG declared a past co-authorship with the authors FC, DP, GD, JT-M, and JG-M to the handling editor.

Publisher's note

Supplementary material

The Supplementary Material for this article can be found online at: https://www.frontiersin.org/articles/10.3389/fvets.2023.1273521/full#supplementary-material

SUPPLEMENTARY FIGURE 1
Genomic organization of the less abundant RNA viruses identified in the noble pen shell *Pinna nobilis* hemocytes. The colored boxes represent the ORFs of genes 1 (yellow) and 2 (green) encoding viral polyproteins 1 and 2, respectively. **(A)** Trinity-assembled contig DN33329_c0_g1 (accession number OR448790); **(B)** Trinity-assembled contig DN33054_c0_g1 (accession number OR448791); **(C)** Trinity-assembled contig DN37302_c0_g1 (accession number OR448792).

References

1. Carella F, Aceto S, Pollaro F, Miccio A, Iaria C, Carrasco N, et al. A mycobacterial disease is associated with the silent mass mortality of the pen shell *Pinna nobilis* along the Tyrrhenian coastline of Italy. *Sci Rep.* (2019) 9:1–12. doi: 10.1038/s41598-018-37217-y

2. Kersting D, Benabdi M, CiŽmek H, Grau A, Jimenez C, Katsanevakis S, et al. *Pinna nobilis. The IUCN Red List of Threatened Species.* (2019). 24 p. Available online at: https://www.iucnredlist.org/species/160075998/160081499

3. Zotou M, Gkrantounis P, Karadimou E, Tsirintanis K, Sini M, Poursanidis D, et al. *Pinna nobilis* in the Greek seas (NE Mediterranean): on the brink of extinction? *Mediterr Mar Sci.* (2020) 21:575–91. doi: 10.12681/mms.23777

4. Carella F, Antuofermo E, Farina S, Salati F, Mandas D, Prado P, et al. In the wake of the ongoing mass mortality events: co-occurrence of *Mycobacterium, Haplosporidium* and other pathogens in *Pinna nobilis* collected in Italy and Spain (Mediterranean Sea). *Front Mar Sci.* (2020) 7:48. doi: 10.3389/fmars.2020.00048

5. Lattos A, Feidantsis K, Georgoulis I, Giantsis IA, Karagiannis D, Theodorou JA, et al. Pathophysiological responses of *Pinna nobilis* individuals enlightens the etiology of mass mortality situation in the mediterranean populations. *Cells.* (2021) 22:2838. doi: 10.3390/cells10112838

6. Katsanevakis S. The cryptogenic parasite *Haplosporidium pinnae* invades the Aegean Sea and causes the collapse of *Pinna nobilis* populations. *Aquat Invasions.* (2019) 14:150–64. doi: 10.3391/ai.2019.14.2.01

7. Vázquez-Luis M, Alvarez E, Barrajon A, García-March JR, Grau A, Hendricks IE, et al. S.O.S. *Pinna nobilis*: a mass mortality event in western Mediterranean Sea. *Front Mar Sci.* (2017) 4:109. doi: 10.3389/fmars.2017.00220

8. Katsanevakis S, Carella F, Çinar ME, Čižmek H, Jimenez C, Kersting DK, et al. The fan musselPinna nobilison the brink ofextinction in the Mediterranean. In: Dellasala DA, Goldstein MI, editors. *Imperiled: the Encyclopedia of Conservation*. Oxford: Elsevier (2022).

9. Darriba S. First haplosporidan parasite reported infecting a member of the Superfamily Pinnoidea (*Pinna nobilis*) during a mortality event in Alicante (Spain, Western Mediterranean). *J Invertebr Pathol.* (2017) 148:14–9. doi: 10.1016/j.jip.2017.05.006

10. Catanese G, Grau A, Valencia JM, Garcia-March JR, Vazquez-Luis M, Alvarez E, et al. Haplosporidium pinnae sp. nov, a haplosporidan parasite associated with mass mortalities of the fan mussel, *Pinna nobilis*, in the Western Mediterranean Sea. *J Invertebr Pathol.* (2018) 157:9–24. doi: 10.1016/j.jip.2018.07.006

11. Carella F, Prado P, García-March JR, Medialdea JT, Cortés Melendreras E. Giménez Casalduero F, et al. *Phagocytosis Based Assay for an In Vitro Assessment of Immunocompetence of the Pen Shell P. nobilis During Mass Mortality Events.* Aberdeen: EAFP European Association of Fish pathologist Congress (2023).

12. Grau A, Villalba A, Navas JI, Hansjosten B, Valencia JM, García-March JR, et al. Wide-geographic and long-term analysis of the role of pathogens in the decline of *Pinna nobilis* to critically endangered species. *Front Mar Sci.* (2022) 9:303. doi: 10.3389/fmars.2022.666640

13. Carella F, Palić D, Šarić T, Župan I, Gorgoglione B, Prado P, et al. Multi-pathogen infections and multifactorial pathogenesis involved in noble pen shell (*Pinna nobilis*) mass mortality events: background and current pathologic approaches. *Vet Pathol.* (2023) 60:560–77. doi: 10.1177/03009858231186737

14. Le Gall O, Christian P, Fauquet CM, King AMQ, Knowles NJ, Nakashima N, et al. *Picornavirales*, a proposed order of positive-sense single-stranded RNA viruses with a pseudo-T = 3 virion architecture. *Arch Virol.* (2008) 153:715. doi: 10.1007/s00705-008-0041-x

15. Wang-Shick R. Chapter 11, picornavirus. In: *Molecular Virology of Human Pathogenic Viruses.* (2017). p. 153–64.

16. Stanway G. Structure, function and evolution of picornaviruses. *J Gen Virol.* (1990) 71(Pt 11):2483–501. doi: 10.1099/0022-1317-71-11-2483

17. Gustavsen JA, Winget DM, Tian X, Suttle CA. High temporal and spatial diversity in marine RNA viruses implies that they have an important role in mortality and structuring plankton communities. *Front Microbiol.* (2014) 5:703. doi: 10.3389/fmicb.2014.00703

18. Whitton JL, Cornell CT, Feuer R. Host and virus determinants of picornavirus pathogenesis and tropism. *Nat Rev Microbiol.* (2005) 3:765–76.

19. Cifuente JO, Moratorio G. Evolutionary and structural overview of human picornavirus capsid antibody evasion. *Front Cell Infect Microbiol.* (2019) 9:283. doi: 10.3389/fcimb.2019.00283

20. Zell R, Delwart E, Gorbalenya E, Hovi T. ICTV virus taxonomy profile. *Picornaviridae.* (2017) 98:2421–2. doi: 10.1099/jgv.0.000911

21. Baltimore D. Expression of animal virus genomes. *Bacteriol Rev.* (1971) 35:235–41. doi: 10.1128/br.35.3.235-241.1971

22. Arcier J-M, Herman F, Lightner DV, Redman RM, Mari J, Bonami JR. A viral disease associated with mortalities in hatchery-reared postlarvae of the giant freshwater prawn *Macrobrachium rosenbergii*. *DAO.* (1999) 38:177–81. doi: 10.3354/dao038177

23. Tang KFJ, Lightner DV. Phylogenetic analysis of Taura syndrome virus isolates collected between 1993 and 2004 and virulence comparison between

two isolates representing different genetic variants. *Virus Res.* (2005) 112:69–76. doi: 10.1016/j.virusres.2005.03.023

24. Kapoor A, Victoria J, Simmonds P, Wang C, Shafer R, Nims W, et al. A highly divergent picornavirus in a marine mammal. i*Virol*. (2008) 82:311–20. doi: 10.1128/JVI.01240-07

25. Shi M, Lin XD, Tian JH, Chen LJ, Chen X, Li CX, et al. Redefining the invertebrate RNA virosphere. *Nature.* (2016) 540:539–43. doi: 10.1038/nature20167

26. Kim J-O, Lee JK, Seo YB, Lim H-K, Kim G-D. Genome sequences of a novel picorna-like virus from Pacific abalone (*Haliotis discus hannai*) in South Korea. *Genome Announc.* (2017) 5:e00484–17. doi: 10.1128/genomeA.00484-17

27. Liu S, Xu T, Wang C, Jia T, Zhang Q. A novel picornavirus discovered in white leg shrimp *Penaeus vannamei*. *Viruses.* (2021) 13:2381. doi: 10.3390/v13122381

28. Belov GA, Nair V, Hansen BT, Hoyt FH, Fischer ER, Ehrenfeld E. Complex dynamic development of poliovirus membranous replication complexes. *J Virol.* (2012) 86:302–12. doi: 10.1128/JVI.05937-11

29. Harak C, Lohmann V. Ultrastructure of the replication sites of positive-strand RNA viruses. *Virology.* (2015) 479–80:418–33. doi: 10.1016/j.virol.2015.02.029

30. Dales S, Eggers HJ, Tamm I, Palade GE. Electron microscopic study of the formation of poliovirus. *Virology*. (1965) 26:379–89. doi: 10.1016/0042-6822(65)90001-2

31. Hsu N-Y, Ilnytska O, Belov G, Santiana M, Chen YH, Takvorian PM, et al. Viral reorganization of the secretory pathway generates distinct organelles for RNA replication. *Cell.* (2010) 141:799–811. doi: 10.1016/j.cell.2010.03.050

32. Suhy DA, Giddings TH Jr, Kirkegaard K. Remodeling the endoplasmic reticulum by poliovirus infection and by individual viral proteins: an autophagy-like origin for virus-induced vesicles. *J Virol.* (2000) 74:8953–65. doi: 10.1128/JVI.74.19.8953-8965.2000

33. Cottam E, Pierini R, Roberts R, Wileman T. Origins of membrane vesicles generated during replication of positive-strand RNA viruses. *Fut. Virol.* (2009) 4:473–85. doi: 10.2217/fvl.09.26

34. Yang JE, Rossignol ED, Chang D, Zaia J, Forrester I, Raja K, et al. Complexity and ultrastructure of infectious extracellular vesicles from cells infected by nonenveloped virus. *Sci Rep.* (2020) 10:1–18. doi: 10.1038/s41598-020-64531-1

35. Welsch S, Müller B, Kräusslich H-G. More than one door - Budding of enveloped viruses through cellular membranes. *FEBS Lett.* (2007) 581:2089–97. doi: 10.1016/j.febslet.2007.03.060

36. den Boon JA, Diaz A, Ahlquist P. Cytoplasmic viral replication complexes. *Cell Host Microbe*. (2010) 8:77–85. doi: 10.1016/j.chom.2010.06.010

37. Prado P, Grau A, Catanese G, Cabanes P, Carella F, Fernández-Tejedor M, et al. *Pinna nobilis* in suboptimal environments are more tolerant to disease but more vulnerable to severe weather phenomena. *Mar Environ Res.* (2021) 163:105220. doi: 10.1016/j.marenvres.2020.105220

38. Gimenez-Casalduero F, Martínez-Fernandez J. El colapso del mar menor: historia de una joya ecol'ogica maltratada. *Metode Rev difusion la Investig.* (2020) 106:22–9.

39. Cortés-Melendreras E, Gomariz-Castillo F, Alonso-Sarría F, Martín FJG, Murcia J, Canales-Cáceres R, et al. The relict population of *Pinna nobilis* in the Mar Menor is facing an uncertain future. *Mar Pollut Bull.* (2022) 185:114376. doi: 10.1016/j.marpolbul.2022.114376

40. Tagliapietra D, Zanon V, Frangipane G, Umgiesser G, Sigovini M. Physiographic zoning of the Venetian lagoon. In: Campostrini P, editor. *Scientific Research and Safeguarding of Venice, vol. VII - 2007-2010*. Venezia: CORILA (2009). p. 161–4.

41. Bolger AM, Lohse M, Usadel B. Trimmomatic: a flexible trimmer for illumina sequence data. *Bioinformatics.* (2014) 30:2114–20. doi: 10.1093/bioinformatics/btu170

42. Langmead B, Salzberg S. Fast gapped-read alignment with Bowtie 2. *Nat Methods.* (2012) 9:357–9. doi: 10.1038/nmeth.1923

43. Danecek P, Bonfield JK, Liddle J, Marshall J, Ohan V, Pollard MO, et al. Twelve years of SAMtools and BCFtools. *GigaScience.* (2021) 10:giab008. doi: 10.1093/gigascience/giab008

44. Grabherr MG, Haas BJ, Yassour M, Levin JZ, Thompson DA, Amit I, et al. Full-length transcriptome assembly from RNA-seq data without a reference genome. *Nat Biotechnol.* (2011) 29:644–52. doi: 10.1038/nbt.1883

45. Li B, Dewey CN. RSEM: accurate transcript quantification from RNA-Seq data with or without a reference genome. *BMC Bioinformat.* (2012) 12:323. doi: 10.1186/1471-2105-12-323

46. Guo J, Bolduc B, Zayed AA, Varsani A, Dominguez-Huerta G, Delmont TO, et al. VirSorter2: a multi-classifier, expert-guided approach to detect diverse DNA and RNA viruses. *Microbiome.* (2021) 9:37. doi: 10.1186/s40168-020-00990-y

47. Chen G, Tang X, Shi M, Sun Y. VirBot: an RNA viral contig detector for metagenomic data. *Bioinformatics.* (2023) 39:btad093. doi: 10.1093/bioinformatics/btad093

48. Kumar S, Stecher G, Li M, Knyaz C, Tamura K. MEGA X: molecular evolutionary genetics analysis across computing platforms. *Mol Biol Evol.* (2018) 35:1547–9. doi: 10.1093/molbev/msy096

49. Lattos A, Papadopoulos DK, Giantsis IA, Feidantsis K, Georgoulis I, Karagiannis D, et al. Investigation of the highly endangered Pinna nobilis mass mortalities: Seasonal and temperature patterns of health status, antioxidant and heat stress responses. *Mar Environ Res.* (2023) 188:105977. doi: 10.1016/j.marenvres.2023.105977

50. Huan P, Wang H, Liu B. Assessment of housekeeping genes as internal references in quantitative expression analysis during early development of oyster. *Gene Genet Syst.* (2016) 91:257–65. doi: 10.1266/ggs.16-00007

51. Srisala J, Thaiue D, Saguanrut P, Taengchaiyaphum, Flegel TW, Sritunyalucksana K. Wenzhou shrimp virus 8 (WzSV8) detection by unique inclusions in shrimp hepatopancreatic E-cells and by RT-PCR. *Aquaculture.* (2023) 572:739483. doi: 10.1016/j.aquaculture.2023.739483

52. Šarić T, Župan I, Aceto S, Villari G, Palic D, De Vico G, et al. Epidemiology of noble pen shell (*Pinna nobilis* L. 1758) mass mortality events in adriatic sea is characterised with rapid spreading and acute disease progression. *Pathogens.* (2020) 9:1–21. doi: 10.3390/pathogens9100776

53. Prado P, Carrasco N, Catanese G, Grau A, Cabanes P, Carella F, et al. Presence of *Vibrio mediterranei* associated to major mortality in stabled individuals of *Pinna nobilis* L. *Aquaculture.* (2020) 519:734899. doi: 10.1016/j.aquaculture.2019.734899

54. English RV, Nelson P, Johnson CM, Nasisse M, Tompkins WA, Tompkins MB. Development of clinical disease in cats experimentally infected with feline immunodeficiency virus. *J Infect Dis.* (1994) 170:543–52. doi: 10.1093/infdis/170.3.543

55. Cusick MF, Libbey JE, Fujinami RS. Picornavirus infection leading to immunosuppression. *Fut Virol.* (2014) 9:475–82. doi: 10.2217/fvl.14.26

56. Oldstone MB. Anatomy of viral persistence. *PLoS Pathog.* (2009) 5:e1000523. doi: 10.1371/journal.ppat.1000523

57. Tizard I. *Secondary Immunodeficiencies*. The Merck Veterinary Manual (2019). Available online at: https://www.merckvetmanual.com/immune-system/immunologic-diseases/secondary-immunodeficiencies#v3277197 (accessed July 22, 2023).

58. Ackley CD, Yamamoto JK, Levy N, Pedersen NC, Cooper MD. Immunologic abnormalities in pathogen-free cats experimentally infected with feline immunodeficiency virus. *J Virol.* (1990) 64:5652–5. doi: 10.1128/jvi.64.11.5652-5655.1990

59. Brown MA, Munkhtsog B, Troyer JL, Ross S, Sellers R, Fine AE, et al. Feline immunodeficiency virus (FIV) in wild Pallas' cats. *Vet Immunol Immunopathol.* (2010) 134:90–5. doi: 10.1016/j.vetimm.2009.10.014

60. Egberink H, Horzinek MC. Animal immunodeficiency viruses. *Vet Microbiol.* (1992) 33:311–31. doi: 10.1016/0378-1135(92)90059-3

61. VandeWoude S, Apetrei C. Going wild: lessons from naturally occurring T-lymphotropic lentiviruses. *Clin Microbiol Rev.* (2006) 19:728–62. doi: 10.1128/CMR.00009-06

62. Lei X, Sun Z, Liu X, Jin Q, He B, Wang J. Cleavage of the adaptor protein TRIF by enterovirus 71 3C inhibits antiviral responses mediated by Toll-like receptor 3. *J Virol.* (2011) 85:8811–8. doi: 10.1128/JVI.00447-11

63. Lee YP, Wang YF, Wang JR, Huang SW, Yu CK. Enterovirus 71 blocks selectively type I interferon production through the 3C viral protein in mice. *J Med Virol.* (2012) 84:1779–89. doi: 10.1002/jmv.23377

64. Son KN, Liang Z, Lipton HL. Mutation of the Theiler's virus leader protein zinc-finger domain impairs apoptotic activity in murine macrophages. *Virus Res.* (2013) 177:222–5. doi: 10.1016/j.virusres.2013.09.001

65. de la Ballina NR, Maresca F, Cao A, Villalba A. Bivalve haemocyte subpopulations: a review. *Front Immunol.* (2022) 13:826255. doi: 10.3389/fimmu.2022.826255

66. Song L, Wang L, Qiu L, Zhang H. Bivalve immunity. *Adv Exp Med Biol.* (2010) 708:44–65. doi: 10.1007/978-1-4419-8059-5_3

67. Cheng TC. Bivalves. In: Ratcliffe NA, Rowley AF, editors. *Invertebrate Blood Cells*. London: Academic Press (1981). p. 233–300.

68. Nakayama K, Nomoto AM, Nishijima M, Maruyama T. Morphological and functional characterization of hemocytes in the giant clam *Tridacna crocea. J Invertebr Pathol*. (1997) 69:105e111. doi: 10.1006/jipa.1996.4626

69. Matozzo V, Pagano M, Spinelli A, Caicci F, Faggio C. *Pinna nobilis*: a big bivalve with big haemocytes? *Fish Shellfish Immunol.* (2016) 55:529–34. doi: 10.1016/j.fsi.2016.06.039

70. Pugliese A, Vidotto V, Beltramo T, Torre D. Phagocytic activity in human immunodeficiency virus type 1 infection. *Clin Diagn Lab Immunol.* (2005) 889–95. doi: 10.1128/CDLI.12.8.889-895.2005

71. Meckes DGJr, Raab-Traub N. Microvesicles and viral infection. *J Virol.* (2011) 85:12844–54. doi: 10.1128/JVI.05853-11

72. Chen YH, Du W, Hagemeijer MC, Takvorian PM, Pau C, Cali A, et al. Phosphatidylserine vesicles enable efficient en bloc transmission of enteroviruses. *Cell.* (2015) 160:619–30. doi: 10.1016/j.cell.2015.01.032

73. Amari L, Germain M. Mitochondrial extracellular vesicles, origins and roles. *Front Mol Neurosci.* (2021) 14:767219. doi: 10.3389/fnmol.2021.767219

74. Geoghegan JL, Duchêne S, Holmes EC. Comparative analysis estimates the relative frequencies of co- divergence and cross- species transmission within viral families. *PLoS Pathog.* (2017) 13:e1006215. doi: 10.1371/journal.ppat.1006215

75. Cheng W, Juang F-M, Chen J-C. The immune response of Taiwan abalone *Haliotis diversicolor supertexta* and its susceptibility to *Vibrio parahaemolyticus* at different salinity levels. *Fish Shellfish Immun.* (2004) 16:295–306. doi: 10.1016/S1050-4648(03)00111-6

76. Hooper C, Hardy-Smith P, Handlinger J. Ganglioneuritis causing high mortalities in farmed Australian abalone (*Haliotis laevigata* and *Haliotis rubra*). *Aust Vet J.* (2007) 85:188–93. doi: 10.1111/j.1751-0813.2007.00155.x

77. Shields JD, Perkins FO. *Parasitological Examination of Wasting Disease in Black Abalone, Haliotis cracherodii: Final Report*. Virginia Institute of Marine Science, William & Mary (1997). Available online at: https://scholarworks.wm.edu/reports/2760

78. Handlinger J, Lleonart M, Powell M. *Development of an Integrated Management Program for the Control of Spionid Mudworms in Cultured Abalone*. Canberra, ACT: FRDC Project No 98/307 Fisheries Research and Development Corporation (2004).

79. Hooper C, Slocombe R, Day R, Crawford S. Leucopenia associated with abalone viral ganglioneuritis. *Aust Vet J.* (2012) 90:24–8. doi: 10.1111/j.1751-0813.2011.00877.x

80. Sun D, Wen X, Wang M, Mao S, Cheng A, Yang X, et al. Apoptosis and Autophagy in Picornavirus Infection. *Front Microbiol.* (2019) 10:2032. doi: 10.3389/fmicb.2019.02032

81. Belov GA, Romanova LI, Tolskaya EA, Kolesnikova MS, Lazebnik YA, Agol VI. The major apoptotic pathway activated and suppressed by poliovirus. *J Virol.* (2003) 77:45–56. doi: 10.1128/JVI.77.1.45-56.2003

82. Croft SN, Walker EJ, Ghildyal R. Picornaviruses and apoptosis: subversion of cell death. *Mbio.* (2017) 8:e01009–17. doi: 10.1128/mBio.01009-17

83. Zhou D, Liu S, Guo G, He X, Xing C, Miao Q, et al. Virome analysis of normal and growth retardation disease-affected *Macrobrachium rosenbergii*. *Microbiol Spectr.* (2022) 10:e0146222. doi: 10.1128/spectrum.01462-22

84. Moreira R, Balseiro P, Planas JV, Fuste B, Beltran S, Novoa B, et al. Transcriptomics of in vitro immune-stimulated hemocytes from the Manila clam Ruditapes philippinarum using high-throughput sequencing. *PLoS ONE.* (2012) 7: e35009. doi: 10.1371/journal.pone.0035009

85. Sadeghi M, Tomaru Y, Ahola T. RNA viruses in aquatic unicellular eukaryotes. *Viruses.* (2021) 25:362. doi: 10.3390/v13030362

86. Shirai Y, Tomaru Y, Takao Y, Suzuki H, Nagumo T, Nagasaki K. Isolation and characterization of a single-stranded RNA virus infecting the marine planktonic diatom *Chaetoceros tenuissimus* meunier appl. *Environ Microbiol.* (2008) 74:4022–7. doi: 10.1128/AEM.00509-08

87. Nagasaki K, Tomaru Y, Katanozaka N, Shirai Y, Nishida K, Itakura S, et al. Isolation and characterization of a novel single-stranded RNA virus infecting the bloom-forming diatom Rhizosolenia setigera. *Appl Environ Microbiol.* (2004) 70:704–11. doi: 10.1128/AEM.70.2.704-711.2004

88. Carballal MJ, Villalba A, Iglesias D, Hine PM. Virus-like particles associated with large foci of heavy hemocytic infiltration in cockles Cerastoderma edule from Galicia (NW Spain). *J Invertebr Pathol.* (2003) 84:234–7. doi: 10.1016/j.jip.2003.11.002

89. Rasmussen LPD. Virus-associated granulocytomas in the marine mussel, *Mytilus edulis*, from three sites in Denmark. *J Invertebrate Pathol.* (1986) 48:117–23. doi: 10.1016/0022-2011(86)90150-3

90. Ip HS, Desser SS. A picornavirus-like pathogen of *Cotylogaster occidentalis* (Trematoda: Aspidogastrea), an intestinal parasite of freshwater mollusks. *J Invertebrate Pathol.* (1984) 43:197–206. doi: 10.1016/0022-2011(84)90138-1

frontiers | Frontiers in Veterinary Science

TYPE Original Research
PUBLISHED 11 January 2024
DOI 10.3389/fvets.2023.1283487

OPEN ACCESS

EDITED BY
Marta Martinez Aviles,
Instituto Nacional de Investigación y Tecnología Agroalimentaria (INIA), Spain

REVIEWED BY
Marta Dec,
University of Life Sciences of Lublin, Poland
Alois Cizek,
University of Veterinary and Pharmaceutical Sciences Brno, Czechia

*CORRESPONDENCE
Jae-Ik Han
✉ jihan@jbnu.ac.kr

†These authors have contributed equally to this work

RECEIVED 26 August 2023
ACCEPTED 20 December 2023
PUBLISHED 11 January 2024

CITATION
Kim M, Kim M, Yeo Y-G, Lee Y-T and Han J-I (2024) Antimicrobial resistance of commensal *Escherichia coli* and *Enterococcus faecalis* isolated from clinically healthy captive wild animals in Seoul zoo.
Front. Vet. Sci. 10:1283487.
doi: 10.3389/fvets.2023.1283487

Antimicrobial resistance of commensal *Escherichia coli* and *Enterococcus faecalis* isolated from clinically healthy captive wild animals in Seoul zoo

Minsu Kim[1,2†], Myeongsu Kim[2†], Yong-Gu Yeo[1], Young-Tae Lee[1] and Jae-Ik Han[2*]

[1]Conservation and Health Center, Seoul Zoo, Gwacheon, Republic of Korea, [2]Laboratory of Wildlife Medicine, College of Veterinary Medicine, Jeonbuk National University, Iksan, Republic of Korea

Despite the importance of antimicrobial resistance, only a few studies on the antimicrobial susceptibility on wild animals have been conducted owing to their population, accessibility, and characteristics. The objective of this study was to investigate the prevalence and characteristics of antimicrobial resistance pattern in *Escherichia coli* and *Enterococcus faecalis* isolated from the feces of captive wild animals in a zoo. A total of 61 captive wild animals were included in this study. *E. coli* was isolated from 58 of the 61 animals and *E. faecalis* was isolated from 29 animals. Among the isolated *E. coli* strains, ampicillin exhibited the highest resistance rate (27/29, 93.1%). Of these, 18 strains (18/29, 62%) showed multidrug resistance. The multilocus sequence typing (MLST) test showed that only ST155 was detected twice, while the other 16 strains showed different ST types. Among the *E. faecalis* strains, two were susceptible to all tested antimicrobials, whereas the remaining 27 strains showed resistance to one or more antimicrobials. Nine strains (9/27, 31%) showed multidrug resistance. Among the *E. faecalis* strains, resistance to quinupristin/dalfopristin was the highest at 96.3% (26/27), while the MLST of the nine MDR strains showed no predominant ST. Genetic association with human isolates or livestock products was observed in the isolated ST types. This indicates that antibiotic resistance in the zoo is responsible for the use of antibiotics and the partial horizontal transmission between humans and animals through feeding or contact.

KEYWORDS

antimicrobial resistance, zoo animals, genotype, *Escherichia coli*, *Enterococcus faecalis*

1 Introduction

Antimicrobial resistance is recognized as a major global health problem (1). The emergence of super bacteria (e.g., methicillin-resistant *Staphylococcus aureus* [MRSA], vancomycin-resistant *S. aureus* [VRSA], vancomycin-resistant *Enterococcus* [VRE], and *Salmonella typhimurium* DT104) that are resistant to antimicrobials and the emergence of multidrug-resistant bacteria that are resistant to various antimicrobials are major global health challenges (2–4). Antimicrobial-resistant bacteria pose the 21st century's greatest public health threat, which the world is actively combating. The emergence of antimicrobial-resistant

bacteria has been systematically researched by the U.S. Food and Drug Administration (FDA) since 1996. In Korea, the National Antimicrobial Resistance Safety Management Project began in 2003. Subsequently, research to analyze the distribution status and pattern of resistant bacteria by isolating various pathogenic bacteria from humans, livestock, fish, and the environment has been earnestly promoted.

Compared with antimicrobial resistance studies on livestock or companion animals in Korea, there are few studies that address the risk of antimicrobial resistance on wild animals. This is presumed to be due to the population of wild animals, conditions of conservation facilities, and the characteristics of individual wild species. While some studies have analyzed the antimicrobial resistance rates of pathogenic *Escherichia coli* isolated from wild animals in Korea (5, 6), there have been few studies on the antimicrobial resistance of indicator bacteria isolated from wild captive animals in Korean zoos.

Escherichia coli, which resides as a normal bacterium in the intestines of mammals such as humans and animals, is an opportunistic bacterium that is always exposed to antimicrobials and can cause disease when immunity is weakened. *E. coli* can easily acquire and transfer antimicrobial resistance and is considered a good bioindicator for observational studies on antimicrobial resistance (7, 8). Therefore, the antimicrobial resistance of target bacteria, such as those found in the environment, meat, and companion animals, are being actively studied. *E. faecalis*, like *E. coli*, is a normal bacterium in the mammalian intestine; however, nosocomial infections in hospitals have recently emerged in humans (9). Additionally, for some antimicrobials, there are intrinsic resistances that induce resistance in bacteria regardless of the use of antimicrobials. Acquired resistance due to the misuse of antimicrobials is also possible, serving as an indicator of antimicrobial resistance (10).

Recently, zoos have tended to focus on animal welfare and species conservation (11); however, some still use methods such as petting for zoo management and increasing public interest. It is possible to become infected with zoonotic pathogens through the ingestion of animal waste through the mouth, direct contact with animals, or contaminated surfaces (12). Another concern is animal-to-human transmission of antimicrobial-resistant bacteria (13). A strong positive correlation may exist between antibiotic use and antibiotic resistance in *E. coli* (14), and several studies have reported the horizontal transmission of zoonotic diseases from zoos or petting farms (15, 16).

The objectives of this study were: (1) to investigate antimicrobial resistance and (2) to analyze the relationship between commensal *E. coli* and *E. faecalis*, which are indicator bacteria, in captive wild animals at Seoul Zoo.

2 Materials and methods

2.1 Sample collection

Samples were collected from animals that needed medical care, e.g., health checkups and anesthesia for movement, but did not show clinical symptoms. A total of 61 healthy animals belonging to 32 species were included in this study. There were 55 mammals of 27 species—including Barbary sheep (*Ammotragus lervia*) and Olive baboons (*Papio Anubis*)—5 birds of 4 species, and 1 reptile of 1 species (dwarf crocodile [*Osteolaemus tetraspis*]). Among these sampled individuals, only black-faced spoonbills (sample no. 11) and Siberian tigers (sample no. 46, 47, 48, with the same parents) were less than 1-year-old. All others were reproductive adults.

Samples were collected through rectal swabs using a sterile transport medium (Asan Pharm, Seoul, Korea) between March 2022 and September 2022. To differentiate between *E. coli* and *E. faecalis* remaining in the soil, only anal swabs were used in this study, and samples were not collected from feces. The patient information is presented in Table 1.

From the perspective of animal ethics, animals were not intentionally captured in this study. Captures and anal swabs were obtained only when medical care was required. Ethical clearance for this study was approved by 2019–008, 2022–004 at the Seoul Zoo IACUC. All sampling was conducted according to the committee criteria.

2.2 Isolation and identification of *Escherichia coli* and *Enterococcus faecalis*

The swab samples were inoculated into thioglycollate medium (BD Difco™, Franklin, NJ, United States) and incubated at 37°C for 24 h, and then the cultured broth was inoculated into CHROMagar™ *E. coli* (CHROMagar™, Paris, France) and CHROMagar™ streptococcus (CHROMagar™) using a sterile loop needle. Bacterial colonies selected according to the criteria for each selective medium were enriched in trypticase soy agar containing 5% sheep blood (Asan Pharm, Seoul, Korea). Species identification was performed based on the sequences of the DNA *gyrase*B gene (*E. coli*) or the 16S ribosomal RNA gene (*E. faecalis*) according to the CLSI guidelines (17). The remaining DNA extract was stored at −20°C for multilocus sequence type (MLST) analysis.

2.3 Antimicrobial susceptibility test

The Kirby-Bauer disk diffusion method was performed according to CLSI guidelines (18). After the turbidity was adjusted as 0.5 McFaland standard, the bacterial suspension was smeared on Muller-Hilton agar (BD BBL™, Franklin, NJ, United States) antimicrobial disks (Oxoid, Hampshire, United Kingdom) were placed at equal intervals, followed by incubation at 37°C for 18 h (vancomycin for 24 h). Subsequently, the size of the inhibition zone was measured, and the presence or absence of antimicrobial resistance was determined according to CLSI guidelines (18). VRE measurements might have an error in the disk diffusion method (19); therefore, they were cross-validated using the E-TEST® strip (bioMerieux SA, Marcy-l'Étoile, France). For the-lactamase test, the double-disk diffusion method was used, and an amoxicillin-clavulanate disk was placed between cefepime and cefotaxime to observe diffusion. Quality control was performed using *E. coli* ATCC 25922, *S. aureus* ATCC 25923, and *E. faecalis* ATCC 29212.

While the resistance of *E. coli* was tested by disks of ampicillin (10 mcg), amoxicillin-clavulanate (30 mcg), cefepime (30 mcg), cefotaxime (30 mcg), meropenem (10 mcg), gentamicin (10 mcg), amikacin (30 mcg), sulfamethoxazole-trimethoprim (25 mcg),

10.3389/fvets.2023.1283487

TABLE 1 The list of zoo animals and antimicrobial resistance included in this study.

Serial	Animals		Antimicrobial resistance*	
	Name	Scientific name	*E. coli*	*E. faecalis*
1	Barbary sheep	*Ammotragus lervia*	No resistance	RD-QD
2	Olive baboon	*Papio anubis*	AMP	No isolation
3	Spotted seal	*Phoca largha*	AMP-CTX-C	No isolation
4	Barbary sheep	*Ammotragus lervia*	No resistance	No isolation
5	Egyptian fruit bat	*Rousettus aegyptiacus*	F-TE	No isolation
6	Puma	*Puma concolor*	AMP-CIP	RD-QD-CIP
7	Amur leopard cat	*Prionailurus bengalensis euptilurus*	AMP-TE-DO-CIP-SXT-C-F	E-DO-TE-RD-CIP-QD
8	Amur leopard cat	*Prionailurus bengalensis euptilurus*	AMP-CTX-TE-CIP-C-SXT	E-RD-QD
9	Red fox	*Vulpes vulpes*	AMP-TE-DO	E-DO-TE-C-QD-RD-CIP
10	Black-handed spider monkey	*Ateles geoffroyi*	AMP-TE-DO	RD-QD
11	Black-faced spoonbill	*Platalea minor*	TE-DO-SXT	No isolation
12	Barbary sheep	*Ammotragus lervia*	No resistance	RD
13	Barbary sheep	*Ammotragus lervia*	No resistance	No isolation
14	Barbary sheep	*Ammotragus lervia*	No resistance	No isolation
15	Barbary sheep	*Ammotragus lervia*	No resistance	No isolation
16	Barbary sheep	*Ammotragus lervia*	No resistance	No isolation
17	North American raccoon	*Procyon lotor*	AMP-FEP-CTX-TE-DO	No resistance
18	Dwarf crocodile	*Osteolaemus tetraspis*	No isolation	No isolation
19	White stork	*Ciconia ciconia*	No isolation	RD-QD
20	Przewalski's horse	*Equus ferus przewalskii*	AMP	No isolation
21	Western chimpanzee	*Pan troglodytes verus*	No resistance	No isolation
22	Black-faced spoonbill	*Platalea minor*	No resistance	QD
23	Spotted hyena	*Crocuta crocuta*	No isolation	QD-RD
24	Guanaco	*Lama guanicoe*	No resistance	No isolation
25	White-handed gibbon	*Hylobates lar*	AMP-TE-DO	No isolation
26	Yellow-throated marten	*Martes flavigula*	AMP-CN-SXT	QD-RD
27	Chattering lory	*Lorius garrulus*	No resistance	QD
28	Collared peccary	*Pecari tajacu*	No resistance	QD-E
29	Barbary sheep	*Ammotragus lervia*	No resistance	RD-QD
30	Barbary sheep	*Ammotragus lervia*	No resistance	No isolation
31	Barbary sheep	*Ammotragus lervia*	AMP-TE-DO-SXT-C	RD-QD
32	Barbary sheep	*Ammotragus lervia*	No resistance	No isolation
33	Barbary sheep	*Ammotragus lervia*	No resistance	No isolation
34	Barbary sheep	*Ammotragus lervia*	No resistance	No isolation
35	Barbary sheep	*Ammotragus lervia*	No resistance	No isolation
36	Indian peafowl	*Pavo cristatus*	No resistance	No isolation
37	Coyote	*Canis latrans*	No resistance	RD-QD
38	Barbary sheep	*Ammotragus lervia*	No resistance	No isolation
39	Bornean orangutan	*Pongo pygmaeus*	No resistance	No isolation
40	American black bear	*Ursus americanus*	AMP-FEP-CTX-CIP	No isolation
41	Mandrill	*Mandrillus sphinx*	No resistance	No isolation
42	Hamadryas baboon	*Papio hamadryas*	AMP-AMC-SXT	No isolation
43	Hamadryas baboon	*Papio hamadryas*	AMP-TE-DO-CIP-SXT	No isolation
44	Hamadryas baboon	*Papio hamadryas*	AMP-TE-DO-C	No isolation

(Continued)

TABLE 1 (Continued)

Serial	Animals		Antimicrobial resistance*	
	Name	Scientific name	*E. coli*	*E. faecalis*
45	Barbary sheep	*Ammotragus lervia*	No resistance	No isolation
46	Siberian tiger	*Panthera tigris altaica*	No resistance	E-QD-DO-TE
47	Siberian tiger	*Panthera tigris altaica*	AMP-AMC-TE-DO-CIP-C	QD
48	Siberian tiger	*Panthera tigris altaica*	No resistance	RD-QD
49	Western chimpanzee	*Pan troglodytes verus*	No resistance	RD-QD
50	Lion	*Panthera leo*	No resistance	E-DO-TE-RD-QD-CIP
51	Eurasian river otter	*Lutra lutra*	AMP-TE-SXT-C	QD
52	Red fox	*Vulpes vulpes*	AMP-FEP-CTX-CN-TE-CIP-SXT	RD-QD-CIP
53	Hamadryas baboon	*Papio hamadryas*	AMP-TE	QD
54	Hamadryas baboon	*Papio hamadryas*	AMP-AMC-SXT	No isolation
55	Banded mongoose	*Mungos mungo*	AMP-AMC-CIP	RD-QD-CIP
56	Hamadryas baboon	*Papio hamadryas*	AMP-AMC-SXT	No isolation
57	Gray wolf	*Canis lupus*	No isolation	E-AMP-QD-CIP
58	Spotted hyena	*Crocuta crocuta*	AMP-AMC-TE	No isolation
59	Barbary sheep	*Ammotragus lervia*	AMP	No isolation
60	Celebes crested macaque	*Macaca nigra*	AMP-AMC	QD-RD
61	Olive baboon	*Papio anubis*	AMP-AMC	No resistance

*AMP, ampicillin; AMC, amoxicillin-clavulanate; TE, tetracycline; DO, doxycycline; CIP, ciprofloxacin; CTX, cefotaxime; FEP, cefepime; CN, gentamicin; SXT, trimethoprim-sulfamethoxazole; C, chloramphenicol; E, erythromycin; RD, rifampin; QD, quinupristin-dalfopristin.

doxycycline (30 mcg), tetracycline (30 mcg), nitrofurantoin (300 mcg), chloramphenicol (30 mcg), and ciprofloxacin (5 mcg), the resistance of *E. faecalis* was tested by disks of penicillin G (10 U), ampicillin (10 mcg), erythromycin (15 mcg), vancomycin (30 mcg), doxycycline (30 mcg), tetracycline (30 mcg), nitrofurantoin (300 mcg), linezolid (30 mcg). chloramphenicol (30 mcg), rifampin (5 mcg), quinupristin/dalfopristin (15 mcg), and ciprofloxacin (5 mcg).

The proportion of antimicrobial-resistant strains was expressed as a percentage by dividing the number of resistant strains by the total number of positive strains. Multidrug-resistant bacteria were defined as strains showing resistance to three or more different classes of antimicrobials (20). The ratio of multi-drug resistant strains is expressed as a percentage of the total number of positive strains.

2.4 Multilocus sequence type

To evaluate the genetic relatedness of the isolated multidrug-resistant (MDR) bacterial clones, 7-gene MLST was conducted (Table 2). These 7 genes were amplified and sequenced to secure the nucleotide sequence of each gene, and the sequence type (ST) was determined by comparison with the PubMLST database.[1] Based on the obtained ST type number, burst analysis was performed to analyze the genetic relationships between clones.[2]

1 https://pubmlst.org/

2 https://online.phyloviz.net/index

2.5 Phylogenetic analysis

To evaluate the relatedness of the isolated *E. coli* strains, neighbor-joining phylogenetic analysis for *gyr*B gene sequence was performed using MEGA X (version 10.1).

3 Results

3.1 Antimicrobial resistance ratio of isolated *Escherichia coli*

The antimicrobial resistance of the isolated *E. coli* strains is shown in Table 1. *E. coli* was isolated from 58 of the 61 animals. Although 29 strains were susceptible to all tested antimicrobials (29/58, 50%), 29 strains were resistant to more than one. The 29 strains that showed resistance to more than one antimicrobial agent were ampicillin (27/29, 93.1%), tetracycline (16/29, 55.2%), sulfamethoxazole-trimethoprim (11/29, 37.9%), doxycycline (10/29, 34.5%), ciprofloxacin (8/29, 27.6%), and amoxicillin-clavulanate (8/29, 27.6%). Conversely, no resistance to meropenem and amikacin was observed. All strains were negative in the double-disk synergy test. Of the 61 samples, 18 strains (18/58, 31%) were MDR. Among the MDR *E. coli* strains, ampicillin resistance was the highest (17/18, 94%), followed by resistance to tetracycline and sulfamethoxazole-trimethoprim. Table 3 summarizes the results for MDR *E. coli*.

Among the species tested, Hamadryas baboons (*Papio hamadryas*; 5/6, 80.3%) and Amur leopard cats (*Prionailurus bengalensis euptilurus*; 2/2, 100%) showed the highest MDR strain retention.

TABLE 2 Oligonucleotide and their reaction conditions of 7-gene multilocus sequence type analysis used in this study.

Species	Locus	Primers	Sequence (5′to 3′)	Annealing temperature (°C)	Allele size (bp)	References
Escherichia coli	adk	ECO_adk_1F ECO_adk_1R	GCAATGCGTATCATTCTGCT CAGATCAGCGCGAACTTCAG	52	536	(42)
	fumC	ECO_FumC_1F ECO_FumC_1R	CCACCTCACTGATTCATGCG CGGTGCACAGGTAATGACTG	52	469	
	gyrB	ECO_gyrB_1F ECO_gyrB_1R	CGGGTCACTGTAAAGAAATTAT GTCCATGTAGGCGTTCAGGG	52	460	
	icd	ECO_icd_1F ECO_icd_1R	TACATTGAAGGTGATGGAATCG GTCTTTAAACGCTCCTTCGG	52	518	
	mdh	ECO_mdh_1F ECO_mdh_1R	TCTGAGCCATATCCCTACTG CGATAGATTTACGCTCTTCCA	52	452	
	purA	ECO_purA_1F ECO_purA_1R	CTGCTGTCTGAAGCATGTCC CAGTTTAGTCAGGCAGAAGC	52	478	
	recA	ECO_recA_1F ECO_RecA_1R	AGCGTGAAGGTAAAACCTGTG ACCTTTGTAGCTGTACCACG	52	510	
Enterococcus faecalis	gdh	EFA_gdh_1F EFA_gdh_1R	GGCGCACTAAAAGATATGGT CCAAGATTGGGCAACTTCGTCCCA	52	530	(43)
	gyd	EFA_gyd_1F EFA_gyd_1R	CAAACTGCTTAGCTCCAATGGC CATTTCGTTGTCATACCAAGC	52	395	
	pstS	EFA_pstS_1F EFA_pstS_1R	CGGAACAGGACTTTCGC ATTTACATCACGTTCTACTTGC	52	583	
	gki	EFA_gki_1F EFA_gki_1R	GATTTTGTGGGAATTGGTATGG ACCATTAAAGCAAAATGATCGC	52	438	
	aroE	EFA_aroE_1F EFA_aroE_1R	TGGAAAACTTTACGGAGACAGC GTCCTGTCCATTGTTCAAAAGC	52	459	
	xpt	EFA_xpt_1F EFA_xpt_1R	AAAATGATGGCCGTGTATTAGG AACGTCACCGTTCCTTCACTTA	52	456	
	yiqL	EFA_yiqL_1F EFA_yiqL_1R	CAGCTTAAGTCAAGTAAGTGCCG GAATATCCCTTCTGCTTGTGCT	52	436	

Contrastingly, MDR *E. coli* was isolated from only one of the 17 barbary sheep, despite the fact that barbary sheep were the largest population tested (17/61, 27.9%). Among the 18 MDR strains, 17 species were carnivores or omnivores and only one (Barbary sheep) was an herbivore.

3.2 Antimicrobial resistance ratio of isolated *Enterococcus faecalis*

The antimicrobial resistance of the isolated *E. faecalis* strains is shown in Table 1. *E. faecalis* was isolated from 29 of the 61 animals. While 2 strains were susceptible to all tested antimicrobials, 27 were resistant to one or more antimicrobials. Resistance to quinipristin/dalfopristin was the highest at 96.3% (26/27), followed by rifampin at 66.7% (18/27), and ciprofloxacin at 25.9% (7/27). No resistance to penicillin, nitrofurantoin, or linezolid was observed. Of the 29 strains, 9 (31.0%) showed MDR. Among the MDR *E. faecalis*, quinupristin/dalfopristin resistance was the highest at 100% (9/9), followed by resistance to rifampin and ciprofloxacin. Compared to the non-MDR *E. faecalis* strain, an increase in ciprofloxacin resistance was observed compared to that of the non-MDR *E. faecalis* strain. All the MDR *E. faecalis* were isolated from carnivores. No vancomycin resistance *E. faecalis* strains were isolated. Table 3 summarizes the results of the MDR *E. faecalis*.

3.3 Multilocus sequence type

Multilocus sequence typing (MLST) was performed on 18 MDR strains of *E. coli* and 9 MDR strains of *E. faecalis*. Seventeen STs were identified among MDR *E. coli* (Table 3). Except for ST155, which was simultaneously detected in Barbary sheep and spotted hyena, all ST types were detected only once. Of the 17 ST types, 7 ST types (ST1994, ST2448, ST5173, ST2161, ST5415, ST7224, and ST12646) were newly discovered. The 10 previously reported ST types have been reported in various sources such as humans, livestock (dogs, cows, pigs, chickens, and turkeys), environments (river, seawater, sewage, and wastewater), wild animals (vultures, elephants, guinea fowls, and hummingbirds), and plants (spinach), suggesting wide horizontal transmission of each clone worldwide (Table 4). Compared with the ST types reported in Korea, 7 ST types (ST90, ST155, ST162, ST206,

TABLE 3 Antimicrobial resistance and MLST type of multidrug-resistant *E.coli* and *E. faecalis* isolated in this study.

Bacteria	Serial	Animal (scientific name)	Antimicrobial resistance*	ST type	Note
Escherichia coli	3	Spotted seal (*Phoca largha*)	AMP-CTX-C	5,415	New ST
	7	Amur leopard cat (*Prionailurus bengalensis euptilurus*)	AMP-TE-DO-CIP-SXT-C-F	164	
	8	Amur leopard cat (*Prionailurus bengalensis euptilurus*)	AMP-CTX-TE-CIP-C-SXT	2,161	New ST
	11	Black-faced spoonbill (*Platalea minor*)	TE-DO-SXT	7,224	New ST
	17	North American raccoon (*Procyon lotor*)	AMP-FEP-CTX-TE-DO	162	
	26	Yellow-throated marten (*Martes flavigula*)	AMP-CN-SXT	38	
	31	Barbary sheep (*Ammotragus lervia*)	AMP-TE-DO-SXT-C	155	
	40	American black bear (*Ursus americanus*)	AMP-FEP-CTX-CIP	349	
	42	Hamadryas baboon (*Papio hamadryas*)	AMP-AMC-SXT	206	
	43	Hamadryas baboon (*Papio hamadryas*)	AMP-TE-DO-CIP-SXT	2,448	New ST
	44	Hamadryas baboon (*Papio hamadryas*)	AMP-TE-DO-C	542	
	47	Siberian tiger (*Panthera tigris altaica*)	AMP-AMC-TE-DO-CIP-C	1994	New ST
	51	Eurasian river otter (*Lutra lutra*)	AMP-TE-SXT-C	5,173	New ST
	52	Red fox (*Vulpes vulpes*)	AMP-FEP-CTX-CN-TE-CIP-SXT	90	
	54	Hamadryas baboon (*Papio hamadryas*)	AMP-AMC-SXT	1,421	
	55	Banded mongoose (*Mungos mungo*)	AMP-AMC-CIP	7,593	
	56	Hamadryas baboon (*Papio hamadryas*)	AMP-AMC-SXT	12,646	New ST
	58	Spotted hyena (*Crocuta Crocuta*)	AMP-AMC-TE	155	
Enterococcus faecalis	6	Puma (*Puma concolor*)	RD-QD-CIP	721	
	7	Amur leopard cat (*Prionailurus bengalensis euptilurus*)	E-DO-TE-RD-CIP-QD	36	
	8	Amur leopard cat (*Prionailurus bengalensis euptilurus*)	E-RD-QD	116	
	9	Red fox (*Vulpes vulpes*)	E-DO-TE-C-QD-RD-CIP	116	
	46	Siberian tiger (*Panthera tigris altaica*)	E-QD-DO-TE	1,362	New ST
	50	Lion (*Panthera leo*)	E-DO-TE-RD-QD-CIP	202	
	52	Red fox (*Vulpes vulpes*)	RD-QD-CIP	32	
	55	Banded mongoose (*Mungos mungo*)	RD-QD-CIP	1,363	
	57	Gray wolf (*Canis lupus*)	E-AMP-QD-CIP	76	

*AMP, ampicillin; AMC, amoxicillin-clavulanate; TE, tetracycline; DO, doxycycline; CIP, ciprofloxacin; CTX, cefotaxime; FEP, cefepime; CN, gentamicin; SXT, trimethoprim-sulfamethoxazole; C, chloramphenicol; E, erythromycin; RD, rifampin; QD, quinupristin-dalfopristin.

ST2161, ST2448, and ST5415) showed single-locus variants with existing Korean isolates, and all strains showing SLV relationships were isolated from humans (Figure 1). Among the 5 MDR strains isolated from hamadryas baboons, 2 showed SLV relationships with each other (ST542 and ST12646), 1 (ST206) with a human isolate, and 1 (ST2161) MDR strain of the amur leopard cat showed SLV relationships with human isolates.

Among the MDR *E. faecalis*, 8 ST were identified, of which 1 (ST1362) was new (Table 3). Interestingly, all but 1 of the previously reported 7 ST types (ST721, ST36, ST116, ST202, ST32, and ST 76) have been reported in humans, except for 1 (ST1363), for which the source was unknown, and 1 (ST32) out of 6 was reported from hospitalized patient specimens in China, Spain, Cuba, Germany, and Portugal. Compared to the ST type reported in Korea, three major clonal complexes containing the ST isolated in this study were identified (Figure 2). Particularly, ST32, ST36, and ST202, isolated from a red fox, amur leopard cat, and lion, respectively, showed SLV relationships with various domestic ST types isolated from pig farms (Table 5). The Puma isolate (ST721) and the spotted hyena isolate (ST984) showed close relationships at the SLV stage.

3.4 Phylogenetic analysis

Among 58 *E. coli* strains, a total of 52 *E. coli* strains were analyzed, including 18 MDR *E coli* strains. As a result of the analysis, the MDR strains were found to belong to the same clade except for one (ST5415; Figure 3). The 17 *E. coli* strains belonging to the same clade were composed of various species and animals with various feeding habits, showing contradictory results to MLST.

4 Discussion

This study was conducted to evaluate the degree and characteristics of antibiotic resistance in *E. coli* and *E. faecalis* in the intestines of clinically healthy zoo-fed wild animals. The results showed that both the isolated *E. coli* and *E. faecalis* were highly resistant to specific antibiotics (ampicillin, tetracycline, trimethoprim/sulfomethoxazole, and ciprofloxacin), besides the intrinsic resistance. Particularly, the incidence of MDR appears to be approximately 30% for both bacteria, suggesting that zoos cannot

TABLE 4 Information of multilocus sequence type and the clonal complex relationship of multidrug-resistant *E. coli* isolated in this study.

ST number	Animal (scientific name)	MLST							SLV* reported in Korea	
		adk	fumC	gyrB	icd	mdh	purA	recA	ST number	Origin
38	Yellow-throated marten (*Martes flavigula*)	4	26	2	25	5	5	19	None	N/A
90	Red fox (*Vulpes vulpes*)	6	4	12	1	20	8	7	410	human
155	Barbary sheep (*Ammotragus lervia*)	6	4	14	16	24	8	14	616	human
155	Spotted hyena (*Crocuta crocuta*)	6	4	14	16	24	8	14	616	human
162	North American raccoon (*Procyon lotor*)	9	65	5	1	9	13	6	517	human, environment
164	Amur leopard cat (*Prionailurus bengalensis euptilurus*)	6	4	32	16	12	8	7	None	N/A
206	Hamadryas baboon (*Papio hamadryas*)	6	7	5	1	8	18	2	793, 8,499	human
349	American black bear (*Ursus americanus*)	34	36	39	87	67	16	4	None	N/A
542	Hamadryas baboon (*Papio hamadryas*)	112	11	5	12	8	8	86	None	N/A
1,421	Hamadryas baboon (*Papio hamadryas*)	8	7	1	8	8	8	2	None	N/A
1994	Siberian tiger (*Panthera tigris altaica*)	83	14	10	14	17	94	28	None	N/A
2,161	Amur leopard cat (*Prionailurus bengalensis euptilurus*)	6	4	5	18	9	8	2	1,295	human
2,448	Hamadryas baboon (*Papio hamadryas*)	6	23	14	18	9	8	14	442	human
5,173	Eurasian river otter (*Lutra lutra*)	81	95	4	18	7	25	6	None	N/A
5,415	Spotted seal (*Phoca largha*)	9	23	64	548	11	8	6	642	human
7,224	Black-faced spoonbill (*Platalea minor*)	13	39	9	13	30	37	26	None	N/A
7,593	Banded mongoose (*Mungos mungo*)	6	29	3	18	11	26	14	None	N/A
12,646	Hamadryas baboon (*Papio hamadryas*)	112	11	5	12	8	445	86	None	N/A

*SLV, single-locus variant.

10.3389/fvets.2023.1283487

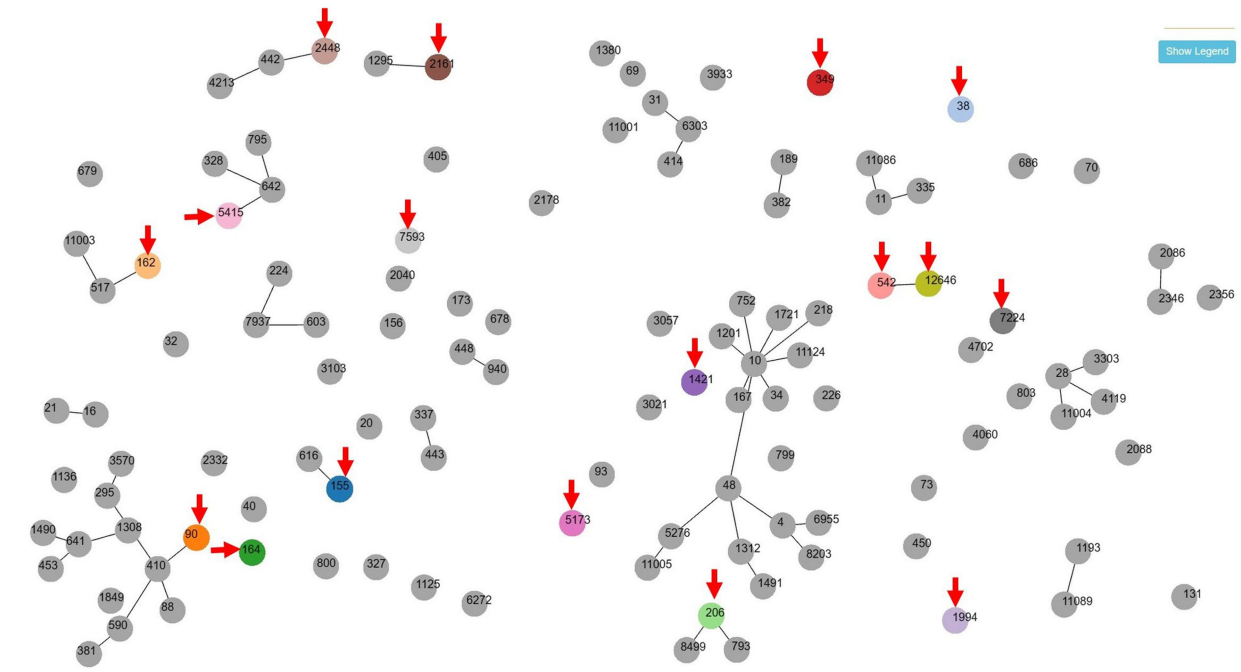

FIGURE 1
goeBURST (PHTLOViZ) analysis between multidrug-resistant *Escherichia coli* isolates of this study and strains reported in human in Korea. Seven zoo animal-origin ST types (ST90, ST155, ST162, ST206, ST2161, ST2448 and ST5415) showed single-locus variant relationships with human-origin existing Korean isolates while one ST type (ST38) was isolated in both of zoo animal (yellow-throated marten) and human. Arrows indicates the isolates of zoo animals in this study.

be an exception to the public health management of antibiotic resistance.

Three reasons have been suggested to explain why bacteria isolated from zoo animals acquire antibiotic resistance. First, owing to the characteristics of zoo animals, it is difficult to properly select antibiotics and administer them at an appropriate dose and duration. In zoo animals, it is often difficult to conduct appropriate tests in a timely manner when there is a need for antibiotics, and it is difficult to evaluate treatment progress. As a result, if the appropriate antibiotic is not used or if it is not used for a sufficient period and dose, it is easy for residual bacteria to acquire antibiotic resistance (21, 22). The *E. coli* isolated in this study showed high frequency of resistance to ampicillin, tetracycline, and trimethoprim/sulfamethoxazole. Owing to their wide application range and easy accessibility, these antibiotics have been widely used as empirical antibiotics in zoos, and the results of this study seem to reflect this. Among similar overseas zoo studies, a study at Chinese zoos showed that ampicillin, tetracycline, sulfamethoxazole-trimethoprim, and doxycycline have the highest *E. coli* resistance, which is similar to our results (23). However, a significant difference was that the ampicillin resistance rate in this study was 93% (27/29), which was higher than the Chinese study result (54.3%, 540/995). In the Petting Zoo of Canada, a study found that tetracycline and ampicillin resistance were the highest in captive wild animals (llamas and birds) targeting the non-O157 STEC serogroup (24). According to the results of a 2012 antimicrobial study conducted in a Japanese zoo, tetracycline, streptomycin, and ampicillin were the most common antibiotic resistance (25), which is largely consistent with the results of this study. Similar to the results of antimicrobial susceptibility studies in livestocks (26), resistance to tetracycline and ampicillin was high. The multidrug resistance rate was also higher than that of cattle (16%) but lower than that of pigs (69.7%) and chickens (82.6%) (26).

Second, food supplied to zoo animals is introduced in a state contaminated with resistant bacteria or resistant genes. The fact that antibiotic-resistant strains are more common in carnivorous and omnivorous mammals than in herbivorous mammals suggests that accumulation in the body of animals higher up in the food chain is also involved in antibiotic resistance. Among the MDR *E. coli* isolates in this study, previously reported ST types were all isolated from livestock products (chicken and cattle) and, for MDR *E. faecalis*, 4 of 7 cases were also reported from livestock products (chicken). Additionally, 17 of the 18 MDR *E. coli* strains were isolated from either carnivores or omnivores, and the fact that all *E. faecalis* isolates were isolated only from carnivores seems to reflect this. In zoos, there are cases where cheap imported food is supplied to breeding animals due to economic factors, and antibiotic resistance can be transferred through this; therefore, management measures for the current status of antibiotic resistance in the importing country or contamination of imported meat are needed.

The third factor is the potential for horizontal transmission between contact groups of animals, including zoo workers. In the case of methicillin-resistant *Staphylococcus pseudintermedius* isolated from dogs (*Canis lupus familiaris*), widespread horizontal transmission of a specific clone has been reported in the United States and Europe but not in Korea (27). A zoo is a closed and distinct ecosystem, a space in which direct contact between working veterinarians, zookeepers, and animals or indirect contact with objects, tools, and food occurs continuously, thus mutual horizontal transmission is possible. Based on the MLST and goeBurst analyses conducted in this study, 7 MDR *E. coli* isolates and three MDR *E. faecalis* isolates were found to be single-locus variants of strains reported from humans in Korea,

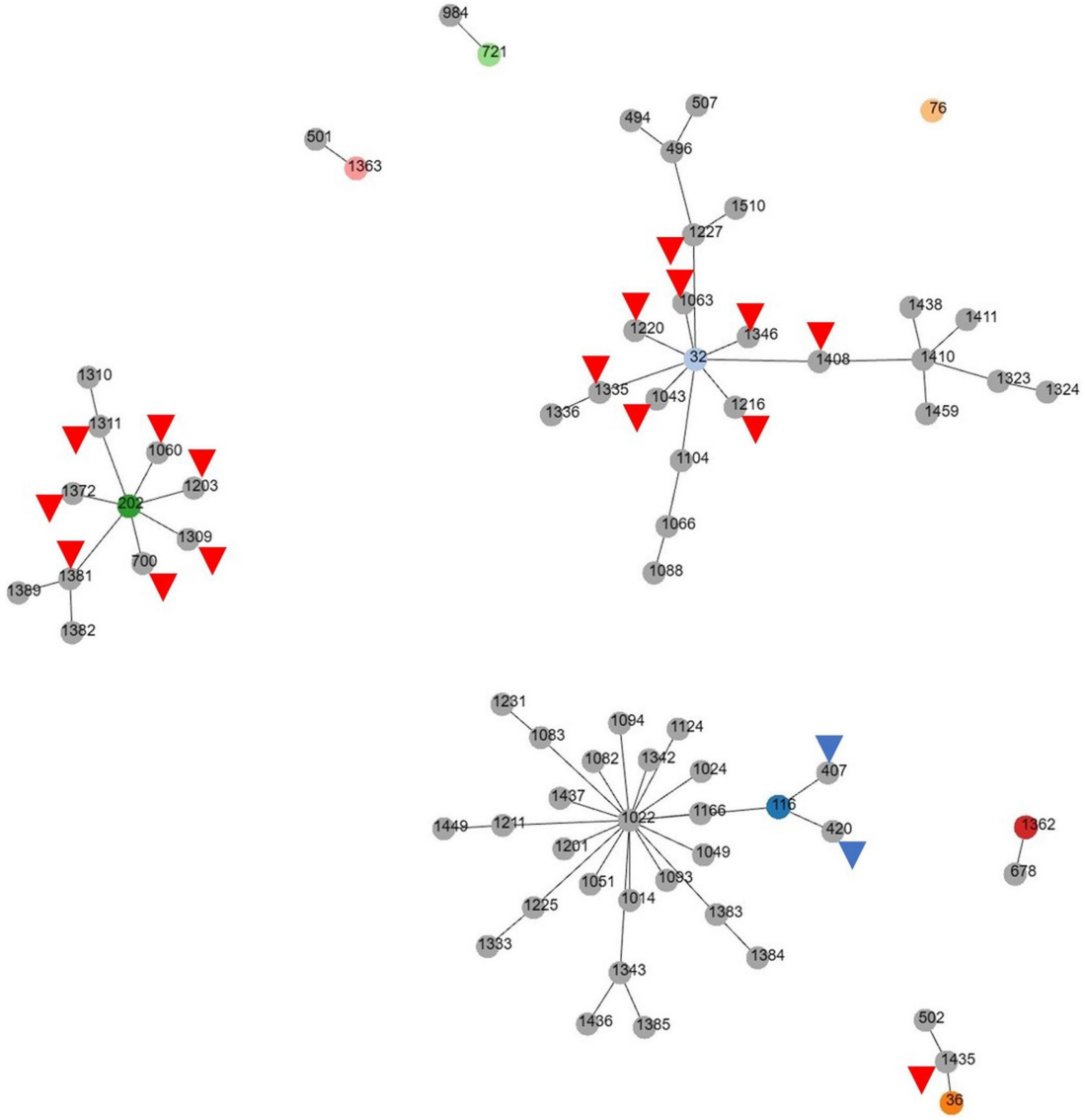

FIGURE 2
goeBURST (PHTLOViZ) analysis of multidrug-resistant *Enterococcus faecalis* reported in Korea. While three major clonal complexes containing the ST type isolated in this study are identified, ST32, ST116 and ST202 show SLV relationships with various domestic ST types isolated from pig farms (red arrowheads) or chicken (blue arrowheads).

suggesting the possibility that it is a change that occurs during the process of horizontal propagation in humans and animals. Therefore, continuous monitoring and investigation for the transmission are required to manage antibiotic resistance.

However, our results suggest that antibiotic resistance in the zoos investigated was not caused by a single factor. For example, in the case of food, carnivores receive meat provided from the same source at the same time daily; therefore, if food is the main entry route for resistance, carnivores should have the same or similar ST type, but this has not been the case. Rather, Barbary sheep and spotted hyenas with the same ST (ST155) have different diets and completely separate breeding areas, suggesting that the possibility of transmission by antibiotic use or contact with people or tools is higher than that by feeding. As a result of MLST for the MDR strain, a wide variety of ST types was detected, and only some shared the same ST, making it difficult to view horizontal transmission through direct or indirect contact between animals and humans or between animals and animals as the main route of antibiotic resistance acquisition. Resistance due to the use of antibiotics had a clear influence on the occurrence of resistance, given that resistance to antibiotics used by zoos was generally high in both strains investigated.

Of the 61 samples, Barbary sheep accounted for the majority (17 cases). The zoo investigated had about 55 Barbary sheep and regularly performed hoof care on about 20 Barbary sheep annually; therefore, the largest number of samples could be tested. All Barbary sheep ate the same feed in the same enclosure; there was little *E. coli* and *E. faecalis* resistance (5.9%, 1/17). However, as described in the results, Hamadryas baboons were the species that have highest frequency of MDR *E. coli* (83.3% 5/6). Similarly, MDR *E. faecalis* has been isolated from all carnivores, including pumas, Amur leopard cats, red foxes, Siberian tigers, lions, banded mongooses, and gray wolves. Various studies have shown that carnivores have higher multidrug resistance than omnivores or herbivores (28). Another factor that makes carnivores more resistant than other species in zoos is that, unlike

10.3389/fvets.2023.1283487

TABLE 5 Information of multilocus sequence type and the clonal complex relationship of multidrug-resistant *E. faecalis* isolated in this study.

ST number	Animal (scientific name)	MLST							SLV* reported in Korea	
		gdh	gyd	pstS	gki	aroE	xpt	yiqL	ST number	Origin
721	Puma (*Puma concolor*)	12	7	3	11	6	20	5	984	Spotted hyena
36	Amur leopard cat (*Prionailurus bengalensis euptilurus*)	16	2	19	16	17	15	11	1,435	Pig
116	Amur leopard cat (*Prionailurus bengalensis euptilurus*)	17	2	22	1	14	14	1	407, 420, 1,166	Chicken, chicken, human
116	Red Fox (*Vulpes vulpes*)	17	2	22	1	14	14	1	407, 420, 1,166	Chicken, chicken, human
1,362	Siberian tiger (*Panthera tigris altaica*)	15	4	37	1	17	1	11	678	Human
202	Lion (*Panthera leo*)	1	7	9	1	1	10	1	700, 1,060, 1,203, 1,309, 1,372	Pig
32	Red fox (*Vulpes vulpes*)	8	7	9	5	4	4	1	1,043, 1,063, 1,216, 1,220, 1,346	Pig
1,363	Banded mongoose (*Mungos mungo*)	12	7	7	5	39	2	36	501	Human
76	Gray wolf (*Canis lupus*)	22	6	7	26	22	4	4	none	

*SLV, single-locus variant.

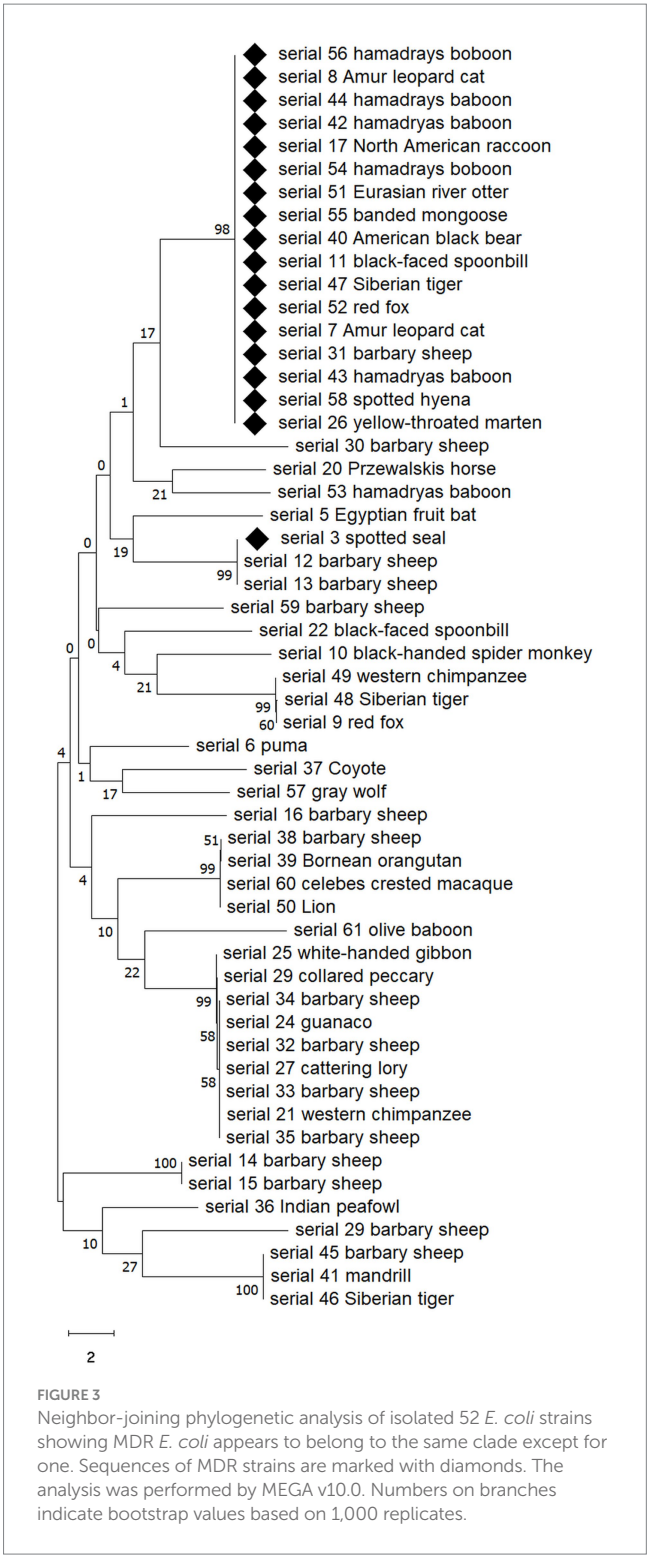

FIGURE 3
Neighbor-joining phylogenetic analysis of isolated 52 *E. coli* strains showing MDR *E. coli* appears to belong to the same clade except for one. Sequences of MDR strains are marked with diamonds. The analysis was performed by MEGA v10.0. Numbers on branches indicate bootstrap values based on 1,000 replicates.

herbivores, carnivores received more antimicrobials because antibiotics can be hidden in their food and can be easily administered. However, given that the biggest difference in feeding management between herbivores and carnivores is meat, the possibility that resistance factors (bacteria or gene) originate from meat cannot be ruled out (29, 30) and additional research is needed.

In this study, 7 MDR strains of *E. coli* showed SLV with human isolates in Korea while 6 MDR strains of *E. faecalis* showed SLV with

human isolates in Korea. Unlike *E. coli*, where it was difficult to determine the origin of SLV because of the lack of data, it was confirmed that three ST types (ST32, ST202 and ST116) of *E. faecalis* linked several SLVs previously identified in pig (ST 32 and ST202) or chicken/human (ST116) in Korea. Interestingly, ST32 was reported to be isolated from chicken meat in Korea (31), and in this study, it was confirmed to be the branched to several ST types isolated from pigs along with ST202. On the other hand, in the case of ST116, it was confirmed that it branched from a human isolate (ST1166) and into two isolates reported in chickens (ST407 and ST420), suggesting the possibility that humans were involved in the introduction into the zoo. However, the fact that different results are obtained from the same species points out that there are various factors involved in the introduction and spread of the bacteria.

What was interesting in this study was that among the 52 isolates of *E. coli* included in the phylogenetic tree analysis, the strains that showed MDR belonged to the same clade, except for one. In particular, they belonged to the same clade regardless of animal taxon, species, or feeding habits, which was contrary to the diversity of MDR *E. coli* ST types shown in MLST. This result suggests that among *E. coli* isolates from the zoo, strains belonging to a specific clade evaluated based on the *gyr*B gene acquired MDR more easily, or that a specific strain, although the origin is unclear, gradually spread and differentiated after acquiring MDR.

Although *Enterococcus* species is a commonly found bacterium in the intestine, *E. faecalis* was isolated from only 48% (29/61) of the animals in this study. While *E. faecalis* and *E. faecium* are known to be the most abundant species in humans (32), the distribution of *Enterococcus* species in animals has been reported to vary (33). In this study, we attempted to isolate and culture *E. faecalis* from various animals raised in zoos, but no consistent pattern was observed in animal taxa, species, or type of food consumed. However, considering that *Enterococcus* species may have a relationship of exchanging resistance with each other, future studies also need to confirm the resistance patterns of major *Enterococcus* species in each animal.

This study investigated the frequency and characteristics of antibiotic-resistant bacteria in zoo wild animals kept in limited spaces. As a result of the investigation, high MDR bacterial isolation was observed in carnivores, and clones isolated from human infection sites were detected, so continuous investigation into the introduction route appears to be necessary.

Data availability statement

The original contributions presented in the study are included in the article/supplementary material, further inquiries can be directed to the corresponding author.

Ethics statement

The animal study was approved by Institutional Animal Care and Use Committee in Seoul zoo. The study was conducted in accordance with the local legislation and institutional requirements.

Author contributions

MiK: Data curation, Formal analysis, Investigation, Methodology, Resources, Writing – original draft. MyK: Data curation, Investigation, Writing – original draft, Formal analysis, Software, Visualization. Y-GY: Data curation, Investigation, Writing – original draft, Resources. Y-TL: Writing – original draft, Data curation, Investigation. J-IH: Conceptualization, Formal analysis, Funding acquisition, Investigation, Methodology, Software, Supervision, Validation, Visualization, Writing – original draft, Writing – review & editing.

Funding

The author(s) declare financial support was received for the research, authorship, and/or publication of this article. This study was supported by the National Institute of Wildlife Disease Control and Prevention as a "Specialized Graduate School Support Project for Wildlife Diseases Specialists."

Acknowledgments

All authors thank the staff of the Seoul zoo for their helps on collecting samples.

Conflict of interest

The authors declare that the research was conducted in the absence of any commercial or financial relationships that could be construed as a potential conflict of interest.

Publisher's note

References

1. Robinson TP, Bu DP, Carrique-Mas J, Fèvre EM, Gilbert M, Grace D, et al. Antibiotic resistance is the quintessential one health issue. *Trans R Soc Trop Med Hyg*. (2016) 110:377–80. doi: 10.1093/trstmh/trw048

2. Ozawa Y, Tanimoto K, Nomura T, Yoshinaga M, Arakawa Y, Ike Y. Vancomycin-resistant enterococci in humans and imported chickens in Japan. *Appl Environ Microbiol*. (2002) 68:6457–61. doi: 10.1128/AEM.68.12.6457-6461.2002

3. Albertini MT, Benoit C, Berardi L, Berrouane Y, Boisivon A, Cahen P, et al. Surveillance of methicillin-resistant *Staphylococcus aureus* (MRSA) and Enterobacteriaceae producing extended-spectrum beta-lactamase (ESBLE) in northern France: a five-year multicentre incidence study. *J Hosp Infect*. (2002) 52:107–13. doi: 10.1053/jhin.2002.1286

4. Murthy R. Implementation of strategies to control antimicrobial resistance. *Chest*. (2001) 119:405S–11S. doi: 10.1378/chest.119.2_suppl.405s

5. Kwak HJ, Lee WW, Kim JH, Chung KT, Woo BG, Lee BG, et al. The antimicrobial susceptibility and plasmid profile of *E coli* isolates from wild bird. *Korean J Vet Ser*. (2006) 29:37–46.

6. Kim KH, Lim HS, Lee JW, Park DH, Yang CR, Cho JK. Antimicrobial resistance of *Escherichia coli* isolated from wild birds in Daegu. *Korean J Vet Ser*. (2021) 44:209–16. doi: 10.7853/kjvs.2021.44.4.209

7. Elena SF, Whittam TS, Winkworth CL, Riley MA, Lenski RE. Genomic divergence of *Escherichia coli* strains: evidence for horizontal transfer and variation in mutation rates. *Int Microbiol*. (2005) 8:271–8.

8. Miller K, O'Neill AJ, Chopra I. *Escherichia coli* mutators present an enhanced risk for emergence of antibiotic resistance during urinary tract infections. *Antimicrob Agents Chemother*. (2004) 48:23–9. doi: 10.1128/AAC.48.1.23-29.2004

9. Murray BE. Diversity among multidrug-resistant enterococci. *Emerg Infect Dis*. (1998) 4:37–47. doi: 10.3201/eid0401.980106

10. Sava IG, Heikens E, Huebner J. Pathogenesis and immunity in enterococcal infections. *Clin Microbiol Infect*. (2010) 16:533–40. doi: 10.1111/j.1469-0691.2010.03213.x

11. Ward SJ, Sherwen S, Clark FE. Advances in applied zoo animal welfare science. *J Appl Anim Welf Sci*. (2018) 21:23–33. doi: 10.1080/10888705.2018.1513842

12. Conrad CC, Stanford K, Narvaez-Bravo C, Callaway T, McAllister T. Farm fairs and petting zoos: a review of animal contact as a source of zoonotic enteric disease. *Foodborne Pathog Dis*. (2017) 14:59–73. doi: 10.1089/fpd.2016.2185

13. Collignon PJ, Conly JM, Andremont A, McEwen SA, Aidara-Kane A, WHO-AGISAR et al. World Health Organization ranking of antimicrobials according to their importance in human medicine: a critical step for developing risk management strategies for the use of antimicrobials in food production animals. *Clin Infect Dis*. (2016) 63:1087–93. doi: 10.1093/cid/ciw475

14. Chantziaras I, Boyen F, Callens B, Dewulf J. Correlation between veterinary antimicrobial use and antimicrobial resistance in food-producing animals: a report on seven countries. *J Antimicrob Chemother*. (2014) 69:827–34. doi: 10.1093/jac/dkt443

15. McMillian M, Dunn JR, Keen JE, Brady KL, Jones TF. Risk behaviors for disease transmission among petting zoo attendees. *J Am Vet Med Assoc*. (2007) 231:1036–8. doi: 10.2460/javma.231.7.1036

16. Stirling J, Griffith M, Dooley JG, Goldsmith CE, Loughrey A, Lowery CJ, et al. Zoonoses associated with petting farms and open zoos. *Vector Borne Zoonotic Dis*. (2008) 8:85–92. doi: 10.1089/vbz.2006.0639

17. Petti CA, Brandt ME, Church DL, Emler S, Simmon K, Zelazny AM. *Interpretive criteria for identification of Bacteria and Fungi by targeted DNA sequencing*. Wayne: Clinical and Laboratory Standards Institute (2018).

18. Lewis JS, Weinstein MP, Bobenchik AM, Campeau S, Cullen SK, Dingle T, et al. *Performance standards for antimicrobial susceptibility testing*. Wayne: Clinical and Laboratory Standards Institute (2022).

19. Lee SY, Park JH, Park HS, Lee MA, Kang ES, Hong KS. Comparison of antimicrobial susceptibility testing methods to detect glycopeptide resistance in enterococci-E-test, Vitek, disk diffusion and agar dilution method. *Korean J Clin Pathol*. (2000) 20:301–7.

20. Magiorakos AP, Srinivasan A, Carey RB, Carmeli Y, Falagas ME, Giske CG, et al. Multidrug-resistant, extensively drug-resistant and pandrug-resistant bacteria: an international expert proposal for interim standard definitions for acquired resistance. *Clin Microbiol Infect*. (2012) 18:268–81. doi: 10.1111/j.1469-0691.2011.03570.x

21. Blue JL, Wooley RE. Antibacterial sensitivity patterns of bacteria isolated from dogs with otitis externa. *J Am Vet Med Assoc*. (1977) 171:362–3.

22. Rodrigues da Costa M, Diana AA. A systematic review on the link between animal welfare and antimicrobial use in captive animals. *Animals (Basel)*. (2022) 12:1025. doi: 10.3390/ani12081025

23. Zhu Z, Jiang S, Qi M, Liu H, Zhang S, Liu H, et al. Prevalence and characterization of antibiotic resistance genes and integrons in *Escherichia coli* isolates from captive non-human primates of 13 zoos in China. *Sci Total Environ*. (2021) 798:149268. doi: 10.1016/j.scitotenv.2021.149268

24. Conrad CC, Stanford K, Narvaez-Bravo C, Neumann NF, Munns K, Tymensen L, et al. Zoonotic fecal pathogens and antimicrobial resistance in Canadian petting zoos. *Microorganisms*. (2018) 6:70. doi: 10.3390/microorganisms6030070

25. Ishihara K, Hosokawa Y, Makita K, Noda J, Ueno H, Muramatsu Y, et al. Factors associated with antimicrobial-resistant *Escherichia coli* in zoo animals. *Res Vet Sci*. (2012) 93:574–80. doi: 10.1016/j.rvsc.2011.09.006

26. Lim SK, Nam HM, Moon DC, Jang GC, Jung SC, Korean V. Antimicrobial resistance of *Escherichia coli* isolated from healthy animals during 2010-2012. *Korean J Vet Res*. (2014) 54:131–7. doi: 10.14405/kjvr.2014.54.3.131

27. Han JI, Rhim H, Yang CH, Park HM. Molecular characteristics of new clonal complexes of *Staphylococcus pseudintermedius* from clinically normal dog. *Vet Q*. (2017) 38:14–20. doi: 10.1080/01652176.2017.1400710

28. Bamunusinghage NPD, Neelawala RG, Magedara HP, Ekanayaka NW, Kalupahana RS, Silva-Fletcher A, et al. Antimicrobial resistance patterns of fecal *Escherichia coli* in wildlife, urban wildlife, and livestock in the eastern region of Sri Lanka, and differences between carnivores, omnivores, and herbivores. *J Wildl Dis*. (2022) 58:380–3. doi: 10.7589/JWD-D-21-00048

29. Rahman MA, Rahman AKMA, Islam MA, Alam MM. Antimicrobial resistance of *Escherichia coli* isolated from milk, beef and chicken meat in Bangladesh. *Bangl J Vet Med*. (2017) 15:141–6. doi: 10.3329/bjvm.v15i2.35525

30. White DG, Zhao S, Simjee S, Wagner DD, McDermott PF. Antimicrobial resistance of foodborne pathogens. *Microbes Infect*. (2002) 4:405–12. doi: 10.1016/s1286-4579(02)01554-x

31. Kim YB, Seo HJ, Seo KW, Jeon HY, Kim DK, Kim SW, et al. Characteristics of high-level ciprofloxacin-resistant *Enterococcus faecalis* and *Enterococcus faecium* from retail chicken meat in Korea. *J Food Prot*. (2018) 81:1357–63. doi: 10.4315/0362-028X.JFP-18-046

32. Zaheer R, Cook SR, Barbieri R, Goji N, Cameron A, Petkau A, et al. Surveillance of *Enterococcus* spp. reveals distinct species and antimicrobial resistance diversity across a one-health continuum. *Sci Rep*. (2020) 10:3937. doi: 10.1038/s41598-020-61002-5

33. Medeiros AW, Blaese Amorim D, Tavares M, de Moura TM, Franco AC, d'Azevedo PA, et al. *Enterococcus* species diversity in fecal samples of wild marine species as determined by real-time PCR. *Can J Microbiol*. (2017) 63:129–36. doi: 10.1139/cjm-2016-0427

frontiers | Frontiers in Veterinary Science

TYPE Opinion
PUBLISHED 17 January 2024
DOI 10.3389/fvets.2024.1313182

OPEN ACCESS

EDITED BY
Chase A. LaDue,
Oklahoma City Zoo and Botanical Garden, United States

REVIEWED BY
Charles Ritzler,
San Antonio Zoo, United States
Sue Margulis,
Canisius College, United States

*CORRESPONDENCE
Matyas Liptovszky
✉ liptovszky@gmail.com

RECEIVED 10 October 2023
ACCEPTED 08 January 2024
PUBLISHED 17 January 2024

CITATION
Liptovszky M (2024) Advancing zoo animal welfare through data science: scaling up continuous improvement efforts.
Front. Vet. Sci. 11:1313182.
doi: 10.3389/fvets.2024.1313182

Advancing zoo animal welfare through data science: scaling up continuous improvement efforts

Matyas Liptovszky[1,2]*

[1]Perth Zoo, South Perth, WA, Australia, [2]School of Veterinary Medicine and Science, University of Nottingham, Sutton Bonington, United Kingdom

KEYWORDS

animal welfare, zoo, data science, continuous improvement, evidence-based decision making, artificial intelligence, machine learning

1 Introduction

Advancing animal welfare in zoos is a multifaceted endeavor that lies at the core of their conservation and educational missions. While zoos have made significant strides in improving the wellbeing of their animal residents, challenges persist in ensuring a comprehensive, evidence-based approach to continuous improvement. Some of these challenges stem from the exponential growth of animal welfare in the last few decades, making it difficult to keep up with ever evolving theories and practical assessment methodologies (1). Others are related to the inherent resource limitations of any organization, including staff time and financial resources dedicated to animal welfare. A significant limitation with the latter is staff time allocated to animal observation and other data collection.

Untapped potential currently exists for data science as a transformative tool to overcome some of these challenges and further advance animal welfare practices in zoos. Data science is an interdisciplinary field that involves the extraction of valuable insights and knowledge from large and complex datasets through a combination of statistical analysis, machine learning, and domain expertise. It encompasses various processes, including data collection, cleaning, and transformation, as well as the application of algorithms and machine learning models to uncover patterns, trends, and correlations within the data. Data science leverages programming languages and tools to process and visualize data, enabling data scientists to interpret and communicate findings effectively. It empowers organizations to make informed decisions, predict future trends, and solve complex problems across diverse domains, from business and healthcare to environmental sciences and beyond. As data continues to proliferate in the digital age, data science plays a crucial role in extracting meaningful knowledge and unlocking the potential for innovation and advancements in numerous fields (2).

The data science lifecycle starts with problem identification and business understanding: the need to deeply understand the operational environment where the data collection and analysis (and any subsequent predictions) will be carried out, and the reasons why we would do that. This provides opportunities for zoos to consider various approaches to how data science can be implemented within existing systems. This can be simple, by analyzing single data sources, or complex, aiming at comprehensive welfare assessments based on all available evidence. A key to the success of this step is domain expertise, in our case expertise from animal care, veterinary and animal behavior and welfare staff. Emphasizing this key first step is also likely an important solution to reduce resistance toward novel technologies and methodologies, as it ensures that the inherent knowledge and expertise of the zoo team are captured.

By adopting a data-driven approach, zoos can capitalize on the wealth of information already available from diverse sources, including readily available daily keeper reports, animal health records, behavioral observations, enclosure data, as well as through emerging technologies such as CCTV footage, environmental sensors, and acoustic recordings. Harnessing the power of data science could allow for efficient and in-depth assessments of animal welfare, enabling zoos to extend their focus to a larger number of animals and make evidence-based decisions for their care. This shift toward data-driven decision-making not only optimizes resource allocation but also leads to a more substantial and positive impact on animal welfare.

Furthermore, integrating data science into daily operations and research can foster collaboration between experts from various fields, including data scientists, academics, and zoo professionals. By encouraging the exchange of knowledge and expertise, this collaborative effort will help zoos address common challenges. Embracing technological change and fostering collaboration will lead to an evidence-based approach for the continuous improvement of animal welfare in zoos. Ultimately, this approach not only benefits the animals under our care but also empowers staff working toward increasingly better animal welfare outcomes and provides vital proof of these efforts for visitors and the broader society.

2 Scalability, efficiency, and impact

Efficiently assessing the welfare of animals in zoos is critical to ensure that resources are allocated appropriately and that continuous improvement efforts are most impactful. Many zoos conduct welfare assessments, carried out through careful observation of animals and/or evaluation of data collected by trained staff. This can be, however, labor intensive, limiting the scale and frequency of such evaluations. The need for scalability and efficiency calls for innovative solutions that can harness the vast amount of data collected daily in zoo environments. Zookeepers record data on animal behavior, nutrition, provision of various aspects of care, including environmental enrichment activities, as well as environmental parameters in general, creating valuable datasets for analysis. Veterinarians and other animal health staff likewise record a plethora of health-related data, including clinical signs, diagnostic test results, preventative health measures, anesthesia data, and drug usage.

For over 1,300 zoos the Species360 Zoological Information Management System (ZIMS) serves as a central repository for animal data, and it currently includes millions of husbandry and health records representing over 50 years from over 10 million individuals of 22,000 species (3). By tapping into this wealth of data and embracing data science techniques and technology, zoos can gain valuable insights into animal behavior and health, identify potential welfare issues, and assess the effectiveness of enrichment programs.

Zoos also increasingly generate data in various other ways, including through CCTV and other audiovisual monitoring, or environmental monitoring and control systems. Some of these systems are installed primarily for animal care purposes, but many others exist for security, environmental, or facility management purposes. Data are also collected on a wide range of other aspects of zoo operations, from visitor attendance, demographics, and spending to weather patterns to maintenance records. In most instances, these data sources currently remain untapped from an animal welfare perspective, as frequently these are collated in isolated business systems specific to their core task. The combination of traditional animal care staff-collected data and these novel data sources could foster a more holistic approach to animal welfare assessment, leading to comprehensive and data-driven decision-making, as well as significantly improved effectiveness.

Machine learning algorithms can analyze this wealth of data and identify patterns that may not be immediately apparent to staff. By automating data collection and analysis, zoos can free up resources that were previously spent on these time-consuming tasks, allowing staff to focus on data interpretation, evidence-based decision-making, and finding the most impactful improvement opportunities. This shift toward data-driven decision-making can lead to more targeted and impactful interventions, promoting the wellbeing of a larger number of animals in the zoo's care, while empowering zoo experts to utilize the best available evidence.

While data science in zoos is still in its early stages, there are some examples of narrow-scale successful implementations. Some zoos have already begun using CCTV footage to analyze animal behavior and the use of enrichment activities. Machine learning algorithms can process vast amounts of video data to identify behavioral patterns and evaluate the effectiveness of enrichment strategies (4–7). However, Zuerl at al. reviewed currently available commercial systems, as well as previously published frameworks to automate the analysis of video streams. This study concluded that while the potential is great to utilize machine learning for this purpose, currently there are few frameworks which would be fully suitable for zoos and further development in this fields is needed (4). Researchers have harnessed large-scale ZIMS datasets for various purposes, including understanding cancer risk in mammals, senescence in testudines, and sex differences in survival and aging in wild mammals (8–10). A broader review of technology to monitor zoo animal welfare highlighted that by combining multiple data sources, continuous automated monitoring of affective state could be achieved in real or near-real time. In addition, this could also increase our knowledge of certain, currently not well-understood conditions (11). Regional zoo associations also identified taxon and veterinary advisors to help assessing population level trends, and making recommendations to improve health, nutrition, and holistic animal welfare.

These examples demonstrate the potential of data-driven approaches to improve animal welfare by providing insights into animal behavior and preferences, as well as other biological phenomena. These technologies also allow individual-level analysis, which can provide optimized care practices and reduce redundant activities, for example, the provision of environmental enrichment that has no utility. Overall, this can lead to increasing efficiency, which, in turn, leads to better scalability and overall impact.

3 Addressing challenges in implementation

Despite the vast potential of data science, several challenges hinder its widespread implementation in zoo settings. Limited access to relevant knowledge and technology, a lack of understanding of data science principles among zoo professionals, resistance to change, concerns about automating a task currently highly trained staff are entrusted to carry out, incomplete record keeping, and reluctance to share data might be among the common barriers. To overcome these challenges, fostering collaboration between data scientists, academics, and zoo professionals is a key aspect. This collaborative effort can facilitate knowledge exchange and skills development, empowering zoo staff to embrace data-driven approaches confidently. Additionally, investing in training and resources for zoo professionals in data science methodologies can help bridge the gap and facilitate the integration of data science into daily zoo operations, as well as reducing fear and suspicion. Emphasizing the practical applications and benefits of data science in enhancing animal welfare can foster a culture of openness to technological change within zoos.

Ensuring ethical data collection and use practices and addressing potential bias in AI systems are also critical considerations. Respecting human privacy and confidentiality is paramount in data collection and analysis, and challenges around this using automated recording systems, like camera traps, have been previously highlighted in wildlife conservation (12). Zoos must establish robust data privacy and security protocols to protect sensitive information collected either for the primary purpose of improving animal welfare or as a side effect. Moreover, AI systems used for welfare assessments must be carefully designed to avoid bias and ensure fair and accurate evaluations. By integrating ethical considerations into the data science process, zoos can build trust with the public and other stakeholders, including staff.

4 Integrating data science into zoo animal welfare

Data science offers opportunities for improving day-to-day zoo operations. By analyzing data on animal behavior, health, and environmental conditions, zoos can optimize resource allocation, develop targeted animal care, veterinary management, and enrichment strategies, therefore enhancing animal welfare. The integration of data science into daily operations fosters a more holistic and data-driven approach to animal care, ultimately improving the quality of life for animals in captivity.

Modern businesses have successfully leveraged data science to optimize processes, gain insights, and make informed decisions, and zoos can benefit from these comparable use cases. Data science is likely already integrated into certain business systems within zoos, and extending this usage to animal welfare can unlock significant benefits. Embracing technological change will position zoos at the forefront of animal welfare innovation and enable them to leverage the full potential of data science for continuous improvement. It also has the potential to ensure the ongoing existence of a social license to operate in an environment that is increasingly critical about industries where live animals are a key part of the business.

The successful implementation of data science in zoos necessitates collaboration among various stakeholders. Data scientists, academics, and zoo professionals each bring unique expertise and perspectives to the table. Collaboration facilitates knowledge exchange, helps address challenges, and encourages the adoption of data-driven approaches. Data scientists can provide guidance on data collection, analysis, and AI model development, while zoo professionals contribute essential insights into animal behavior, care, and welfare priorities. Together, these collaborative efforts ensure that data science serves as a transformative tool for advancing animal welfare in zoos.

5 Conclusion

Data science presents a transformative opportunity for advancing animal welfare in zoos. By adopting a data-driven approach, zoos can efficiently and effectively assess the wellbeing of a larger number of animals, optimize resource allocation, and make evidence-based decisions. The integration of diverse data sources allows for comprehensive welfare assessments and enriches our understanding of animal behavior and health. Addressing challenges related to knowledge, technology, and resistance to change requires collaboration and investment in training and resources. Ensuring ethical data collection and use, as well as addressing bias in AI systems are essential considerations. Embracing technological change and fostering collaboration between experts are pivotal for success. Data science offers a compelling path forward, empowering zoos to embrace a more evidence-based, data-driven approach to continuously improve animal welfare. This collective effort could positively impact animals, visitors, and staff alike, further elevating the vital role zoos play in conservation, education, and research.

Author contributions

ML: Conceptualization, Writing – original draft, Writing – review & editing.

Funding

The author(s) declare that no financial support was received for the research, authorship, and/or publication of this article.

Acknowledgments

I am grateful to Brian Carter and Emily Polla for the inspiring conversations through our collaborative project about artificial intelligence in zoo animal welfare. Thanks to Rachel Thompson

and Lorraine Miller for providing valuable feedback on the draft manuscript.

Conflict of interest

The author declares that the research was conducted in the absence of any commercial or financial relationships that could be construed as a potential conflict of interest.

Publisher's note

References

1. Freire R, Nicol C. A bibliometric analysis of past and emergent trends in animal welfare science. *Anim welf.* (2019) 28:465–85. doi: 10.7120/09627286.28.4.465

2. Cao L. Data science: a comprehensive overview. *ACM Comput Surv.* (2018) 50:1–42. doi: 10.1145/3076253

3. Species360 Zoological Information Management System (ZIMS). zims.Species360.org. Minneapolis, MN (2024). Available online at: https://species360.org/serving-conservation/citation-guidelines/

4. Zuerl M, Stoll P, Brehm I, Raab R, Zanca D, Kabri S, et al. Automated video-based analysis framework for behavior monitoring of individual animals in zoos using deep learning-a study on polar bears. *Animals.* (2022) 12:692. doi: 10.3390/ani12060692

5. Brookes O, Gray S, Bennett P, Burgess KV, Clark FE, Roberts E, et al. Evaluating cognitive enrichment for zoo-housed gorillas using facial recognition. *Front Vet Sci.* (2022) 9:886720. doi: 10.3389/fvets.2022.886720

6. Congdon JV, Hosseini M, Gading EF, Masousi M, Franke M, MacDonald SE. The future of artificial intelligence in monitoring animal identification, health, and behaviour. *Animals.* (2022) 12:1711. doi: 10.3390/ani12131711

7. Polla E, Carter B, Liptovszky M. AI for animal welfare: a strategic partnership to advance zoo animal welfare utilising artificial intelligence technology. In: *Zoo and Aquarium Association (Australasia) Annual Conference Melbourne: Zoo and Aquarium Association (Aus tralasia).* Melbourne (2022).

8. Lemaître JF, Ronget V, Tidière M, Allainé D, Berger V, Cohas A, et al. Sex differences in adult lifespan and aging rates of mortality across wild mammals. *Proc Natl Acad Sci USA.* (2020) 117:8546–53. doi: 10.1073/pnas.1911999117

9. Silva R da, Conde DA, Baudisch A, Colchero F. Slow and negligible senescence among testudines challenges evolutionary theories of senescence. *Science.* (2022) 376:1466–70. doi: 10.1126/science.abl7811

10. Vincze O, Colchero F, Lemaître JF, Conde DA, Pavard S, Bieuville M, et al. Cancer risk across mammals. *Nature.* (2022) 601:263–7. doi: 10.1038/s41586-021-04224-5

11. Diana A, Salas M, Pereboom Z, Mendl M, Norton T. A systematic review of the use of technology to monitor welfare in zoo animals: is there space for improvement? *Animals.* (2021) 11:3048. doi: 10.3390/ani11113048

12. Sharma K, Fiechter M, George T, Young J, Alexander JS, Bijoor A, et al. Conservation and people: towards an ethical code of conduct for the use of camera traps in wildlife research. *Ecol Solut Evidence.* (2020) 1:e12033. doi: 10.1002/2688-8319.12033

frontiers | Frontiers in Veterinary Science

TYPE Original Research
PUBLISHED 12 March 2024
DOI 10.3389/fvets.2024.1305643

OPEN ACCESS

EDITED BY
Carlos Sacristán Yagüe,
Centro de Investigación en Sanidad Animal (CISA), Spain

REVIEWED BY
Jose Angel Barasona,
Complutense University of Madrid, Spain
Giovanni Sgroi,
Experimental Zooprophylactic Institute of Southern Italy (IZSM), Italy

*CORRESPONDENCE
Lea Tummeleht
✉ lea.tummeleht@emu.ee

RECEIVED 02 October 2023
ACCEPTED 15 February 2024
PUBLISHED 12 March 2024

CITATION
Tummeleht L, Häkkä SSS, Jürison M, Vilem A, Nurmoja I and Viltrop A (2024) Wild boar (*Sus scrofa*) carcasses as an attraction for scavengers and a potential source for soil contamination with the African swine fever virus. *Front. Vet. Sci.* 11:1305643. doi: 10.3389/fvets.2024.1305643

Wild boar (*Sus scrofa*) carcasses as an attraction for scavengers and a potential source for soil contamination with the African swine fever virus

Lea Tummeleht[1]*, Susanna Suvi Siviä Häkkä[1], Margret Jürison[2], Annika Vilem[1,3], Imbi Nurmoja[3] and Arvo Viltrop[1]

[1]Institute of Veterinary Medicine and Animal Sciences, Estonian University of Life Sciences, Tartu, Estonia, [2]Institute of Agricultural and Environmental Sciences, Estonian University of Life Sciences, Tartu, Estonia, [3]The National Centre for Laboratory Research and Risk Assessment, LABRIS, Tartu, Estonia

The wild boar (*Sus scrofa*) is a social animal species native to Eurasia. During the last decade, the wild boar population in Estonia has been severely affected by the African swine fever virus (ASFV), which has also affected domestic pig farming. The potential transmission routes of ASFV remain unclear and are currently under intensive investigation. This pilot study aimed to clarify the frequency and characteristics of contacts between living wild boars and the carcasses of their conspecifics, which could play a role in the transmission of ASFV. Wild animals' contact and scavenging behavior on wild boar carcasses were studied using trail cameras in an experimental setting on Hiiumaa, Western Estonia. Four legally hunted carcasses were used in the present study. This study aimed to determine whether intraspecies scavenging occurs in wild boars. The persistence of ASFV DNA in soil contaminated with infected wild boar carcasses was investigated separately. Among the 17 identified wildlife species that visited wild boar carcasses, the common raven (*Corvus corax*) was the most frequent one (37.26%), followed by raccoon dogs (*Nyctereutes procyonoides*; 4.25%), carcass conspecific/wild boars (3.16%), and red foxes (*Vulpes vulpes*; 2.14%). Regarding the direct contact with the carcass, the same species ranking was detected: common raven (74.95%), raccoon dogs (9.94%), wild boars (4.21%), and red foxes (4.21%). No clear signs of cannibalism were noted among the wild boars, although brief physical contact with the carcasses was evident. The persistence of ASFV DNA in soil contaminated by infected wild boar carcasses was investigated separately. This study revealed that ASFV DNA from infected carcasses could be detected in forest soil for prolonged periods, even after removing the carcasses. Hence, the carcasses of infected wild boars may play an important role in spreading the African swine fever virus in wild boar populations; thus, prompt removal and disinfection of the soil could be considered necessary to limit the spread of the infection.

KEYWORDS

common raven (*Corvus corax*), ASFV infection, virus DNA, ASFV p72 gene, carcass decomposition

1 Introduction

Scavenging infected animal carcasses is considered a potential transmission route for many pathogens in wildlife (1). There are several potentially scavenging-mediated infectious diseases including tuberculosis, brucellosis, anthrax, tularemia, and African swine fever (ASF), as the causative agents can be ingested [e.g., (1–4)]. Furthermore, the opening of the carcass by vertebrate scavengers can cause pathogens (e.g., anthrax-causing bacteria *Bacillus anthracis*) to depart the carcass, contaminate the environment, or facilitate further spread by vectors (1). However, especially for birds of prey, eating carcasses helps reduce the potential of an infected source to spread infection (1). It has been shown that, in the specialized digestive system of raptors (e.g., low gastric pH and specialized microbiomes), most pathogens will not survive [e.g., (5)], and removing carcasses quickly from the environment prevents heavy pathogen loads in the substrate below the carcass (6). The other factor that reduces the infection load of carcasses is the natural decomposition process that occurs relatively rapidly. As a result, there is only limited availability of carrions for scavengers to consume (6). However, almost all carnivorous vertebrates should be regarded as facultative scavengers because they frequently contact and/or consume fresh carcasses when available (6). Hence, scavenging refers to a process that should be followed to understand disease outbreaks and reservoirs in wildlife better.

Since 2007, when African swine fever virus genotype II was first detected in Eastern Europe, wild boars (*Sus scrofa*) have played an important role in the rapid spread of the disease (7, 8), which was also observed in Estonia. Wild boars have experienced re-emerging outbreaks since the introduction of the African swine fever virus (ASFV) in Estonia in September 2014 (9, 10). Intraspecies scavenging among wild boars has been suggested as a possible means of transmission of ASFV; however, the scavenging behavior of wild boars has not been extensively studied, and it seems that wild boar behavior differs between countries (11–13). As social animals, suids do not always scavenge but investigate their deceased conspecifics and use their natural rooting behavior to search for the soil under the carcass [e.g., (12)]. Physical contact with pathogen-positive carcasses or the substrates beneath them poses an equal risk of ASFV infection. A large-scale study in Germany showed that ∼30% of the encounters of wild boars with dead conspecifics led to direct contact: sniffing and poking on the carcasses, whereby animals were particularly interested in soil under and around the carcasses (12). We did not observe any evidence of intraspecific scavenging. Regarding contact with wild boar carcasses, either via hunting or otherwise, it is recognized that humans are the main contributors to virus transmission and virus introduction into domestic pig farms (14).

Recent studies have concluded that ASFV exhibits exceptional environmental stability and resilience (15). Infected tissues and organs from decomposing carcasses that persist in the environment for a long time can be the sources of ASFV infection for several months, particularly at low temperatures (15, 16).

The general objective of this pilot study was to discuss the scavenging behavior of Estonian wildlife on wild boar carcasses. The study specifically focused was on wild boar behavior to detect cannibalism or other types of physical contact with dead conspecifics to understand the role of wild boar behavior in spreading ASFV within the population. Additionally, in a separate experiment, the resilience of the ASF viral DNA in the soil under the infected carcass was tested over time.

2 Materials and methods

2.1 Study design

2.1.1 Study 1. Investigating wild boar behavior concerning a conspecific carcass

The field experiment was conducted in a forest on the Hiiumaa island (58°53′ 3″N, 22°38′40″ E), the second largest island in Estonia, located in the Baltic Sea, which is 22 km west of the mainland.

This location was selected for four reasons: First, to date, no cases of ASF were detected in Hiiumaa, and the experimental work did not interfere with the infectious status of the island. Second, since there was a legal obligation to remove all wild boar carcasses found in the forest in infected areas by hunters in Estonia, other locations were not qualified for this study. Third, ASF was a highly lethal disease, especially when first discovered, so there were not enough wild boars in study areas where ASFV spreads. The holders of the hunting grounds agreed to deliver the hunted carcasses. Being able to buy the carcasses was highly valuable as, at that time, most of the wild boar population of the country had been decreased by the disease, and the hunters were not interested in discarding the hunted game. Fourth, the hunting grounds were easily accessible.

Four legally hunted wild boar carcasses were purchased from local hunters. All carcasses tested negative for ASFV at the Estonian National Center for Laboratory Research and Risk Assessment (LABRIS; Tartu, Estonia; https://labris.agri.ee/en). For carcass testing, serum samples were collected and analyzed by real-time PCR using ASFV p72 gene-targeting forward and reverse primers and TaqMan probes, as mentioned in the study conducted by Tignon et al. (17).

Table 1 shows the details of the carcasses used in this study. No animals were killed during this study.

The animals were monitored using the UOVision (Shenzhen, China) trail camera, which is a UM595-2G model (infrared heat and motion-sensitive wireless digital devices). The monitoring period was from 21.11.2016 to 18.10.2017, which lasted for 332 days. Two cameras were set to simultaneously focus on the carcasses (in the case of carcass 4, besides the gut pile) from different directions. The cameras were fixed on trees 5 m from the placed carcass and at a height of 1.5 m above the ground. The cameras were programmed to take three photos when activated by animal movements, with a 1-min pause between every subsequent activation.

One of the cameras stopped working a couple of times and did not film during the following periods: 26 November 2016–13 December 2016, 25 January 2017–14 April 2017, and 8 June 2017–25 July 2017. In total, 16,967 individual pictures from the two cameras were collected and included in the analysis. Examples of the trail camera photographs are shown in Figure 1.

TABLE 1 Parameters and persistence of carcasses used for the scavenging experiment.

Carcass ID	Sex	Age (years)	Weight (kg)	Date of placing	Date of only bones and skin left	Persistence of carcass in days	Remarks
Carcass 1	Female	2+	90	21.11.2016	26.12.2016	35	
Carcass 2	Male	4	70	11.01.2017	29.01.2017	18	
Carcass 3	Male	4–5	100	13.02.2017	27.03.2017	42	
Carcass 4	Male	2+	60	06.8.2017	14.08.2017	8	Head removed; gut pile placed aside

FIGURE 1
Trail camera photographs of random visitors of experimentally placed wild boar carcasses in the study area—forest on the island Hiiumaa.

2.1.2 Study 2. Estimating the persistence of soil contamination under the ASFV-infected wild boar carcass

To estimate how long the ASFV DNA released from infected wild boar carcasses was detectable, soil samples were collected from the carcasses of infected dead wild boars (infection confirmed at the LABRIS) after removing the carcasses. In total, between 2016 and 2017, samples were collected from 11 sites in four Estonian counties (Järvamaa, Jõgevamaa, Lääne-Virumaa, and Raplamaa) where wild boar carcasses were found. In total, 107 soil samples were collected at ∼1–2 week intervals.

In July 2016, a pilot study was conducted to optimize the methodology by sampling the soil from three nearby ASFV-infected carcasses. Samples were manually collected from the surface of each site using a latex glove. A handful of soil was taken, and the glove was pulled from the hand around the sample, tied, placed in a sealable transportation container, and transported to the laboratory within 24 h. Samples were collected for 2–4 weeks (see Supplementary Table 1), with two samples per site at every sampling event.

Sampling in October 2016 and February 2017 was performed using a sampling tool consisting of a 50 ml plastic syringe, the top of which was cut off. The syringe was pushed into the soil, and the sample stuck in a barrel (up to 50 ml) was pushed into a sample container using a plunger. Separate syringes were used at each sampling site. Three samples were collected underneath each carcass at every sampling point and were transported to the laboratory within 24 h. All samples were stored at −20°C until further analysis. The samples were collected from the carcasses discovered in October over 1 month, unless the sampling site was destroyed by plowing or flooding (see Supplementary Table 1). From the carcasses discovered in February, samples were collected for 4 months, assuming a longer survival time for the virus in winter.

Viral DNA analyses were performed periodically after collecting samples from several sites, rather than immediately after sampling. According to the manufacturer's guidelines, total viral DNA was isolated from the soil samples using the PowerSoil DNA Isolation Kit (MO BIO Laboratories, Carlsbad, California, United States). The DNA samples were analyzed by real-time PCR using ASFV p72 gene-targeting forward and reverse primers and TaqMan probes, as detailed by Tignon et al. (17). Samples were considered negative when there was no threshold cycle (Ct value) or the Ct value was >40 in the PCR analysis.

Virus DNA-positive soil samples were investigated at the Friedrich-Loeffler Institute (Germany) for the presence of viable viruses. No virus was isolated from cell cultures (data not shown).

2.2 Data analysis

Each photo was visually assessed by one author (S.H.) to determine the animal species in the photo and to record the scavenging behavior of the animal (such as tearing, removing, chewing, or breaking down soft tissues and bones). When additional assistance was required, a wildlife veterinarian (M.L.) was consulted to determine the species in the photograph. The data from the trail camera recordings based on the information in the pictures were collected using an MS Excel spreadsheet. The variables recorded were as follows: date of the event; the beginning of the event when the animal/animals were first seen on camera; end of the event when the animal/animals were last seen on camera; species; the number of animals of the same species in an event; camera ID; air temperature (°C); detection of contact with the carcass (yes/no); the number of animals in contact during the event, and extra notes when necessary.

The collected data were analyzed, and graphs were constructed using MS Excel.

3 Results

3.1 Animals visiting wild boar carcasses

From the camera recordings, 17 vertebrate species, 10 mammals, and 7 avian species roamed around the experimentally placed wild boar carcasses; there were 4,337 individual encounters. Most observed encounters were birds (79.59%): common raven (*Corvus corax*), common buzzard (*Buteo buteo*), common crane (*Grus grus*), Eurasian magpie (*Pica pica*), hooded crow (*Corvus cornix*), golden eagle (*Aquila chrysaetos*), and white-tailed eagle (*Haliaeetus albicilla)*. Among all the recorded animals belonging to mammalian species (20.41%), the distribution is as follows: raccoon dog (*Nyctereutes procyonoides*), wild boar (*Sus scrofa*), red fox (*Vulpes vulpes*), gray wolf (*Canis lupus*), European pine marten (*Martes martes*), roe deer (*Capreolus capreolus*), red deer (*Cervus elaphus*), European elk (*Alces alces*), and domestic cat (*Felis catus*). Additionally, unidentified mammalian and avian species were grouped. Common ravens were the most frequently identified ($n = 3{,}231$), followed by raccoon dogs ($n = 369$), wild boars ($n = 268$), and red foxes ($n = 186$).

A total of 2,303 encounters from 11 identified species and two unidentified mammal species were found to have direct contact with wild boar carcasses (Tables 2, 3). All species in contact, excluding wild boars and Eurasian magpies, were also found scavenging on the carcass. Peaks in animals detected and in contact occurred 1 week or less, before only bones and skin were left from the carcass. Common ravens were the most common species in contact with wild boar carcasses, followed by raccoon dogs. The third highest frequency rank of contact with the carcass was shared between the red fox and wild boar.

The cameras recorded a total of 268 wild boar visits (the total number of counted wild boars in photos from one visitation event) to the site where carcasses were placed (which accounted for 6.18% of the total number of all animal encounters), while 97 of these visits (33.92%) were instances where wild boars came into direct contact with the carcasses. The period from the placement of the carcass to the first contact with the wild boar varied between 0 and 2 days. The availability of soft tissues from the carcasses (excluding the skin) varied from ∼7–44 days (Table 3). The shortest wild boar contact lasted 1 s, the longest was 22 min 32 s, and the median value of boar contacts was 4 min 30 s. However, there were no clear signs of intraspecies scavenging in wild boars. Piglets or their mothers were in contact with several wild boars. In addition, piglets were often observed when no contact was recorded.

TABLE 2 Number and percentage of individual animals of different species in contact with the carcasses.

Species	Number of individuals in contact	Percentage of all individuals in contact
Common raven (*Corvus corax*)	1,726	74.95%
Raccoon dog (*Nyctereutes procyonoides*)	229	9.94%
Wild boar (*Sus scrofa*)	97	4.21%
Red fox (*Vulpes vulpes*)	97	4.21%
Common buzzard (*Buteo buteo*)	63	2.74%
White-tailed eagle (*Haliaeetus albicilla)*	33	1.43%
Hooded crow (*Corvus cornix*)	22	0.96%
Gray wolf (*Canis lupus*)	15	0.65%
Eurasian magpie (*Pica pica*)	8	0.35%
Golden eagle (*Aquila chrysaetos*)	6	0.26%
European pine marten (*Martes martes*)	5	0.22%
Unidentified mammal	2	0.09%
Total number of individuals in contact	2,303	100%

Wild boar visits were recorded throughout the year, with the lowest number in November ($n = 2$) and the highest in September ($n = 37$). Most contacts with carcasses occurred in June ($n = 22$) and April ($n = 21$). No contact was observed between September and November (Figure 2).

3.2 ASFV soil contamination persistence in time

Of the 11 collection sites in the two individual sites, the soil samples were negative from the first sampling event. At one of these sites, the removed carcass was an ∼1.5-month-old skeleton. In the other case, there was a fresh carcass that was 1–2 days old.

The first soil samples were ASFV DNA-positive at the nine sampling sites, whereas the removed carcass characteristics varied greatly (Table 4). There were carcasses ranging from 1–2 days old to 2–3 weeks old, some of which were intact while others had already been eaten by wild animals. Natural decomposition was already in progress in some cases. ASFV DNA was detectable in average after 28 ± 24 (mean ± SD) days after the first sampling event. The site with the longest detectable ASFV DNA presence was after 82 days (from 17 February 2017 to 10 May 2017), and the shortest period

TABLE 3 Characteristics of wild boar visits to the carcasses.

Carcass ID	Date of placing	Date of only bones and skin left	Total no of wild boar visited (in contact)	First wild boar visits to the carcass	First wild boar contacts with the carcass (description)
Carcass 1	21.11.2016	26.12.2016	41 (11)	22.11.2016	03.12.2016 (piglets, adult avoiding the carcass)
Carcass 2	11.01.2017	29.1.2017	20 (10)	11.01.2017	26.01.2017 (one adult); 30.01.2017 (eight animals, mother and piglets)
Carcass 3	13.02.2017	27.3.2017	150 (74)	15.02.2017	26.03.2017 (two adults)
Carcass 4	06.08.2017	14.8.2017	57 (3)	08.08.2017	8.08.2017 (one adult)

The observational period of one carcass is counted from the date of placing this carcass until the day next carcass was placed.

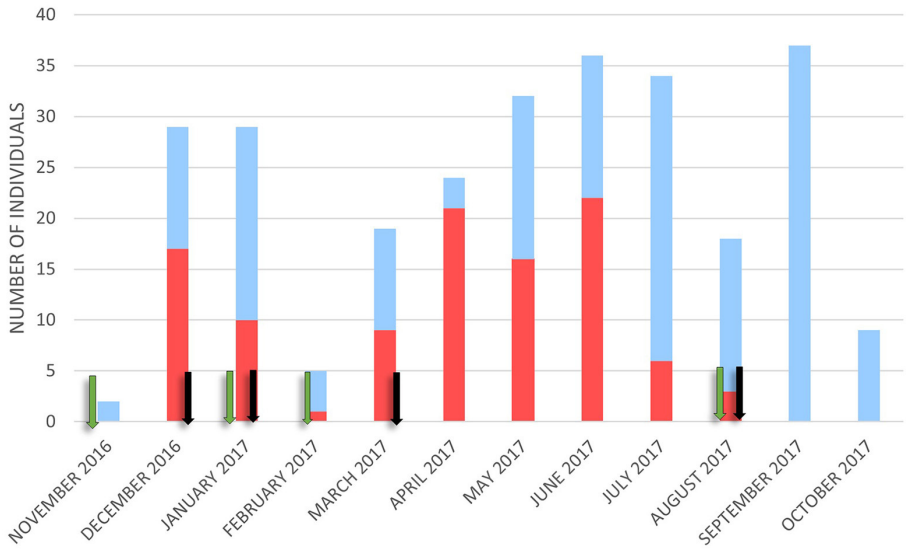

FIGURE 2
The number of wild boars was detected in contact (red bar) and not in contact (blue bar) with the carcasses monthly. Green arrows represent when new carcasses were placed and black arrows indicate when only bones and the skin were left.

was <7 days (10 October 2016 positive; after a week, faded). The carcass conditions are shown in Table 4.

4 Discussion

4.1 Animals visiting wild boar carcasses

Vertebrate animals, 4,337 individual encounters, were detected by trail cameras to visit the wild boar carcasses in this study belonged to 10 different mammal species and seven avian species. Furthermore, avian visits were more frequent. The ranking of the animal species most frequently identified and in physical contact with the carcass fully coincided as follows: common raven, raccoon dog, wild boar, and red fox. The most common raven carcass contact was detected during winter (January and December). Similarly, Probst et al. (4) used wild boar carcasses to collect data on vertebrate scavengers in northeast Germany. Their analysis revealed that birds were the first to detect carcasses in winter/spring or forest clearings when the data were analyzed separately by seasons and site visibility. However, in the summer/autumn and closed forests, mammals were first found at the site of the carcass (4). Unfortunately, in the current study, we did not have enough carcasses for statistical power to investigate the species abundance between seasons.

Among mammalian species, raccoon dogs and red foxes were the most frequently expected visitors around the carcasses in the forest in Hiiumaa. Similarly, the study by Probst et al. (4), performed in northeast Germany, found that raccoon dogs were the most frequent (44% of the observations) mammal species visiting the wild boar carcasses. Raccoon dogs and red foxes were scavenging on wild boar carcasses. In addition, six other mammalian species were considered as potential scavengers, i.e., wild boars, raccoons (*Procyon lotor*), martens (*Martes sp.*), polecats (*Mustela putorius*), water voles (*Arvicola terrestris*), and domestic dogs (*Canis familiaris*) (4). A comprehensive study of 214 naturally occurring carcasses in Poland also ranked red foxes and raccoon dogs as the most frequently scavenged mammals in temperate European woodlands (18). Although the overall composition of the fauna is different in central Spain, a study by Carrasco-Garcia et al. (2) showed that red foxes were among the most frequent scavengers, followed by griffon vultures (*Gyps fulvus*), and common ravens.

10.3389/fvets.2024.1305643

TABLE 4 African swine fever virus (ASFV) positive samples collected in the site of the removed infected wild boar carcasses.

ID of carcass	Month of discovery	No of samples	No of positive samples	% Of positive samples	No of days virus detectable	Conditions of the carcass when found
V1	July	6	4	66.7%	15	Adult female. Fresh carcass of 1–2 days. Located in open area exposed to the sun.
V2	July	4	0	0.0%	0	Adult female. Fresh carcass of 1–2 days. Located under the trees in shadow.
V3	July	4	1	25.0%	7	Adult female. Carcass of approximately a week old; decomposed. Located under the trees in shadow.
V4	July	8	0	0.0%	0	Approximately 1.5 months old carcass of only bones left.
H1	October	12	8	66.7%	43	Fresh carcass of 1–2 days. No signs of hemorrhage.
O1	October	9	2	22.2%	15	Fresh carcass of about 1 day. Symptoms of ASF: bleeding eyes and gums; bruises on the mucous membrane, reddened groin and armpits.
SO1	October	4	1	25.0%	1	Fresh carcass of about 2–3 days. The scavengers have eaten the head and behind. No signs of hemorrhage.
SA1	October	9	3	33.3%	19	Fresh carcass of about 2–3 days. The scavengers have eaten the behind. Symptoms of ASF: bleeding eyes and gums; bruises on the mucous membrane, reddened groin and armpits.
VI1	October	9	5	55.6%	34	Fresh carcass of about 3–4 days. Scavengers have eaten the behind. Bruises in the armpits, eyes slimy.
US1	February	21	9	42.9%	82	Skeleton; age > 1 month.
US2	February	21	14	66.7%	82	Carcass of 2–3 weeks; half body eaten by scavenger; the rest of the remains frozen.

The first contact of the wild boar with their conspecific carcass occurred 2 days after the carcass placement. Wild boars were most often detected to root in the remains of carcasses, bones, and skin. A similar behavioral trend has been observed in Germany (4).

Although wild boars were in direct contact with the carcass, none of them were detected in the acts of cannibalism. Direct contact with the carcasses was not frequent and usually of short duration, lasting 1–3 min. Although no direct eating of carcasses was observed, the contact with carcasses can be assumed to be intense enough for virus transmission to occur if the infectious virus was present in the carcass or the contaminated soil around it. Unfortunately, no quantification supporting this hypothesis was found in the scientific literature. Studies conducted in experimental settings have demonstrated that contact with an environment contaminated with ASFV can lead to infection in susceptible pigs (19).

The lack of signs of cannibalism in our pilot study differed from those reported in other European countries [e.g., (11, 13)]. As our study was conducted on an island and at one location, it represents the behavior of a limited metapopulation of wild boars in Estonia. Therefore, it is impossible to extrapolate these findings to the entire population of a country. Nevertheless, these findings coincide with the results of a much larger study conducted by Probst et al. (12) conducted in Northern Germany, where wild boar scavenging on red deer (*Cervus elaphus*) and roe deer (*Capreolus capreolus*) carcasses was observed; however, there were no clear signs of intraspecies scavenging, even when direct contact was recorded (12). Differently, one study in the Czech Republic with placed carcasses found wild boar contact with the carcass in 81% of the records. Contrastingly, in this study, cannibalism was observed in 9.8% of all recorded wild boar visits (13). In the study of wild boars in Poland, Merta et al. (11) reported that their stomach contents consisted of other animal tissues and residues of conspecifics

hinting at scavenging wild boar carcasses. Nevertheless, since wild boars are omnivorous animals exhibiting strong rooting behavior, even when not scavenging, they significantly impact the surfaces on which they forage (20). Hence, deliberate or accidental consumption of carcasses or invasive contact with carcasses can be foreseen.

Cannibalistic behavior may be related to the availability of resources for wild boars. In the northern latitudes, the density of wild boars is generally lower than that in the southern latitudes [e.g., (21)]. On the one hand, this is due to the difference in available feeding resources. Still, on the other hand, a higher density means more competition for resources between animals, which may lead to different animal behaviors (22). We may also speculate that wild boars in Southern and Central Europe may have more hybrids with domestic pigs, whereas, in the northern latitudes, wild boars seem to be of pure wild boar genotype (23). Since cannibalism is common in domestic pigs and may have a genetic background, northern wild boars might have less cannibalism. However, this hypothesis requires further investigation. A study conducted in Germany, to assess wild boar behavior concerning dead conspecifics, observed wild boars scavenging red deer (*Cervus elaphus*) and roe deer (*Capreolus capreolus*) carcasses. Still, there were no clear signs of intraspecies scavenging even when direct contact was recorded (12).

However, we observed many wild boar contacts with the remains of the carcasses (bones and the skin) and rooting of the soil around the carcasses; this could indicate that the sites of carcass decomposition remain attractive for wild boars for extended periods and may serve as hubs for virus transmission, as long as the virus persists in the carcass or the surrounding soil. Wild boars' natural behavior of rooting, wallowing, and investigating objects can be a risk factor for acquiring the infection when living in a virus-contaminated environment. Pepin et al. (24) developed a model (Bayesian computation) of ASFV in wild boars to estimate the virus transmission via carcasses in Eastern European wild boars. They inferred 53–66% of carcass-based transmission events when live conspecifics were in contact.

4.2 The persistence of ASFV DNA in the soil contaminated with infected wild boar carcasses

Infected carcasses are a potential source of environmental contamination, particularly the soil under the carcass and other objects around [e.g., (25, 26)]. The results of soil contamination testing in this study showed that viral DNA was detectable in soil contaminated with ASFV-infected carcasses, long after the carcasses were removed. Viral DNA contamination in the soil was detectable on average 1 month after carcass removal, independent of the season. When planning the current pilot study, we based the preliminary knowledge on half-lives of ASFV DNA in tissue samples stored at 20°C from 1.7 to 7.4 days (27). Hence, the sampling period was ∼2 months. Therefore, real DNA persistence times often exceed the planned sampling periods.

Although we could not detect the total disappearance of DNA in the soil at every study site, the sites of ASFV-infected carcasses seemed to show the longest detectable viral DNA traces discovered in winter (February), followed by the sites discovered in autumn (October). The shortest persistence of viral DNA was observed in samples from sites detected in July. We could not test whether ambient temperature and season effects were statistically significant due to insufficient data. However, it is generally established that ASFV persists longer at low temperatures, particularly in raw meat products [e.g., reviewed by Chenais et al. (14)]. Under laboratory conditions, a study investigated the soil samples and tested the survival of ASFV under different temperatures. The virus was detectable at day 112 when stored at 4°C, and the genome copy numbers were constant over 210 days after soil inoculation, showing a clear temperature dependency (28). Often, the persistence of ASFV in soil is determined by parameters other than temperature, such as soil pH. For example, in acidic soil, the virus disappears more quickly (29).

The presence of viral DNA in soil does not directly indicate that the soil is infectious. However, this proves that the virus reaches the soil from the carcasses; therefore, the soil is also a potential source of infection. A study in Lithuania (30) tested the persistence of ASFV in buried ASFV-infected wild boar carcasses using *in vitro* assays and viral DNA. At most sites, excavated carcass samples were positive for the ASFV genome, whereas no livable ASFV was isolated from any of the carcasses. Similarly, a study conducted in the Tavush region of Armenia investigated the presence of ASFV DNA in bone, bone marrow, and porcine tissue samples obtained from skeletons and carcasses found in forests and excavated from cemeteries; however, the study found that infectious ASFV could not be isolated (31).

It is important to conclude that, although direct contact between wild boars and the carcasses of their conspecifics was not frequent, the rooting behavior and intensive investigation of the remains of young pigs should be considered as critical factors in the chain of disease transmission. Therefore, it is crucial to quickly remove ASFV-infected carcasses from the environment. Furthermore, directly causing infection to the visiting wild boar, the carcass can also provide a basis for the virus to be carried by potential arthropod vectors. ASFV DNA was detected in the soil at the carcass removal site for weeks. Although the potential for live virus has not been studied, infected carcasses not removed from the site could increase the risk of indirect virus spread.

Data availability statement

The original contributions presented in the study are included in the article/Supplementary material, further inquiries can be directed to the corresponding author.

Ethics statement

Ethical approval was not required for the study involving animals in accordance with the local legislation and institutional requirements because, the wild boar carcasses were legally hunted. No animals were killed for the purpose of this study. Animals

filmed by cameras were not disturbed nor harmed during the study.

Author contributions

LT: Conceptualization, Data curation, Formal analysis, Investigation, Supervision, Visualization, Writing—original draft, Writing—review & editing. SH: Conceptualization, Data curation, Formal analysis, Investigation, Visualization, Writing—original draft. MJ: Data curation, Formal analysis, Investigation, Writing—review & editing. AVile: Data curation, Formal analysis, Writing—review & editing. IN: Formal analysis, Project administration, Writing—review & editing. AVilt: Conceptualization, Data curation, Funding acquisition, Project administration, Resources, Supervision, Writing—original draft, Writing—review & editing.

Funding

The author(s) declare that financial support was received for the research, authorship, and/or publication of this article. The study was financed by the Estonian Ministry of Agriculture, project contract No 184: "*SAK viiruse vastupidavust looduslikus keskkonnas soodustavad tegurid*," 2016–2017.

Acknowledgments

We thank the wildlife veterinarian Madis Leivits (ML) for his help in identifying avian species (raptors), Hunter Marko Pruul, and other hunters from the Emmaste hunting club in Hiiumaa for providing wild boar carcasses and the experimental area for this study. We also thank Heli Kirik for helping collect the soil samples and several hunters on the Estonian mainland for helping us find the sites of dead-infected wild boars.

Conflict of interest

The authors declare that the research was conducted in the absence of any commercial or financial relationships that could be construed as a potential conflict of interest.

The author(s) declared that they were an editorial board member of Frontiers, at the time of submission. This had no impact on the peer review process and the final decision.

Publisher's note

Supplementary material

The Supplementary Material for this article can be found online at: https://www.frontiersin.org/articles/10.3389/fvets.2024.1305643/full#supplementary-material

References

1. Vicente J, VerCauteren K. The role of scavenging in disease dynamics. In: Olea P, Mateo-Tomás P, Sánchez-Zapata J, editors. *Carrion Ecology and Management. Wildlife Research Monographs, vol 2*. Cham: Springer (2019). p. 161–82.

2. Carrasco-Garcia R, Barroso P, Perez-Olivares J, Montoro V, Vicente J. Consumption of big game remains by scavengers: a potential risk as regards disease transmission in central Spain. *Front Vet Sci.* (2018) 5:4. doi: 10.3389/fvets.2018.00004

3. Hestvik G, Uhlhorn H, Koene M, Åkerström S, Malmsten A, Dahl F, et al. Francisella tularensis in Swedish predators and scavengers. *Epidemiol Infect.* (2019) 147:e293. doi: 10.1017/S0950268819001808

4. Probst C, Gethmann J, Amler S, Globig A, Knoll B, Conraths FJ. The potential role of scavengers in spreading African swine fever among wild boar. *Sci Rep.* (2019) 9:1–13. doi: 10.1038/s41598-019-47623-5

5. Blumstein DT, Rangchi TN, Briggs T, De Andrade FS, Natterson-Horowitz B. A systematic review of carrion eaters' adaptations to avoid sickness. *J Wildl Dis.* (2017) 53:577–81. doi: 10.7589/2016-07-162

6. DeVault TL, Rhodes OE, Shivik JA. Scavenging by vertebrates: behavioral, ecological, and evolutionary perspectives on an important energy transfer pathway in terrestrial ecosystems. *Oikos.* (2003) 102:225–34. doi: 10.1034/j.1600-0706.2003.12378.x

7. Cwynar P, Stojkov J, Wlazlak K. African swine fever status in europe. *Viruses.* (2019) 11:1–17. doi: 10.3390/v11040310

8. Schulz K, Staubach C, Blome S, Nurmoja I, Viltrop A, Conraths FJ, et al. How to demonstrate freedom from African swine fever in wild boar-Estonia as an example. *Vaccines.* (2020) 8:1–14. doi: 10.3390/vaccines8020336

9. Nurmoja I, Petrov A, Breidenstein C, Zani L, Forth JH, Beer M, et al. Biological characterization of African swine fever virus genotype II strains from North-Eastern Estonia in European wild boar. *Transbound Emerg Dis.* (2017) 64:2034–41. doi: 10.1111/tbed.12614

10. Vilem A, Nurmoja I, Tummeleht L, Viltrop A. Differentiation of African swine fever virus strains isolated in estonia by multiple genetic markers. *Pathogens.* (2023) 12:720. doi: 10.3390/pathogens12050720

11. Merta D, Mocała P, Pomykacz M, Frackowiak W. Autumn-winter diet and fat reserves of wild boars (Sus scrofa) inhabiting forest and forest-farmland environment in south-western Poland. *Folia Zool Brno.* (2014) 63:95–102. doi: 10.25225/fozo.v63.i2.a7.2014

12. Probst C, Globig A, Knoll B, Conraths FJ, Depner K. Behaviour of free ranging wild boar towards their dead fellows: potential implications for the transmission of African swine fever. *Royal Soc Open Sci.* (2017) 4:170054. doi: 10.1098/rsos.170054

13. Cukor J, Linda R, Václavek P, Mahlerová K, Šatrán P, Havránek F. Confirmed cannibalism in wild boar and its possible role in African swine fever transmission. *Transbound Emerg Dis.* (2020) 67:1068–73. doi: 10.1111/tbed.13468

14. Chenais E, Depner K, Guberti V, Dietze K, Viltrop A, Ståhl K. Epidemiological considerations on African swine fever in Europe 2014-2018. *Porcine Health Manag.* (2019) 5:6. doi: 10.1186/s40813-018-0109-2

15. Guberti V, Khomenko S, Masiulis M, Kerba S. *African Swine Fever in Wild Boar—Ecology and Biosecurity. FAO Animal Production and Health Manual No. 28*. 2nd ed. Rome: FAO, World Organisation for Animal Health and European Commission (2022).

16. Fischer M, Hühr J, Blome S, Conraths FJ, Probst C. Stability of African swine fever virus in carcasses of domestic pigs and wild boar experimentally infected with the ASFV "Estonia 2014" isolate. *Viruses.* (2020) 12:1118. doi: 10.3390/v12101118

17. Tignon M, Gallardo C, Iscaro C, Hutet E, Van der Stede Y, Kolbasov D, et al. Development and inter-laboratory validation study of an improved new real-time

PCR assay with internal control for detection and laboratory diagnosis of African swine fever virus. *J Virol Methods.* (2011) 178:161–70. doi: 10.1016/j.jviromet.2011.09.007

18. Selva N, Jędrzejewska B, Jędrzejewska W, Wajrak A. Factors affecting carcass use by a guild of scavengers in European temperate woodland. *Can J Zool.* (2005) 83:1590–601. doi: 10.1139/z05-158

19. Olesen AS, Lohse L, Boklund A, Halasa T, Belsham GJ, Rasmussen TB, et al. Short time window for transmissibility of African swine fever virus from a contaminated environment. *Transbound Emerg Dis.* (2018) 65:1024–32. doi: 10.1111/tbed.12837

20. Barrios-Garcia MN, Ballari SA. Impact of wild boar (*Sus scrofa*) in its introduced and native range: a review. *Biol Invasions.* (2012) 14:2283–300. doi: 10.1007/s10530-012-0229-6

21. Pittiglio C, Khomenko S, Beltran-Alcrudo D. Wild boar mapping using population-density statistics: from polygons to high resolution raster maps. *PLoS ONE.* (2018) 13:e0193295. doi: 10.1371/journal.pone.0193295

22. May R, Conway G, Hassell M, Southwood T. Time delays, density-dependence and single-species oscillations. *J Anim Ecol.* (1974) 3:747–70. doi: 10.2307/3535

23. Iacolina L, Pertoldi C, Amills M, Kusza S, Megens HJ, Bâlteanu VA, et al. Hotspots of recent hybridization between pigs and wild boars in Europe. *Sci Rep*. (2018) 8:17372. doi: 10.1038/s41598-018-35865-8

24. Pepin KM, Golnar AJ, Abdo Z, Podgórski T. Ecological drivers of African swine fever virus persistence in wild boar populations: insight for control. *Ecol Evol.* (2020) 10:2846–59. doi: 10.1002/ece3.6100

25. De Carvalho Ferreira HC, Weesendorp E, Quak S, Stegeman JA, Loeffen WLA. Quantification of airborne African swine fever virus after experimental infection. *Vet Microbiol.* (2013) 165:243–51. doi: 10.1016/j.vetmic.2013.03.007

26. Nuanualsuwan S, Songkasupa T, Boonpornprasert P, Suwankitwat N, Lohlamoh W, Nuengjamnong C. Persistence of African swine fever virus on porous and non-porous fomites at environmental temperatures. *Porcine Health Manag.* (2022) 8:34. doi: 10.1186/s40813-022-00277-8

27. De Carvalho Ferreira HC, Weesendorp E, Quak S, Stegeman JA, Loeffen WLA. Suitability of faeces and tissue samples as a basis for non-invasive sampling for African swine fever in wild boar. *Vet Microbiol.* (2014) 172:449–54. doi: 10.1016/j.vetmic.2014.06.016

28. Prodelalova J, Kavanova L, Salat J, Moutelikova R, Kobzova S, Krasna M, et al. Experimental evidence of the long-term survival of infective African swine fever virus strain Ba71V in soil under different conditions. *Pathogens.* (2022) 11:648. doi: 10.3390/pathogens11060648

29. Carlson J, Fischer M, Zani L, Eschbaumer M, Fuchs W, Mettenleiter T, et al. Stability of African swine fever virus in soil and options to mitigate the potential transmission risk. *Pathogens.* (2020) 9:977. doi: 10.3390/pathogens9110977

30. Zani L, Masiulis M, Bušauskas P, Dietze K, Pridotkas G, Globig A, et al. African swine fever virus survival in buried wild boar carcasses. *Transbound Emerg Dis.* (2020) 67:2086–92. doi: 10.1111/tbed.13554

31. Arzumanyan H, Hakobyan S, Avagyan H, Izmailyan R, Nersisyan N, Karalyan Z. Possibility of long-term survival of African swine fever virus in natural conditions. *Vet World.* (2021) 14:854–9. doi: 10.14202/vetworld.2021.854-859

frontiers | Frontiers in Veterinary Science

TYPE Original Research
PUBLISHED 17 June 2024
DOI 10.3389/fvets.2024.1389029

OPEN ACCESS

EDITED BY
Marta Martinez Aviles,
Instituto Nacional de Investigación y Tecnología Agroalimentaria (INIA), Spain

REVIEWED BY
Peter A. Durr,
Commonwealth Scientific and Industrial Research Organisation (CSIRO), Australia
Mary-Louise Penrith,
University of Pretoria, South Africa

*CORRESPONDENCE
Georgina Limon
✉ georgina.limon-vega@pirbright.ac.uk

†These authors have contributed equally to this work and share first authorship

‡These authors have contributed equally to this work and share last authorship

RECEIVED 20 February 2024
ACCEPTED 03 June 2024
PUBLISHED 17 June 2024

CITATION
Ludi AB, Baker H, Sanki R, De Jong RMF, Maryan J, Walker M, King DP, Gubbins S, Limon G and Officer K (2024) Epidemiological investigation of foot-and-mouth disease outbreaks in a Vietnamese bear rescue centre.
Front. Vet. Sci. 11:1389029.
doi: 10.3389/fvets.2024.1389029

Epidemiological investigation of foot-and-mouth disease outbreaks in a Vietnamese bear rescue centre

Anna B. Ludi[1†], Hannah Baker[1†], Rachel Sanki[2], Rosanne M. F. De Jong[3], Julie Maryan[1], Martin Walker[3,4], Donald P. King[1], Simon Gubbins[1], Georgina Limon[1,3*‡] and Kirsty Officer[2,5‡]

[1]The Pirbright Institute, Pirbright, United Kingdom, [2]Animals Asia Foundation, Hanoi, Vietnam, [3]Veterinary Epidemiology, Economics and Public Health Group, Department of Pathobiology and Population Sciences, WOAH Collaborating Centre in Risk Analysis and Modelling, Royal Veterinary College, University of London, London, United Kingdom, [4]Department of Infectious Disease Epidemiology, Imperial College, London, United Kingdom, [5]School of Veterinary Medicine, Murdoch University, Murdoch, WA, Australia

Foot-and-mouth disease (FMD) outbreaks affecting Asiatic black bears (*Ursus thibetanus*) and a Malayan sun bear (*Helarctos malayanus*) were previously reported in 2011 in two housing facilities at a Vietnamese bear rescue centre. In this study, demographic data of all animals housed in the centre at the time of the outbreaks ($n = 79$) were collected. Blood samples drawn from 23 bears at different timepoints were tested for FMDV-specific antibodies targeting using a non-structural protein (NSP) ELISA and by virus neutralisation test (VNT). The relationship between seroconversion and clinical signs was explored and epidemic curves and transmission diagrams were generated for each outbreak, where FMD cases were defined as animals showing FMD clinical signs. Outbreak-specific attack rates were 18.75 and 77.77%, with corresponding basic reproduction numbers of 1.11 and 1.92, for the first and second outbreaks, respectively. Analyses of risk factors showed that after adjusting for sex there was strong evidence for a decrease in odds of showing clinical signs per year of age. All samples collected from bears before the outbreak tested negative to NSP and VNT. All cases tested positive to VNT following onset of clinical signs and remained positive during the rest of the follow up period, while only 6 out of 17 cases tested positive to NSP after developing clinical signs. Six animals without clinical signs were tested post outbreaks; five seroconverted using VNT and three animals were seropositive using NSP ELISA. This study provides initial epidemiological parameters of FMD in captive bears, showing that FMDV is easily spread between bears in close proximity and can cause clinical and subclinical disease, both of which appear to induce rapid and long-lasting immunity.

KEYWORDS

foot-and-mouth disease, epidemiology, outbreak investigation, Asiatic black bear, Malayan sun bear, rescue centre

1 Introduction

Foot-and-mouth disease (FMD) is a highly contagious, acute viral disease typically affecting cloven-hoofed livestock. FMD follows infection with foot-and-mouth disease virus (FMDV; family *Picornaviridae*, genus *Aphthovirus*) and is clinically characterised by fever and vesicular lesions in the mouth and on the lips, teats and feet (1). FMDV has seven known serotypes (A, O, C, SAT1, SAT2, SAT3, and Asia1) which are endemic to different regions of the world (2). The features of FMDV, including a broad host range, high transmissibility, subclinical persistence and environmental stability contribute to the transboundary threats posed by FMD and highlight the importance of international efforts to control the disease to facilitate trade (3).

Despite all cloven-hoofed animals (order *Artiodactyla*) being susceptible to FMDV, cloven-hoofed domestic livestock species, such as cattle, sheep, goats and pigs, play the most significant role in the epidemiology of FMD due to the intra- and inter-herd proximity, quantity, movement and management of livestock creating opportunities for the introduction, transmission and establishment of FMD. The World Organisation for Animal Health (WOAH) estimates that FMD circulates in 77% of the world's global livestock population, occurring in Africa, Asia and a part of South America (4). Although FMD is primarily documented in domestic livestock, FMDV has been reported to cause disease in over 70 wildlife species (5). Impalas (*Aepyceros melampus*) in close proximity with buffalo herds can become infected, develop clinical signs, and infect susceptible livestock (6, 7). However, only African buffalo (*Syncerus caffer*) is known to play an important role in maintaining FMD SAT-serotypes (8–10).

FMD outbreaks have also been documented in non-cloven-hoofed as well as hoofed wildlife species (11). For example, there are reports of natural FMDV infection in the, Arabian Oryx (*Oryx Leucoryx*), Impala (*Aepyceros melampus*), kudu (*Tragelaphus strepsiceros*) Asiatic elephant (*Elephas maximus*), capybara (*Hydrochoerus hydrochaeris*), European hedgehog (*Erinaceus europaeus*), eastern grey kangaroo (*Macropus giganteus*), domestic dog (*Canis lupus familiaris*) among others (6, 12–17). However, it should be noted that most of these outbreaks occurred in captive wild animals who, although they live under human supervision, are not confined and are instead part of wildlife parks adjacent to livestock. Experimental infection with FMDV has also been demonstrated in various atypical animals including armadillo, birds, cats, dogs, marsupials, moles, monotremes, primates, reptiles and rodents (17). As FMD research is primarily livestock-orientated, its epidemiological manifestation in atypical species is poorly documented or understood and warrants attention.

There have been three reports of FMD in brown bear (*Ursus arctos*), Asiatic black bears (ABB) (*Ursus thibetanus*) and Malayan sun bear (MSB) (*Helarctos*) (18–20). However, except for the manuscript by Officer, FMDV could not be isolated. The identification of FMDV in these papers, is based on clinical signs, which appear to be severe and limited to the footpads (19), and linked to FMDV outbreaks in surrounding area.

The Vietnam Bear Rescue Centre (VBRC) reported a period of 15 days in August 2011 when 13 Asiatic black bears and one Malayan sun bear displayed signs of lethargy and developed footpad vesicles, which were consistent with clinical signs of FMD and warranted further investigation. A minority of the bears in contact with these infected bears remained asymptomatic, while signs in the infected bears resolved by the end of September (20). Additionally, clinical records indicated FMD cases had occurred in a second location earlier in 2011. This provided an ideal opportunity for serological analysis to look for evidence of FMDV circulation in asymptomatic bears. Through virus isolation and sequencing FMDV serotype O was confirmed to be responsible for the outbreak, and it was hypothesised that the source of infection was a closely related isolate that may have been circulating in rural Vietnamese pigs at the time, although direct evidence is lacking since the FMD outbreak reporting rate in the country is low (20). Building on the previous study, the aims of this investigation were to (i) undertake a descriptive epidemiological analysis of the outbreak which includes the estimation of epidemiological parameters, (ii) identify risk factors and (iii) determine the nature of the antibody response, including longevity, in these unusual host species. Of particular interest was to elucidate persistence and differences in antibody titres between bear species, cubs and adult bears, and antibody responses in those bears that did not exhibit clinical signs of FMD.

2 Materials and methods

In 2011, the VBRC housed 79 bears: 73 Asiatic black bears and 6 Malayan sun bears. The age range of the bears was 0.5–15 years, and time residing in the sanctuary ranged between 1–48 months. The centre comprised 5 houses: the Mountain House (17 bears), River House (19 bears), cub house (2 bears), H01-1 (5 bears), H01-2 (15 bears) and H02 (21 bears) (Figure 1). Bear-keeping staff lived in the nearby rural area and changed boots upon arrival, walked through 2% bleach footbaths when entering and leaving a bear house, and did not work between houses.

2.1 Study design

The study was performed following two FMDV outbreaks among captive bears at Animal Asia's Vietnam Bear Rescue Centre (VBRC) in Tam Dao National Park, Vietnam. A total of 77 sera samples from 23 bears (22 Asiatic black bears and one Malayan sun bear) were tested during varying time points pre- and post-outbreak (between 24 months prior to 55 months post development of clinical signs), in order to characterise FMD antibody responses over time.

2.2 Animal selection

Bears were included in the analysis if they either displayed clinical signs of FMD, or if they did not display clinical signs but were in direct contact with those that did, for example, through open bars in adjacent dens. Bears included in the analysis were from two different houses: Mountain House and River House (Figure 1). Slides between dens could be opened and bears moved between dens for cleaning or enrichment sessions. The Asiatic black bears ranged from cubs through to adults and included both males and females. The one Malayan sun bear sampled was a female yearling exhibiting clinical signs of FMD. Blood samples were opportunistically

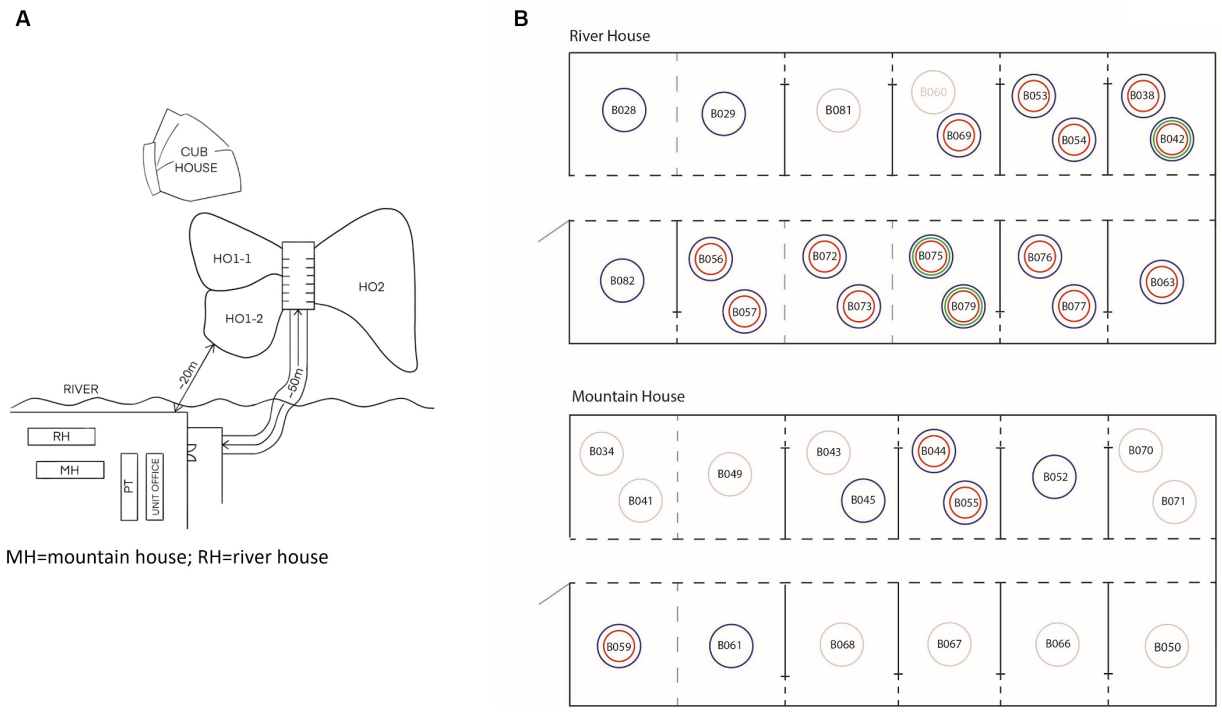

FIGURE 1
Enclosure layout of Vietnam Bear Rescue Centre **(A)**. Layout and location of bears in Mountain House and River House in 2011 **(B)**. Bears IDs are shown within circles; with grey ID indicating a deceased bear. A red circle indicates bears that displayed FMD clinical signs; a green circle indicates bears with positive test result for FMDV by virus isolation, PCR or ELISA [in the previous study (20)]; a blue circle indicates bears with serum sample/s collected and tested in the current study; a grey circle indicates bears with no clinical signs or testing. A grey dashed line indicates bears in neighbouring dens are integrated and have use of both dens; a solid line with black dashed portion indicates neighbouring bears are not integrated but have contact through den bars; a long horizontal black dashed line indicates den bars facing the central corridor. Figure is not to scale and for demonstrative purposes only.

collected during routine health checks; therefore time-points vary between subjects. Both pre- and post-outbreak samples were available for analysis.

2.3 Sampling and serology

After whole blood samples were aseptically collected from the jugular vein, sera were separated and frozen at −80°C. The serum samples were transported to the FAO World Reference Laboratory for FMD (WRLFMD) at The Pirbright Institute (TPI) under CITES export permit number 17VN2492N/CT-KL and importer permit number 556181/02. These sera were shipped on ice, where they were heat inactivated in a water bath at 56°C for 30 min and stored at 4.5°C ± 3.5°C prior to serological testing. The samples were tested by non-structural protein (NSP) ELISA using the commercially available PrioCHECK® FMDV NS kit (Lot No.: F161002LA) from Prionics Lelystad B.V., following the technical insert version 1.0_e, which was adapted to allow testing using two wells per sample. Percent inhibitions greater than or equal to 50% were considered positive. Further analysis was conducted through the well-established Virus Neutralisation Test (VNT) method using IB-RS-2 cells and testing for anti FMDV neutralising antibodies against an isolate from the O/ME-SA/PanAsia lineage: O VIT 28/2014 (21). The neutralisation titre is the reciprocal of the serum dilution where 50% of the wells are protective at a virus dose of 100$TCID_{50}$ (32 $TCID_{50}$–320 $TCID_{50}$). Neutralisation titres above or equal to 45 were considered positive while values less than 16 were considered negative. Neutralisation titres in-between were considered inconclusive.

2.4 Data management

All data were collated and stored in Excel. Data included the house layouts, characteristics of all animals ($n = 79$), description of clinical signs, dates of onset/regression of FMD clinical signs ($n = 17$), dates of sera collection and FMDV-antibody test results measured by non-structural proteins (NSP) and virus neutralisation tests (VNT) ($n = 23$).

2.5 Statistical analysis

Descriptive statistics were conducted. Temporal and spatio-temporal patterns of each outbreak were described by producing epidemic curves (Figure 2) and describing case-data and likely transmission chains. Clinical signs of FMD cases were described and tabulated.

The outbreak specific attack rates of FMD were estimated by dividing the number of bears developing clinical signs of FMD by bears present in the house where each phase of the outbreak happened. Given the sanctuary lay-out and geographical separation with other houses (Figure 1) only bears present in the affected houses were

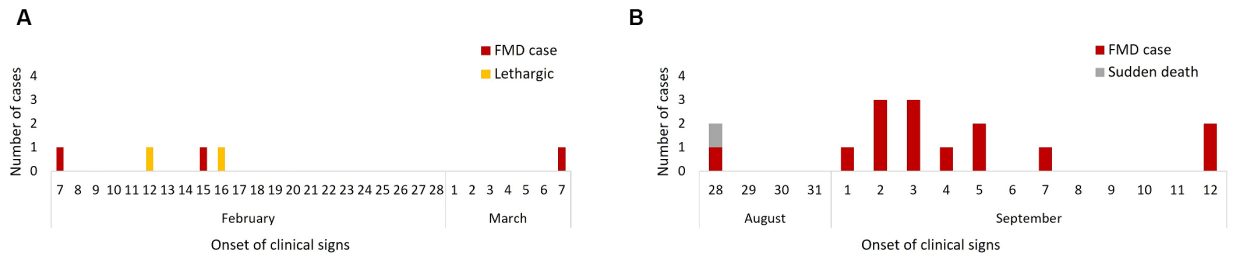

FIGURE 2
Epidemic curves of cases of FMD by date of clinical signs onset in the 2011 FMD outbreak: February–March ($n = 3$) **(A)** and August–September ($n = 17$) **(B)**.

considered. The attack rates were used to calculate the basic reproduction numbers (R_0) for the two outbreaks.

Multivariable analysis using a binomial logistic regression model was conducted to determine the extent to which sex and age were associated with FMD status (i.e., showing/not showing FMD clinical signs). Only bears housed in Mountain House or River House at the start of each outbreak were considered. Sex was analysed as a categorical variable whereas age was analysed as continuous. Differences between species were not considered due to lack of variability (only 1 Malayan sun bear). A p-value of <0.05 was deemed to indicate statistical significance. Likelihood ratio test was used to assess which model fit the data best (including both variables vs. only one of them).

The time to detection of FMDV-antibodies (seroconversion) was analysed by plotting overall and bear-specific VNT titres and NSP percentage inhibition against months pre- and post-onset of clinical signs or outbreak start for FMD cases and non-cases, respectively. McNemar's chi-squared test for paired data and kappa statistics were used to assess whether there was a statistically significant difference in the proportion of positives between NSP and VNT tests, and to what extent they were correlated.

All statistical analyses were conducted in R.4.2.0 (R Core Team, 2022) using packages epiR (function epi.kappa) (22), lme4 (function glm) (23) and R0 (function estimate.R) (24).

3 Results

Bears displaying clinical signs consistent with FMD were recorded in the Mountain House ($n = 3$; February–March 2011) and River House ($n = 14$; August–September 2011). Both houses consisted of rows of indoor dens only along a central corridor, and bears in neighbouring dens could have physical contact through metal bars. Each den was separated by a sliding metal bar door, the bears could be moved between adjacent dens during cleaning and enrichment set-up sessions (Figure 1). The first outbreak exclusively affected the Mountain House and started on February 7 (day 1), when a female Asiatic black bear (B055) demonstrated signs of FMD, after which another adult Asiatic black bear (B044) in the same den was found to have signs on day 9 and a final case (B059) developed clinical signs on day 29. Two adult bears (B043, B070) in in the same house demonstrated lethargy on day 6 and 9 of the outbreak but showed no other clinical signs of FMD. No diagnostic testing was carried out during this outbreak.

The second outbreak affected only the River House with the first case reported on August 28 (day 1) when an adult male Asiatic black bear (B069) showed clinical FMD and a second bear (B060) in the same den suddenly died with non-specific clinical signs (lethargy and inappetence only). Post-mortem examination was undertaken and there were no gross signs of FMD. Samples had not been taken from this bear and was not considered in the rest of the analysis. Four days later (day 5) an adult female bear (B054) in a neighbouring den developed FMD signs followed by her den-mate (B053) on day 7. Simultaneously, from days 6–8 all 6 animals (5 juveniles – B056, B057, B072, B073, B075, 1 adult – B079) in a den across the corridor from the index case developed signs of FMD, followed by 2 cubs in the adjacent den on day 9. Two days later (day 11) a Malayan sun bear in the den next to the cubs showed clinical FMD, followed by the 2 final cases in adult Asiatic black bears (B038, B042) on days 15 and 16. Diagnostic work ups were performed on three affected bears (B079, B075, and B042), with FMDV positive RT-PCR results recorded for all three cases, and isolation of FMDV from B079 and B042 (ref the original paper). Faeces from B063 and samples opportunistically collected 10 days after the onset of signs from B038 tested negative. Epidemic curves suggested a propagated and a point-source outbreak (Figures 2A,B).

The attack rate of FMD during the first outbreak was 18.75% (95% confidence interval (CI): 4.97–46.3%). The second outbreak had a higher attack rate of 77.77% (95% CI: 51.92–92.63%). Based on these attack rates the basic reproduction number (R_0) for the Mountain House outbreak was 1.11 (95% CI: 0.99–1.27), while for the River House outbreak it was 1.93 (95% CI, 1.50–3.61).

All affected bears ($n = 17$) developed blister-like lesions on all their foot-pads, presenting as noticeably more severe in younger animals. Of all cases, 35.29% ($n = 6$) and 11.76% ($n = 2$) also developed blisters on their nose and lips, respectively (Table 1). Blisters on the nose appeared 2–11 days (mean = 4.83 days) after blisters on footpads. Fifteen bears exhibited reduced activity for periods ranging from 1–12 days (mean = 5.53 days, 95% CI: 3.85–7.21), with the remaining 2 cases, the cubs, showing no change in activity. Nine cases (52.94%) had appetite reductions lasting from 1–4 days post-onset of clinical signs (mean = 1.72 days, 95% CI: 0.84–2.61). Footpad lesions took 16–17 days to fully heal (based on 4 observations) and sloughed between 2–21 days (based on 11 observations). From all cases, 14 animals (82.35%) were administered analgesia (tramadol, $n = 2$; meloxicam, $n = 12$), antibiotics (cephalexin, $n = 12$; amoxicillin clavulanate, $n = 1$) and/or a neuroleptic agent (acepromazine, $n = 1$).

TABLE 1 Summary of clinical signs of FMD cases in bears from both outbreaks ($n = 17$) in Vietnam Bear Rescue Centre, 2011.

Clinical sign[1]	Number of days	FMD cases ($n = 17$)	
		n	%
Blisters on foot pads		17	100
Blisters on nose		6	35.3
Blisters on lips		2	11.8
Reduced activity (number of days post onset of signs)	0	2	11.8
	1–5	7	41.2
	6–10	6	35.3
	11+	2	11.8
Reduced appetite (number days post onset of signs)	0	8	47.1
	1	5	29.4
	2–4	4	25.5

FMD, foot-and-mouth disease.
[1]Clinical signs were observed and reported by staff working at each house.

TABLE 2 Demographic characteristics of FMD cases in the Mountain House (February–March 2011; $n = 3$) and River House (August–September 2011; $n = 14$) in the Vietnam Bear Rescue Centre.

Characteristic	Category	Mountain House outbreak (February–March 2011)				River House outbreak (August–September 2011)			
		Subjects		FMD Cases		Subjects		FMD Cases	
		n	%[1]	*n*	%[2]	*n*	%	*n*	%
Total		**16**	**100**	**3**	**18.75**	**18**	**100**	**14**	**77.78**
Species	Asian black bear	16	100	3	18.8	17	94.4	13	76.5
	Malayan sun bear	–	–	–	–	1	5.6	1	100
Sex	Male	9	56.3	1	11.1	7	38.9	5	71.4
	Female	7	43.8	2	28.6	11	61.1	9	81.8
Age group (years)	Cub (0)	0	0	0	0	2	11.1	2	100
	Yearling (1)	0	0	0	0	7	38.9	6	85.7
	Adult (2–9)	8	50.0	2	25.0	7	38.9	6	85.7
	Adult (10+)	8	50.0	1	12.5	2	11.1	0	0
Time in sanctuary (months)	0–6	0	0	0	0	5	27.8	3	60.0
	7–12	11	68.8	3	27.3	5	27.8	5	100
	13–24	5	31.3	0	0	8	44.4	6	75.0

[1]Indicates percentage of animals in the house in the category (row %).
[2]Indicates percentage of animals in category with FMD (column %).

Overall, three out of 16 (18.8%) and 14 out of 18 (77.8%) bears in the affected houses developed clinical signs of FMD in the first and second outbreak, respectively (Table 2). All cases affected Asiatic black bears, with the exception of one Malayan sun bear which was the only Malayan sun bear housed in an FMD-affected house. In both outbreaks, a slightly greater proportion of females contracted FMD compared to males. Younger animals appeared to have an increased incidence of FMD (mean age of cases = 3.9 years), with all cubs ($n = 2$) and 85.7% ($n = 6$) of yearlings becoming infected as opposed to none of the adults aged 10+ years and older ($n = 2$) in the River House outbreak (Table 2).

The odds of showing clinical signs were higher in females [adjusted odds ratio (AOR): 11.58; 95% CI: 1.29–293.6; $p = 0.06$] and decreased with age (AOR: 0.51; 95% CI: 0.30–0.73; $p = 0.003$).

3.1 Relationship between seroconversion and clinical signs

Figure 3 shows the FMDV-specific antibody levels in FMD cases (defined as presence of clinical signs) ($n = 17$) and non-cases (defined as absence of clinical signs) ($n = 6$), from both outbreaks, measured by VNT and NSP ELISA over time relative to the date of onset of clinical signs (for cases) or start of the outbreak (for non-cases). Not all bears had samples collected (see Supplementary Table S1), and therefore only bears with samples collected are presented in Figure 3. All cases tested positive to VNT following onset of clinical signs and remained positive for the rest of the follow up period. Two animals were sampled only 1 day post onset of clinical signs and tested negative to VNT in this sampling; however, they were positive in the following sampling.

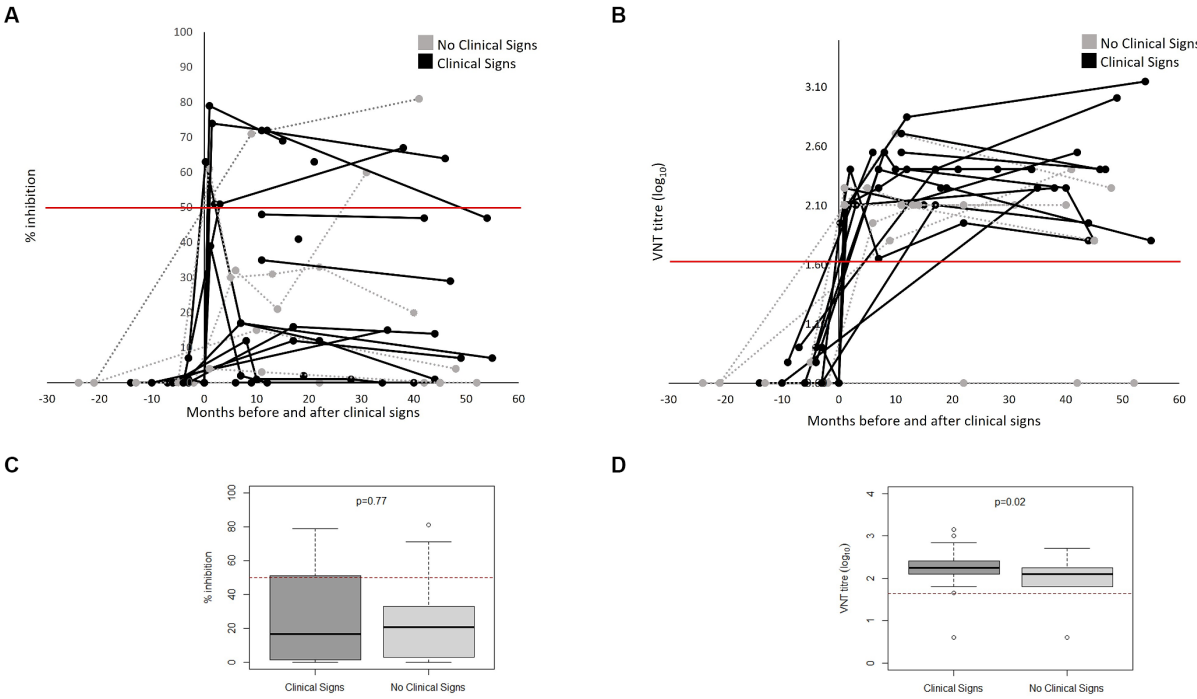

FIGURE 3
FMDV-antibodies in bears FMD cases ($n = 17$) and non-cases ($n = 6$) from both outbreaks as measured by NSP **(A)** and VNT **(B)** antibody tests over months pre- and post-onset of clinical signs (for cases) or pre- and post-outbreak (for non-cases) in Vietnam Bear Rescue Centre. FMD cases were defined as bears demonstrating clinical signs of FMD. Clinical signs were first observed at x = 0. For non-cases, x = 0 indicates the start of the outbreak. Antibody tests were deemed positive if VNT titre >45 and NSP percent inhibition ≥50, represented with a red line. Boxplots comparing titles as measured by NSP **(C)** and VNT **(D)** of clinical and non-clinical bears considering results from x = 0 onwards.

TABLE 3 **Concordance between number of positive and negative results using NSP and VNT tests.**

	VNT		*p*-value†	Kappa statistic
	Number of negative	Number of positive		
All samples ($n = 77$)				
NSP				
Number of negative	24	38	<0.001	0.19
Number of positive	0	15		
Samples from animals with clinical signs ($n = 40$)				
NSP				
Number of negative	2*	27	<0.001	0.04
Number of positive	0	11		
Samples from animals without clinical signs ($n = 26$)				
NSP				
Number of negative	11	11	0.002	0.23
Number of positive	0	4		

†McNemar test.
A significant test suggests strong disagreement between the tests.
*These bears were tested 1 day after clinical signs onset.

Only 6 out of 17 cases tested positive to NSP following the development of clinical signs. Of the 6 non-cases tested, 5 seroconverted to VNT, 3 to NSP post-outbreak and one remained negative to both assays. There was a significant difference and only slight agreement between NSP and VNT for samples from cases (kappa statistic 0.04) and fair agreement for those from non-cases (kappa statistic 0.23) (Table 3). All samples collected from animals before the first outbreak tested negative to both tests (NSP and VNT). All bears that seroconvert in the River House were after the onset of the second outbreak.

4 Discussion

This study provides a description of two incursions of an FMD outbreak in captive bears. Understanding the evolution of the outbreak, transmission dynamics and clinical presentation in bears provides essential information on the potential impacts of future FMD outbreaks, informing disease control measures (25) and the design of bear sanctuaries and their biosecurity protocols.

The attack rate of FMD during the first outbreak was 18.75% while the second outbreak had a higher attack rate of 77.77%. The corresponding basic reproduction numbers (R_0) were 1.11 and 1.93, respectively, which are close to the epidemic threshold at $R_0 = 1$, especially in the first phase of the outbreak. They are also much lower than is reported for outbreaks in typical hosts ($R_0 \sim 10–20$) such as cattle in previously naïve populations (26) or African buffalo under experimental conditions (27), but similar to values in cattle in endemic populations ($R_0 \sim 1.26–2.52$) (25). This could reflect lower transmissibility of FMDV in bears but could also reflect the reduced opportunity for contact between individuals because of the way the bears were housed.

After adjusting for sex, there was a strong association ($p = 0.003$) between age and the presentation of FMD clinical signs, with decreased odds of FMD signs per year of age (AOR = 0.51). In addition, younger animals showed more severe blister-like lesions. These findings are in line with current literature in other species (28, 29). It is plausible that the higher proportion of younger bears kept in River House at the time of the second outbreak contributed to the increased cases and level of transmission in this incursion. Additionally, despite the River House enforcing control measures on day 6 of the outbreak, all animals tested from the River House were seropositive. This highlights the need to take immediate action to control the spread of the virus, especially as it is still unknown whether bears are infectious prior to the onset of clinical signs.

Following the second outbreak, biosecurity protocols were reviewed and updated including requiring the staff to change clothes before entering and upon exiting the sanctuary, as some of the staff keep livestock and feed their animals before going to work. All personnel must now also go through Virkon footbaths when entering and exiting bear housing areas and all guests on site must also follow the biosecurity change in/change out policy if they enter bear housing areas during their visit. In addition, all bears are placed into quarantine for 30-45 days when they arrive to allow for close observation of any health issues and to treat if necessary, as well as allowing rapport building with staff to gain trust in the bears. Since the biosecurity measures were strengthened no outbreaks have been reported in the centre even though FMDV is still circulating in rural areas nearby.

Serological analysis found that both symptomatic and asymptomatic infection with FMD conferred rapid and long-lasting antibody responses in bears, which supports current literature (7, 30, 31). This study highlights the general importance of collecting sera routinely, not just during infectious disease outbreaks, but also for retrospective analyses to better understand transmission dynamics.

All FMD cases seroconverted post-outbreak by VNT and 35.3% ($n = 6/17$) when using NSP. A similar pattern was observed in non-cases. Although occasional disagreement between the NSP and VNT could be expected as the tests detect different subsets of antibodies, we observed significant differences and only weak concordance between them. Considering just bears that developed clinical signs, the sensitivity of VNT was 100% (CI 89–100%) while the sensitivity of NSP was 27% (CI 15–44%). All bears that seroconverted to VNT remained sero-positive until the end of the follow up period, which in some bears was up to 4.5 years after infection. We note that the NSP ELISA kit is not validated for the use in bears and therefor the precise cut-off for positive samples is not known. Some samples showed toxicity in the VNT which could have caused false negatives in the NSP ELISA as these samples were not titrated. In addition, a limitation of this study is the irregular intervals at which serum samples were collected, suggesting that initial antibody responses may have been missed. However, given samples were derived from large carnivores with serum sample collection requiring general anaesthesia, this limitation is attributed to the nature of the study population. For similar reasons, clinical signs of FMD were observed only through protected contact conscious examinations through den bars, not through hands-on close examination, meaning less severe signs may have been missed, leading to differential misclassification and an underestimation of the effect estimates.

Animals can contract FMDV through inhalation, ingestion, or direct contact with viral particles. Additionally, FMDV can remain viable in the environment for up to 2 weeks (32–34). The environmental persistence of FMDV could explain why the first outbreak appeared to have a propagated source. Moreover, as the infectiousness of subclinical FMD cases is not well known, asymptomatic cases which seroconverted post-outbreak may have played a role in FMD transmission within the house.

Further research on the contribution of subclinical FMD in bears to disease transmission, the duration of infectiousness, and the level of antibody response required to confer FMDV-immunity warrants attention. Previous research reports differences between inter- and intra-species FMD transmissibility, such as increased cattle-cattle transmission compared to cattle-sheep or sheep-sheep (35, 36). The role of bears in inter-species FMD transmission therefore comprises an important area of future research, particularly when considering the potential of wildlife-livestock interactions and introduction to rescue centres. Results from this outbreak investigation suggest that bears were infected by an external source on two separate occasions, and by adhering to strict biosecurity and quarantine protocols, bears in rescue centres or zoos can be kept FMD free in areas where FMD is endemic.

5 Conclusion

FMDV can cause clinical and subclinical disease in bears, both of which appear to confer rapid and long-lasting antibody responses. This study provides initial epidemiological parameters of FMD in bears and suggests that bears were accidental hosts in this outbreak, and FMD outbreaks can be prevented if strict biosecurity protocols are put in place.

Data availability statement

The original contributions presented in the study are included in the article/Supplementary material, further inquiries can be directed to the corresponding author.

Ethics statement

The animal study was approved by Social Science Research Ethical Review Board (SSRERB) (URN SR2020-0176), Royal Veterinary College, UK. The study was conducted in accordance with the local legislation and institutional requirements.

Author contributions

AL: Conceptualization, Data curation, Visualization, Writing – original draft, Writing – review & editing. HB: Methodology, Writing – review & editing. RS: Writing – original draft, Writing – review & editing. RJ: Data curation, Formal analysis, Writing – review & editing. JM: Methodology, Project administration, Writing – review & editing. MW: Supervision, Writing – review & editing. DK: Conceptualization, Funding acquisition, Resources, Writing – review & editing. SG: Formal analysis, Supervision, Writing – review & editing. GL: Conceptualization, Formal analysis, Writing – original draft, Writing – review & editing. KO: Conceptualization, Funding acquisition, Methodology, Writing – original draft, Writing – review & editing.

Funding

The author(s) declare financial support was received for the research, authorship, and/or publication of this article. Work at the Pirbright Institute was supported by the Department for Environment, Food, and Rural Affairs (Defra; UK) research grant SE1131 and funding provided by the European Union (via a contract from EuFMD, Rome, Italy). The views expressed herein can in no way be taken to reflect the official opinion of the European Union. The Pirbright Institute receives strategic funding from the UKRI Biotechnology and Biological Sciences Research Council of the United Kingdom (projects BB/X011038/1 and BB/X011046/1) (20).

Acknowledgments

We acknowledge the Vietnam Bear Rescue Centre staff for collecting blood samples and sharing records, and in particular Mandala Hunter-Ishikawa for her early input to this project.

Conflict of interest

The authors declare that the research was conducted in the absence of any commercial or financial relationships that could be construed as a potential conflict of interest.

The author(s) declared that they were an editorial board member of Frontiers, at the time of submission. This had no impact on the peer review process and the final decision.

Publisher's note

Supplementary material

The Supplementary material for this article can be found online at: https://www.frontiersin.org/articles/10.3389/fvets.2024.1389029/full#supplementary-material

References

1. Eschbaumer M, Stenfeldt C, Rekant SI, Pacheco JM, Hartwig EJ, Smoliga GR, et al. Systemic immune response and virus persistence after foot-and-mouth disease virus infection of naive cattle and cattle vaccinated with a homologous adenovirus-vectored vaccine. *BMC Vet Res*. (2016) 12:205. doi: 10.1186/s12917-016-0838-x

2. Paton DJ, Sumption KJ, Charleston B. Options for control of foot-and-mouth disease: knowledge, capability and policy. *Philos Trans R Soc Lond Ser B Biol Sci*. (2009) 364:2657–67. doi: 10.1098/rstb.2009.0100

3. Alexandersen S, Mowat N. Foot-and-mouth disease: host range and pathogenesis. *Curr Top Microbiol Immunol*. (2005) 288:9–42. doi: 10.1007/3-540-27109-0_2

4. World Organisation for Animal Health (2023). *Technical disease card [online]*. WOAH, Paris, France. Available at: https://www.woah.org/en/disease/foot-and-mouth-disease/ (Accessed 27 July 2023).

5. Thomson GR, Vosloo W, Bastos ADS. Foot and mouth disease in wildlife. *Virus Res*. (2003) 91:145–61. doi: 10.1016/S0168-1702(02)00263-0

6. Hargreaves SK, Foggin CM, Anderson EC, Bastos AD, Thomson GR, Ferris NP, et al. An investigation into the source and spread of foot and mouth disease virus from a wildlife conservancy in Zimbabwe. *Rev Sci Tech*. (2004) 23:783–90. doi: 10.20506/rst.23.3.1519

7. Vosloo W, Thompson PN, Botha B, Bengis RG, Thomson GR. Longitudinal study to investigate the role of impala (*Aepyceros melampus*) in foot-and-mouth disease maintenance in the Kruger National Park, South Africa. *Transbound Emerg Dis*. (2009) 56:18–30. doi: 10.1111/j.1865-1682.2008.01059.x

8. Anderson EC, Foggin C, Atkinson M, Sorensen KJ, Madekurozva RL, Nqindi J. The role of wild animals, other than buffalo, in the current epidemiology of foot-and-mouth disease in Zimbabwe. *Epidemiol Infect*. (1993) 111:559–64. doi: 10.1017/s0950268800057289

9. Maree F, de Klerk-Lorist LM, Gubbins S, Zhang FQ, Seago J, Perez-Martin E, et al. Differential persistence of foot-and-mouth disease virus in African Buffalo is related to virus virulence. *J Virol*. (2016) 90:5132–40. doi: 10.1128/Jvi.00166-16

10. Samara SI, Pinto AA. Detection of foot-and-mouth-disease carriers among water Buffalo (Bubalus-Bubalis) after an outbreak of the disease in cattle. *Vet Rec*. (1983) 113:472–3. doi: 10.1136/vr.113.20.472

11. Weaver GV, Domenech J, Thiermann AR, Karesh WB. Foot and mouth disease: a look from the wild side. *J Wildl Dis*. (2013) 49:759–85. doi: 10.7589/2012-11-276

12. Bhattacharya S, Banerjee R, Ghosh R, Biswas A, Chatterjee A. Identification of foot-and-mouth disease from a captive kangaroo in a zoological garden in India. *Vet Rec*. (2003) 153:504–5. doi: 10.1136/vr.153.16.504

13. Frolich K, Hamblin C, Jung S, Ostrowski S, Mwanzia J, Juurgen Streich W, et al. Serologic surveillance for selected viral agents in captive and free-ranging populations of Arabian oryx (oryx leucoryx) from Saudi Arabia and the United Arab Emirates. *J Wildl Dis*. (2005) 41:67–79. doi: 10.7589/0090-3558-41.1.67

14. Hedger RS, Brooksby JB. FMD in an Indian elephant. *Vet Rec*. (1976) 99:93. doi: 10.1136/vr.99.5.93-a

15. Mc LJ, Henderson WM. The occurrence of foot-and-mouth disease in the hedgehog under natural conditions. *J Hyg (Lond)*. (1947) 45:474–9. doi: 10.1017/s0022172400014194

16. Pyakural S, Singh U, Singh NB. An outbreak of foot-and-mouth disease in Indian elephants (Ellphas maximus). *Vet Rec*. (1976) 99:28–9. doi: 10.1136/vr.99.2.28

17. Waters RA, Wadsworth J, Mioulet V, Shaw AE, Knowles NJ, Abdollahi D, et al. Foot-and-mouth disease virus infection in the domestic dog (*Canis lupus familiaris*), Iran. *BMC Vet Res*. (2021) 17:63. doi: 10.1186/s12917-021-02769-1

18. Grosso AM. La fiebre aftosa en el jardin zoologico de Buenos Aires en los ultimos quince años. *Gaceta Veterinaria*. (1957) 19:54–5.

19. Neugebauer W. Maul-und Klauenseuche bei Kragenbären (*Ursus thibetanus*). *Zool Garten NF*. (1976) 46:195–7.

20. Officer K, Lan NT, Wicker L, Hoa NT, Weegenaar A, Robinson J, et al. Foot-and-mouth disease in Asiatic black bears (*Ursus thibetanus*). *J Vet Diagn Invest*. (2014) 26:705–13. doi: 10.1177/1040638714547256

21. World Organisation for Animal Health (2023). Chapter 3.1.8 Foot and mouth disease (infection with foot and mouth disease virus). WOAH, Paris, France. Available at: https://www.woah.org/en/disease/foot-and-mouth-disease/ (Accessed August 1 2023).

22. Stevenson M.S., Evan (2023). epiR: tools for the analysis of epidemiological data. Available at: https://CRAN.R-project.org/package=epiR

23. Bates D, Mächler M, Bolker BM, Walker SC. Fitting linear mixed-effects models using lme4. *J Stat Softw*. (2015) 67:1–48. doi: 10.18637/jss.v067.i01

24. Obadia T, Haneef R, Boelle PY. The R0 package: a toolbox to estimate reproduction numbers for epidemic outbreaks. *BMC Med Inform Decis Mak*. (2012) 12:147. doi: 10.1186/1472-6947-12-147

25. Tadesse B, Molla W, Mengsitu A, Jemberu WT. Transmission dynamics of foot and mouth disease in selected outbreak areas of Northwest Ethiopia. *Epidemiol Infect*. (2019) 147:e189. doi: 10.1017/S0950268819000803

26. Chis Ster I, Dodd PJ, Ferguson NM. Within-farm transmission dynamics of foot and mouth disease as revealed by the 2001 epidemic in Great Britain. *Epidemics*. (2012) 4:158–69. doi: 10.1016/j.epidem.2012.07.002

27. Jolles A, Gorsich E, Gubbins S, Beechler B, Buss P, Juleff N, et al. Endemic persistence of a highly contagious pathogen: foot-and-mouth disease in its wildlife host. *Science*. (2021) 374:104-+. doi: 10.1126/science.abd2475

28. Dukpa K, Robertson ID, Edwards JR, Ellis TM. A retrospective study on the epidemiology of foot-and-mouth disease in Bhutan. *Trop Anim Health Prod*. (2011) 43:495–502. doi: 10.1007/s11250-010-9722-z

29. Nyaguthii DM, Armson B, Kitala PM, Sanz-Bernardo B, Di Nardo A, Lyons NA. Knowledge and risk factors for foot-and-mouth disease among small-scale dairy farmers in an endemic setting. *Vet Res*. (2019) 50:33. doi: 10.1186/s13567-019-0652-0

30. Cox SJ, Carr BV, Parida S, Hamblin PA, Prentice H, Charleston B, et al. Longevity of protection in cattle following immunisation with emergency FMD A22 serotype vaccine from the UK strategic reserve. *Vaccine*. (2010) 28:2318–22. doi: 10.1016/j.vaccine.2009.12.065

31. Hayer SS, VanderWaal K, Ranjan R, Biswal JK, Subramaniam S, Mohapatra JK, et al. Foot-and-mouth disease virus transmission dynamics and persistence in a herd of vaccinated dairy cattle in India. *Transbound Emerg Dis*. (2018) 65:e404–15. doi: 10.1111/tbed.12774

32. Colenutt C, Brown E, Nelson N, Paton DJ, Eble P, Dekker A, et al. Quantifying the transmission of foot-and-mouth disease virus in cattle via a contaminated environment. *MBio*. (2020) 11:e00381. doi: 10.1128/mBio.00381-20

33. de Rueda CB, de Jong MCM, Eble PL, Dekker A. Quantification of transmission of foot-and-mouth disease virus caused by an environment contaminated with secretions and excretions from infected calves. *Vet Res*. (2015) 46:43. doi: 10.1186/s13567-015-0156-5

34. Woodbury EL. A review of the possible mechanisms for the persistence of foot-and-mouth-disease virus. *Epidemiol Infect*. (1995) 114:1–13. doi: 10.1017/S0950268800051864

35. de Rueda CB, de Jong MCM, Eble PL, Dekker A. Estimation of the transmission of foot-and-mouth disease virus from infected sheep to cattle. *Vet Res*. (2014) 45:58. doi: 10.1186/1297-9716-45-58

36. Orsel K, Dekker A, Bouma A, Stegeman JA, de Jong MCM. Vaccination against foot and mouth disease reduces virus transmission in groups of calves. *Vaccine*. (2005) 23:4887–94. doi: 10.1016/j.vaccine.2005.05.014

frontiers | Frontiers in Veterinary Science

TYPE Case Report
PUBLISHED 22 August 2024
DOI 10.3389/fvets.2024.1439432

OPEN ACCESS

EDITED BY
Bruce Arthur Young,
A.T. Still University, United States

REVIEWED BY
Viktor Palus,
Neurovet, Slovakia
Catherine Carr,
University of Maryland, United States
James Adams,
A.T. Still University, United States

*CORRESPONDENCE
Alessandro Vetere
✉ alessandro.vetere88@gmail.com

RECEIVED 27 May 2024
ACCEPTED 01 August 2024
PUBLISHED 22 August 2024

CITATION
Vetere A, Camera ND, Cococcetta C, Paoletti C, Dondi M, Biaggi F and Ianni FD (2024) Case report: Evaluation of head trauma in a tawny owl (*Strix aluco*) with advanced imaging diagnostic, FVEP and BAER test.
Front. Vet. Sci. 11:1439432.
doi: 10.3389/fvets.2024.1439432

Case report: Evaluation of head trauma in a tawny owl (*Strix aluco*) with advanced imaging diagnostic, FVEP and BAER test

Alessandro Vetere[1]*, Nicola Della Camera[2], Ciro Cococcetta[3], Carlo Paoletti[4], Maurizio Dondi[1], Fabio Biaggi[1] and Francesco Di Ianni[1]

[1]Department of Veterinary Science, Università Degli Studi di Parma, Parma, Italy, [2]Clinica Veterinaria Pedrani, Zugliano, Italy, [3]Department of Exotic Animals, Centre Hospitalier Vétérinaire Saint-Martin, Allonzier-la-Caille, France, [4]Department of Exotic Animals, Centre Hospitalier Vétérinaire ADVETIA, Vélizy-Villacoublay, France

An adult pet tawny owl (*Strix aluco*) presented to a veterinary hospital at Parma University with a history of head trauma. After a critical care protocol including thermal, oxygen and fluid support aimed at stabilizing the patient, a neurological examination was performed. During neurological evaluation, marked lethargy and an inability to rise from a recumbent position was noted. Anisocoria was also present, with a mydriatic left pupil exhibiting no pupillary light response (PLR) even on direct illumination of both eyes. On ocular fundus examination, retinal hemorrhage and retinal detachment were observed. Based on these clinical findings, a complete work-up was performed, including hematological exams and total body X-ray studies followed by a computed tomography (CT) scan. Additional examinations, such as brainstem auditory evoked response (BAER) measurement and flash visual evoked potential (FVEP) recording, were performed. FVEP measurements performed on the left eye exhibited no peaks in either series of stimulations, indicating an altered functional integration within the visual pathway. A CT scan revealed a large hypoattenuating lesion within the right cerebral hemisphere, suspected to be intraparenchymal edema. The BAER test demonstrated an altered trace consistent with brainstem involvement and left hypoacusis due to cranial nerve VIII deficiency. Head trauma can result in significant neurological impairments in birds, impacting their behavior, mobility, and cognitive abilities. FVEP recordings, BAER tests and CT scans may be useful diagnostic tools in clinical practice. Understanding the causes and neurologic presentation of avian traumas is essential for effective prevention, diagnosis and treatment of affected birds.

KEYWORDS

raptors, birds of prey, head trauma, BAER, tawny owl, FVEP, advanced imaging

1 Introduction

In wild birds, common types of trauma include cuts, abrasions, fractures, punctures, sprains, dislocations, concussions, and internal organ damage (1). The causes of bird trauma are multifaceted and can be broadly categorized into natural and anthropogenic factors (2). Natural causes include predator attacks, territorial disputes, adverse weather conditions, and collisions

with trees in flight. Anthropogenic causes encompass a range of human activities, such as electrocution from power lines, vehicle collisions, entanglement in man-made structures such as nets and fences or collisions against glass or windows (1–3). Traumas can result in neurological manifestations in birds, leading to a range of behavioral, sensory, motor, and cognitive impairments. Common neurologic presentations in birds include altered responsiveness, abnormal posture or movement, impaired flight or balance, loss of coordination, abnormal reflexes, and sensory deficits (2–4). Accurate diagnosis through thorough neurologic examinations, advanced imaging techniques, and laboratory tests can guide appropriate treatment strategies, including supportive care, pain management, surgical interventions, and rehabilitation (5). Recently, Foss et al. (6) established a Modified Glasgow Coma Scale for avian species to serve as a prognostic indicator in raptors with head trauma. This proposed scale demonstrated good to excellent inter-rater agreement among evaluators from diverse backgrounds in assessing raptors with head trauma. Furthermore, it has been correlated with the probability of survival within the first 48 h after presentation to rehabilitation facilities for raptors suffering from head trauma.

Computed tomography (CT) scanning has emerged as a powerful imaging modality, providing detailed cross-sectional images of avian patients (7, 8). CT scanning involves the use of an x-ray tube revolving around the subject while opposed detectors quantify how much of the x-ray beam is attenuated as it passes through the body. These attenuation values are processed by a computer algorithm to construct detailed cross-sectional images, or slices, of the bird's body. CT scans play a crucial role in the assessment and management of head traumas in birds, as they provide detailed imaging of cranial structures, facilitating the identification and characterization of traumatic lesions (4, 8). By visualizing bone, soft tissue, and the brain, CT scans aid in detecting fractures, skull deformities, hemorrhages, contusions, foreign bodies, and other traumatic abnormalities (4, 9, 10). These images enable clinicians to assess the extent and localization of the injuries, guiding appropriate treatment decisions and surgical interventions (4, 7). Magnetic resonance imaging (MRI) is ideally suited for soft tissue assessment because of its excellent soft tissue contrast and its ability to image directly in any plane. However, MRI comes with higher costs, is less widely accessible, and typically necessitates longer periods of anesthesia (8). Moreover, the very small size of the brain in most birds results in poor anatomic detail (8, 10, 11).

Brainstem auditory evoked response (BAER) tests are non-invasive and evaluate components of the external ear canal; middle and inner ear cavities; cranial nerves VIII (BAER and the afferent limb of the acoustic reflex), V and VII (both involved in the afferent branches of the acoustic reflex); and.

selected areas of the brainstem and cerebral cortex (12, 13). In fact, the results obtained in conscious and unconscious patients are similar; therefore, this test can be useful to better specify the degree of involvement of brainstem structures during sensory obtundation (13). In practice, BAER measurement requires three electrodes (recording, ground, and reference), an amplifier, and a stimulator (12). The response to the stimuli is recorded as a series of peaks (waves I–V) at approximately 1 ms intervals. The origin of peak I (eighth pair of cranial nerves) is usually easily recognized; peak II arises in the cochlear nucleus, peak III in the inferior olive complex and peaks IV and V in the inferior colliculus (11). Several studies have been conducted on the use of the BAER test in healthy birds, highlighting different responses with respect to the perception of sound waves in nocturnal and diurnal birds, birds of prey and those born in captivity (10–16).

Flash visual evoked potentials (FVEPs) are non-invasive electrodiagnostic tests used to diagnose neurological disorders (17, 18). FVEPs have clinical applications in ophthalmological retinal pathology and neurological pathology related to the optic nerve and/or brain. FVEPs allow the detection of altered functional integration within the visual pathway originating from the retina to the cortical areas through the optic nerve as a result of light stimulation. The triggering of these neuro-anatomic pathways is represented on the recorded waveforms as a series of distinct peaks (positive or negative) according to the variation in the electric field over time. In birds, the use of FVEPs was demonstrated in pigeons (*Columba livia*) and zebra finch (*Taeniopygia guttata*) to assess the origin of the potential of the involved structures of the visual pathways (19–21). The feasibility of FVEP recording has also been evaluated in four species of diurnal birds of prey: Harris's hawk (*Parabuteo unicinctus*), lanner falcon (*Falco biarmicus*), gyrfalcons (*Falco rusticolus*), and saker falcon (*Falco cherrug*) under general anesthesia (21). Despite the small number of birds involved in the study, FVEPs were considered safe, easy to perform and useful for the assessment of visual function. The case reported herein provides the first description of a traumatic brain injury evaluated using BAER testing as an indirect test to assess the brainstem as well as the hearing integrity in a pet tawny owl. Additional examinations, such as flash visual evoked potential (FVEP) recording and CT scan, were also performed.

2 Case description

A captive-bred, adult male pet tawny owl (*Strix aluco*) weighing 500 g was presented to a veterinary hospital in Parma because of a history of head trauma against a window while attempting to escape out of the house. The trauma occurred almost 13 h before the clinical examination. Upon clinical examination, the animal appeared to have good nutritional status but was unable to fly and exhibited obtunded senses. A large, dark red hematoma extending into the acoustic meatus was noted in the left ear. At the opening of the oral cavity, the palatine fissure exhibited small blood clots. For a duration of 12 h, the owl was hospitalized and placed under oxygen in an incubator at 30°C (100% sat, 4 L/min), and warm fluids (Ringer solution) S.a.l.f. Spa, Via Guglielmo Marconi, 2, 24,069 Cenate sotto BG (Italy) (50 mL/kg, SC) (5) and vitamin B12 (Dobetin 500 µg/mL injectable Via Amelia 70, 00181, Roma, Italia) (0.5 mg/kg IM) (19) were administered subcutaneously. A single dose of tramadol [Nargesic®, Acme Srl, Via Portella della Ginestra 9, 42,025 Z.I. Corte Tegge (RE), Italy] was administered at 15 mg/kg PO. Meloxicam at 0.5 mg/kg (Metacam® 5 mg/mL, Boehringer Ingelheim S.p. A, Noventana, Italy) was administered orally twice a day. Gavage feeding was performed [Emeraid Exotic Carnivore, 30 mL orally, every 6–8 h, Slow Global, Corso Liberta' 262, 13,100 Vercelli (VC), Italy] for an additional 12 h. Once stabilized, the tawny owl was placed under gaseous general anesthesia (2% isoflurane) (Isoflo® Zoetis Italia S.r.l, Via Andrea Doria, 41 M, 00,192 Roma RM), and two radiograph projections

Abbreviations: BAER, brainstem auditory evoked response; CT, computed tomography; FVEPs, flash visual evoked potentials; HU, Hounsfield units; CBC, complete blood cell.

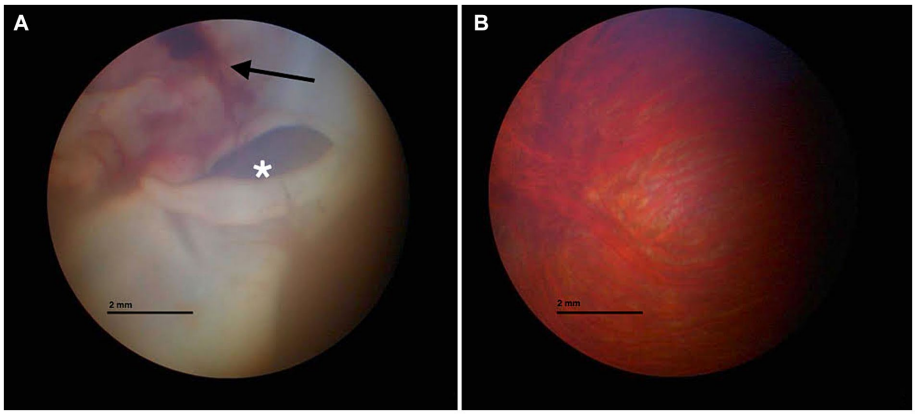

FIGURE 1
Fundus inspection of the left **(A)** and right eyes **(B)**. **(A)** Vitreal hemorrhage (black arrow) and retinal detachment (white asterisk) are visible. **(B)** Normal fundus appearance.

(latero-lateral and dorsal-ventral) were performed. No fractures or other pathological findings were noted. A 2 mL sample of venous blood was drawn from the ulnar vein for a complete blood cell (CBC) count and biochemical analysis, demonstrating no alterations compared with the published reference values for the species (22). An ophthalmic exam was performed. The right eye examination was unremarkable. The left pupil was mydriatic, and no sign of vision was observed. Indirect ophthalmoscopy revealed diffuse retinal edema and detachment. The left pecten was hypotrophic compared with the right pecten. Fundus inspection revealed vitreal hemorrhages and retinal detachments (Figure 1). For two additional days, the owl continued to receive supportive care with subcutaneous fluid therapy of 20 mL NaCl 0.9% followed by intravenous infusion of Ringer's lactate and 5-mL tube feeding with EmerAid Carnivore (EmerAid Intensive Care Carnivore, Cornell, IL, United States) q12h. Meloxicam and tramadol were used to minimize pain and inflammation (Topalgic 100 mg/mL, Sanofi Aventis, Paris, France) at 30 mg/kg PO q12h.

The clinical state of the tawny owl remained stable. However, to advance the diagnostic process and gain crucial insights into vision prognosis, a comprehensive whole-body CT scan was selected. The owl was placed under gaseous general anesthesia (2% isoflurane), and a total body CT scan without the use of contrast media was performed using a single-slice spiral scanner (SOMATOM EMOTION, Siemens Spa, Milano, Italy). An intraxial, ill defined, ovalar and hypoattenuating (75 HU) lesion was reported in the right cerebral hemisphere. No skull fractures were identified. Based on these findings, post-traumatic cerebral edema was hypothesized, such as from severe non-hemorrhagic cerebral contusion (Figure 2).

To better investigate this result, FVEP tests were performed. The test was recorded using Electromyography and Evoked Potentials Systems (MyoHandy, Micromed, Treviso, Italy). The animals were placed in sternal recumbency with their heads elevated using a support to facilitate proper light stimulation. VEPs were recorded using a bipolar method utilizing stainless-steel needle electrodes (size 10 × 0.25 mm). These electrodes were applied subcutaneously at specific locations: the midline of the forehead between the eyes (Fpz) served as the negative electrode, the occipital region on the nuchal crest (Oz) served as the positive electrode, and a ground electrode was positioned subcutaneously at Cz (vertex). Before the recordings,

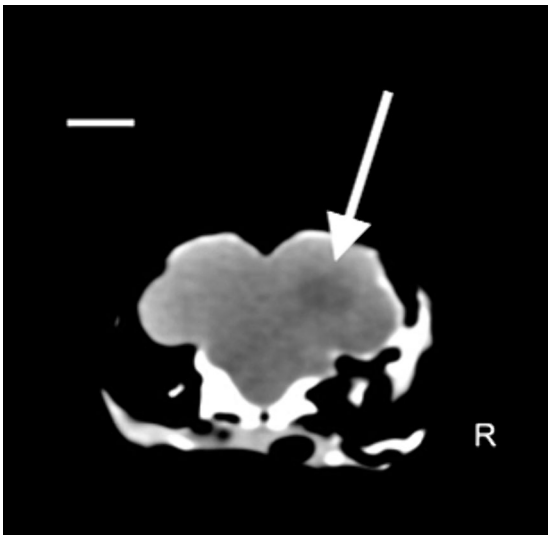

FIGURE 2
Coronal plane image with soft tissue algorithm in the brain window. Scale bar = 8 mm. A hypoattenuating ovalar intra-axial lesion with ill-defined margin is observed at level of parieto-temporal area at the level of the right cerebral hemisphere (white arrow) (Pitch 0.562, slice thickness: 1.25 mm).

mydriatic drugs were not administered, as adequate mydriasis was achieved as part of the anesthetic plan. Throughout the recording sessions, artificial tears (Epigel®, Trebifarma s.r.l, Viale Ammiraglio Giorgio Des Geneys, 60R, 16,148 Genova GE) were applied to keep the eyes moistened. The recordings took place in a quiet and well-lit room with the animal exposed to light for at least 30 min before the session to ensure proper adaptation of the eyes to the light conditions. Each stimulus was a flash of light at an intensity of 10,000 millicandelas per square meter (mcd s/m^2). These flashes were generated using a xenon lamp photostimulator (Flash Stimulator, Micromed® Treviso, Italy). This device produces bright white light that closely resembles natural sunlight. To trigger the xenon lamp, the Flash Stimulator was directly connected to MyoHandy® (Micromed group, Via Giotto, 2, 31,021 Zona Industriale S.p.z. TV, Italy) device. The xenon lamp unit

was positioned 15 cm in front of the eye being examined. The eyelid of the eye under examination was gently opened, and the contralateral eye was covered with a black eye patch to ensure that the light stimulus was specific to the eye under observation. Each eye underwent two consecutive series of stimulations. The first series involved flashes at a frequency of 1 Hz, followed by the second series with flashes at a frequency of 6 Hz. There was a 2-min interval between the two series to allow for adequate recovery and adaptation between stimulations. The duration of the light stimulus was approximately 20 µs. The traces of the left eye revealed no peaks in either series of stimulations, reflecting an altered functional integration within the visual pathway (Figure 3), whereas traces of the right eye were normal.

The subject underwent the BAER examination, performed with acoustic stimulation in the form of Click Standard, with an intensity of 80 dB nHL. This test was performed under the same anesthesia, as all the monitored parameters were stable. Subcutaneous monopolar scalp electrodes were positioned based on previously described conditions in healthy Strigiformes birds (23): a positive electrode on the vertex, a negative electrode near the auditory meatus and a neutral electrode in the retro-occipital area. A monaural click stimulus at 80 dB, able to generate the square wave, was sent to the patient, and only the rise/fall time parameter was considered, usually very fast: slew rate measured in µV/s. The duration of the stimulus was approximately 10 ms, each recording was obtained from an average of approximately 500 stimuli, and all tracings were recorded in duplicate to ensure repeatability of the graph and to eliminate any artifacts.

As observed in Figure 4, in comparison with a physiological tracing from a healthy, captive-bred tawny owl obtained from another owner (Figure 4B), both tracings obtained were characterized by the complete absence of waves from III to V as a suspected general involvement of the brainstem structures, according to the clinical evaluation. However, on the left, as suspected given the involvement of the internal auricular portions, there is hypoacusis at 80 dB, resulting in the disappearance of wave I (cranial nerve VIII) and subsequently the disappearance of the others.

The length of the entire diagnostic procedure was approximately 20 min. The tawny owl died during recovery from anesthesia without any evident cause. Necropsy was refused by the owner.

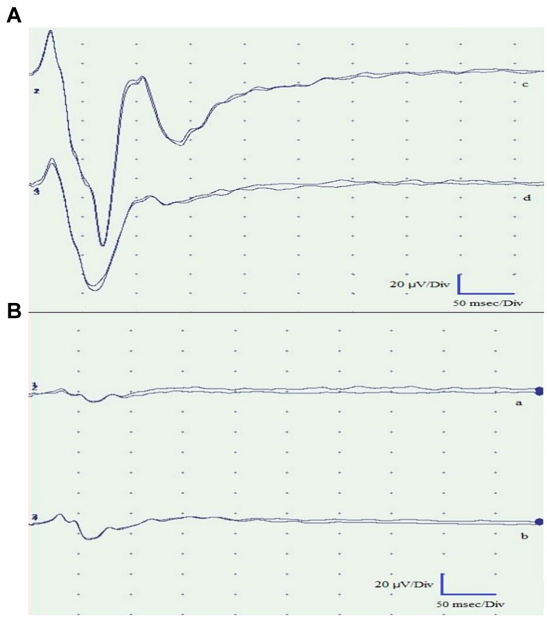

FIGURE 3
Flash visual evoked potentials of the right eye **(A)** and left eye **(B)**. Traces a and c were obtained by light stimulation with the eyes open. Traces b and d were obtained with the eyes closed. The recorded traces from the left eye exhibited pathological findings, demonstrating the absence of peaks in both stimulations. Conversely, the traces obtained from the right eye were normal and exhibited the expected peaks.

3 Discussion

Head trauma in birds is one of the most common causes of neurological disfunction (1, 24, 25) and is often related to collisions (24–28). Comprehensive and meticulous observations, along with several controlled experiments, have demonstrated that, as a general trend, birds do not perceive clear or reflective glass or plastic panes as barriers to be avoided (24–28). Hence, it is unsurprising that the same holds true for pet birds kept in domestic environments. Fractures are a common finding in wild birds that have experienced blunt trauma (24–28). In the case described herein, skull fractures were not evident on either radiographic or CT scan examination. As the traumatic event occurred indoors, it is possible that the short distance covered by the tawny owl prior to hitting the glass was not sufficient to cause bone injuries. However, as literature regarding indoor blunt traumas in birds is scarce, every hypothesis about this finding remains speculative. Ocular injuries are a prevalent aspect of head trauma in birds, with an incidence of over 30% among traumatized avian individuals (29, 30), because of the large orbit, which accommodates their relatively large eyes and scleral ossicles (30). Owl species tend to experience ocular lesions more frequently compared with other birds of prey, primarily due to the unique anatomical and orbital structure of their eyes (31). In this case, we observed vitreal hemorrhages, retinal detachments and hypotrophy of the left pecten relative to the right pecten during the fundus inspection. CT scan revealed a blurry hypoattenuating area within the right cerebral hemisphere. A significant region of cerebral edema was present throughout much of the deep interior of the right cerebral hemisphere. Although the cause is not definitively known, a non-hemorrhagic cerebral contusion is a possible etiology. Bilaterally, there was no visualization of ventricles, sulci, fissures, or cisterns, suggesting increased intracranial pressure. Therefore, differential diagnosis should include cerebral edema secondary to cerebral contusion due to the blunt trauma (32). CT scans have proven to be clinically useful for imaging the brain in birds (33). The decision to perform CT instead of MRI was made for two reasons. The first is related to the duration of anesthesia necessary for the different procedures, with CT needing only a short duration because the procedure is so fast, relative to MRI, which is lengthy As reported in dogs, prolonged anesthesia times after head trauma promote an increased risk of anesthesia and post anesthesia complications (8, 34). Increased intracranial pressure from the administration of anesthetic drugs would, based on the Monroe Kelly doctrine, result in an increased risk of cerebral or cerebellar herniation (35). The second aspect is related to the better evaluation of acute hemorrhage and bone fracture with CT relative to MR imaging, as reported in dogs and cats (36). The limitation of this procedure was related to the absence of contrast medium injection that restrict evaluation of other pathologic areas, if present, or a well

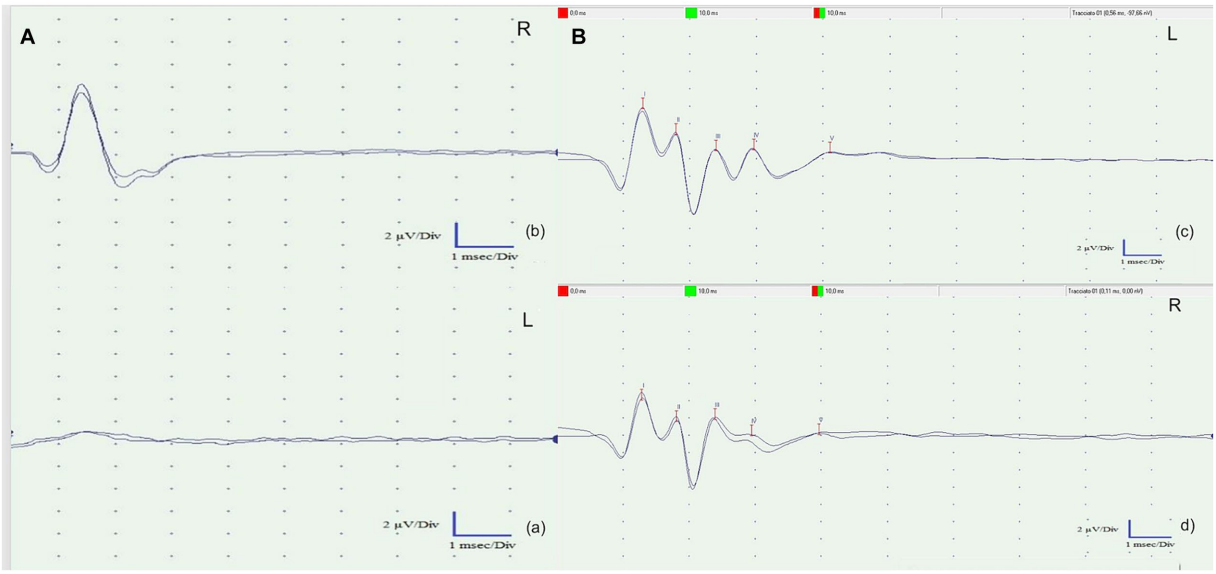

FIGURE 4
(A) Brainstem auditory evoked response (BAER) tests of the left ear **(A)** and the right ear (b). Both recorded tracings exhibited a complete absence of waves III to V, suggesting a likely overall involvement of the brainstem structures, as indicated by the clinical evaluation. However, on the left side (a), there is probable involvement of the inner ear. This hearing impairment resulted in the disappearance of wave I (cranial nerve VIII) and subsequent waves in the recordings. **(B)** Left (c) and right (d) BAER tracks of a clinically healthy tawny owl (*Strix aluco*) used to compare the BAER tracks obtained from the patient. The presence of five physiological waves (I–V) is evident.

clarification of which kind of lesion was observed. Among disorders affecting the posterior eye segment (fundus oculi) in birds, trauma-related hemorrhages are the most frequently diagnosed (37). When the choroid and retina experience traumatic injury, there is a rapid exudation of fluid and cells into the subretinal space, ultimately causing retinal detachment (38). Moreover, the energy transfer from the rigid sclera to the internal structures of the eye could have had a profound impact on the integrity of the retina. In fact, as energy propagates through the semiliquid retinal tissues, it exerts a disruptive force on the most delicate layer of the retina (39). A characteristic of the avian retina that contributes to a higher risk of damage in trauma cases is its avascular nature. When subjected to impact, the globe expands along the equatorial plane, causing destabilization of the uveoscleral interface. Unlike in vascularized retinas, the avascular structure lacks the tensile support provided by the retinal vascular network. This absence of support makes the otherwise semiliquid retinal tissue susceptible to additional shearing, especially in response to oscillating, lower-amplitude pressure wave reflections that occur following the initial short-duration, high-amplitude shock waves typical of blunt traumas (40).

Flash visual evoked potential measurements performed on the left eye exhibited no peaks in either series of stimulations, indicating an altered functional integration within the visual pathway. In birds, invasive techniques involving visual evoked potentials were employed to discern the origin of the potential from individual structures within the visual pathways (17, 18). In dogs, the utility of the fVEP test lies in its ability to correlate the function of specific structures in the visual pathway with the presence of distinct peaks on the recordings. This allows for the identification of the neuroanatomical location of visual lesions, either by the absence of certain potentials or by observing an increase in their latency times (41). Drawing similar conclusions in birds of prey is challenging due to the lack of precise data on their neurofunctional anatomy (20). Despite the existence of significant neuroanatomical similarities with the visual pathways of mammals, which could enable the formation of parallel hypotheses, the absence of accurate information hinders such definitive assessments. Indeed, in birds of prey, there are two parallel visual pathways known as the tectofugal and thalamofugal pathways. The tectofugal pathway corresponds to the extrageniculostriate system observed in mammals, especially in primates, whereas the thalamofugal pathway corresponds to the geniculostriate system. In detail, the tectofugal (collothalamic) pathway consists of optic nerve axons that intersect to varying degrees depending on the species to form the optic chiasm. These fibers then travel to the optic tectum, followed by the round nucleus of the thalamus and finally to the extrastriate cortex (41). With respect to physiological BAER values in birds, literature is lacking. Based on a recent study by Garello et al. (23) on 28 clinically healthy nocturnal raptors (including 4 tawny owls), the most prominent and consistent waves on tracks were the P1, the P2, and the P3. These peaks corresponded to the stimulation of the eighth cranial nerve, the cochlear nucleus, and the lower olivary complex, respectively. These findings were consistent with the track obtained from a clinically healthy tawny owl used as a comparison. The patient exhibited a complete absence of waves III to V, suggesting potential overall involvement of the brainstem structures based on the clinical evaluation. Notably, on the left side, there was probable involvement of the internal auricular portions, leading to 80 dB hearing loss, which resulted in the disappearance of wave I (cranial nerve VIII) and subsequently all other waves. The death of the tawny owl during the recovery from anesthesia could be related to the severity of the injuries, to the anesthesia itself, or both. In fact, due to its impact on central and peripheral control mechanisms, isoflurane has the potential to induce cardiac and respiratory depression in both mammals and birds (42). Moreover, isoflurane has been shown to have dose-dependent respiratory depressant effects in several avian species (43–45). It is possible that the length of the entire diagnostic procedure (approximately 20 min) might have affected the already weakened

nervous system. Furthermore, the newly developed Avian Modified Glasgow Coma Scale, which is useful as a prognostic indicator in cases of raptors presenting with head trauma, was not available at the time of the described case (6). The authors cannot state with certainty whether or not this new scale would have provided a positive prognostic index for the case described so far. However, this demonstrates the existence of an additional tool for defining the diagnostic and therapeutic plan in the course of head trauma in avian species.

4 Conclusion

Head trauma can have a profound impact on birds, leading to notable neurological impairments that affect their behavior, mobility, and cognitive abilities. Utilizing diagnostic tools such as FVEP recordings, BAER tests, and CT scans can be valuable in a clinical setting to assess and understand the extent of neurological damage. It is crucial for clinicians to comprehend the causes and neurological manifestations of avian trauma to ensure effective prevention, accurate diagnosis, and appropriate treatment for affected birds.

Data availability statement

The raw data supporting the conclusions of this article will be made available by the authors, without undue reservation.

Ethics statement

The animal studies were approved by Ethics Committee of the University of Parma (PROT. N. 15/CESA/2023). The studies were conducted in accordance with the local legislation and institutional requirements. Written informed consent was obtained from the owners for the participation of their animals in this study.

Author contributions

AV: Writing – original draft, Writing – review & editing. NC: Conceptualization, Data curation, Formal analysis, Funding acquisition, Investigation, Methodology, Project administration, Resources, Software, Supervision, Validation, Visualization, Writing – review & editing. CC: Conceptualization, Data curation, Formal analysis, Funding acquisition, Investigation, Methodology, Project administration, Resources, Software, Supervision, Validation, Visualization, Writing – review & editing. CP: Conceptualization, Data curation, Formal analysis, Funding acquisition, Investigation, Methodology, Project administration, Resources, Software, Supervision, Validation, Visualization, Writing – review & editing. MD: Visualization, Writing – review & editing, Conceptualization, Data curation, Formal analysis, Funding acquisition, Investigation, Methodology, Project administration, Resources, Software, Supervision, Validation. FB: Conceptualization, Data curation, Formal analysis, Funding acquisition, Investigation, Methodology, Project administration, Resources, Software, Supervision, Validation, Visualization, Writing – review & editing. FDI: Conceptualization, Data curation, Formal analysis, Funding acquisition, Investigation, Methodology, Project administration, Resources, Software, Supervision, Validation, Visualization, Writing – review & editing.

Funding

The author(s) declare that no financial support was received for the research, authorship, and/or publication of this article.

Conflict of interest

The authors declare that the research was conducted in the absence of any commercial or financial relationships that could be construed as a potential conflict of interest.

Publisher's note

References

1. Cococcetta C, Coutant T, Collarile T, Vetere A, Di Ianni F, Huynh M. Causes of raptor admission to the wildlife rehabilitation centre in Abruzzo (Central Italy) from 2005-2016. *Animals*. (2022) 12:1916. doi: 10.3390/ani12151916

2. Stenkat J, Krautwald-Junghanns ME, Schmidt V. Causes of morbidity and mortality in free-living birds in an urban environment in Germany. *EcoHealth*. (2013) 10:352–65. doi: 10.1007/s10393-013-0868-9

3. Morishita TY, Fullerton AT, Lowenstine LJ, Gardner IA, Brooks DL. Morbidity and mortality in free-living raptorial birds of northern California: a retrospective study, 1983-1994. *J Avian Med Surg*. (1998) 12:78–81.

4. Baptista CS, Monteiro C, Fernandes H, Canadas A, Guardão L, Santos JC. Acute intraparenchymal cerebral haemorrhage in an Iberian golden eagle - a case report. *BMC Vet Res*. (2018) 14:60. doi: 10.1186/s12917-018-1379-2

5. Avanzi M, Crosta L, Peccati C, Selleri P. Diagnosi E Terapia Delle Malattie Degli Animali Esotici. Coniglio, Furetto, Pappagalli, Tartarughe. Milano: Elsevier (2008).

6. Foss KD, Keller KA, Reich SK, Franzen-Klein D, Scott D, Sosa-Higareda M, et al. An avian modified Glasgow coma scale as a prognostic indicator in raptors with head trauma. *J Am Vet Med Assoc*. (2023) 261:1–8. doi: 10.2460/javma.23.05.0225

7. Lautenschlager S, Bright JA, Rayfield EJ. Digital dissection - using contrast-enhanced computed tomography scanning to elucidate hard- and soft-tissue anatomy in the common buzzard *Buteo buteo*. *J Anat*. (2014) 224:412–31. doi: 10.1111/joa.12153

8. Jolly M. Treatment of traumatic brain injury in Morepork owls: a review of diagnostic and treatment options. *Proc Assoc Avian Vet*. (2015) 23:31–9.

9. Witmer LM, Ridgely RC, Dufeau DL, Semones MC. Using CT to peer into the past: 3D visualization of the brain and ear regions of birds, crocodiles, and nonavian dinosaurs In: H Endo and R Frey, editors. Anatomical imaging: towards a new morphology. Tokyo: Springer (2008). 67–87.

10. Brittan-Powell EF, Lohr B, Hahn DC, Dooling RJ. Auditory brainstem responses in the eastern screech owl: an estimate of auditory thresholds. *J Acoust Soc Am*. (2005) 118:314–21. doi: 10.1121/1.1928767

11. Strain GM. Brainstem auditory evoked response (BAER) In: GM Strain, editor. Deafness in dogs and cats. Wallingford: CAB International (2011). 83–107.

12. Webb AA. Brainstem auditory evoked response (BAER) testing in animals. *Can Vet J*. (2009) 50:313–8.

13. Cuddon PA. Electrodiagnosis in veterinary neurology: electromyography, nerve conduction studies, and evoked responses. Loveland: Veterinary Specialists of Northhern Colorado (2000).

14. Brittan-Powell EF, Dooling RJ, Gleich O. Auditory brainstem responses in adult budgerigars (*Melopsittacus undulatus*). *J Acoust Soc Am*. (2002) 112:999–1008. doi: 10.1121/1.1494807

15. Brittan-Powell EF, Dooling RJ. Development of auditory sensitivity in budgerigars (*Melopsittacus undulatus*). *J Acoust Soc Am*. (2004) 115:3092–102. doi: 10.1121/1.1739479

16. Kraemer A, Baxter C, Hendrix A, Carr CE. Development of auditory sensitivity in the barn owl. *J Comp Physiol A*. (2017) 203:843–53. doi: 10.1007/s00359-017-1197-1

17. Parker DM, Delius JD. Visual evoked potentials in the forebrain of the pigeon. *Exp Brain Res*. (1972) 14:198–209. doi: 10.1007/bf00234799

18. Engelage J, Bischof HJ. Flash evoked potentials in the ectostriatum of the zebra finch: a current source-density analysis. *Exp Brain Res*. (1989) 74:563–72. doi: 10.1007/bf00247358

19. Engelage J, Bischof HJ. Development of flash-evoked responses in the ectostriatum of the zebra finch: an evoked potential and current-source-density analysis. *Vis Neurosci*. (1990) 5:241–8. doi: 10.1017/s0952523800000316

20. Dondi M, Biaggi F, Di Ianni F, Dodi PL, Quintavalla F. Flash visual evoked potentials in diurnal birds of prey. *PeerJ*. (2016) 4:e2217. doi: 10.7717/peerj.2217

21. Samour J. Appendix 8, pharmaceutics commonly used in avian medicine In: J Samour, editor. Avian medicine. London: Mosby (2000). 388–418.

22. Spagnolo V, Crippa V, Marzia A, Alberti I, Sartorelli P. Hematologic, biochemical, and protein electrophoretic values in captive tawny owls (*Strix aluco*). *Vet Clin Pathol*. (2008) 37:225–8. doi: 10.1111/j.1939-165X.2008.00038.x

23. Garello A, Dondi M, Biaggi F. Brainstem auditory evoked responses in strigiformes birds. Master thesis. Parma, UK: Università di Parma (2020).

24. Klem D. Bird injuries, cause of death, and recuperation from collisions with windows (Heridas, causas de muerte y restablecimiento de aves que chocan con ventanas). *J Field Ornithol*. (1990) 61:115–9.

25. Basilio LG, Moreno DJ, Piratelli AJ. Main causes of bird-window collisions: a review. *An Acad Bras Cienc*. (2020) 92:e20180745. doi: 10.1590/0001-3765202020180745

26. Klem D. Glass: a deadly conservation issue for birds. *Bird Obs*. (2006) 34:73–81.

27. Gelb Y, Delacretaz N. Avian window strike mortality at an urban office building. *Kingbird*. (2006) 56:190–8.

28. Hager SB, Trudell H, McKay KJ, Crandall SM, Mayer L. Bird density and mortality at windows. *Wilson J Ornithol*. (2008) 120:550–64. doi: 10.1676/07-075.1

29. Seruca C, Molina-López R, Peña T, Leiva M. Ocular consequences of blunt trauma in two species of nocturnal raptors (*Athene noctua* and *Otus scops*). *Vet Ophthalmol*. (2012) 15:236–44. doi: 10.1111/j.1463-5224.2011.00976.x

30. Demir A, Ozsemir KG. Ocular lesions and neurologic findings in traumatic birds: a retrospective evalution of 114 cases. *Erciyes Üniv Vet Fak Derg*. (2021) 18:19–25. doi: 10.32707/ercivet.878004

31. Murphy CJ, Kern TJ, McKeever K, McKeever L, MacCoy D. Ocular lesions in free-living raptors. *J Am Vet Med Assoc*. (1982) 181:1302–4.

32. Schwarz T, Saunders J. Veterinary computed tomography. Hoboken, NJ: John Wiley & Sons (2011).

33. Krautwald-Junghanns ME, Kostka VM, Dörsch B. Comparative studies on the diagnostic value of conventional radiography and computed tomography in evaluating the heads of psittacine and raptorial birds. *J Avian Med Surg*. (1998) 12:149–57.

34. Hicks JA, Kennedy MJ, Patterson EE. Perianesthetic complications in dogs undergoing magnetic resonance imaging of the brain for suspected intracranial disease. *J Am Vet Med Assoc*. (2013) 243:1310–5. doi: 10.2460/javma.243.9.1310

35. Neff S, Subramaniam RP. Monro-Kellie doctrine. *J Neurosurg*. (1996) 85:1195. doi: 10.3171/jns.1996.85.6.1195

36. Dewey CW, Da Costa RC. Practical guide to canine and feline neurology. Hoboken, NJ: John Wiley & Sons (2016).

37. Carter RT, Lewin AC. Ophthalmic evaluation of raptors suffering from ocular trauma. *J Avian Med Surg*. (2021) 35:2–27. doi: 10.1647/1082-6742-35.1.2

38. Davidson M. Ocular consequences of trauma in raptors. *Semin Avian Exot Pet Med*. (1997) 6:121–30. doi: 10.1016/S1055-937X(97)80019-9

39. Moore BA, Teixeira LBC, Sponsel WE, Dubielzig RR. The consequences of avian ocular trauma: histopathological evidence and implications of acute and chronic disease. *Vet Ophthalmol*. (2017) 20:496–504. doi: 10.1111/vop.12453

40. Sims MH, Laratta LJ, Bubb WJ, Morgan RV. Waveform analysis and reproducibility of visual-evoked potentials in dogs. *Am J Vet Res*. (1989) 50:1823–8.

41. Shimizu T, Bowers AN. Visual circuits of the avian telencephalon: evolutionary implications. *Behav Brain Res*. (1999) 98:183–91. doi: 10.1016/s0166-4328(98)00083-7

42. Jaensch SM, Cullen L, Raidal SR. Comparative cardiopulmonary effects of halothane and isoflurane in galahs (*Eolophus roseicapillus*). *J Avian Med Surg*. (1999) 13:15–22.

43. Ludders JW, Rode JA, Mitchell GS. Isoflurane ED50 and cardiopulmonary dose-response during spontaneous and controlled breathing in sandhill cranes (*Grus-canadensis*). *Vet Surg*. (1988) 17:174–5.

44. Ludders JW, Rode J, Mitchell GS. Isoflurane anesthesia in sandhill cranes (*Grus canadensis*): minimal anesthetic concentration and cardiopulmonary dose-response during spontaneous and controlled breathing. *Anesth Analg*. (1989) 68:511–6. doi: 10.1213/00000539-198904000-00016

45. Ludders JW, Mitchell GS, Rode J. Minimal anesthetic concentration and cardiopulmonary dose response of isoflurane in ducks. *Vet Surg*. (1990) 19:304–7. doi: 10.1111/j.1532-950x.1990.tb01193.x

frontiers | Frontiers in Veterinary Science

TYPE Original Research
PUBLISHED 02 September 2024
DOI 10.3389/fvets.2024.1276436

OPEN ACCESS

EDITED BY
Irene Iglesias,
National Institute for Agricultural and Food Research and Technology, Spain

REVIEWED BY
Ana Carolina Ewbank,
University of São Paulo, Brazil
David John Beale,
Commonwealth Scientific and Industrial Research Organisation (CSIRO), Australia

*CORRESPONDENCE
Brian Oakley
✉ boakley@westernu.edu

RECEIVED 11 August 2023
ACCEPTED 20 August 2024
PUBLISHED 02 September 2024

CITATION
Guan J, Ramírez GA, Eng C and Oakley B (2024) Microbiome resilience of three-toed box turtles (*Terrapene carolina triunguis*) in response to rising temperatures. *Front. Vet. Sci.* 11:1276436. doi: 10.3389/fvets.2024.1276436

Microbiome resilience of three-toed box turtles (*Terrapene carolina triunguis*) in response to rising temperatures

Jimmy Guan[1], Gustavo A. Ramírez[1,2], Curtis Eng[1] and Brian Oakley[1]*

[1]College of Veterinary Medicine, Western University of Health Sciences, Pomona, CA, United States, [2]Department of Biological Sciences, California State University Los Angeles, Los Angeles, CA, United States

The gastrointestinal (GI) microbiome of chelonians (testudines) plays an important role in their metabolism, nutrition, and overall health but the GI microbiome of three-toed box turtles (*Terrapene carolina triunguis*) has yet to be characterized. How the GI microbiome responds to rapidly rising environmental temperatures has also not been studied extensively in ectotherms, specifically chelonians. In this study, twenty (20) *T.c.triunguis* were split into control and experimental groups. The experimental group experienced 4.5°C increases every two weeks while the control group stayed at a constant ambient temperature (24°C) through the entirety of the experiment. Before each temperature increase, all turtles had cloacal swab samples taken. These samples underwent DNA extraction followed by 16S rRNA gene sequencing and microbial community analyses. Differences in diversity at the community level in the controls compared to the experimental groups were not statistically significant, indicating microbiome resilience to rapid temperature changes in *T.c.triunguis*, although some differentially abundant lineages were identified. Interestingly, an amplicon sequence variant belonging to the *Erysipelothrix* spp. was exclusively enriched in the highest temperature group relative to controls. Overall, our work suggests that there may be an innate robustness to rapid temperature swings in the microbiome of *T.c.triunguis* which are native to temperate North America. Despite this resilience, *Erysipelothrix* spp. was enriched at the highest temperature. Phylogenetic analysis of this amplicon variant showed that it is a close relative of *Erysipelothrix rhusiopathiae,* a pathogen of zoonotic importance associated with both wildlife and livestock.

KEYWORDS

microbiome, chelonians, zoonosis, global warming, *Erysipelothrix* spp.

Introduction

The GI microbiome is a complex community of microorganisms that are a vital part of the hosts' health, acting as a symbiosis contributing to various functions such as energy metabolism, immune system modulation, behavior, and even neurodevelopment (1, 2). These complex communities are directly tied to the health and disease of the host. Although numerous studies have been able to provide valuable insights into the GI microbiome in mammals (3–6), such studies have yet to be done extensively on reptiles, specifically members of the order *Testudines*, commonly referred to as turtles and tortoises. Throughout this study we will use the names

chelonian and testudines interchangeably for the name of the taxonomic order containing all turtles and tortoises. *Testudines* currently contains 357 recognized species, over half (51%) of which are considered globally threatened. This makes turtles and tortoises one of the most threatened groups of vertebrates (7). Members of this order can be roughly divided into aquatic, semi-aquatic, and terrestrial species. Microbial community studies have been done on various aquatic species such as the green sea turtle (*Chelonia mydas*) (8), eastern-short neck turtle (*Emydura macquarii macquarii*) (9), red eared slider (*Trachemys scripta elegans*), and Chinese three-keeled pond turtle (*Chinemys reevesii*) (10) as well as terrestrial species such as Aldabra giant tortoises (*Aldabrachelys gigantea*), gopher tortoises (*Gopherus polyphemus*), and Bolson tortoises (*Gopherus flavomarginatus*) (11). Interestingly, the microbiome of semi-aquatic turtles has yet to be characterized.

Three-toed box turtles (*Terrapene carolina triunguis*) are semi-aquatic turtles belonging to the genus *Terrapene*. These terrestrial turtles are found throughout North America, characterized by a movable hinged plastron that can completely close (12). *T.c.triunguis* spends most of the time on land among ground covers that aid in thermoregulation, and generally only enter bodies of water during periods of high temperatures and drought (13). Like all ectotherms, *T.c.triunguis* relies entirely on environmental temperatures in order to thermoregulate. Because ambient temperature directly affects body temperature, environmental temperatures have a strong influence on ectotherm physiology, behavior, and performance (14). The rapidly warming climate of the Anthropocene (15) challenges *T.c.triunguis* and other turtles/tortoises with these unnatural thermal increases. Climate change has had important documented effects on the individual, population, and community ecology of *Testudines* (16), but the effects of increased ambient temperature on the GI microbiome, to our knowledge, have not been previously examined.

As an ectotherm, *T.c.triunguis* and its microbiota are particularly susceptible to fluctuations in temperature. Temperature-driven microbiome changes may alter the abundance of key lineages, including potential human and animal pathogens, affecting turtle health. Ambient temperature increases are known to perturb host-associated microbial communities in ectotherms and can result in dysbiosis and possible shedding of pathogens. For example, recent observations made in wild western fence lizards (*Sceloporus accidentalis*) exposed to increasing temperatures showed significant changes in their gastrointestinal microbiome, including overall increases in putative pathogenic clades (17).

The objective of this study was to understand the effects of increasing ambient temperature on the gastrointestinal microbiota in *T.c.triunguis*. The changes observed provide important insight into microbial changes in a clade of vertebrates that are globally threatened and highly susceptible to heat stress. Not only is this important to animal health, but there are important public health implications. Both captive and wild-caught reptiles that are asymptomatic have been shown to harbor and excrete a wide array of pathogens that could impact human health. Common turtle-hosted enteric bacteria that are of zoonotic importance include *Salmonella* spp., *Escherichia coli, Kiebsiella* spp., *Campylobacter* spp., and *Yersinia* spp. (18). As reptiles, especially turtles/tortoises, become more popular to keep as pets, this study may inform human and veterinary medicine from a One Health perspective about how rapidly changing environmental temperatures can affect both reptiles and humans.

Abbreviations: GI, Gastrointestinal; ASV, Amplicon sequence variant; DADA2, Divisive amplicon denoising algorithm 2; MAFFT, Multiple Alignment Using Fast Fourier Transform; NMDS, Non-metric multidimensional scaling; PERMANOVA, Permutational multivariate analysis of variance; RAxML, Randomized axelerated maximum likelihood.

Methods

Animal husbandry

Over twenty adult *T.c.triunguis* were obtained from a local turtle/tortoise rescue and housed together in a large group for 2 weeks before the start of the experiment in order to ensure they were equally exposed to the same environment and diet and were considered healthy for the study. All animals were medically evaluated by an experienced exotic animal veterinarian (CE), and any turtles that were deemed unhealthy were removed prior to the start of the study. Blood samples could not be taken due to funding limitations and lack of manpower as this study occurred during the SARS-CoV2 pandemic. Twenty turtles were split equally between males and females into control and experimental groups. Sex was presumed based on sexual dimorphism; females had brown iris color, shorter tails and a flat plastron shape while males had red to orange iris color, longer tails and had a more concave shaped plastron (19). One turtle experienced lethargy, inappetence, and blepharitis during the first week of the study and was removed. The removal of one turtle during the study resulted in the control group with 9 turtles and the experimental with 10. The two groups were housed in separate 50-gallon Rubbermaid stock tanks covered with heavy-duty plastic to create and maintain a microenvironment providing consistent lighting, temperature and humidity. Turtles were housed on 5″ deep cypress mulch substrate (ZooMed Forest Floor) and allowed free access to water. All turtles were free fed as a group approximately 200 g of pellets (Mazuri® Tortoise Diet) supplemented with approximately 100 g of thoroughly rinsed mixed greens, 10–15 red wriggler worms, and powdered calcium (ZooMed ReptiCalcium) three times a week. All diets fed to both groups were obtained from identical sources. UVB lighting was provided 12 h a day using four-foot-long T-5 high output UVB light fixtures (ZooMed ReptiSun).

Five 100-watt ceramic heat emitters (ZooMed Repticare Ceramic Infrared Heat Emitter) were placed approximately 50 cm above the enclosures and connected to digital thermostat controllers (ZooMed ReptiTemp). The control group was maintained at 24°C for the duration of the experiment. This temperature was considered within the lower range of the preferred optimal temperature zone (POTZ) for this species (20). The experimental group experienced 4.5°C increases in temperature every two weeks from 24°C to 28.5°C and finally 33°C. The final temperature point was considered within the higher range of the POTZ (20) without the possibility of resulting in hyperthermia since animals would be exposed to this temperature consistently. Whereas, in the wild animals have the ability to seek shade or swim into deeper areas where temperatures are noticeably cooler. Humidity was maintained between 50–60% in both enclosures for the duration of the experiment. Ambient temperature and humidity were monitored by three different digital temperature and humidity gauges (ZooMed) and recorded daily. Carapace and plastron

temperatures were also taken on each turtle with an infrared thermometer (ZooMed ReptiTemp) and recorded daily. The carapace and plastron temperatures were averaged to obtain accurate total body temperature. Appetite, activity, health, and hydration were subjectively recorded three times a week on a plus-minus scale. All animals were given free access to any location in the enclosure to allow for behavioral thermoregulation. Any turtles that spent a subjectively large amount of time under a heat source or burrowed in the substrate were noted and confirmed to have higher or lower than expected body temperature, respectively. Weights were recorded twice a week with a precision scale.

Sample collection and DNA purification

Every two weeks, before increasing the ambient temperature in the experimental group, all turtles had cloacal swab samples taken. The perineal area was wiped down with square gauze and 70% isopropyl alcohol to clean and disinfect the site. Thermo Scientific™ Remel BactiSwab™ culturette swabs were inserted into the cloaca until the cotton portion was not visible and spun 4–5 times for adequate sample collection. The swabs were placed into the provided culturette tubes with a sponge soaked in liquid transport medium and stored at −20°C. Within 3 months of collection, the stored samples were slowly thawed in an ice bath for DNA extraction. The entire cotton tip and liquid transport medium were used to extract and purify DNA with the QIAmp® PowerFecal® Pro DNA kit. One uL of purified DNA was placed onto a Thermo Scientific NanoDrop™ for nucleic acid quantification. The purified DNA samples were stored at −20°C.

16S rRNA amplicon sequencing, amplicon sequence variant (ASV) generation, and statistical analyses

16S rRNA genes were targeted from DNA samples via PCR using the 519F and 926R (V4-V5 region) primers as previously described (21). Raw sequence Illumina fastq files are deposited in the NCBI SRA archive under the following BioProject number: PRJNA924021.

Amplicon Sequence Variants (ASVs) were generated from high-quality 16S rRNA gene sequences using Divisive Amplicon Denoising Algorithm 2 (DADA2) (22) implemented in the RStudio software. Briefly, forward and reverse reads were trimmed with the filterAndTrim() command using the following parameters: trimLeft = c(20,20), maxEE = c(2,2), rm.phix = TRUE, multithread = TRUE, minLen = 130, truncLen = c(290,200). Subsequently we performed an error assessment followed by independent dereplication of forward and reverse reads. Sequence error removal was performed with the dada() command. Next, error-free forward and reverse reads were merged using the mergePairs() command. Prokaryotic 16S rRNA gene Amplicon Sequence Variants (ASVs) were assigned taxonomy using the SILVA 132 database. ASV-based community composition was visualized in R using ggplot2 implemented in Phyloseq (23) and custom plot scripts.

Microbial community differences between (experimental and control groups) and within (differences among week sampling points) treatment groups were explored with permutational multivariate analysis of variance using the ADONIS function of the R package Vegan (24) implemented on Bray-Curtis distances. Final probabilities were adjusted for multiple comparison inflation by implementing Benjamini-Hochberg correction via the p.adjust (24) function in R. Differential abundance analysis of microbial taxa was performed using the R package *DeSeq2* (25). Specifically, per ASV count data was fitted to a negative binomial distribution model which allows coefficients (log2-fold counts) and standard error estimates for each sample group. A Wald Test, using maximum likelihood estimates of our ASV model coefficients, was then used to test (Pval = 0.05) the following hypothesis between sample groups: H_0 = *no differential abundance*.

Phylogenetic analysis

A comparative phylogenetic analysis of the Eysipelotrichaceae family 16S rRNA gene was performed using the sequence alignment program Multiple Alignment Using Fast Fourier Transform (MAFFT) (26) with the following command parameters: mafft --maxiterate 1,000 –localpair seqs.fasta > aligned.seqs.fasta. Maximum likelihood trees with 100 bootstrap supports were constructed with the Randomized Axelerated Maximum Likelihood (RAxML) program (27) as follows: raxmlHPC -f a -m GTRGAMMA -p 12345 -x 12,345 -# 100 -s aligned.seqs.fasta -n T.tree, −T 4 ML search + bootstrapping. Newick tree files were uploaded to FigTree v1.4.2 for visualization. An *E. coli* (accession: AB681728) sequence was used as the tree outgroup.

Results

Control vs. experimental measurements

For the control group, ambient temperature and body temperature did not change significantly through the course of the experiment, with an average ambient temperature of 23.6°C (Figure 1A) and average body temperature of 24.3°C (Figure 1B). In contrast, the experimental group experienced significant changes ($p < 0.0001$) in both ambient temperature (Figure 1C) and body temperature (Figure 1D). For weeks 1–2, body temperature averaged 22.9°C and ambient temperature averaged 24.8°C. During weeks 3–4, body temperature averaged 26.7°C and ambient temperature averaged 28.5°C. During weeks 5–6, body temperatures averaged 30.4°C and ambient temperature averaged 33°C (Figure 1). Average body weights at the beginning of the experiment were not significantly different between the control animals (mean 400.8 g) and the experimental animals (mean 420.9 g) with neither group changing significantly throughout the experiment (Figure 2; Supplementary Table S1).

Community analysis

Microbial community composition for both experiment and control groups across all time/temperature steps was predominantly (>75% relative abundance) comprised of *Firmicutes*, *Bacteroidetes*, and *Proteobacteria* phyla members (Supplementary Figure S1). More

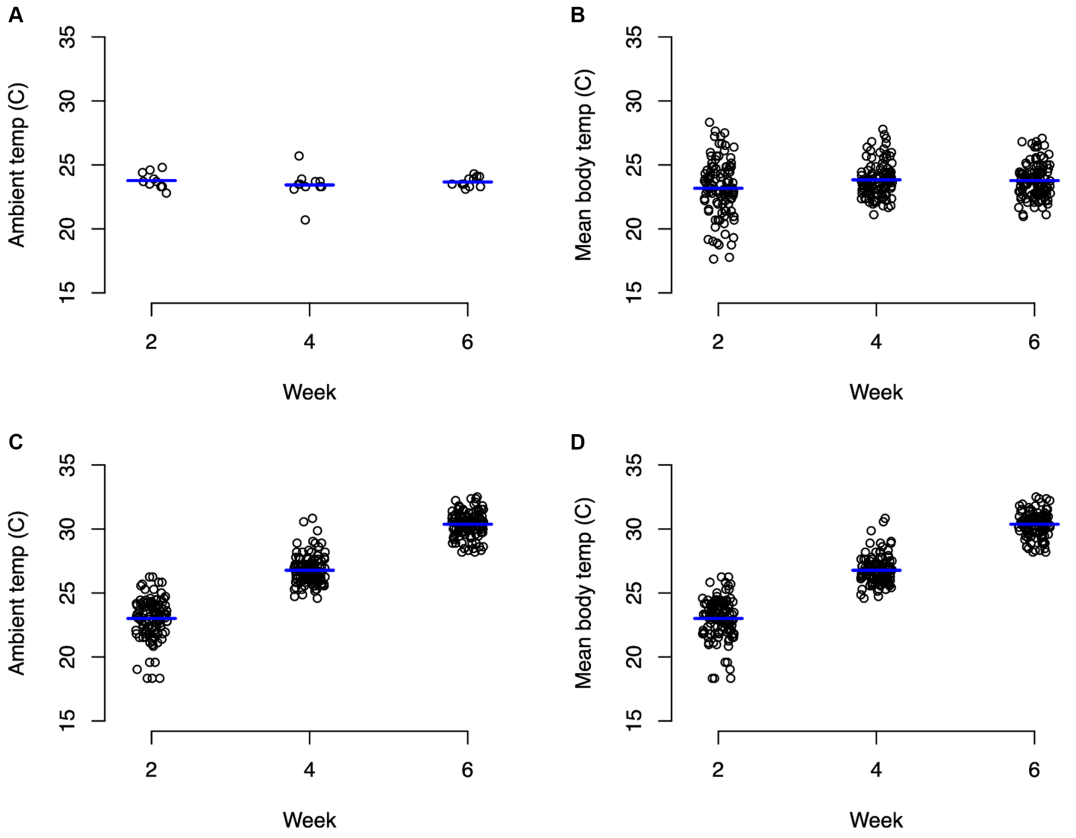

FIGURE 1
Strip charts of recorded ambient and body temperatures in Celsius. **(A)** Represents ambient temperature for animals in the control group, **(B)** represents body temperature for control turtles, **(C)** represents ambient temperature for animals in the experimental group, and **(D)** represents body temperature for experimental turtles. Significant ($p < 0.0001$) differences in ambient and body temperature for the experimental group between every time point.

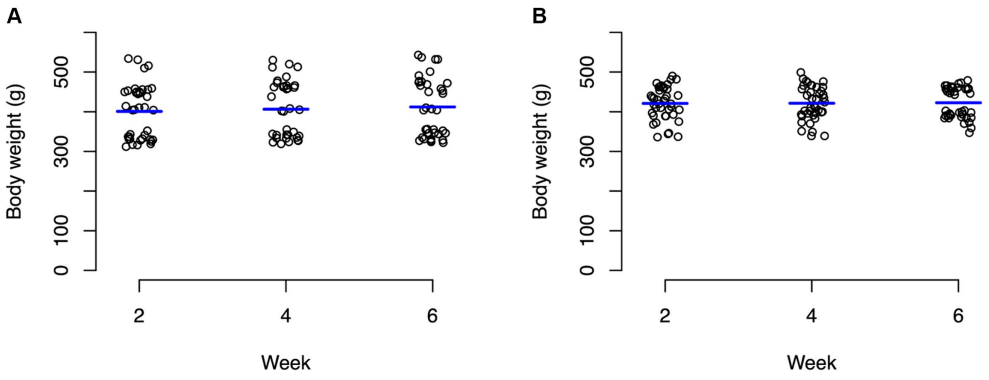

FIGURE 2
Strip charts of baseline body weights of all turtles in grams. **(A)** Control turtles and **(B)** experimental turtles. No significant changes in weight were observed in both groups through the entirety of the experiment.

specifically, members of the following classes within these three phyla were dominant: *Alphaproteobacteria*, *Gammaproteobacteria*, *Bacteroidia*, *Clostridia*, and *Bacilli* (Figure 3).

Alpha diversity metrics showed no significant differences (student *t*-test, Pval >0.05) between control and experimental groups at any collection time (Supplementary Figure S2). Similarly, non-metric multidimensional scaling (NMDS) of all turtles across all the time points showed no significant structuring [Benjamini-Hochberg corrected permutational multivariate analysis of variance (PERMANOVA) $p < 0.01$; Figure 4] between control and experimental groups at any collection time. No temperature driven changes were noted in stress-related organisms; however, there were high degrees of variation within both control and experimental groups at week 2 (Supplementary Figure S3).

10.3389/fvets.2024.1276436

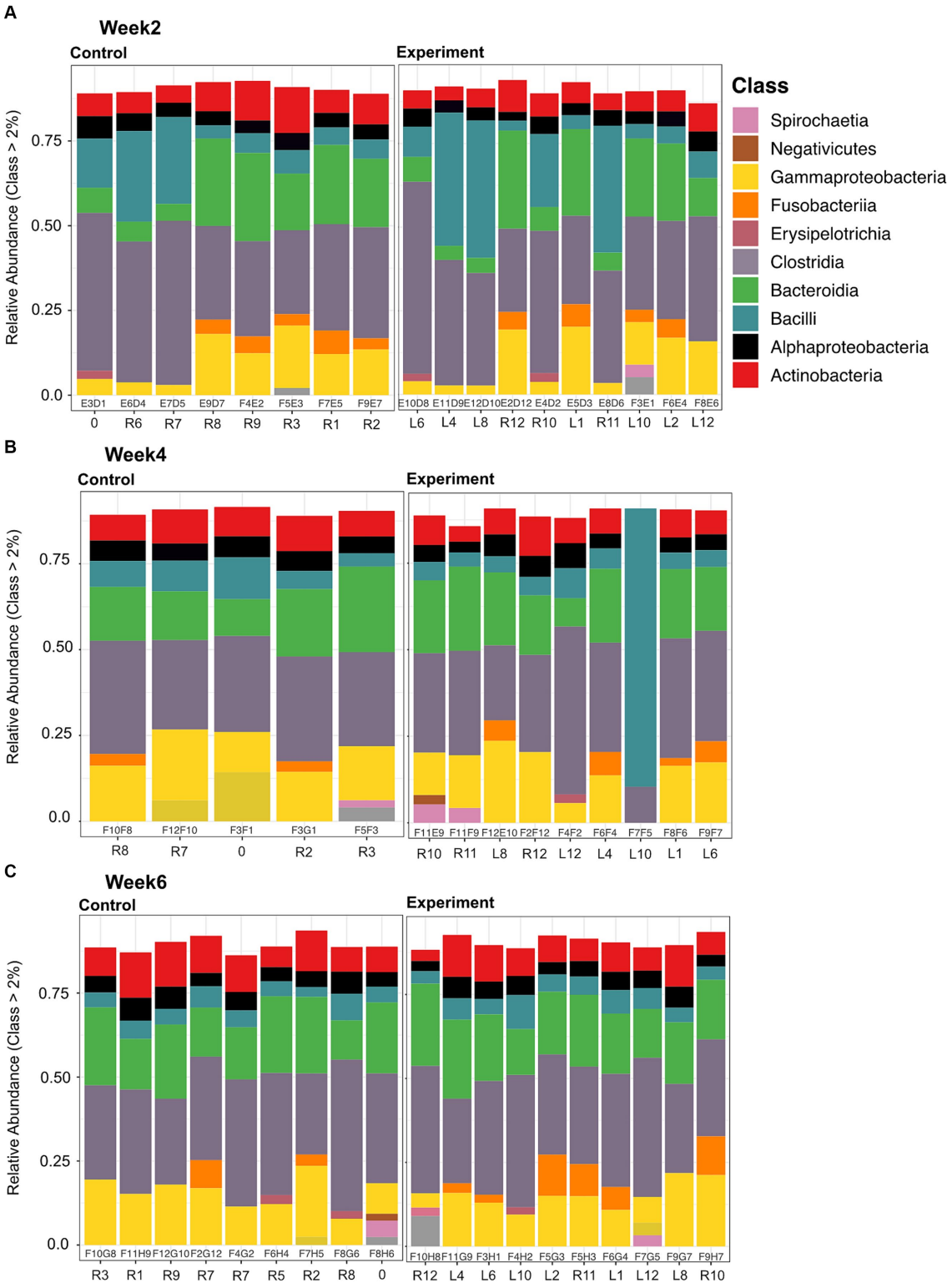

FIGURE 3
Stacked bar plots of relative abundance at the class level for samples collected between control and experimental at each time point (Weeks 2, 4, and 6 depicted in panels **A**, **B**, and **C**, respectively). Each bar plot is labeled with a sequencing ID (within the box) and a Turtle ID (outside the box). Predominant classes present between all samples are: *Alphaproteobacteria*, *Gammaproteobacteria*, *Bacteroidia*, *Clostridia*, and *Bacilli*. Alpha numerical column labels within the black outline boxes represent sequencing identifier. For column labels outside the boxes, the "R" stands for right and "L" stands for left, denoting marking of the carapacial marginal scutes in order to identify individuals (e.g., R8 -> right scute 8), "0" is a turtle we marked on the middle scute.

Enriched genera

Despite its non-significant community-level effect, temperature change elicited significant differential abundances (Wald Test, Pval <0.01) of some individual ASV lineages in the experiment versus control groups (Figure 5). This temperature-driven differential abundance trend between the control and experimental groups was strongest in week 4. Interestingly, despite most of the genera that became more abundant in the controls belonging to known commensal organisms, a temperature enriched ASV in week six was

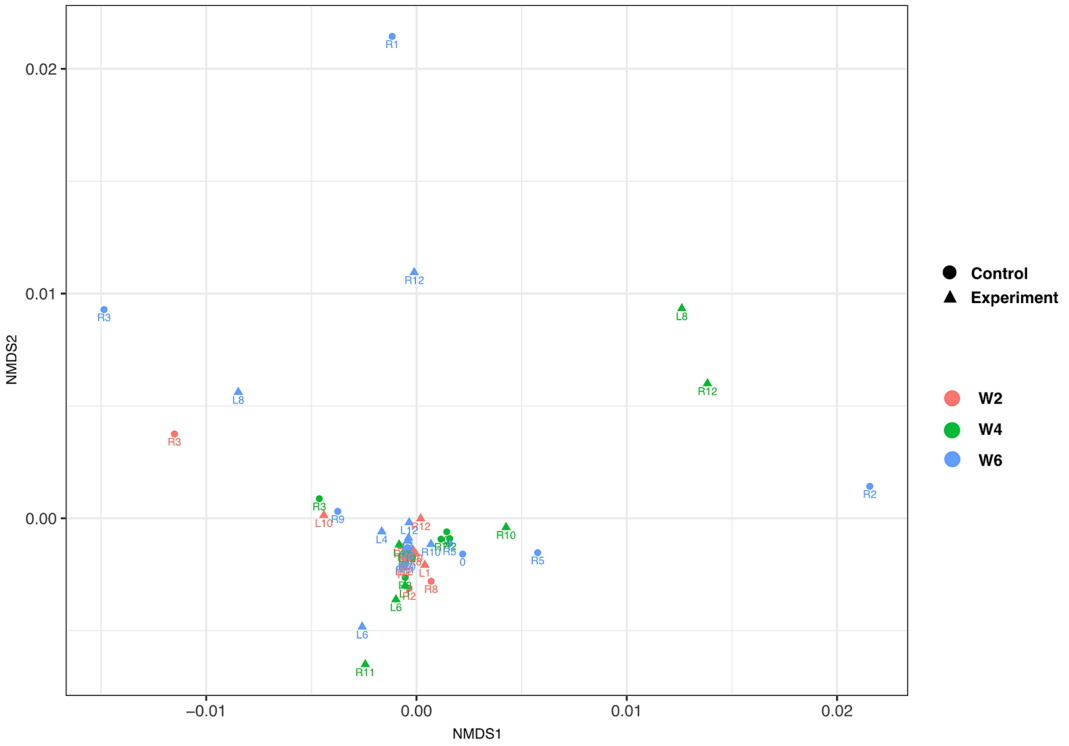

FIGURE 4
Non-metric multidimensional scaling of individual turtles. Triangles and circles depict experimental and control samples, respectively. Collection times week 2, week 4, and week 6 are depicted in red, green, and blue color, respectively. The data, based on Benjamini-Hochberg corrected permutational multivariate analysis of variance (PERMANOVA) $p < 0.01$, failed to show experiment group- or time of collection-driven structuring.

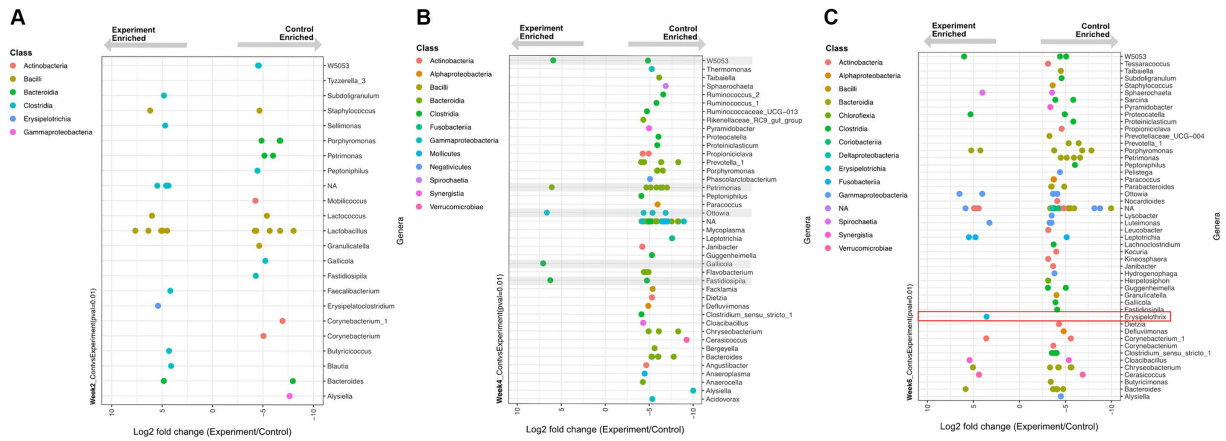

FIGURE 5
Differentially enriched (Wald Test, $p < 0.01$) genera between experimental and control group samples at time **(A)** week 2, **(B)** week 4, and **(C)** week 6. Each dot represents a differentially enriched ASV with experiment and control enrichment for negative and positive Log2 fold-change values, respectively. Each ASV is color coded as a function of taxonomic class and plotted on rows that represent genus-level assignments. **(B)** Grey boxes depict five ASVs enriched under experimental conditions. **(C)** The specific sequence type of *Erysipelothrix* spp. enriched in experimental group is highlighted in the red box.

identified as a member of the *Erysipelothrix* spp., a well-known genus for pathogenic and zoonotic members. A genus-specific phylogenetic analysis of this ASV placed it in a sister clade to the *Erysipelothrix* Clostridium cluster XVI (Figure 6).

Discussion

This study provides insights into the temperature-induced GI microbiome dynamics of semi-aquatic turtles, a group of largely understudied *Testudines*. All turtles in the experimental group experienced a significant change in ambient-induced body temperature at each time point. Three animals from the control group and two from the experimental group were removed from the data set because they experienced prolonged higher or lower temperatures than expected due to observed behavioral thermoregulation. Despite some individual lineages being identified as differentially abundant due to temperature change (Figure 5), the magnitude of temperature change and/or the total exposure time in our experiment failed to elicit significant diversity or community composition changes in the experimental relative to control groups (Figures 3, 4; Supplementary Figure S1). Our results contrast with other studies investigating effects of warming climates on the vertebrate and invertebrate gastrointestinal microbiome where significant decreases in both diversity and community structure have been reported (28, 29).

T.c.triunguis are commonly found in the midwestern and southern United States (e.g., Alabama, Arkansas, Georgia, Illinois, Kansas, Louisiana, Mississippi, Missouri, Oklahoma, Texas) (7) which experience a wide range of temperature differences from periods of extreme cold to extreme heat. Free ranging box-turtles have been observed to be active at temperature ranges from 11.0°C to 36.0°C (30). Unlike most reptiles, ectotherms native to these areas must be able to rapidly adapt to temperature swings. These adaptations may include rapid changes to their microbiome or alternatively, as reported here, a microbial community that exhibits minimal change despite environmental temperature shifts. The lack of significant community-level change between the two groups in our experiment could be due to the fact that the microbiome of *T.c.triunguis* has a level of innate robustness against rapid temperature swings.

Recent work with active-season ground squirrels showed that the microbiome did not change at different timepoints in the seasons, which the authors identified as a potential insensitivity to change of the obligate hibernator microbiome (31). Similarly, metatranscriptomic work on arctic ground squirrels shows that active season cecal microbiome composition is insensitive to seasonal time of collection and high versus low fat diet, however, both variables indeed affect microbiome transcriptional patterns (32). These hibernating mammal studies, despite not being directly comparable to our ectotherm study model, suggests that animals living in habitats with extreme seasonality may be adapted to resist change in their gastrointestinal microbiome during the active season. The compositional robustness of the microbiome may allow for time-optimal energy harvesting needs. Further, the unchanging diversity of the microbiome throughout the active season also suggests a highly diverse GI microbial functional repertoire that through transcriptomic responses, as reported elsewhere (32), may optimally address environmental/dietary seasonality. Future work involving the effect of temperature on the metatranscriptomic dynamics of the *T.c.triunguis* GI microbiome is warranted. Although there were no significant changes induced by temperature in the *T.c.triunguis* microbiome at the community level, we detected significant experiment group-driven differential abundance of a few dozen individual lineages or ASVs (Figure 5). Despite these few taxa exhibiting differential abundance driven by temperature, their net contribution to community-wide alpha diversity and ordination clustering is negligible.

At week 2 (24°C ambient temperature), there was a total of 16 and 21 differentially enriched lineages in the experimental and control group, respectively (Figure 5A). No obvious enrichment trends were observed in terms of the number or taxonomic affiliation of these lineages. Given that there was no difference in temperature between the control and experimental group at this time point, we consider this observation to reflect minor methodological or biological variance in our data.

At week 4 (28.5°C ambient temperature) the experimental group had experienced an increase of 3.1° C mean body temperature for two weeks relative to controls. Here a clear enrichment trend emerged: 75 lineages were significantly enriched in the controls relative to only 5 enriched in the experimental group (Figure 5B). This trend indicates that most differentially abundant taxa were

FIGURE 6
Erysipelothrix spp. phylogenetic tree (100 bootstraps iterations) for various environmental- and host-associated members of this genus. Sequence type ASV 2078, shown in bold red, is the *Erysipelothrix* spp. lineage differentially enriched in week 6 under experimental conditions relative to the control. An *E. coli* sequence (accession AB681728) was used as an outgroup.

disproportionally depleted in the experiment group (with increased temperature) and therefore enriched in the control group. This observation, despite being inconsequential to community-level diversity metrics, supports the notion of a net decrease in abundance of 75 microbiome members in response to a sustained average temperature increase of only 3.1°C.

At week 6 (33°C ambient temperature) the experimental group experienced an additional step increase in temperature of 3.7°C for two weeks (i.e.: a net increase of 6.8°C relative to controls over the previous two weeks). Here, a similar pattern as observed in week 4 was evident: more lineages (78 total) were depleted from the experimental group (enriched in the controls) while only 19 lineages were enriched by the sustained temperature increase (Figure 5C).

Within the thermal and temporal range of our experiment (two week-spaced stepwise increases in temperature by 3.4°C), many lineages were disproportionally depleted in abundance by rising temperatures. Perhaps longer experimental time windows (> 4 weeks) or more drastic temperature increases (>6.8°C) could have resulted in more dramatic differential abundance trends leading to potential impacts on community-level metrics.

Interestingly, one of the 19 temperature-enriched lineages observed at week 6 is a member of the *Erysipelothrix* spp. (Figure 6). Members of this genus are ubiquitous Gram-positive bacteria that can infect a wide variety of hosts such as mammals, reptiles, fish, birds, and even insects (33). The genus is comprised of several species, the most notable is *Erysipelothrix rhusiopathiae,* causing significant clinical disease in livestock and has zoonotic potential. Classically *E. rhusiopathiae* is the causative agent of swine erysipelas resulting in significant losses in outbreaks due to acute septicemia, endocarditis, cutaneous lesions, and chronic arthritis (34). It is also a pathogen of zoonotic concern causing erythematous cutaneous lesions (erysipeloid) and possible fatal endocarditis if left untreated (35, 36). Zoonotic infection with *E.rhusiopathiae* is most commonly as a result of handling infected animals (37). This pathogen notably has also caused clinical disease and zoonotic transmission in American alligators (*Alligator mississippiensis*) and American crocodiles (*Crocodylus acutus*) (38), and has been isolated from a common snapping turtle (*Chelydra serpentina*) (39). Phylogenetic analysis (Figure 6) of the sequences recovered here placed the week 6 experimentally enriched *Erysipelothrix* spp. sequence within a clade that is most similar to previously sequenced *E.rhusiopathiae*. Although considered environmentally ubiquitous, the ASV sequenced in this experiment was most abundant relative to controls in the experimental group at the highest temperature. Enrichment of this ASV at this temperature may be expected since *Erysipelothrix* spp. is optimally incubated at 37°C (36, 40). This supports the likelihood that this ASV would appear in the experimental group at the highest temperature step.

Conclusion

To our knowledge, this study is the first to characterize the cloacal microbial community of a semi-aquatic turtle (*T.c.triunguis*). Our results suggest a level of innate robustness in response to rapid temperature changes, perhaps related to the natural life history of *Terrapene* spp. in North America. Although there were no significant community-wide changes in abundance and diversity in response to temperature increases covering a total range of 9°C over a 6-week experiment, we detected some temperature-driven differentially abundant lineages. One such lineage, with increasing abundance with temperature, was identified as a member of the *Erysipelothrix* spp. which contains many pathogenic species. This observation suggests that the increases in environmental temperature such as those induced here may contribute to enrichment of potential pathogens. Overall, our works indicates that some members of the microbiomes of ectotherms such as *T.c.triunguis* could potentially be affected by increasing environmental temperatures. Future studies to support the innate robustness of *T.c.triunguis* utilizing metabolomics, transcriptomics, proteomics, or gene expression of the microbiome are required to confirm our hypothesis.

Data availability statement

The datasets presented in this study can be found in online repositories. The names of the repository/repositories and accession number(s) can be found at: https://www.ncbi.nlm.nih.gov/genbank/, SRX19164472-SRX19164523.

Ethics statement

This experiment was approved by the Western University of Health Sciences Institutional Animal Care and Use Committee, Protocol R20IACUC011. The study was conducted in accordance with the local legislation and institutional requirements.

Author contributions

JG: Conceptualization, Data curation, Formal analysis, Funding acquisition, Investigation, Methodology, Project administration, Writing – original draft, Writing – review & editing. GR: Formal analysis, Investigation, Supervision, Validation, Visualization, Writing – review & editing. CE: Conceptualization, Funding acquisition, Investigation, Methodology, Project administration, Resources, Supervision, Validation, Writing – review & editing. BO: Data curation, Formal analysis, Funding acquisition, Investigation, Project administration, Supervision, Validation, Visualization, Writing – review & editing.

Funding

The author(s) declare that financial support was received for the research, authorship, and/or publication of this article. Funding was provided by Western University of Healthy Sciences College of Veterinary Medicine "Small Grants for Projects Involving Students" to supply materials required for sample collection, sample purification, and equipment.

Acknowledgments

We thank Zoo Med Laboratories for donating all the husbandry supplies. We would like to extend our gratitude to the San Diego Turtle and Tortoise Society for providing the animals required for this study. We would also like to thank Dominique Griffon and Western University of Health Sciences CVM Office of Research for continued support in student led research.

Conflict of interest

The authors declare that the research was conducted in the absence of any commercial or financial relationships that could be construed as a potential conflict of interest.

Publisher's note

Supplementary material

The Supplementary material for this article can be found online at: https://www.frontiersin.org/articles/10.3389/fvets.2024.1276436/full#supplementary-material

References

1. Barko PC, McMichael MA, Swanson KS, Williams DA. The gastrointestinal microbiome: a review. *J Vet Intern Med*. (2018) 32:9–25. doi: 10.1111/jvim.14875

2. Siddiqui R, Maciver SK, Khan NA. Gut microbiome-immune system interaction in reptiles. *J Appl Microbiol*. (2022) 132:2558–71. doi: 10.1111/jam.15438

3. Colston TJ, Jackson CR. Microbiome evolution along divergent branches of the vertebrate tree of life: what is known and unknown. *Mol Ecol*. (2016) 25:3776–800. doi: 10.1111/mec.13730

4. de Jonge N, Carlsen B, Christensen MH, Pertoldi C, Nielsen JL. The gut microbiome of 54 mammalian species. *Front Microbiol*. (2022) 13:886252. doi: 10.3389/fmicb.2022.886252

5. Moeller AH, Sanders JG. Roles of the gut microbiota in the adaptive evolution of mammalian species. *Philos Trans Royal Soc B*. (1808) 375:20190597. doi: 10.1098/rstb.2019.0597

6. Wu X, Wei Q, Wang X, Shang Y, Zhang H. Evolutionary and dietary relationships of wild mammals based on the gut microbiome. *Gene*. (2022) 808:145999. doi: 10.1016/j.gene.2021.145999

7. Rhodin AGJ, Iverson JB, Bour R, Fritz U, Georges A, Shaffer HB, et al. Turtles of the world: annotated checklist and atlas of taxonomy, synonymy, distribution, and conservation status. *Chelonian Res Monographs*. (2021) 8:1–472. doi: 10.3854/crm.8.checklist.atlas.v9.2021

8. Bloodgood JCG, Hernandez SM, Isaiah A, Suchodolski JS, Hoopes LA, Thompson PM, et al. The effect of diet on the gastrointestinal microbiome of juvenile rehabilitating green turtles (*Chelonia mydas*). *PLoS One*. (2020) 15:e0227060. doi: 10.1371/journal.pone.0227060

9. Beale DJ, Nguyen TV, Shah RM, Bissett A, Nahar A, Smith M, et al. Host–gut microbiome metabolic interactions in PFAS-impacted freshwater turtles (*Emydura macquarii macquarii*). *Meta*. (2022) 12:747. doi: 10.3390/metabo12080747

10. Qu YF, Wu YQ, Zhao YT, Lin LH, Du Y, Li P, et al. The invasive red-eared slider turtle is more successful than the native Chinese three-keeled pond turtle: evidence from the gut microbiota. *PeerJ*. (2020) 8:e10271. doi: 10.7717/peerj.10271

11. Sandri C, Correa F, Spiezio C, Trevisi P, Luise D, Modesto M, et al. Fecal microbiota characterization of Seychelles Giant tortoises (*Aldabrachelys gigantea*) living in both Wild and controlled environments. *Front Microbiol*. (2020) 11:569249. doi: 10.3389/fmicb.2020.569249

12. Espinheira Gomes F, Brandao J, Sumner J, Kearney M, Freitas I, Johnson J 3rd, et al. Survey of ophthalmic anterior segment findings and intraocular pressure in 95 north American box turtles (Terrapene spp.). *Vet Ophthalmol*. (2016) 19:93–101. doi: 10.1111/vop.12257

13. Fredericksen TS. Thermal regulation and habitat use of the eastern box turtle in southwestern Virginia. *Northeast Nat*. (2014) 21:554–64. doi: 10.1656/045.021.0406

14. Roe JH, Wild KH, Hall CA. Thermal biology of eastern box turtles in a longleaf pine system managed with prescribed fire. *J Therm Biol*. (2017) 69:325–33. doi: 10.1016/j.jtherbio.2017.09.005

15. Crutzen PJ. The "Anthropocene" In: E Ehlers and T Krafft, editors. Earth system science in the Anthropocene. Berlin: Springer Berlin Heidelberg (2006). 13–8.

16. Butler CJ. A review of the effects of climate change on chelonians. *Diversity*. (2019) 11:138. doi: 10.3390/d11080138

17. Moeller AH, Ivey K, Cornwall MB, Herr K, Rede J, Taylor EN, et al. The Lizard gut microbiome changes with temperature and is associated with heat tolerance. *Appl Environ Microbiol*. (2020) 86:e01181. doi: 10.1128/AEM.01181-20

18. Ebani VV. Domestic reptiles as source of zoonotic bacteria: a mini review. *Asian Pac J Trop Med*. (2017) 10:723–8. doi: 10.1016/j.apjtm.2017.07.020

19. West JM, Klukowski M. Demographic characteristics of the eastern box turtle, *Terrapene carolina carolina*, in a relictual, suburban, wetland habitat of middle Tennessee, USA. *Herpetol Conserv Biol*. (2016) 11:459–66.

20. Parlin AF, Do Amaral JPS, Dougherty JK, Stevens MHH, Schaeffer PJ. Thermoregulatory performance and habitat selection of the eastern box turtle (*Terrapene carolina carolina*). *Conserv Physiol*. (2017) 5:cox070. doi: 10.1093/conphys/cox070

21. Ramírez GA, Mara P, Sehein T, Wegener G, Chambers CR, Joye SB, et al. Environmental factors shaping bacterial, archaeal and fungal community structure in hydrothermal sediments of Guaymas Basin, gulf of California. *PLoS One*. (2021) 16:e0256321. doi: 10.1371/journal.pone.0256321

22. Callahan BJ, McMurdie PJ, Rosen MJ, Han AW, Johnson AJA, Holmes SP. DADA2: high-resolution sample inference from Illumina amplicon data. *Nat Methods*. (2016) 13:581–3. doi: 10.1038/nmeth.3869

23. McMurdie PJ, Holmes S. Phyloseq: an R package for reproducible interactive analysis and graphics of microbiome census data. *PLoS One*. (2013) 8:e61217. doi: 10.1371/journal.pone.0061217

24. Oksanen J. (2010). Vegan: community ecology package. R package version 1.17. 9.

25. Love MI, Huber W, Anders S. Moderated estimation of fold change and dispersion for RNA-seq data with DESeq2. *Genome Biol*. (2014) 15:550. doi: 10.1186/s13059-014-0550-8

26. Katoh K, Standley DM. MAFFT multiple sequence alignment software version 7: improvements in performance and usability. *Mol Biol Evol*. (2013) 30:772–80. doi: 10.1093/molbev/mst010

27. Stamatakis A. RAxML version 8: a tool for phylogenetic analysis and post-analysis of large phylogenies. *Bioinformatics*. (2014) 30:1312–3. doi: 10.1093/bioinformatics/btu033

28. Bestion E, Jacob S, Zinger L, Di Gesu L, Richard M, White J, et al. Climate warming reduces gut microbiota diversity in a vertebrate ectotherm. *Nat Ecol Evol*. (2017) 1:161. doi: 10.1038/s41559-017-0161

29. Sepulveda J, Moeller AH. The effects of temperature on animal gut microbiomes. *Front Microbiol*. (2020) 11:384. doi: 10.3389/fmicb.2020.00384

30. Parlin AF, Nardone JA, Kelly Dougherty J, Rebein M, Safi K, Schaeffer PJ. Activity and movement of free-living box turtles are largely independent of ambient and thermal conditions. *Mov Ecol*. (2018) 6:12. doi: 10.1186/s40462-018-0130-8

31. Grond K, Kurtz CC, Hatton J, Sonsalla MM, Duddleston KN. Gut microbiome is affected by gut region but robust to host physiological changes in captive active-season ground squirrels. *Animal Microbiome*. (2021) 3:56. doi: 10.1186/s42523-021-00117-0

32. Hatton JJ, Stevenson TJ, Buck CL, Duddleston KN. Diet affects arctic ground squirrel gut microbial metatranscriptome independent of community structure. *Environ Microbiol*. (2017) 19:1518–35. doi: 10.1111/1462-2920.13712

33. Opriessnig T, Forde T, Shimoji Y. *Erysipelothrix* Spp.: past, present, and future directions in vaccine research. *Front Vet Sci*. (2020) 7:174. doi: 10.3389/fvets.2020.00174

34. Morimoto M, Kato A, Nogami K, Akaike Y, Furusawa T, Kojima H, et al. The swine erysipelas vaccine SER-ME effectively protects pigs against challenge with the *Erysipelothrix rhusiopathiae* M203/I257 SpaA-type variant. *Vet Sci*. (2022) 9:382. doi: 10.3390/vetsci9080382

35. Wang T, Khan D, Mobarakai N. *Erysipelothrix rhusiopathiae* endocarditis. *IDCases*. (2020) 22:e00958. doi: 10.1016/j.idcr.2020.e00958

36. Jean S, Lainhart W, Yarbrough Melanie L. The brief case: *Erysipelothrix* bacteremia and endocarditis in a 59-year-old immunocompromised male on chronic high-dose steroids. *J Clin Microbiol*. (2019) 57:e02031–18. doi: 10.1128/JCM.02032-18

37. Forde T, Biek R, Zadoks R, Workentine ML, De Buck J, Kutz S, et al. Genomic analysis of the multi-host pathogen *Erysipelothrix rhusiopathiae* reveals extensive recombination as well as the existence of three generalist clades with wide geographic distribution. *BMC Genomics*. (2016) 17:461. doi: 10.1186/s12864-016-2643-0

38. Johnson-Delaney CA. Chapter 79 – reptile Zoonoses and threats to public health In: DR Mader, editor. Reptile medicine and surgery (second edition). Saint Louis: W.B. Saunders (2006). 1017–30.

39. Elliott RJ. Infectious diseases and pathology of reptiles: Color atlas and text. Boca Raton: CRC Press (2007).

40. Fidalgo SG, Wang Q, Riley TV. Comparison of methods for detection of *Erysipelothrix* spp. and their distribution in some Australasian Seafoods. *Appl Environ Microbiol*. (2000) 66:2066–70. doi: 10.1128/AEM.66.5.2066-2070.2000

frontiers | Frontiers in Veterinary Science

TYPE Original Research
PUBLISHED 01 November 2024
DOI 10.3389/fvets.2024.1483922

OPEN ACCESS

EDITED BY
Marta Martinez Aviles,
Spanish National Research Council (CSIC), Spain

REVIEWED BY
Andrew S. Lang,
Memorial University of Newfoundland, Canada
Wendy Blay Puryear,
Tufts University, United States
Hon Ip,
United States Geological Survey, United States

*CORRESPONDENCE
Katherine H. Haman
✉ Katherine.haman@dfw.wa.gov

RECEIVED 20 August 2024
ACCEPTED 09 October 2024
PUBLISHED 01 November 2024

CITATION
Haman KH, Pearson SF, Brown J, Frisbie LA, Penhallegon S, Falghoush AM, Wolking RM, Torrevillas BK, Taylor KR, Snekvik KR, Tanedo SA, Keren IN, Ashley EA, Clark CT, Lambourn DM, Eckstrand CD, Edmonds SE, Rovani-Rhoades ER, Oltean H, Wilkinson K, Fauquier D, Black A and Waltzek TB (2024) A comprehensive epidemiological approach documenting an outbreak of H5N1 highly pathogenic avian influenza virus clade 2.3.4.4b among gulls, terns, and harbor seals in the Northeastern Pacific.
Front. Vet. Sci. 11:1483922.
doi: 10.3389/fvets.2024.1483922

A comprehensive epidemiological approach documenting an outbreak of H5N1 highly pathogenic avian influenza virus clade 2.3.4.4b among gulls, terns, and harbor seals in the Northeastern Pacific

Katherine H. Haman[1]*, Scott F. Pearson[1], Justin Brown[2], Lauren A. Frisbie[3], Sara Penhallegon[4], Azeza M. Falghoush[5], Rebecca M. Wolking[5], Brandi K. Torrevillas[5], Kyle R. Taylor[5,6], Kevin R. Snekvik[5,6], Sarah A. Tanedo[1], Ilai N. Keren[1], Elizabeth A. Ashley[7], Casey T. Clark[1], Dyanna M. Lambourn[1], Chrissy D. Eckstrand[5,6], Steven E. Edmonds[5,6], Emma R. Rovani-Rhoades[5,6], Hanna Oltean[3], Kristin Wilkinson[8], Deborah Fauquier[9], Allison Black[3] and Thomas B. Waltzek[5,6]

[1]Wildlife Program, Science Division, Washington Department of Fish and Wildlife, Olympia, WA, United States, [2]Department of Veterinary and Biomedical Sciences, Pennsylvania State University, University Park, PA, United States, [3]Washington State Department of Health, Shoreline, WA, United States, [4]Center Valley Animal Rescue, Quilcene, WA, United States, [5]Washington Animal Disease Diagnostic Laboratory, Pullman, WA, United States, [6]Department of Veterinary Microbiology and Pathology, Washington State University College of Veterinary Medicine, Pullman, WA, United States, [7]EpiCenter for Disease Dynamics, One Health Institute, School of Veterinary Medicine, University of California Davis, Davis, CA, United States, [8]West Coast Regional Office, National Marine Fisheries Service, Seattle, WA, United States, [9]Office of Protected Resources, National Marine Fisheries Service, Silver Spring, MD, United States

Highly pathogenic avian influenza viruses (HPAIV) H5N1 clade 2.3.4.4b continue to have unprecedented global impacts on wild birds and mammals, with especially significant mortality observed in colonial surface-nesting seabirds and in some marine mammal species. In July of 2023 H5N1 HPAIV 2.3.4.4b was detected in Caspian terns nesting on Rat Island, Washington USA. An estimated 1,800–1,900 adult terns populated the breeding colony, based on aerial photographs taken at the start of the outbreak. On a near-weekly basis throughout July and August, we counted and removed carcasses, euthanized moribund birds, and collected swab and tissue samples for diagnostic testing and next-generation sequencing. We directly counted 1,101 dead Caspian tern adults and 520 dead chicks, indicating a minimum 56% loss of the adult colony population and potential impacts to reproductive success. Combining the observed mortality on Rat Island with HPAI-related Caspian tern deaths recorded elsewhere in Washington and Oregon, we estimate that 10–14% of the Pacific Flyway population was lost in the summer of 2023. Comparatively few adult Glaucous-winged gulls (hybrids) nesting on Rat Island died (~3% of the local population), although gull chick mortality was high. Sixteen harbor seals in the immediate or nearby area stranded during the outbreak, and H5N1 HPAIV was detected in brain and/or lung tissue of five seals. These cases are the first known detections of HPAIV in a marine

mammal on the Pacific coast of North America. Phylogenetic analyses support the occurrence of at least three independent avian-mammalian virus spillover events (tern or gull to harbor seal). Whole genome sequencing indicated that H5N1 HPAIV may have been introduced to Washington from Caspian terns in Oregon. Ongoing monitoring and surveillance for H5N1 HPAIV in the marine environment is necessary to understand the epidemiology of this virus, assess conservation impacts to susceptible species, and provide support for data-driven management and response actions.

KEYWORDS

gull, highly pathogenic avian influenza (HPAI H5N1), H5N1 2.3.4.4b, marine mammals, harbor seal, tern

1 Introduction

Since 2020, H5N1 clade 2.3.4.4b highly pathogenic avian influenza virus (HPAIV) has caused significant impacts to wild birds and mammals globally, with confirmed detections in millions of animals and over 500 species (1). Historically HPAIV were rarely detected in wild birds, but rather emerged in poultry after a wild bird-origin low pathogenic avian influenza virus (LPAIV) was introduced and adapted to a gallinaceous host (2). A paradigm-shift emerged in the early 2000s as the number of H5N1 wild birds became increasingly involved in HPAI epidemiology (3). This shift initially manifested as sporadic wild bird mortalities associated with H5N1 HPAIV and, subsequently, long distance dissemination of the virus by wild birds (2, 3). With the emergence of H5 clade 2.3.4.4b HPAIV, the extent and diversity of hosts, virulence, and transmission and maintenance dynamics associated with HPAIV radically changed (2, 4–6). H5N1 clade 2.3.4.4b HPAIV has caused sporadic deaths and mass die-offs in wildlife across Europe, Africa, Asia, North America, and South America since 2020 (7–12). In addition to wild birds, thousands of domestic and wild mammals have died because of spillover events and, in certain cases, likely mammal-mammal transmission (13–16). Thus, while HPAI has always posed a threat to domestic animal health, commercial agriculture, and food security, its risk to public health and wildlife conservation has drastically intensified.

Despite the apparent widespread distribution and continued circulation of H5N1 HPAIV in wildlife, disease presentations and outcomes vary among avian and mammalian hosts. The pathobiology of HPAIV is complex and involves the interaction of multiple factors related to level of exposure, viral strain, and host (17). A wide range of clinical responses to H5N1 HPAIV have been documented in taxonomically similar species, even under controlled experimental conditions (18–23). Interspecific variation in susceptibility to infection and disease is magnified by differences in the biology and behaviors of different species that may impact viral exposure, as well as any pre-existing immunity from prior low pathogenic avian influenza (LPAI) virus infections (3, 19, 24, 25). Regarding avian-origin influenza A viruses (IAVs), gulls and terns (Family Laridae) are frequently discussed as a collective group. However, while gulls are well-studied hosts of LPAI and HPAI viruses, there is a dearth of information on IAV pathobiology and ecology in terns, and field observations during the ongoing H5N1 HPAIV panzootic suggest important differences may exist between the two avian groups.

Gulls are recognized reservoirs for LPAIV and can be infected with a wide-diversity of subtypes, including the gull-adapted H13 and H16 subtypes (26, 27). Gulls are clinically susceptible to H5N1 HPAIV (18, 19); however, some field evidence suggests lower mortality rates in adult gulls relative to juveniles, presumably associated with preexisting immunity. In contrast to gulls, large scale mortality events in terns associated with H5N1 HPAIV have been evident since 2020. For example, Sandwich terns (*Thalasseus sandvicensis*) were susceptible to H5N1 HPAIV, with extremely high mortality observed in both adults and juveniles on nesting colonies in the Netherlands (12). Mortality in Sandwich terns across Northwestern Europe is thought to have resulted in a 17% loss of the global breeding population (28). In the United States, there were reports of high mortality rates in Caspian terns (*Hydroprogne caspia*) in the Great Lakes region of Michigan and Wisconsin (29, 30), though published epidemiological data are limited. The distinct lack of information on IAVs in terns limits our ability to interpret the short and long-term impacts of H5N1 HPAIV, particularly when only mortality data are available.

There are numerous challenges associated with discerning epidemiological patterns of HPAIV outbreaks, especially in free-ranging wildlife when only field observations are available. This is true for both individual mortality events and for events over greater spatial and temporal scales. Pairing on-the-ground outbreak investigation and surveillance efforts with viral molecular epidemiology is crucial to understanding patterns of transmission. It is also of critical importance to combine disease surveillance with population monitoring to provide a denominator for simple mortality counts and assess immediate and long-term implications for wildlife conservation and management.

Adopting a comprehensive approach, we describe an H5N1 HPAIV mass mortality event that affected Caspian terns, Glaucous-winged and Western gull hybrids (*Larus occidentalis x glaucenscens*), and harbor seals (*Phoca vitulina*) on Rat Island, Washington USA in the summer of 2023. This event occurred approximately 16 months after the first detection of H5N1 HPAI virus in a wild bird in Washington and involved the first confirmed detection of HPAIV in a marine mammal in the Northeast Pacific. We combine traditional surveillance and outbreak investigation approaches with population monitoring and molecular epidemiology to describe the mass mortality event and quantify its impact on the Pacific Flyway Caspian tern population.

2 Materials and methods

2.1 Study area and species

This study occurred primarily on Rat Island in the Salish Sea, but also includes data on Caspian tern mortality in other localities in the Salish Sea and on the lower Columbia River estuary of Oregon and

Washington (Figure 1). The Salish Sea is a 16,925 km^2 inland sea extending from Olympia, Washington, USA, north to Campbell River, British Columbia, Canada, and includes Puget Sound, the Strait of Georgia, and the Strait of Juan de Fuca. Rat Island is in Puget Sound's Port Townsend Bay. It is a low-lying and sparsely vegetated island (primarily by grasses and herbaceous flowering plants) that is approximately 4.26 ha in size and 0.61 km at its longest axis. The island is used by migrating and over-wintering waterfowl and shorebirds and by several species of breeding birds and one mammal including, Caspian terns, Glaucous-winged and Western gull hybrids (hereafter gulls), black oystercatchers (*Haematopus bachmani*), savannah sparrows (*Passerculus sandwichensis*), song sparrows (*Melospiza melodia*), and harbor seals. Only gulls, terns and seals were observed dead or moribund on Rat Island during carcass collection trips (described below).

Caspian terns are migratory and populations on the U.S. West Coast spend their winters primarily in southern California and Mexico and return to the Salish Sea in late April and early May. They breed in large and dense colonies where they form depressions in the soil and lay 2–3 eggs. Gulls are found on Rat Island year-round and lay 2–3 egg clutches annually in June. On Rat Island in 2023, tern eggs started hatching in early July and continued to hatch through August. Harbor seals use Rat Island year-round as a haulout and pupping site, or rookery. The number of harbor seals hauled out at any given time ranges from zero to 234 non-pups (adults, subadults, and weaned pups) and zero to 54 pups, depending on the year, day, and tide conditions [raw counts are published in (31)]. Harbor seal pupping occurred in late June and continued through early August of 2023, which is typical of most years. Prior to the outbreak on Rat Island, H5N1 HPAI virus had been circulating in Washington State since March of 2022. The virus was primarily detected in waterfowl, shorebirds and predatory and scavenging bird and mammal species and was not associated with this marine ecosystem.

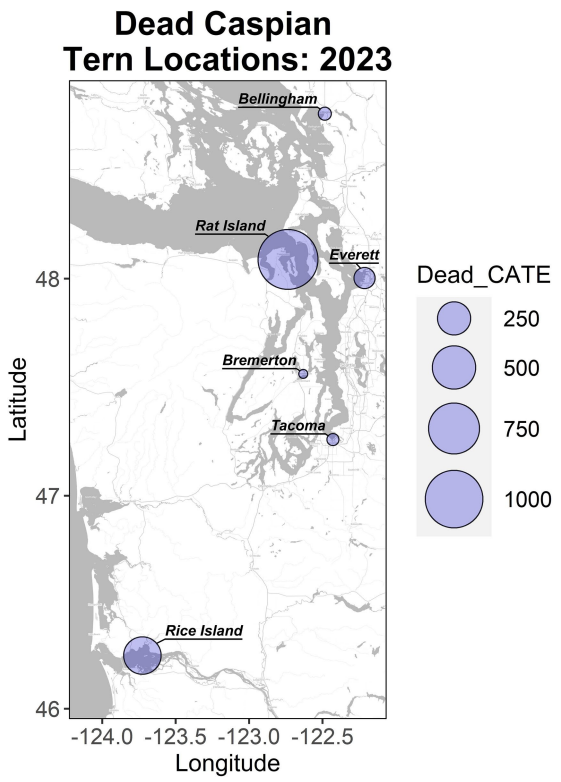

FIGURE 1
Localities and magnitude of Caspian tern mortality in Washington and Oregon in the summer of 2023. Rat Island incurred the largest mortality and is the focus of this study. The Rice Island location along the lower Columbia River includes birds from East Sand Island and Astoria, which are located downstream of this location.

2.2 General surveillance and disease outbreak investigation

The first reports of sick or dead Caspian terns were made to the Washington Department of Fish and Wildlife on July 10, 2023. Given the proximity of Rat Island to Fort Flagler State Park, a very populated state park and campground, we began visiting the island to remove carcasses on July 17, 2023. During this active outbreak, we conducted near weekly site visits for sample collection for pathogen surveillance and carcass counting and removal through August 11, 2023. We also conducted two additional site visits after what we considered to be the active outbreak period, in mid-September and early October (Supplementary Tables S1, S2).

2.3 Sample collection

Over the course of the outbreak select carcasses were sampled for IAV testing. Briefly, for wild avian species, pooled choanal / cloacal samples collected with sterile polyester tipped plastic handle swabs (Puritan, Maine USA®) were collected from individual birds and placed in viral transport media (BD Universal Viral Transport for Viral, Chlamydial, Mycoplasmal, and Ureaplasmal Specimens, New Jersey USA). Swab samples were stored on ice packs in the field and shipped on ice packs to the Washington Animal Disease Diagnostic Laboratory (WADDL) within 48 h of collection. If shipment could not occur within 48 h, samples were frozen at −20C until shipped. Wild bird carcasses were not submitted for postmortem examination due to the ongoing H5N1 HPAIV outbreak in Washington and the known impacts on wild birds.

Harbor seals that were found dead, either by WDFW staff or reported to the local Marine Mammal Stranding Network in the immediate geographic area (within approximately 2 km) of Rat Island, were initially sampled by collecting a nasopharyngeal and a rectal swab in separate vials of transport media. Similar to the avian samples, these were maintained on ice packs in the field and submitted to WADDL within 48 h of being collected, or frozen if shipped after 48 h. However, after several harbor seals stranded dead in the immediate area, we included additional tissue samples for diagnostic testing. If the carcass was small enough to ship (e.g., pup), the whole carcass was submitted to WADDL. From larger individuals (e.g., adults) we sampled lung and the whole head for submission to WADDL for IAV matrix PCR, histology, and immunohistochemistry. All samples were shipped frozen.

2.4 Movement patterns of Caspian terns

We recovered federal bands from the legs of dead Caspian terns. The bands were removed, and the unique identification numbers on the bands were sent to the researchers responsible for banding the

terns and tracking their resights. Banding data included the original banding location, age of banding (adult or chick), and summaries of re-sights (location and year). This information was used to compare the movement patterns of terns prior to the disease outbreak with the pattern of disease spread observed in Washington and Oregon and to examine potential long-distance movement of H5N1 HPAIV by Caspian terns.

2.5 Population estimates

To estimate the number of nesting terns and gulls on Rat Island, oblique aerial photographs were taken on July 17, 2024 during four passes over the island from an airplane flying at ~244-meter altitude and travelling at 148–167 km/h using a digital single lens reflex camera with a 100–400 mm lens with camera speed and International Organization for Standardization (ISO) adjusted to maximize resolution. The photographs included four series of overlapping photos from each pass over the Island that were stitched together in Adobe Photoshop to create a single complete view of the colony from each overflight (overlapping areas were removed to avoid double counting using landmarks) and the following variables were counted from each of the four series of photographs: Caspian tern = live adults, dead adults, nests; gulls = live adults; harbor seals = pups, non-pups (Supplementary Figure S1). Gull nests were difficult to identify from aerial counts because many were obscured by vegetation or driftwood and no dead adult gulls were identified in the photographs. Many dead terns collected during carcass collections were in an incubating position and would have been impossible to distinguish from live, incubating birds from aerial counts. As a result, we did not use the photographs to estimate tern mortality. We combined counts of live and dead adult terns to estimate the total number of adult terns on the colony just prior to the first carcass collection, which served as our estimate of the total number of Caspian terns associated with the Rat Island breeding colony. Each nest or animal was counted in Adobe Photoshop using the count tool to avoid double counting and to help us enumerate all variables (e.g., nests, adults) given the close proximity of nests and birds in the colony.

2.6 Documenting mortality and estimating mortality rates

During the active H5N1 HPAIV outbreak we collected all carcasses from Rat Island in four primary sweeps (8–11 days apart) on July 17, July 25, August 2, and August 11, 2023. We conducted two additional sweeps later in the reproductive season (September 13 and October 3, 2023) and consider these dates past the active outbreak window (Supplementary Table S2). The purpose of the delay was to avoid disturbing fledgling Caspian terns. During sweeps, all gull and tern carcasses were counted (adults and chicks), bagged, and removed from the island. All personnel wore hooded Tyvek suits, rubber boots, gloves, goggles, and N95 masks. All non-disposable equipment, including inflatables and life jackets, was disinfected with a 10% household bleach solution immediately after each visit to the island.

Observed mortality data included six carcass collection dates where we conducted total counts of chick and adult Caspian tern carcasses and chick and adult Glaucous-winged gull carcasses. These counts are either culminations of daily mortalities that occurred between collection periods (known periods of time) or, in the case of the first collection (July 17, 2023), an unknown period of daily mortalities.

To describe daily mortality rates as a continuous exponential curve over unobserved times, we used JAGS 4.3.1 (32) to construct a nonhomogeneous Poisson state-space MCMC model. Thus, each observed count Y_i, is a random variable from a Poisson distribution with rate R_i

$$Y_i \sim Pois\left(R_i\right) i \in \left\{1,2,3,4,5\right\}$$

where $R_i = \sum M_t I\left(t\left(i-1\right) \le t \le t\left(i+1\right)\right)$ is the cumulation of continuous mortality (M_t) between collection dates. We placed a 7-to-21-day uniform prior around time 0, the date of the first carcass collection. Although this is an informative prior, it could be considered diffuse given the observed rate of HPAI growth in poultry (33, 34). We wanted to limit this initial growth period because the colony was under daily observation when the first few carcasses were observed on 10 July 2023, 7 days prior to the first carcass collection. Because the colony was being observed daily by both kayakers watching the island as part of natural history tours and by education volunteers with scopes pointed at the colony, we believe the initial observations of carcasses at the edge of the colony were early in the outbreak. At the same time, because the observers could not see into the middle of the colony, it is probable that the disease started to spread within the colony prior to its first detection (hence the 7–21 days). Published research that estimated secondary cases caused by the infection from one individual (R_0) suggests initial exponential spread and that this spread continues for a few weeks and is faster than the rate of decrease (33, 34). Although these results are for poultry farms, the Caspian tern nest density in the wild [up to 1.48 nests/m^2; (35)] is not unlike bird densities observed in poultry farms. Therefore, rather than fitting a symmetric logistic growth curve we modeled the likelihood of the latent continuous mortalities as an asymmetric sigmoid:

$$M_t = \psi(e^{-t/\sigma^2} - e^{-t/\phi}).$$

where $\phi < \sigma^2$ are mortality rates before and after the inflection point and ψ is a scaling factor for the asymptote.

We placed fully diffused priors on all hyper parameters. However, while the prior on ψ was the improper Gamma (0,0) distribution, the prior for σ^2 was restricted as uniform Beta (1,1) inverse ratio of ϕ. Similarly, we placed a minimum precision half normal prior on ϕ but centered it around the natural log of the $\frac{y_1}{t_0}$ suggesting the inflection point likely occurred during around the time of first collection. For consistency, we fit the same model for the Caspian tern chicks as the adults, except we did not need to estimate t_0 because chick mortality started about the same date as the first carcass collection (July 17, 2023).

2.7 Histology and immunohistochemistry

No samples from wild birds were collected for histology. Whole body cadaver or formalin-fixed tissues were submitted from harbor seals found freshly dead on Rat Island, Ft Flagler, or Indian Island (Supplementary Table S1). Tissues were fixed in 10% neutral-buffered

formalin and sections embedded in paraffin for standard H&E slide preparation and examination by veterinary anatomic pathologists. Immunohistochemistry was performed on select sections of brain from two harbor seal cases using the Ultra View Red Detection Kit (Roche Indiana, USA) on the Discovery Ultra (Roche Diagnostics, Indiana, USA) automated platform. Before applying the primary antibodies, slides were pretreated with protease 1 enzyme (Roche). Influenza A primary antibody (Meridian Bioscience) was used at a 1:400 dilution in antibody diluent (Roche Indiana, USA) and incubated for 28 min. Slides were briefly counterstained with hematoxylin. Applied antibody diluent without the primary antibody served as the negative control.

2.8 Nucleic acid extraction and RT-qPCR for the detection of IAV

Pooled avian choanal/cloacal swabs, nasopharyngeal swabs from harbor seals, and select tissues from harbor seals (lung, brain) were submitted to WADDL for IAV screening with reverse transcription quantitative PCR (RT-qPCR). Nucleic acid extractions of swabs and tissues were performed using a MagMAX™96 Viral RNA Isolation Kit as per the manufacturer's instructions (Thermo Fisher Scientific, Washington USA). RT-qPCR targeting the IAV matrix gene segment was performed as previously described (36). Samples with evidence of IAVs were submitted to the United States Department of Agriculture (USDA)'s National Veterinary Services Laboratory for confirmatory testing, subtyping, and pathotyping.

2.9 Twist comprehensive viral research panel (CVRP) sequencing and molecular analyses

RNA extracts from non-negative samples (those yielding IAV matrix gene segment RT-qPCR cycle threshold (Ct) values <30) were selected for next-generation sequencing (NGS). The sequencing library was constructed using the Twist Library Preparation EF Kit 2.0 (Twist Bioscience, California USA) followed by viral enrichment by hybrid capture using the Twist CVRP with Standard Hybridization v2 reagents [Twist Bioscience, California USA, (37)]. Hybrid capture was performed according to manufacturer's instructions. Briefly, a ProtoScript II First Strand cDNA synthesis kit (New England Biolabs, Massachusetts USA) was used to synthesize first strand cDNA, immediately followed by second-strand synthesis using a NEBNext Ultra II Non-Directional RNA Second Strand Synthesis kit (New England Biolabs, Massachusetts USA). After cDNA purification, enzymatic fragmentation, telomere repair, and dA-Tailing, barcoded universal adapters provided by Twist Bioscience were ligated to the cDNA and then purified. The purified barcoded libraires were then PCR-amplified for 15–20 cycles, followed by purification. The DNA concentration of the sequencing libraries was then quantified using a Qubit dsDNA High Sensitivity Assay Kit (Invitrogen, Massachusetts USA) and batches of four to six prepared libraries were pooled by equal mass up to 2 µg total DNA as recommended by Twist Bioscience. Pooled libraries were incubated with hybridization reagents and 1 unit of biotinylated CVRP probes for 15–17 h. Streptavidin beads were then used to purify viral library fragments bound to the CVRP probes. Post-capture PCR was conducted for 12 cycles as recommended by Twist Bioscience to amplify the enriched libraries. The mean fragment length (base pairs) of enriched pools was estimated using a High Sensitivity NGS Fragment Analysis kit (Advanced Analytical, Massachusetts USA) on a Fragment Analyzer capillary electrophoresis system. The concentration of functional, sequenceable molecules in the enriched pools was determined using a KAPA Library Quantification Kit (Roche, Indiana USA). The mean fragment length values and functional concentration values of enriched pools were then used to combine pools to generate the final equimolar library. The final sequencing library was then diluted to 7pM and sequenced on an Illumina MiSeq using a 600-cycle v3 kit.

To generate the consensus genomes, we used QIAGEN CLC Genomics workbench (version 24.0.1). Raw fastq files were imported into CLC Genomics Workbench. Paired-end reads were quality and adapter-trimmed using default parameters (< 2 ambiguities and quality score > 0.05 per read) and aligned to GISAID EpiFlu reference sequence EPI_ISL_18311027. Consensus sequences were called by base majority frequency and no infilling of zero coverage regions, using default parameters. The coding sequences for individual segments comprising the IAV genomes sequenced at WADDL were deposited in GenBank under accession numbers: PQ118625-PQ118632, PQ118638-PQ118645, PQ118399-PQ118406, PQ118380- PQ118387, PQ118169-PQ118176, PQ118050-PQ118057, PQ118039-PQ118046, PQ118001-PQ118008, PQ113434-PQ113441, PQ113408-PQ113415, PQ113396-PQ113403, PQ113381-PQ113388 (Supplementary Table S3).

2.10 Dataset curation for phylogenetic analysis

To provide background genomic context for the outbreak sequences, we sourced all hemagglutinin (HA) segment sequences from human and animal hosts, sampled from anywhere in the world, with collection dates between January 1, 2020 through June 5, 2024. Data were downloaded from GISAID.[1] The metadata for the GISAID sequences in addition to the 12 sequences generated for this study were then assessed for quality and completeness. Briefly, we used seqtk (V1.4) (38) to deduplicate any sequences generated from the same specimen, a process that can occur when originating labs and confirmatory-testing labs both conduct whole genome sequencing. Using custom R scripts, we excluded all sequences generated from samples with egg passage history and any samples with incomplete dates lacking year, month and day of sample collection. Metadata for all samples were then reformatted into the Nextstrain metadata ingest format. This process yielded a dataset of 11,422 cleaned, deduplicated H5N1 HA segments to use as input to phylogenetic analysis in Nextstrain.

2.11 Phylogenetic inference using HA gene segments

Using the dataset described above, we performed phylogenetic inference using the Nextstrain software suite (39). This workflow enables subsampling of the data, sequence data alignment, genetic

1 gisaid.org

divergence and temporally resolved phylogenetic tree inference, and visualization of the resulting tree using a browser-based package. Briefly, the metadata and fasta files for the 11,422 HA segments were used as the input to Nextstrain Augur. The first step in the pipeline performs subsampling of the genomic data in a tiered way with regard to sampling location. We specified that all sequences sampled from Washington, Oregon, Idaho and British Columbia should be included in the build. Then, sequences sampled from other geographic locations should be sampled at random from the input dataset up to a specified maximum threshold. For sequences sampled from other parts of North America (excluding WA, ID, OR, and BC) we specified inclusion of up to 400 sequences per month per year, and for any geographic location outside of North America, only 2 sequences per month per year should be sampled and included in the build. This subsampling procedure resulted in a dataset of 4,293 HA gene segments used for phylogenetic inference.

As specified within our Nextstrain pipeline, the 4,293 HA segments were aligned with MAFFT (55). The alignment was trimmed to the reference sequence, and a maximum likelihood genetic divergence tree was inferred using IQ-TREE (40). Using the TreeTime package (41), a molecular clock was inferred from the dataset and used to temporally-resolve the tree. The tree structure and associated information were exported as a JSON file for viewing using Nextstrain Auspice. Additional information about the sequences generated for this study were integrated with the genomic analysis using Nextstrain's metadata overlay feature.

2.12 Phylogenetic inference of concatenated whole genome sequences

As a segmented virus, IAV phylogenetic trees are often inferred segment by segment (e.g., one tree for HA, one tree for neuraminidase, etc.). This approach ensures that reassortment events, which can bring together segments with different evolutionary histories, do not confound phylogenetic inference. However, looking at single gene segments yields much shorter sequences, and therefore less visibility into sequence evolution, which can reduce our ability to understand within-outbreak dynamics (42). In cases where reassortment is unlikely, such as geographically limited outbreaks occurring over short timescales, one can concatenate gene segments together to create a whole genome dataset for higher resolution phylogenetic inference.

To perform whole genome phylogenetic inference of the outbreak clade, we concatenated gene segments into a single full-length genome for 17 outbreak-associated viruses that grouped together in a single clade in the HA tree. These 17 sequences included the 12 viruses sequenced at WADDL and five available from GISAID. To ensure proper rooting of this smaller tree, we used an H5N1 concatenated whole genome sampled from a chicken in Oklahoma (*A/chicken/Oklahoma/USDA-013220-001/2022*) as an outgroup. We performed phylogenetic inference as described above, with the addition of reconstructing host species state for internal nodes using TreeTime (41) in Nexstrain. Newick files were visualized with Nextstrain Auspice, and as before we used the Nextstrain metadata overlay feature to integrate additional epidemiological and ecological information with the genomic data.

3 Results

3.1 General surveillance and disease outbreak investigation

Dead terns and gulls that tested positive for H5N1 HPAIV were first detected on the lower Columbia River in mid-June (2023) and then observed in July and August at multiple locations across the Puget Sound (Washington) including Tacoma, Everett, Bellingham and Rat Island (Figure 1). We focused our intensive investigation of mortality on Rat Island, Washington. The active H5N1 HPAIV outbreak period occurred from early July through the end of August 2023. We visited Rat Island to count and remove carcasses a total of four times during the active H5N1 HPAIV outbreak and two additional times at the end of the outbreak (Supplementary Table S2). During the active outbreak visits, we collected a total of 1,580 Caspian terns, including 1,055 adults, 525 young-of-year, and a total of 211 gulls, including 12 adults and 199 young-of-year. After the active outbreak period, on September 13, 2023, we visited Rat Island and collected 74 terns (30 adults and 44 young-of-year) and 87 gulls (13 adults and 74 young-of-year). At this time, all the Caspian tern carcasses had a prolonged postmortem interval resulting in poor diagnostic quality while 2 adult and 13 young-of-year gull carcasses were considered recently dead (i.e., likely <1 week postmortem). During our final trip to Rat Island on October 3, 2023, we collected 50 young-of-year Caspian terns and 22 young-of-year gull carcasses but found no adult bird carcasses. All the Caspian tern young-of-year carcasses had a prolonged postmortem interval while five of the young-of-year gulls were considered recently dead (Supplementary Table S2). Because of the prolonged postmortem interval in the later carcass collection trips, these birds were not used in generating the mortality curves below. Additional carcasses from these species were collected from Fort Flagler and other areas in Western Washington, as reported to WDFW (Supplementary Table S2).

3.2 Sampling

A total of 13 birds (9 terns and 4 gulls) were sampled for diagnostic testing. Of these, six terns (2 young of year and 4 adult) and four gulls (2 young-of-year and 2 adult) were sampled from Rat Island. An additional three terns (all adult) were sampled from surrounding areas (Supplementary Table S1). All nine terns and three of four gulls were IAV-positive via RT-qPCR, and H5N1 clade 2.3.4.4b HPAIV was identified and confirmed in all IAV-positive samples.

A total of 16 harbor seals (6 non-pups and 10 pups) were reported stranded alive ($n = 1$) or dead ($n = 15$) either on Rat Island or nearby Fort Flagler or Indian Island between July 15 and September 10, 2023. All dead stranded harbor seals were in good post-mortem condition except one, that was too heavily scavenged and autolyzed to warrant further investigation (Supplementary Table S1). Dead stranded harbor seals appeared in good body condition with no evidence of gross trauma. Brain, lung, and/or nasopharyngeal swab samples from five harbor seals tested positive for IAV via RT-qPCR; H5N1 clade 2.3.4.4b HPAI virus was identified in all IAV-positive samples. Notably, two harbor seals tested negative for IAV on nasopharyngeal swabs alone but had IAV-positive brain and/or lung tissue samples.

3.3 Movement patterns of banded Caspian terns

Band data were recovered from 16 Caspian tern carcasses, including one that was captured/banded as an adult and all the others were banded as chicks. The birds were banded between 1997 and 2010 (13–26 years old) and were banded at relatively close locations 32–47 km from Rat Island (Dungeness Spit Washington, $n = 1$; Bellingham Washington, $n = 1$), locations 140 km to the southwest along the lower Columbia River (East Sand Island, n = 7; Rice Island, $n = 1$), 177 km to the east in the Columbia Basin (Goose Island, $n = 1$), and 1,132 km to the south in San Francisco Bay (Brooks Island, $n = 1$). Some of these birds were never resighted ($n = 4$) prior to their death. Most were resighted multiple times and one was resighted 142 times. All resights appear to be at breeding colonies. In Figure 2, we show representative movement patterns of six of these birds among colonies and regions based on their original banding location and their resight history. These do not represent annual movements but lifetime movements; a single colony location may represent multiple years breeding at that site before moving to the next site. The most common movement between colonies was between the lower Columbia River and Rat Island, which are the locations where we observed cases of HPAI in terns and matches the timing of mortality and the apparent movement of the disease based on our molecular results below. No movement data were available for seals.

3.4 Population estimates, mortality, and daily mortality rates

Only gulls, terns and seal carcasses were observed and collected on Rat Island, and we focus on those species here. Using the maximum number of animals counted from aerial photographs taken on July 17, 2023, we estimate there were 1,942 adult Caspian terns, 1,100 adult gulls and 130 harbor seals (7 of which were pups) on Rat Island (Table 1). For terns, we counted 1,045 nests in the photographs and the vast majority consisted of an adult sitting on the nest incubating eggs (Table 1). If we assume a pair associated with each nest, there were 2,090 breeding adults, which is a difference of only 148 terns from our maximum count of adults.

Using either the maximum count of adult terns (11,942) or doubling the number of nests (2,090), we estimate that at least 53–56% of the adult Rat Island tern population died during the event. Though we base our population estimate on aerial photographs collected at the onset of the H5N1 outbreak, this may be an underestimation because adult Caspian terns could have been away from the colony foraging at the time of the flight. It is also likely that some terns may have died elsewhere or that carcasses could have washed away with the tides and not been counted. In contrast to the Caspian terns, we estimate that only 2–3% of the adult gull population died. We do not know how many of the eggs from tern nests hatched (many eggs associated with tern nests did not hatch, presumably as the result of adults that died or became ill during the incubation period) and therefore we cannot estimate the proportion of the chicks lost. Nearly all of the gull nests had hatched just prior to the outbreak, and we could not get estimate gull nests or chicks because they were concealed in vegetation. Both gull and tern young of year died at high rates (Table 1). In addition to the mortality documented on Rat Island (Table 1), another 78 terns died in Everett, Bellingham, and Tacoma, Washington and 350 terns died along the lower Columbia River, primarily on Rice Island ($n = 201$) but also in Astoria and East Sand Island, Oregon. In total, 1,529 dead terns were found throughout western Oregon and Washington localities in July and August (Figure 1). We emphasize that these are minimal counts because many carcasses could have been washed out into the Salish Sea or gone undetected, especially along the lower Columbia River. For each of these locations, only a small subset of the dead or moribund birds were sampled for diagnostic testing but all carcasses tested were positive for H5N1 HPAIV (Supplementary Table S1).

Our model of daily mortality for Rat Island suggests that adult terns started dying around July 3, 2023, and the outbreak lasted through the end of August 2023, with a peak in mortality around July 15, with approximately 50 bird deaths per day (Figure 3). For tern chicks, mortality started around July 17 (coincident with the first hatching nests) and lasted until the end of August, with the peak in chick mortality occurring around July 22 with approximately 24 deaths per day. Because hatching continued over several weeks, patterns of mortality in chicks differed from that of adults.

While it is possible not all harbor seal mortalities were recovered, given the surveillance efforts on Rat Island and adjacent Fort Flagler, we believe we found most harbor seal carcasses ($n = 16$), which indicates approximately 12% mortality of the harbor seal associated with Rat Island, based on the one count available ($n = 130$). Since we do not know how many pups were born on Rat Island during this outbreak, we cannot speak to the impacts of H5N1 on adults relative to juvenile harbor seals.

3.5 Harbor seal histology and immunohistochemistry

Histology was performed on various tissues from all harbor seals confirmed to be positive for H5N1 HPAIV by RT-qPCR (Supplementary Table S1). Histologic findings included meningeoencephalitis, neuronal necrosis and perivascular cuffing, myocarditis, non-suppurative inflammation in the brain and heart, pulmonary edema and hemorrhage (Supplementary Table S1). For the cases with a meningeoencephalitis, all exhibited locally extensive or widespread neuronal necrosis and marked meningoencephalitis of the cerebrum and cerebellum (Figure 4), with a mixed leukocyte population of predominantly lymphocytes and plasma cells, as well as macrophages and rare neutrophils along with proteinaceous edema expanding the leptomeninges and Virchow-Robin space (Figure 5). Rarely, leukocytes extended into the neuroparenchyma. Immunohistochemical staining exhibited prominent immunoreactivity to the influenza A nucleoprotein in neuronal cell bodies and processes, as well as glial cells (Figure 6).

3.6 RT-qPCR for IAV detection

Twelve of 13 birds and five of 15 harbor seals screened for IAV via RT-qPCR ultimately tested positive for H5N1 HPAIV. Early in the

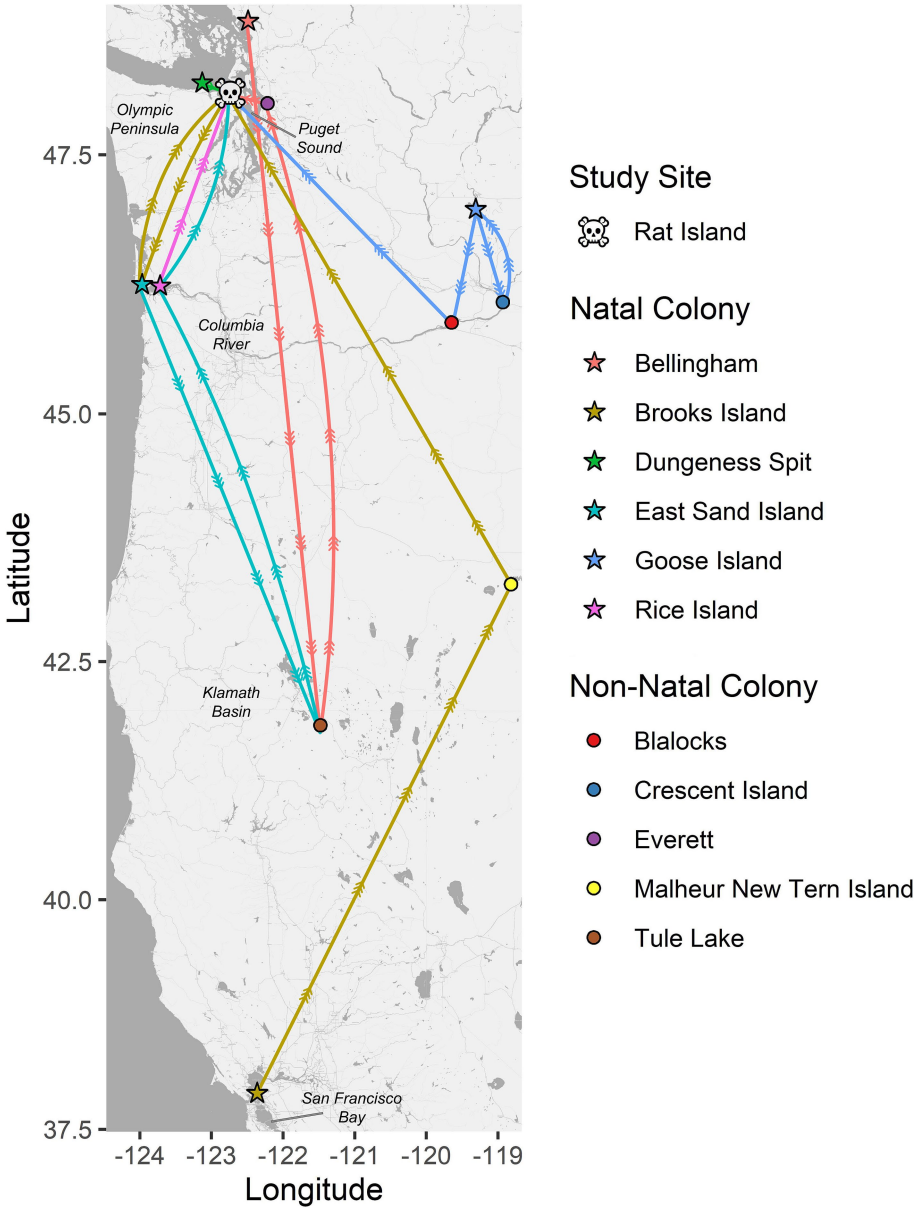

FIGURE 2
Pathways between natal colonies (stars) and resight locations for six color-banded Caspian terns (each represented by a unique color). All six of these birds died on Rat Island (skull and crossbones) in 2023 during the HPAI outbreak where their bands were recovered. The circles represent non-natal colonies where these birds were resighted. These six birds are representative of the resight pathways followed by the other 10 banded terns recovered on Rat Island and that were also banded on their natal colonies in Puget Sound, lower Columbia River, Columbia Basin (Goose Island area) and San Francisco Bay. These movement patterns have implications for the spread of diseases by terns and suggest that terns move both long and short distances among breeding colonies, they move regularly during their lifetimes, and that the most common pattern of movement, between the lower Columbia River and Puget Sound, is the pattern observed for the spread of H5N1 HPAI virus among terns in the region. Note that these movement patterns only represent movement among breeding colonies and not non-breeding movements to southern localities like Mexico or California and are likely biased by locations where there is a higher probability of detection and documentation such as where active research and observation is occurring.

outbreak, only nasopharyngeal swabs were tested from seals. Approximately 1 month into the outbreak, in mid-August, the marine mammal stranding network highlighted the relative increase in harbor seal mortalities in the immediate geographic area around Rat Island. Given this apparent increase, lung and brain tissue were tested as well as nasopharyngeal swabs from three seals that stranded on August 18 and August 25, 2023. Of these three, the nasopharyngeal swab from only one seal was positive for H5N1, while the tissues (lung and/or brain) from all three were positive for H5N1 HPAIV. Given these findings, archived tissues were submitted from the previously dead stranded cases for which tissues had been saved (Supplementary Table S1). Only two of the five harbor seals determined to be positive for H5N1 HPAIV had detectable concentrations of the virus on nasopharyngeal swabs.

10.3389/fvets.2024.1483922

3.7 Molecular epidemiology of H5N1 2.3.4.4b on Rat Island

Whole genome sequencing of H5N1 HPAIV-positive diagnostic specimens yielded 17 complete IAV genome sequences from multiple animal species (12 bird; 5 seal) infected during the outbreak event and sampled between June 15 and August 31, 2023. These data include five sequences sampled from five unique harbor seals, nine sequences from Caspian terns sampled from three different geographic locations along the Puget Sound, and three sequences from infected gulls. Phylogenetic inference performed using HA segment sequences show that all sequences sampled during the outbreak event descend from a single common ancestor, indicating that this outbreak resulted from a single introduction event (Figures 7A,B). Fifteen of the sequences group together in a monophyletic clade with strong bootstrap support, which we refer to as the primary outbreak clade (Figure 7B). Two samples, one sampled from a gull in Oregon and one from a Caspian tern sampled during the outbreak even in Washington, outgroup the primary outbreak clade, though all of these sequences do still share a single common ancestor. The sequence sampled from the Oregon gull is the most basal sequence amongst the 17 sequences explored here and has an identical HA sequence to the inferred common ancestor of all 17 sequences. This finding is consistent with observed patterns of H5N1 detection in terns where mortalities were first observed in Oregon in June and then later in Washington in July, suggesting the Oregon transmission likely preceding the start of the outbreak in Washington. This timing is consistent with when outbreaks were observed to begin in these different regions, where dead birds were first observed in June in Oregon along the lower Columbia River and then in the Puget Sound Region of Washington in July and August.

Within the primary outbreak clade, we observe that the five sequences sampled from unique harbor seals cluster into three separate clades with bootstrap support of 70% or higher (Figure 7B). This is consistent with three separate virus introduction events from gulls or terns into harbor seals. Two of the clades group two harbor seal sequences together, while one clade groups sequences from a single harbor seal sequence and a single Caspian tern sequence. In one of the harbor seal clades, both harbor seal samples have identical HA

TABLE 1 Maximum number of live adults, pups (harbor seals only), and nests (terns only) on Rat Island at the time of the outbreak as determined by aerial photographs taken on July 17, 2023.

Counts of live animals		
Species	Adults (non-pups)	Nests/Pups
Caspian terns	1942	1,045
Glaucous-winged gulls	1,100	
Harbor seals	123	7

Counts of dead animals		
Species	Adults	Young-of-Year/ Pups
Caspian terns	1,101	520
Glaucous-winged gulls	27	298
Harbor seals	6	10

Total counts of dead animals collected at four time points during the active H5N1 HPAIV outbreak and two time points post-outbreak. For harbor seals, numbers include stranded animals from the immediate surrounding area (Fort Flagler and Indian Island).

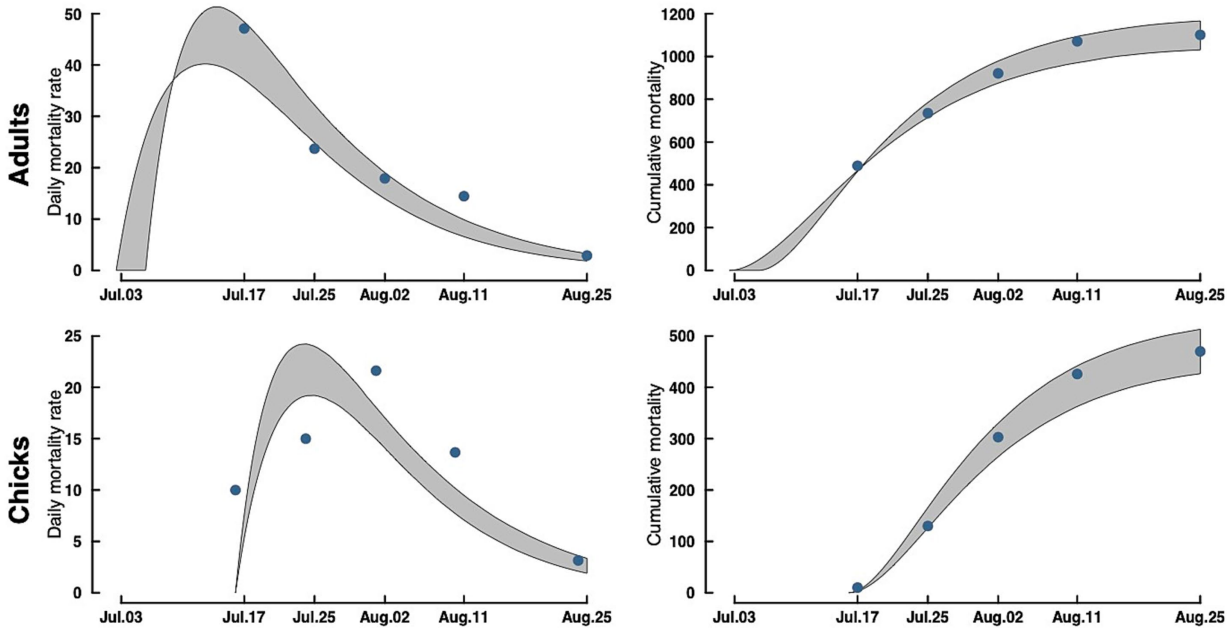

FIGURE 3
Adult (top) and chick (bottom) Caspian tern daily mortality rates (left) and cumulative mortality (right) during the 2023 Rat Island H5N1 HPAI virus event. Gray bands are a 95% CrI around the estimate. Dots in the accumulation curves represent the observed cumulative removals from the Island. The dots in the mortality rate curves are the actual counts of carcasses removed rescaled to daily mortalities (observed counts/ave. time difference between collections).

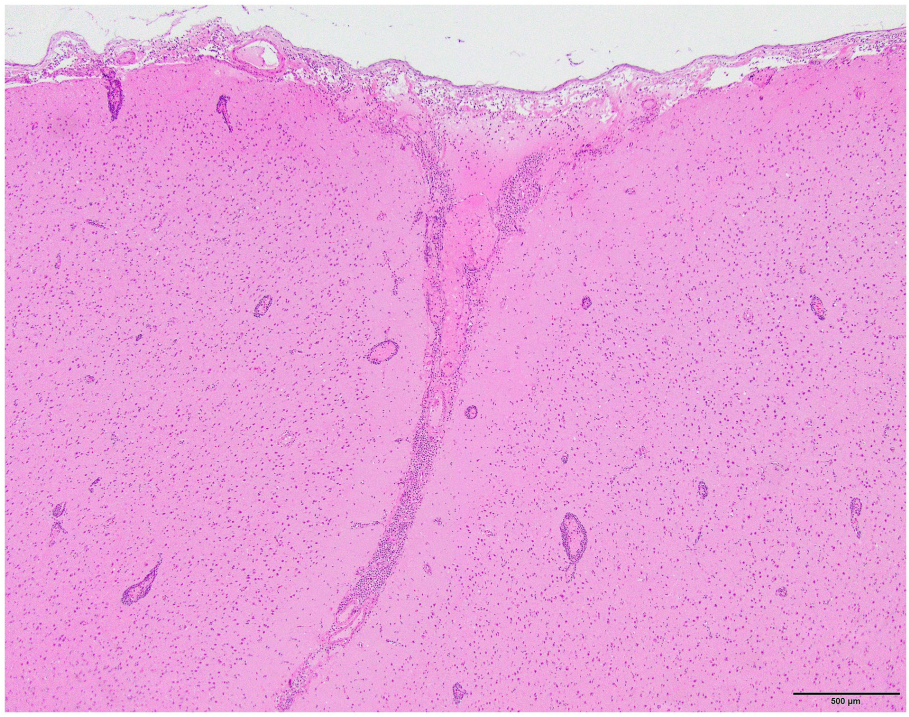

FIGURE 4
Harbor seal cerebrum exhibiting meningoencephalitis (H&E).

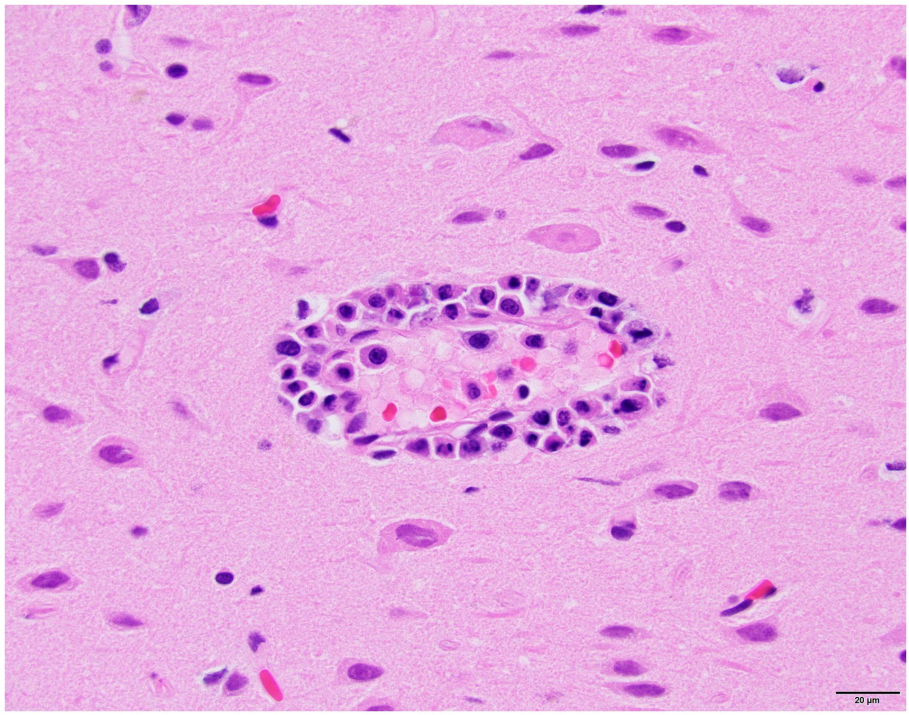

FIGURE 5
Harbor seal cerebrum. Cuffing in Virchow-Robin space, largely lymphoplasmacytic, associated with adjacent neuronal necrosis (H&E, 600x).

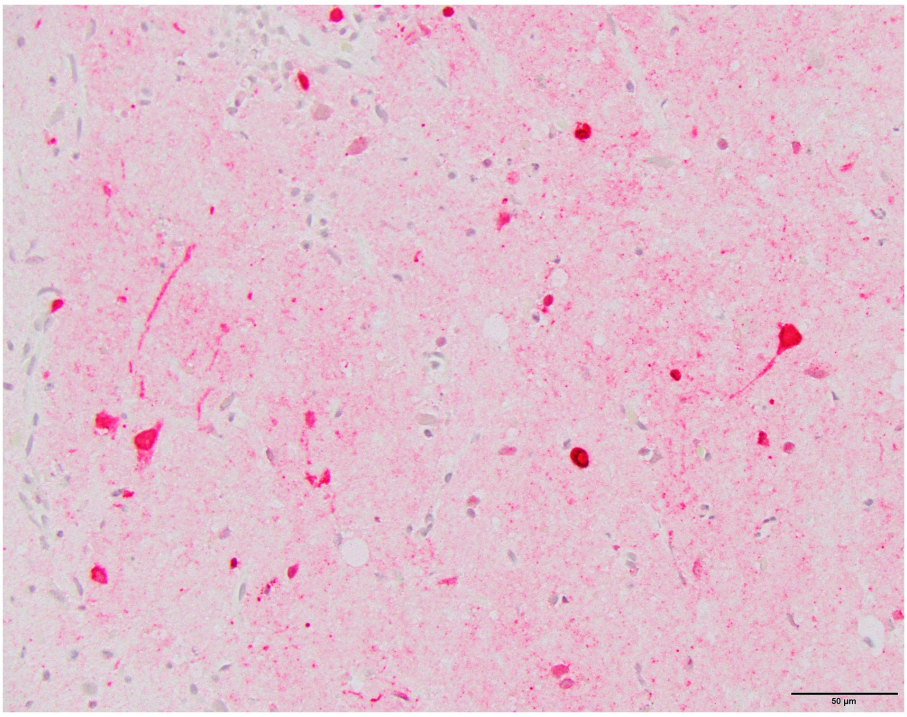

FIGURE 6
Harbor seal cerebrum. Immunoreactivity to influenza A nucleoprotein in neurons and glial cells (Immunohistochemistry, 400x).

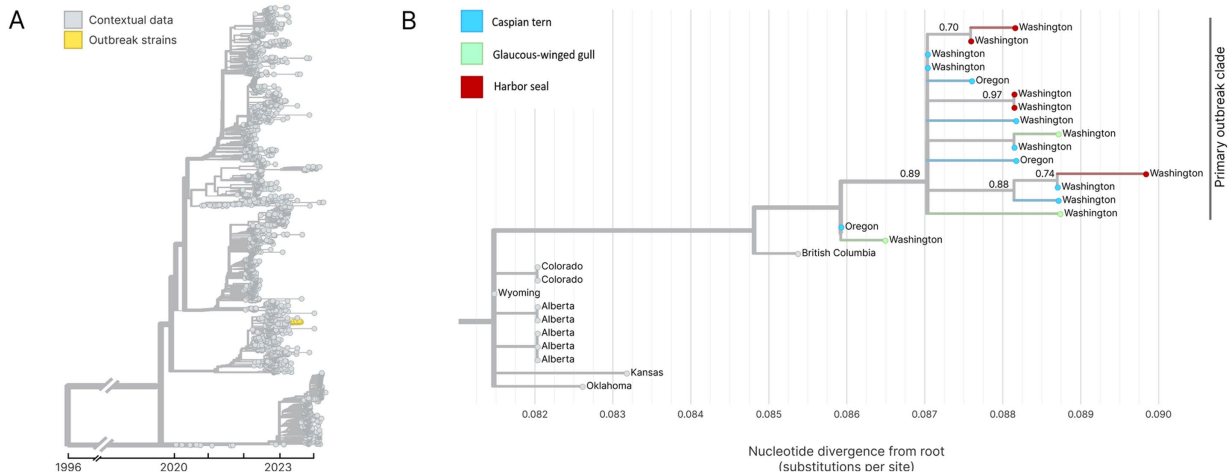

FIGURE 7
(A) Temporally resolved H5N1 HA segment phylogenetic with contextual data. Outbreak viruses are shown colored in yellow, contextual data is colored in grey. **(B)** Maximum likelihood genetic divergence tree of the H5N1 HA outbreak clade. Outbreak clade viruses of interest (colored yellow in panel A) are colored by host animal; light blue indicates a Caspian tern, green indicates Glaucous-winged gull and red indicates harbor seal. Geographic location where the virus was sampled from are annotated at the tips. Bootstrap support values are indicated at key nodes.

gene sequences (Figure 7B). To further explore these spillover events and attempt to differentiate bird-to-seal and seal-to-seal transmission, we performed phylogenetic analysis and ancestral host state reconstruction. Given that the primary outbreak clade sequences are collected over a short time window, during an acute outbreak event, and had greater than 99% nucleotide identity across all genome segments, we did not expect reassortment to impact phylogenetic analysis of the primary outbreak clade sequences. For this analysis we therefore used the concatenated whole genome sequences.

Figure 8 shows the whole genome phylogenetic tree for the primary outbreak clade, with harbor seal clades indicated. Though use of the whole genome provides higher resolution to observe genetic distance resulting in different branch lengths between samples, the topology of the whole genome tree is consistent with the HA tree. As

before, the data support at least three introductions of H5N1 HPAIV from terns into harbor seals. Harbor seal clades one and three (Figure 8) each group together two harbor seal sequences that descend from the same common ancestor and are more closely related to one another than to tern/gull viruses. The four nucleotide mutations defining Seal Clade 1 yielded no amino acid changes. Seal Clade 2 had one amino acid mutation in PB2 (E192K), which is a known, low-frequency mammalian pathogenicity-associated mutation that increases polymerase activity in mammalian hosts (43). Seal Clade 3 viruses shared three amino acid mutations (M646V in PB1, V11A in HA, and A30S in M2).

4 Discussion

During the H5N1 HPAIV clade 2.3.4.4b epizootic on Rat Island, Washington in summer of 2023, there were clear epidemiological patterns for infected host species, with host age class (adult vs. young of year) being an apparent key factor for mortality differences between terns and gulls. For both gulls and terns, conspecifics appeared to be in close contact and at relatively high densities. However, while both adult and young-of-year terns suffered very high mortality, only the gull young-of-year were similarly impacted by the H5N1 HPAIV. This result in adult mortality between species suggests differences in susceptibility and indicates that terns and gulls should not be viewed as having similar responses to IAV, especially H5N1 HPAIV.

Both gulls and Caspian terns are relatively long-lived species (several of the terns observed in this study were older than 20 years), which would provide ample opportunity for exposure to IAVs. It is well documented that many gull species are exposed to a wide diversity of LPAIV subtypes and adults yield a high seroprevalence when surveyed (44–46). This high level of LPAIV exposure may result in immunity and affords protection from H5N1 HPAIV infection or disease. While there is extensive data on IAVs infection in gulls, there are few corresponding studies for terns, especially Caspian terns. Interestingly, one study did find comparatively high seroprevalence in brown and lesser noddies, both terns in the family Laridae (47). This highlights the need for more surveillance and research in gulls and terns to better define the complex topic of IAV immunity in this group of birds, and complicates the interpretation of our results in the absence of serological data. Regardless, the pattern of mortality in adult and juvenile Caspian terns associated with the H5N1 HPAIV outbreak on Rat Island compared to gulls suggests that the Caspian terns may lack protective immunity to H5N1 HPAIV and all life stages are thus more susceptible to fatal infection. Understanding immune responses may not only help predict which species are most susceptible in the face of the ongoing H5N1 HPAIV wild bird panzootic, but also predict future temporal trends as the virus is maintained on land and seascapes.

In addition to prior exposure and immune status, H5N1 HPAIV disease characteristics may be influenced by viral dose and route of exposure. For example, the nesting ecology of Caspian terns is rather distinct compared to Glaucous-winged gulls. On Rat Island and elsewhere, the terns make nests, or scrapes, in a small area with the individual scrapes being extremely close to one another (35). In contrast, the gulls tend to nest on the margins of the island just above the rocky, debris filled high tide line. The gull nests are dispersed and further apart than terns. Given that H5N1 HPAIV can transmit directly or indirectly (through the environment) between birds, the proximity of the tern scrapes may have enhanced viral transmission in the nesting colony. Regardless, given that both the adult and juvenile gulls were scavenging moribund and dead Caspian terns, viral exposure and transmission in the gulls should have also been

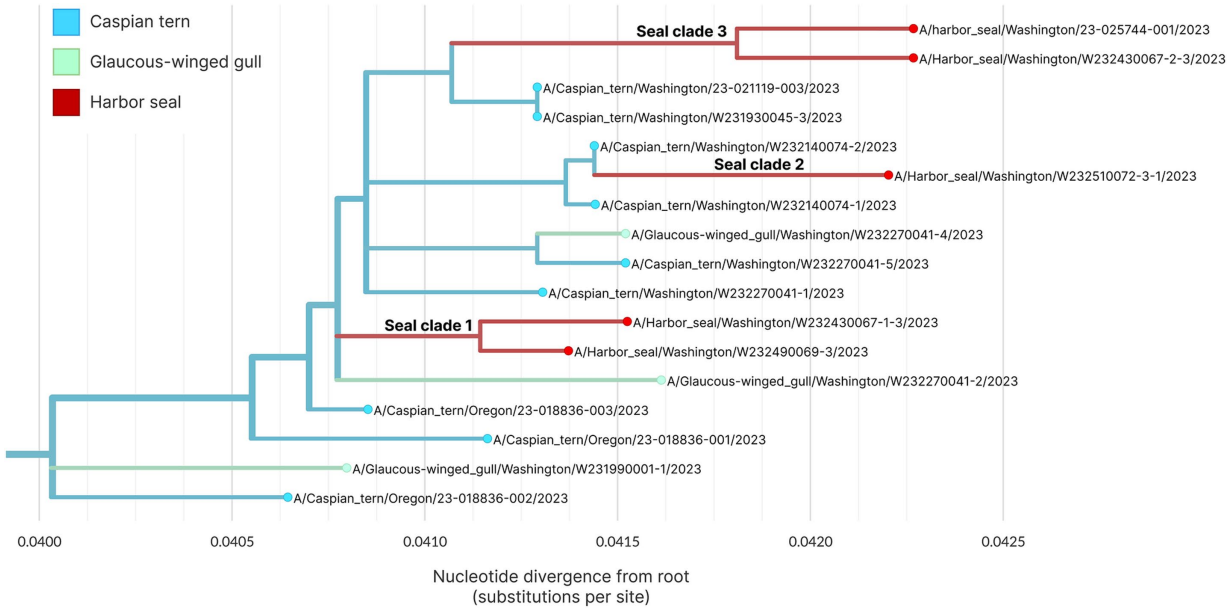

FIGURE 8
Maximum likelihood genetic divergence tree of the H5N1 whole genome outbreak clade. Tips and inferred internal node host state are colored by animal: light blue indicates a Caspian tern, green indicates Glaucous-winged gull and red indicates harbor seal. The three seal introductions are labeled.

extensive. Ingesting infected tissues has experimentally been documented as a method of transmission for H5N1 HPAV in gulls (19). On several occasions, we observed gull chicks and adults scavenging/foraging on both dead and moribund terns, suggesting considerable exposure. The difference in mortality rates in adult Caspian terns compared to adult gulls highlights critical gaps in our understanding of host and viral dynamics and interactions that are key variables in driving disease and spread of H5N1 HPAIV across the global landscape.

Like many seabirds, Caspian terns have a relatively low annual reproductive output and relatively long-life expectancy (48). Based on information obtained from banded Caspian terns found dead on Rat Island, the age of the nesting adults ranged from 13 to 26 years. We estimate that at least 53–56% of the breeding adult tern population on Rat Island died during the H5N1 HPAIV event in 2023. While there were concurrent HPAIV-associated mortalities in other Caspian tern breeding colonies along the Pacific Flyway, tern carcasses were not systematically collected or counted, so the overall impact remains unknown. When we combined the number of dead breeding adult terns at Rat Island ($n = 1{,}101$) with other areas in Washington ($n = 78$) and those collected from Oregon ($n = 350$), the total observed mortality of Caspian terns in 2023 associated with H5N1 HPAI virus was 1,529. The 2021 flyway posteriori population estimate is 10,862 (49). Consequently, the proportion of adult Caspian terns lost during this mortality event in the Pacific Flyway was 10–14%. This is likely a minimum count of the 2023 tern mortality in Oregon and Washington due to the lack of a complete count of dead terns at other breeding colonies. This disease related mortality occurred when the population was already rapidly declining. A census-based minimum population estimate in 2021 indicates that the Pacific Flyway breeding population of Caspian terns declined by 54% since 2008, with most of this decline occurring between 2015 and 2021 (49). Our results indicate the population level impacts of these types of events and how they can compound population losses due to other factors.

The five harbor seals with H5N1 HPAIV virus clade 2.3.4.4b infection are the first documented cases of HPAIV in a marine mammal in the Northeast Pacific. Findings in the seals were similar to H5N1 HPAIV outbreaks in seals documented in 2022 in Quebec, Canada (50) and in Maine (51). Although there have been large mortality events associated with this virus in pinnipeds in South America (16), such extensive mortality was not observed in harbor seals in Washington or the other North American seal outbreaks. Given differences in apparent mortality rates between pinnipeds in South America and Washington, it is possible that, like the species-specific differences observed in susceptibility between the Caspian terns and gulls, such differences may also exist between species of marine mammals. Alternatively, the mechanism(s) of exposure may have differed between events as there is evidence that the H5N1 HPAIV strain affecting pinnipeds in South America may have possessed a greater ability to infect and/or transmit among mammals, compared to the virus infecting harbor seals in Washington (16). Further research is needed to better understand viral transmission dynamics and host susceptibility to H5N1 HPAIV in marine mammals.

The finding of brain positive samples when nasopharyngeal swabs were negative in seals highlights the importance of submitting multiple types of samples (e.g., nasopharyngeal swab, lung, brain) from wild mammals suspected to be infected/exposed to H5N1 HPAIV. Brain positive samples are consistent with observations in other wild terrestrial mammals (52), and these data highlight that H5N1 HPAI virus 2.3.4.4b has a strong tropism for the nervous system. This is supported in the histological findings from the harbor seals infected by H5N1 HPAIV that had widespread neuronal necrosis and a marked meningoencephalitis associated with H5N1 HPAI virus based on the immunohistochemical analyses. Interestingly, neurotrophic H5N1 HPAIV virus strains have not been reported in recent dairy cattle outbreaks, which have been detected in lung, mammary, and conjunctival samples (53, 54), highlighting that continued sampling of multiple organ systems are warranted in wild animals.

The H5N1 HPAIV sequences associated with the mortality event on Rat Island indicates very little genetic variation in the viral genome sequence during the active outbreak and mortality event (July–August 2023). This supports the host susceptibility differences we observed in the mortality data. More research is needed to better understand IAV exposure and immunological characteristics of Caspian terns relative to their gull counterparts on Rat Island and elsewhere.

Comparison of Washington and Oregon H5N1 HPAIV HA segments recovered from Oregon Caspian terns with those from Washington Caspian terns indicates that the virus was likely introduced to Washington from Oregon. This is also supported by the regular movement of banded birds between these regions and by the pattern of mortality, with the first virus detections and mortalities in terns observed in Oregon and then later in Washington. However, given the relatively sparse genomic sampling over the course of this event ($n = 17$), July–September 2023, this linkage may not be direct. The observed genomic pattern is also consistent with viral movement from Oregon to another, unsampled geographic location, with subsequent introduction to Washington. Under either scenario, genomic data support an outbreak event in Oregon preceding the Washington outbreak, with the Washington outbreak descending from the viral diversity circulating in Oregon.

Phylogenetic analysis of whole H5N1 HPAIV genomes sampled from avian hosts and harbor seals associated with the outbreak on Rat Island indicate that there were at least three unique avian-to-seal spillover events. This finding indicates that the mammalian outbreak was driven in part by multiple spillover events, though the reconstruction of two internal nodes as likely circulating in seals supports that some seal-to-seal transmission may have occurred as well. To better understand patterns of transmission both within and among species, more detailed sampling and viral sequencing throughout the outbreak would be necessary. In summary, we find strong evidence for multiple spillover events from terns/gulls into harbor seals on Rat Island. Local spillover from birds to mammals is supported by the fact that the seal event was limited in time and space, and no additional seal mortality events have occurred over the last 12 months. Finally, this local spillover from birds to mammals is consistent with the pattern observed in other outbreaks in North America (50, 51).

5 Conclusion

The global impact of H5N1 HPAIV clade 2.3.4.4b on wild birds and mammals is considerable based on raw mortality counts. However, few studies have accurately assessed the actual mortality and pattern of mortality across an entire outbreak or combined disease

surveillance data with population monitoring (prior to the outbreak) to assess local colony and population impacts. Our investigation of the Rat Island outbreak employed comprehensive and multifaceted approaches that are uncommon in published studies of HPAI in free-ranging wildlife. In addition to the mortality event investigation, we also conducted population monitoring of Caspian terns at the onset of the outbreak, which allowed us to estimate total mortality. Using raw carcass counts collected nearly weekly during the outbreak, we were able to calculate population impacts of this outbreak on the terns. This was combined with diagnostic and genomic data confirming H5N1 HPAIV clade 2.3.4.4b infections in several hosts, including the first documentation of HPAI in a marine mammal in the Northeast Pacific. We document clear host susceptibility differences between breeding adult Caspian terns and gulls nesting at the same colony and in close proximity, with significant population level impacts for Caspian terns in the Pacific Flyway, yet very little impact to adult gulls. Finally, we found consistent patterns of the timing of H5N1 detection, the pattern of virus mutation, and the pattern of bird movement.

As comprehensive as our data are, we still lack a full understanding of these species' immunological response(s) to IAV infections, especially H5N1 HPAIV, and how this affects susceptibility and disease outcomes in face of acute HPAI outbreaks and ongoing circulation of IAVs in the environment. This information gap and our findings highlight the importance of combining population monitoring, traditional and molecular epidemiological tools, and serologic surveillance for investigating wildlife morbidity and mortality events to better understand their impacts. We recommend expanding our wildlife health approach beyond mortality surveillance efforts (i.e., counting the dead) to also focus on population-level impacts and how environmental, behavioral, and immunological differences influence host susceptibility to disease, especially as H5N1 HPAI continues to devastate wildlife around the globe.

Data availability statement

The datasets presented in this study can be found in online repositories. The names of the repository/repositories and accession number(s) can be found in the article/Supplementary material.

Ethics statement

The animal study was approved by Washington Department of Fish and Wildlife, Wildlife Health. The study was conducted in accordance with the local legislation and institutional requirements.

Author contributions

KHH: Conceptualization, Data curation, Formal analysis, Funding acquisition, Investigation, Methodology, Project administration, Resources, Software, Supervision, Validation, Visualization, Writing – original draft, Writing – review & editing. SFP: Conceptualization, Data curation, Formal analysis, Funding acquisition, Investigation, Methodology, Project administration, Resources, Software, Supervision, Validation, Visualization, Writing – original draft, Writing – review & editing. JB: Conceptualization, Methodology, Resources, Writing – original draft, Writing – review & editing. LF: Data curation, Formal analysis, Methodology, Software, Writing – original draft, Writing – review & editing. SP: Data curation, Investigation, Methodology, Resources, Writing – review & editing. AF: Data curation, Formal analysis, Methodology, Writing – original draft, Writing – review & editing. RW: Data curation, Investigation, Methodology, Writing – review & editing. BT: Data curation, Formal analysis, Investigation, Methodology, Writing – review & editing. KT: Data curation, Formal analysis, Investigation, Methodology, Writing – original draft, Writing – review & editing. KS: Investigation, Methodology, Supervision, Writing – review & editing. ST: Formal analysis, Methodology, Writing – review & editing. IK: Data curation, Formal analysis, Methodology, Writing – review & editing. EA: Writing – original draft, Writing – review & editing. CC: Data curation, Investigation, Methodology, Writing – review & editing. DL: Data curation, Investigation, Methodology, Writing – review & editing. CE: Data curation, Investigation, Methodology, Writing – review & editing. SE: Data curation, Investigation, Methodology, Writing – review & editing. ER-R: Data curation, Investigation, Methodology, Writing – review & editing. HO: Investigation, Resources, Supervision, Writing – review & editing. KW: Investigation, Methodology, Writing – review & editing. DF: Investigation, Methodology, Writing – review & editing. AB: Conceptualization, Formal analysis, Funding acquisition, Investigation, Methodology, Software, Supervision, Writing – original draft, Writing – review & editing. TW: Funding acquisition, Investigation, Methodology, Project administration, Software, Supervision, Writing – original draft, Writing – review & editing.

Funding

The author(s) declare that financial support was received for the research, authorship, and/or publication of this article. This work was supported through the Washington Department of Fish and Wildlife, Washington Department of Health, and WADDL. Sequencing and genomic analysis were supported by the CDC Pathogen Genomics Centers of Excellence (NU50CK000630) and CDC Enhancing Epidemiology and Laboratory Capacity AMD Sequencing and Analytics (NU50CK000515). NOAA John H. Prescott Marine Mammal Rescue Assistance Grant Program provided funding to the Marine Mammal Stranding Network Partners.

Acknowledgments

We are grateful to WDFW biologists Katie Laushman, Chad Norris, Devin Walker, James McKinlay, Bryan Murphie, Shelly Ament, Jen Mannas, and Kurt Licence and WDFW marine mammal intern Matthew Sherrard for helping collect carcasses on Rat Island. We are grateful for our partners at the Washington Department of Public Health, Dr. Beth Lipton and Dr. Hannah Schnitzler, for helping address public health concerns and biosecurity practices for human safety during carcass collection. We thank Kirsten Bixler and Dan Roby for sharing banded tern resight information and

M. James Lawonn for sharing tern mortality information from Oregon. Park rangers at Fort Flagler State Park (Aaron Terada, Miles Carignan, and Karl Fisch) along with the Friends of Fort Flagler were instrumental in providing information to the public regarding the status of the H5N1 outbreak on Rat Island, informing us of sick/dead bird and seal reports, and helping collect carcasses around the beaches of Fort Flagler. Betsy Carlson and the Port Townsend Marine Science Center's Marine Mammal Stranding Network provided information about reported sick/dead stranded marine mammals. Responses to stranded marine mammals were conducted under 109(h) authority or 112(c) agreements under the Marine Mammal Protection Act. We thank the public health nurses that monitored the health of the field teams after potential exposures. We thank our colleagues at the National Veterinary Services Laboratory, including Dr. Mia Torchetti, for providing confirmatory results of all samples associated with this project. The scientific results and conclusions and any views or opinions expressed herein are those of the authors and do not necessarily reflect the views or policies of the U.S. government, its agencies, or any of the included organizations.

Conflict of interest

The authors declare that the research was conducted in the absence of any commercial or financial relationships that could be construed as a potential conflict of interest.

Publisher's note

Supplementary material

The Supplementary Material for this article can be found online at: https://www.frontiersin.org/articles/10.3389/fvets.2024.1483922/full#supplementary-material

References

1. Food and Agriculture Organization of the United Nations. Global avian influenza viruses with zoonotic potential situation update bird species affected by H5Nx HPAI. (2024). Available at: https://www.fao.org/animal-health/situation-updates/global-aiv-with-zoonotic-potential/bird-species-affected-by-h5nx-hpai/en (Accessed July 23, 2024).

2. Ramey AM, Hill NJ, DeLiberto TJ, Gibbs SEJ, Hopkins MC, Lang AS, et al. Highly pathogenic avian influenza is an emerging disease threat to wild birds in North America. *J Wildl Manag*. (2022) 86:e22171. doi: 10.1002/jwmg.22171

3. Swayne DE. Understanding the complex pathobiology of high pathogenicity avian influenza viruses in birds. *Avian Dis*. (2007) 51:242–9. doi: 10.1637/7763-110706-REGR.1

4. Charostad J, Rukerd MRZ, Mahmoudvand S, Bashash D, Hashemi MA, Nakhaie M, et al. A comprehensive review of highly pathogenic avian influenza (HPAI) H5N1: An imminent threat at doorstep. *Travel Med Infect Dis*. (2023) 55:102638. doi: 10.1016/j.tmaid.2023.102638

5. Verhagen JH, Fouchier RAM, Lewis N. Highly pathogenic avian influenza viruses at the wild-domestic bird interface in Europe: future directions for research and surveillance. *Viruses*. (2021) 13:212. doi: 10.3390/v13020212

6. Webby RJ, Uyeki TM. An update on highly pathogenic avian influenza a (H5N1) virus, clade 2.3.4.4b. *J Infect Dis*. (2024) 230:533–42. doi: 10.1093/infdis/jiae379

7. Abolnik C, Phiri T, Peyrot B, de Beer R, Snyman A, Roberts D, et al. The molecular epidemiology of clade 2.3.4.4B H5N1 high pathogenicity avian influenza in southern Africa, 2021-2022. *Viruses*. (2023) 15:1383. doi: 10.3390/v15061383

8. Ariyama N, Pardo-Roa C, Munoz G, Aguayo C, Avila C, Mathieu C, et al. Highly pathogenic avian influenza a (H5N1) clade 2.3.4.4b viruses in wild birds, Chile. *Emerg Infect Dis*. (2023) 29:1842–5. doi: 10.3201/eid2909.230067

9. Campagna C, Uhart M, Falabella V, Campagna J, Zavattieri V, Vanstreels RET, et al. Catastrophic mortality of southern elephant seals caused by H5N1 avian influenza. *Mar Mamm Sci*. (2024) 40:322–5. doi: 10.1111/mms.13101

10. Fusaro A, Zecchin B, Giussani E, Palumbo E, Aguero-Garcia M, Bachofen C, et al. High pathogenic avian influenza a(H5) viruses of clade 2.3.4.4b in Europe – why trends of virus evolution are more difficult to predict. *Virus Evolution*. (2024) 10:27. doi: 10.10903/ve/veae027

11. Letsholo SL, James J, Meyer SM, Byrne AMP, Reid SM, Settypalli TBK, et al. Emergence of high pathogenicity avian influenza virus H5N1 clade 2.3.4.4b in wild birds and poultry in Botswana. *Viruses*. (2022) 14:2601. doi: 10.3390/v14122601

12. Rijks JM, Leopold MF, Kühn S, Veld R, Schenk F, Brenninkmeijer A, et al. Mass mortality caused by highly pathogenic influenza a(H5N1) virus in sandwich terns, the Netherlands, 2022. *Emerg Infect Dis*. (2022) 28:2538–42. doi: 10.3201/eid2812.221292

13. Caserta LC, Frye EA, Butt SL, Laverack M, Nooruzzaman M, Covaleda LM, et al. Spillover of highly pathogenic avian influenza H5N1 virus to dairy cattle. *Nature*. (2024). doi: 10.1038/s41586-024-07849-4

14. Plaza PI, Gamarra-Toledo V, Eugi JR, Lambertucci SA. Recent changes in patterns of mammal infection with highly pathogenic avian influenza a (H5N1) virus worldwide. *Emerg Infect Dis*. (2024) 30:444–52. doi: 10.3201/eid3003.231098

15. Puryear WB, Runstadler JA. High-pathogenicity avian influenza in wildlife: a changing disease dynamic that is expanding in wild birds and having an increasing impact on a growing number of mammals. *J Am Vet Med Assoc*. (2024) 262:601–9. doi: 10.2460/javma.24.01.0053

16. Uhart M, Vanstreels RET, Nelson MI, Olivera V, Campagna J, Zavattieri V, et al. Massive outbreak of influenza a H5N1 in elephant seals at Península Valdés, Argentina: Increased evidence for mammal-to-mammal transmission. *Biorxiv*. (2024). doi: 10.1101/2024.05.31.596774

17. Patin-Jackwood MJ, Swayne DE. Pathogenesis and pathobiology of avian influenza virus infection in birds. *Rev Sci Tech*. (2009) 28:113–36.

18. Brown JD, Stallknecht DE, Beck JR, Suarez DL, Swayne DE. The susceptibility of north American ducks and gulls to H5N1 highly pathogenic avian influenza viruses. *Emerg Infect Dis*. (2006) 12:1663–70. doi: 10.3201/eid1211.060652

19. Brown JD, Stallknecht DE, Swayne DE. Transmission of H5N1 high pathogenicity avian influenza virus to herring gulls (*Larus argentatus*) through intranasal inoculation of virus and ingestion of virus-infected chicken meat. *Avian Pathol*. (2008) 37:393–7. doi: 10.1080/03079450802216595

20. Brown JD, Stallknecht DE, Swayne DE. Infectious and lethal doses of H5N1 highly pathogenic avian influenza virus for house sparrows (*Passer domesticus*) and rock pigeons (*Columbia livia*). *J Vet Diagn Investig*. (2009) 21:437–45. doi: 10.1177/104063870902100404

21. Keawcharoen J, van Riel D, van Amerongen G, Bestebroer T, Beyer WE, van Lavieren R, et al. Wild ducks as long-distance vectors of highly pathogenic avian influenza virus (H5N1). *Emerg Infect Dis*. (2008) 14:600–7. doi: 10.3201/eid1404.071016

22. Perkins LE, Swayne DE. Pathobiology of a/chicken/Hong Kong/220/97 (H5N1) avian influenza virus in seven gallinaceous species. *Vet Pathol*. (2001) 38:149–64. doi: 10.1354/vp.38-2-149

23. Perkins LE, Swayne DE. Pathogenicity of a Hong Kong–origin H5N1 highly pathogenic avian influenza virus for emus, geese, ducks, and pigeons. *Avian Dis*. (2002) 46:53–63. doi: 10.1637/0005-2086(2002)046[0053:POAHKO]2.0.CO;2

24. Berhane Y, Leith M, Embury-Hyatt C, Neufeld J, Babiuk S, Hisanaga T, et al. Studying possible cross-protection of Canada geese pre-exposed to north American low pathogenicity avian influenza virus strains (H3N8, H4N6, and H5N2) against an H5N1 highly pathogenic avian influenza challenge. *Avian Dis*. (2010) 54:548–54. doi: 10.1637/8841-040309-Reg.1

25. Costa TP, Brown JD, Howerth EW, Stallknecht DE, Swayne DE. Homo- and heterosubtypic low pathogenic avian influenza exposure on H5N1 highly pathogenic avian influenza virus infection in wood ducks (*Aix sponsa*). *PLoS One*. (2011) 6:e15987. doi: 10.1371/journal.pone.0015987

26. Rasmussen EA, Czaja A, Cuthbert FJ, Tan GS, Lemey P, Nelson MI, et al. Influenza a viruses in gulls in landfills and freshwater habitats in Minnesota, United States. *Front Genet*. (2023) 14:1172048. doi: 10.3389/fgene.2023.1172048

27. Verhagen JH, Herfst S, Fouchier RAM. Infectious disease. How a virus travels the world. *Science*. (2015) 347:616–7. doi: 10.1126/science.aaa6724

28. Knief U, Bregnabelle T, Alfarwi I, Ballmann MZ, Brenninkmeijer A, Bzoma S, et al. Highly pathogenic avian influenza causes mass mortality in sandwich tern (*Thalasseus sandvicensis*) breeding colonies across North-Western Europe. *Bird Conserv Int*. (2023) 34:1–11. doi: 10.1017/S0959270923000400

29. Billau. Waterbird researcher surveys how many Caspian terns survived bird flu in Northern Michigan. (2023) Available at: https://lsa.umich.edu/umbs/news-events/all-news/search-news/waterbird-researcher-surveys-how-many-caspian-terns-survived-bir.html (Accessed August 15, 2024).

30. USDA. Detections of Highly Pathogenic Avian Influenza in Wild Birds. (2024) Available at: https://www.aphis.usda.gov/livestock-poultry-disease/avian/avian-influenza/hpai-detections/wild-birds (Accessed August 19, 2024).

31. Pearson SF, Amburgey SM, Clark CT, Tanedo SA, London JM, Huber HR, et al. Trends and status of harbor seals in Washington state, USA (1977-2023). *Mar Mamm Sci*. (2024). doi: 10.1111/mms.13161

32. Plummer M. (2003). JAGS: a program for analysis of Bayesian graphical models using Gibbs sampling. Proceedings of the 3rd international workshop on distributed statistical computing (DSC 2003), Vienna, 20–22 march 2003, 1–10.

33. Kim WH, Cho S. Estimation of the basic reproduction numbers of the subtypes H5N1, H5N8, and H5N6 during the highly pathogenic avian influenza epidemic spread between farms. *Front Vet Sci*. (2021) 8:597630. doi: 10.3389/fvets.2021.597630

34. Ward WP, Maftei D, Apostu C, Suru A. Estimation of the basic reproductive number (R0) for epidemic, highly pathogenic avian influenza subtype H5N1 spread. *Epidemiol Infect*. (2009) 137:219–26. doi: 10.1017/S0950268808000885

35. Antolos M, Roby DD, Lyons DE, Anderson SK, Collis K. Effects of nest density, location, and timing of breeding success of Caspian terns. *Waterbirds*. (2006) 29:465–72. doi: 10.1675/1524-4695(2006)29[465:EONDLA]2.0.CO;2

36. Spackman E, Senne DA, Myers TJ, Bulaga LL, Garber LP, Perdue ML, et al. Development of a real-time reverse transcriptase PCR assay for type a influenza virus and the avian H5 and H7 hemagglutinin subtypes. *J Clin Microbiol*. (2002) 40:3256–60. doi: 10.1128/jcm.40.9.3256-3260.2002

37. Metsky CM, Siddle KJ, Gladden-Young A, Qu J, Yang DK, Brehio P, et al. Capturing sequence diversity in metagenomes with comprehensive and scalable probe design. *Nat Biotechnol*. (2019) 37:160–8. doi: 10.1038/s41587-018-0006-x

38. Shen W, Le S, Li Y, Hu F. SeqKit: a cross-platform and ultrafast toolkit for FASTA/Q file manipulation. *PLoS One*. (2016) 11:163962. doi: 10.1371/journal.pone.0163962

39. Hadfield J, Megill C, Bell SM, Huddleston J, Potter B, Callender C, et al. Nextstrain: real-time tracking of pathogen evolution. *Bioinformatics*. (2018) 34:4121–3. doi: 10.1093/bioinformatics/bty407

40. Nguyen LT, Schmidt HA, von Haeseler A, Minh BQ. IQ-TREE: a fast and effective stochastic algorithm for estimating maximum-likelihood phylogenies. *Mol Biol Evol*. (2014) 32:268–74. doi: 10.1093/molbev/msu300

41. Sagulenko P, Puller V, Neher RA. TreeTime: maximum-likelihood phylodynamic analysis. *Virus Evol*. (2018) 4:vex042. doi: 10.1093/ve/vex042

42. Dudas G, Bedford T. The ability of single genes vs full genomes to resolve time and space in outbreak analysis. *BMC Evol Biol*. (2019) 19:232. doi: 10.1186/s12862-019-1567-0

43. Lee CY, An SH, Choi JG, Lee YJ, Kim JH, Kwon HJ. Rank orders of mammalian pathogenicity-related PB2 mutations of avian influenza a viruses. *Sci Rep*. (2020) 10:5359. doi: 10.1038/s41598-020-62036-5

44. Brown JD, Luttrell MP, Berghaus RD, Kistler W, Keeler SP, Howey A, et al. Prevalence of antibodies to type a influenza virus in wild avian species using two serologic assays. *J Wildl Dis*. (2010) 46:896–911. doi: 10.7589/0090-3558-46.3.896

45. Guinn K, Fojtik A, Davis-Fields N, Poulson RL, Krauss S, Webster RG, et al. Antibodies to influenza a viruses in gulls at Delaware Bay, USA. *Avian Dis*. (2016) 60:341–5. doi: 10.1637/11103-042115-Reg

46. Toennessen R, Kristoffersen AB, Jonassen CM, Hjortaas MJ, Hansen EF, Rimstad E, et al. Virological and serological surveillance for type a influenza in the black-legged kittiwake (*Rissa tridactyla*). *Virol J*. (2013) 10:112. doi: 10.1186/1743-422X-10-112

47. Lebarbenchon C, Jaeger A, Feare C, Bastien M, Dietrich M, Larose C, et al. Influenza a virus on oceanic islands: host and viral diversity in seabirds in the Western Indian Ocean. *PLoS Pathog*. (2015) 11:e1004925. doi: 10.1371/journal.ppat.1004925

48. Cuthbert FJ, Wires LR. Caspian tern (*Hydroprogne caspia*), version 1.0 In: SM Billerman, editor. Birds of the world. Ithica, NY, USA: Cornell Lab of Ornithology (2020)

49. Lawes T., Roby D.D., Lyons D.E.. Final annual report 2021 Pacific flyway Caspian tern population monitoring. Submitted to U.S. Fish and Wildlife Service, legacy region 1, migratory birds and habitat program. Portland: Migratory Birds and Habitat Program, (2021).

50. Lair S, Quesnel L, Signore AV, Delnatte P, Embury-Hyatt C, Nadeau M, et al. Outbreak of highly pathogenic avian influenza a (H5N1) virus in seals, St. Lawrence estuary, Quebec, Canada. *Emerg Infect Dis*. (2024) 30:1133–43. doi: 10.3201/eid3006.231033

51. Puryear W, Sawatzki K, Hill N, Foss A, Stone JJ, Doughty L, et al. Highly pathogenic avian influenza a(H5N1) virus outbreak in New England seals, United States. *Emerg Infect Dis*. (2023) 29:786–91. doi: 10.3201/eid2904.221538

52. Elsmo EJ, Wunschmann A, Beckmen KB, Broughton-Neiswanger LE, Buckles EL, Ellis J, et al. Highly pathogenic avian influenza a (H5N1) virus clade 2.3.4.4b infections in wild terrestrial mammals, United States 2022. *Emerg Infect Dis*. (2023) 29:2451–60. doi: 10.3201/eid2912.230464

53. Burrough ER, Magstadt DR, Petersen B, Timmermans SJ, Gauger PC, Zhang J, et al. Highly pathogenic avian influenza virus infection in domestic dairy cattle and cats, United States 2004. *Emerg Infect Dis*. (2024) 30:1335–43.

54. Eisfeld AJ, Biswas A, Guan L, Gu C, Maemura T, Trifkovic S, et al. Pathogenicity and transmissibility of bovine H5N1 influenza virus. *Nature*. (2024) 633:426–32. doi: 10.1038/s41586-024-07766-6

55. Katoh K, Standley DM. MAFFT multiple sequence alignment software version 7: improvements in performance and usability. *Mol Biol Evol*. (2016) 30:772–780. doi: 10.1093/molbev/mst010

Frontiers in Veterinary Science

Transforms how we investigate and improve animal health

The third most-cited veterinary science journal, bridging animal and human health with a comparative approach to medical challenges. It explores innovative biotechnology and therapy for improved health outcomes.

Discover the latest Research Topics

See more →

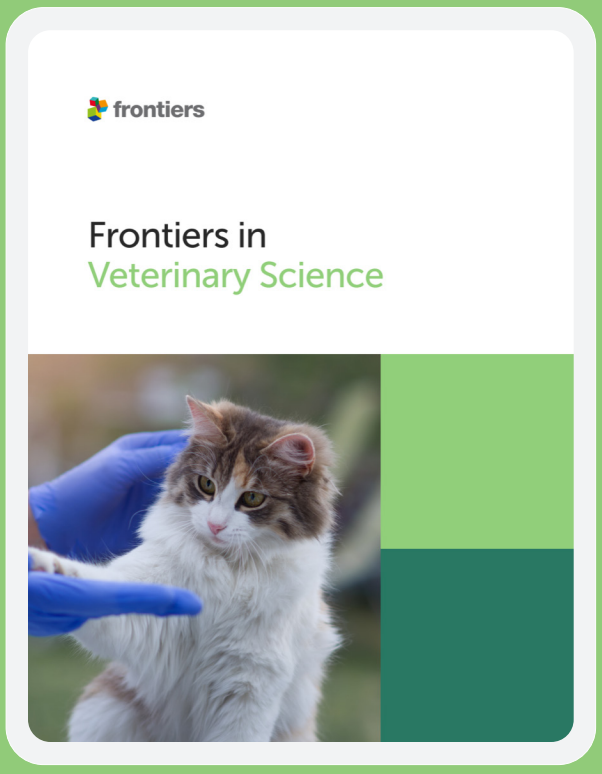

Frontiers

Avenue du Tribunal-Fédéral 34
1005 Lausanne, Switzerland
frontiersin.org

Contact us

+41 (0)21 510 17 00
frontiersin.org/about/contact